PB81-232365

Formation and Fate of Atmospheric Nitrates Workshop Proceedings

(U.S.) Environmental Science Research Lab.
Research Triangle Park, NC

Jun 81

U.S. Department of Commerce
National Technical Information Service
NTIS

United States
Environmental Protection
Agency

Environmental Sciences Research
Laboratory
Research Triangle Park NC 27711

EPA-600/9-81-025
June 1981

PB81-232365

Research and Development

EPA

Formation and Fate of Atmospheric Nitrates

Workshop Proceedings

REPRODUCED BY
NATIONAL TECHNICAL
INFORMATION SERVICE
U.S. DEPARTMENT OF COMMERCE
SPRINGFIELD, VA 22161

TECHNICAL REPORT DATA

(Please read Instructions on the reverse before completing)

1. REPORT NO. EPA-600/9-81-025	2.	3. RECIPIENT'S ACCESSION NO. PB81 232365
4. TITLE AND SUBTITLE FORMATION AND FATE OF ATMOSPHERIC NITRATES Workshop Proceedings		5. REPORT DATE June 1981
		6. PERFORMING ORGANIZATION CODE
7. AUTHOR(S) H.M. Barnes, Editor		8. PERFORMING ORGANIZATION REPORT NO.
9. PERFORMING ORGANIZATION NAME AND ADDRESS Environmental Sciences Research Laboratory - RTP, NC Office of Research and Development U.S. Environmental Protection Agency Research Triangle Park, North Carolina 27711		10. PROGRAM ELEMENT NO. CABN1D/10-0548 (FY-81)
		11. CONTRACT/GRANT NO.
12. SPONSORING AGENCY NAME AND ADDRESS Same as #9		13. TYPE OF REPORT AND PERIOD COVERED In-house
		14. SPONSORING AGENCY CODE EPA/600/09

15. SUPPLEMENTARY NOTES

16. ABSTRACT

Articles based on formal presentations given October 22-23, 1979, at the "Workshop on the Formation and Fate of Atmospheric Nitrates" are documented in the report. The authors discuss nitrate formation from both theoretical (gas and aerosol formation models) and applied (smog chamber and field measurement programs) aspects. The fate of atmospheric nitrates is discussed in terms of wet and dry removal processes.

17. KEY WORDS AND DOCUMENT ANALYSIS

a. DESCRIPTORS	b. IDENTIFIERS/OPEN ENDED TERMS	c. COSATI Field/Group

18. DISTRIBUTION STATEMENT RELEASE TO PUBLIC	19. SECURITY CLASS (This Report) UNCLASSIFIED	21. NO. OF PAGES 217
	20. SECURITY CLASS (This page) UNCLASSIFIED	22. PRICE

EPA Form 2220-1 (Rev. 4-77) PREVIOUS EDITION IS OBSOLETE

EPA-600/9-81-025
June 1981

FORMATION AND FATE OF ATMOSPHERIC NITRATES

Workshop Proceedings

Edited by

H.M. Barnes
Aerosol Research Branch
Environmental Sciences Research Laboratory
Research Triangle Park, North Carolina 27711

ENVIRONMENTAL SCIENCES RESEARCH LABORATORY
OFFICE OF RESEARCH AND DEVELOPMENT
U.S. ENVIRONMENTAL PROTECTION AGENCY
RESEARCH TRIANGLE PARK, NORTH CAROLINA 27711

DISCLAIMER

This report has been reviewed by the Environmental Sciences Research Laboratory, U.S. Environmental Protection Agency, and approved for publication. Mention of trade names or commercial products does not constitute endorsement or recommendation for use.

FOREWORD

The Environmental Sciences Research Laboratory (ESRL) of the U.S. Environmental Protection Agency at Research Triangle Park, North Carolina, (EPA-RTP) conducts an intramural and extramural research program to detect, define, and quantify the effects of air pollution on urban, regional, and global atmospheres (and the subsequent impact on water quality and land use). Within ESRL, the Aerosol Research Branch conducts laboratory and field studies on the chemical and physical properties and mechanisms of formation and removal of aerosol particles.

In performance of this role, ESRL conducted a workshop on "Formation and Fate of Atmospheric Nitrates" in Research Triangle Park, North Carolina, on October 22 and 23, 1979. This report represents one important product of that meeting.

A.H. Ellison, Acting Director
Environmental Sciences Research
Laboratory

ABSTRACT

Articles based on formal presentations given October 22-23, 1979, at the "Workshop on the Formation and Fate of Atmospheric Nitrates" are documented in the report. The authors discuss nitrate formation from both theoretical (gas and aerosol formation models) and applied (smog chamber and field measurement programs). The fate of atmospheric nitrates is discussed in terms of wet and dry removal processes.

In the Introduction, H. M. Barnes summarizes the workshop presentations and the discussion session following them. B. Dimitrades begins the presentations with a discussion of the overall question of nitrates as an air pollution problem and the relevant questions to be addressed. S. K. Friedlander discusses the thermodynamic and kinetic considerations of ammonium nitrate formation. D. G. Hendry reports on the analysis of smog chamber data for the predominant NO_x gas phase reactions leading to nitric acid formation. The important gas-solid NO_x interactions are discussed by H. S. Judeikis. H. E. Jeffries and K. Sexton report on the comparisons of six photochemical models for predictng the fate of NO_x in irradiated hydrocarbon-NO_x mixtures. The importance of wet deposition for nitrates is discussed by G. J. Stensland, who reports on nitrate measurement in rainwater at a Midwest field site. C. W. Spicer reports on a multi-year research program at Battelle-Columbus concerning the measurement, distribution, and reaction rate of NO_x/NO_3^- in the ambient air. Problems in the sampling of ambient air nitrates are addressed by B. R. Appel et al. Nitric acid measurements in clean air near Boulder, Colorado, are reported by D. H. Stedman and T. J. Kelly. The historical trends of nitrate wet depositon in the eastern United States are described and discussed by M. L. Miller and A. G. Everett. The reactions of NO_x in the aqueous phase as they apply to atmospheric processes are described by S. E. Schwartz. The Discussion includes the following topics: (1) Natural vs. anthropogenic NO_x sources, (2) Wet deposition measurements, (3) Dry deposition measurements, (4) Smog chamber measurements, (5) Laboratory studies, (6) General observations.

CONTENTS

Foreword iii
Abstract iv
Figures viii
Tables xii
Acknowledgment xiv

INTRODUCTION 1
H. M. Barnes

THE ISSUE OF NITRATES IN THE ATMOSPHERE 5
Basil Dimitriades

Introduction 5
Conclusions 6
Recommendations 6
The Issues 7
References 14

THERMODYNAMICS AND KINETICS OF AEROSOLS CONTAINING AMMONIUM NITRATE. . . 16
Sheldon K. Friedlander

Introduction 16
Thermodynamic Considerations 17
Kinetics of NH_4NO_3 Formation: Effects of SO_2 Oxidation 20
Application to Field Studies 22
References 23

ATMOSPHERIC NITROGEN CHEMISTRY 25
Dale G. Hendry

Introduction 25
Conclusions and Recommendations 26
Analysis of Smog Chamber Nitrogen Balance 26
Alternative NO_x Loss Reactions 29
References 36

HETEROGENEOUS NO_X REACTIONS IN THE ATMOSPHERE 38
Henry S. Judeikis

Introduction 38
Experimental 39
Results 40
Discussion 42
References 47

MODELING ASPECTS OF NITROGEN OXIDES USING SMOG CHAMBER DATA 49
Harvey Jeffries and Ken Sexton

Introduction 49
Conclusions and Recommendations 49
Nitrogen Transformation Process 50
Mechanism Characteristics 51
Chamber Experiments and Simulations 54
Results and Discussion 56
Nitric Acid Special Experiments 66
References 94

NITRATE MEASUREMENTS IN PRECIPITATION FOR THE STUDY OF TRENDS, PATTERNS, AND SCAVENGING PROCESS 96
Gary J. Stensland

Introduction 96
Conclusions 96
Patterns and Trends for Nitrate in Precipitation 97
Daily Precipitation and Aerosol Data for Illinois 103
Precipitation Scavenging of Nitrate 108
Acknowledgments 115
References 115

REACTION OF NO_X IN SMOG CHAMBERS AND URBAN ATMOSPHERES 118
Chester W. Spicer

Introduction 118
Results and Discussion 118
Acknowledgment 127
References 137

SAMPLING OF NITRATES IN AMBIENT AIR 138
Bruce R. Appel, Y. Tokiwa, and M. Haik

Introduction 138
Conclusions 138
Recommendations 139
Experimental 139
Results and Discussion 140
Acknowledgments and Disclaimer 145
References 154

NITRIC ACID MEASUREMENTS IN CLEAN AIR 156
Donald Stedman and Thomas J. Kelly

Introduction 156
Experimental 156
Results 157
Acknowledgments 160
References 161

HISTORY AND TRENDS OF ATMOSPHERIC NITRATE DEPOSITION IN THE EASTERN U.S.A. 162
M. L. Miller and A. Gordon Everett

Introduction 162
Conclusions 162
Natural vs. Anthropogenic Sources 163
Variability in Sample Collection 166
Analytical Uncertainties 167
Long-Term Study Results 168
Ice-Core and Buffering-Effect Analyses 173
References 174

AQUEOUS PHASE NO_x PROCESSES IN THE ATMOSPHERE 179
Stephen E. Schwartz

DISCUSSION 196
W. E. Wilson

Natural vs. Anthropogenic NO_x Sources 196
Wet Deposition Measurements 196
Dry Deposition Measurements 197
Smog Chamber Studies 197
Laboratory Studies 198
General Observations 199

LIST OF ATTENDEES 200

FIGURES

Number Page

THERMODYNAMICS AND KINETICS OF AEROSOLS CONTAINING AMMONIUM NITRATE
S. K. Friedlander

1 The product $[NH_3][HNO_3]$ for West Covina compared with equilibrium theory 19

ATMOSPHERIC NITROGEN CHEMISTRY: NO_x LOSS REACTIONS
D. G. Hendry

1 SAPRC propene run EC-314 27
2 Nitrogen balance: propene 28
3 SAPRC n-butane run EC-306 30
4 Nitrogen balance 30
5 SAPRC toluene run EC-266 31
6 Nitrogen balance: toluene 31
7 Decomposition of PBzN at 300K 32
8 Missing nitrogen relative to toluene loss 34

MODELING ASPECTS OF NITROGEN OXIDES USING SMOG CHAMBER DATA
H. E. Jeffries
K. Sexton

1 Nitrogen transformation processes 69
2 Experimental data from UNC outdoor smog chamber 70
3 Experimental data from UNC outdoor smog chamber 70
4 Experimental data from UNC outdoor smog chamber 71
5 Experimental nitrogen balance 72
6 Experimental carbon balance 72
7 Simulation with CARTER mechanism 73
8 Simulation with CARTER mechanism 73
9 Minor nitrogen species in CARTER mechanism 74
10 Minor nitrogen species in CARTER mechanism 74
11 Experimental data from UNC outdoor smog chamber 75
12 Simulation nitrogen balance 75
13 Simulation with DODGE mechanism 76

Number Page

14 Simulation with CBII mechanism 76
15 Simulation with CBII mechanism 77
16 Simulation with LLOYD mechanism 77
17 Simulation with DERMJ mechanism 78
18 Simulation with JEFFRIES mechanism 78
19 Simulation with CBII mechanism 79
20 Simulation with LLOYD mechanism 79
21 Reaction sequence from LLOYD mechanism 80
22 Experimental data from UNC outdoor smog chamber 80
23 Simulation of propylene-butane experiment using DODGE mechanism 81
24 Simulation of propylene-butane experiment using DODGE mechanism 81
25 Simulation of propylene-butane experiment using CBII mechanism 82
26 Simulation of mix experiment using CBII mechanism 82
27 Simulation of mix experiment using DERMJ mechanism 83
28 Simulation of mix experiment using LLOYD mechanism 83
29 Simulation of mix experiment using LLOYD mechanism 84
30 Comparison of NO, NO_2, and O_3 profiles 84
31 Simulation with DODGE mechanism 85
32 Simulation with CBII using variable temperatures 85
33 Simulation with DERMJ mecahanism 86
34 Simulation with LLOYD mechanism 86
35 Experimental data from UNC outdoor smog chamber 87
36 Simulation results for UNCR propylene 88
37 Simulation results for UNCB toluene-propylene 89
38 Simulation results for UNCB toluene-propylene 90
39 Experimental data from UNC chamber at night 91
40 Simulation including heterogeneous N_2O_5 chemistry 91
41 Simulation omitting heterogeneous N_2O_5 chemistry 92
42 Experimental data from UNC outdoor smog chamber 92
43 Experimental data from UNC outdoor smog chamber 93
44 Experimental data from UNC chamber using chemiluminescent nitric acid analyzer 93

NITRATE MEASUREMENTS IN PRECIPITATION FOR THE STUDY OF TRENDS, PATTERNS, AND SCAVENGING PROCESSES

G. J. Stensland

1 Precipitation chemistry sampling sites 98
2 Contours of NO_3^- concentrations for the Junge network 100
3 Contours of NO_3^- concentrations from NADP results 100
4 Emission trends for NO_x and SO_x 102
5 Daily nitrate concentrations, Champaign, Illinois 104
6 Monthly average nitrate concentrations, Champaign 104
7 Monthly average sulfate concentrations, Champaign 105
8 Daily aerosol concentrations for four filter setups 107
9 SCORE-78 network and beginning times of rainfall 109

Number Page

10 Ending time of rainfall 110
11 Spatial variation of sample volume and pH 111
12 Spatial variation of $SO_4^=$, NO_3^-, Ca, and Mg 112
13 Spatial variation of K, Cl, Na, and NH_4^+ 113

REACTION OF NO_x IN SMOG CHAMBERS AND URBAN ATMOSPHERES
C. W. Spicer

1 Comparison of nitrate mass on various filters 128
2 Artifact nitrate as a function of $HONO_2$ exposure 129
3 Average diurnal air quality and meteorological profile,
  West Covina 130
4 Composite profiles of F_n* in St. Louis and West Covina 131
5 Oxidized nitrogen distribution, Philadelphia 132
6 F_n vs. reaction time 132
7 Results of irradiation of urban HC mix and NO_x 133
8 $HONO_2$ yield vs. initial NO_x 134
9 Air parcel trajectory, Boston, August 23, 1978 135
10 First order plot for flights of August 23, 1978 136

SAMPLING NITRATES IN AMBIENT AIR
B. R. Appel
Y. Tokiwa
M. Haik

1 Total particulate nitrate filter 146
2 Glass fiber filters as total nitrate samplers 146
3 HNO_3 collection efficiency of nylon and W41 filters 147
4 HNO3 collection, nylon vs. NaCl/W41 filters 147
5 Comparison of HNO_3 by filter collection and "by difference"
  using unheated samplers 148
6 Comparison of HNO3 by filter collection and "by difference"
  using heated samplers 149
7 Comparison of HNO_3 by long path Fourier transform and
  "by difference" 150
8 Comparison of particulate NO_3^- levels by Teflon prefilters
  and by the total particulate NO_3^- sampler with
  unheated samplers 151
9 Comparison of particulate NO_3^- levels by Teflon prefilters
  and by the total particulate NO_3^- samplers with
  heated samplers 151
10 Diurnal variations for HNO_3, true particulate NO_3^-,
  and O_3 152
11 Diurnal variations for HNO_3, particulate acidity, and
  gaseous NH_3 152
12 Fraction of NO_3^- on afterfilter 153
13 Fraction of NO_3^- on afterfilter 153

Number Page

NITRIC ACID MEASUREMENTS IN CLEAN AIR

D. H. Stedman
T. J. Kelly

1 Inlet system block diagram for mobile NOx detector 157
2 Concentrations of NO_2 and HNO_3, Erie, Colorado 158
3 Typical NO_x and HNO_3 data from Niwot Ridge 159
4 NO_x/HNO_3 ratio vs. NO_x, Niwot Ridge 160

HISTORY AND TRENDS OF ATMOSPHERIC NITRATE DEPOSITION IN THE EASTERN U.S.A.

M. L. Milller
A. G. Everett

1 Frequency and distribution of lightning 164
2 pH of precipitation at Hubbard Brook 169
3 Hubbard Brook precipitation sampling sites 169
4 pH of precipitation vs. time, New York locations 170
5 NO_3^- vs. time, New York locations 170

AQUEOUS PHASE NO_x PROCESSES IN THE ATMOSPHERE

S. E. Schwartz

1 Nitrogen oxide and oxyacid equilibria 180
2 Henry's Law coefficient vs. normal boiling point for various gases 181
3 Partial pressure of HNO_3 above dilute solution 182
4 Partial pressure of HNO_3 at 1 ppb 183
5 Partial pressure of HNO_3 as a function of pH 184
6 Nitrous acid characteristics 184
7 Partial pressure of HNO_2 as a function of pH 185
8 Plot of literature data for equilibrium constant and free energies of formation 186
9 NO_2/NO ratio at various partial pressures 187
10 Concentration of HNO_3 at various partial pressures 187
11 Partial pressure of gas phase NO_2 or HNO_3 188
12 Thermochemical cycles and Henry's Law coefficient 190
13 Mechanism describing phase mixed system 190
14 Second-order rate law and partial pressure of NO_2 191

TABLES

Number Page

ATMOSPHERIC NITROGEN CHEMISTRY: NO_x LOSS REACTIONS

D. G. Hendry

1 Inorganic Nitrogen Chemistry 25

HETEROGENEOUS NO_x REACTIONS IN THE ATMOSPHERE

H. S. Judeikis

1 Experimental Reactivities for NO_2 41
2 Atmospheric Nitrate Burdens from NO_2--Aerosol Reactions 44

MODELING ASPECT OF NITROGEN OXIDES USING SMOG CHAMBER DATA

H. E. Jeffries
K. Sexton

1 Characteristics of Simulation Mechanisms Used in This Study . . . 52
2 Rate Constants for Selected Reactions 52
3 Chamber Experiments and Simulations 55
4 1978 UNC Simulated Urban HC Mix 55
5 Input Data and Parameters for Models 57
6 N-BAL at O_3 Maximum 57
7 N-BAL at O_3 Maximum 61
8 Input Data and Parameters for Models 62
9 N-BAL at O_3 Max 62
10 Initial HC Concentrations in Simulation Models 64
11 N-BAL at O_3 Max 65
12 Nighttime Ozone/Nitrogen Dioxide Mechanism 67

Number Page

NITRATE MEASUREMENTS IN PRECIPITATION FOR THE STUDY OF TRENDS, PATTERNS, AND SCAVENGING PROCESSES

G. J. Stensland

1 NO_3^- Concentrations, Recent and Historical 99
2 Median NO_3^- and $SO_4^=$ Concentrations, Champaign 106
3 A. Numerical Data, 7/1/78 Event, SCORE 114
B. Ion Concentrations, 7/1/78 Event 114
4 Ratios of Ion Concentrations from Single Rain Cell Samples . . . 115

REACTION OF NOx IN SMOG CHAMBERS AND URBAN ATMOSPHERES

C. W. Spicer

1 Gaseous Nitrate Measurement Methods 119
2 Average Pair-Wise NO_3^- Differences 120
3 Oxidized Nitrogen Distribution 121
4 Atmospheric Nitrate Distribution 123
5 Atmospheric Nitrogen Balance 125
6 NO_x Removal Rate, Boston Plume Study 127

SAMPLING OF NITRATES IN AMBIENT AIR

B. R. Appel
Y. Tokiwa
M. Haik

1 Filter Media Studies for Artifact Formation 140
2 Artifact NO_3^- Formation at 50 Percent RH 141
3 Comparison of Atmospheric NO_3^- and Artifact NO_3^- 141
4 Loss of HN_4NO_3 from Teflon Filter 143

HISTORY AND TRENDS OF ATMOSPHERIC NITRATE DEPOSITION IN THE EASTERN U.S.A.

M. L. Miller
A. G. Everett

1 pH Trends for USGS Sites 171
2 NO_3^- Trends for USGS Sites 171
3 NO_3^- Trends for USGS Sites 172
4 NO_3^-/pH Relationship for USGS Data Base 172

AQUEOUS PHASE NO_x PROCESSES IN THE ATMOSPHERE

S. E. Schwartz

1 Aqueous Phase Concentrations Using Henry's Law Coefficients 181

ACKNOWLEDGMENT

The editor wishes to thank Ms. Jan Parsons, Northrop Services, Inc., for her assistance and efforts in arranging this workshop and in the preparation of this document.

INTRODUCTION

H. M. Barnes

Environmental Sciences Research Laboratory
U.S. Environmental Protection Agency
Research Triangle Park, North Carolina 27711

The U.S. EPA sponsored a workshop to discuss the formation and removal processes for nitrogen oxides/nitrates in the ambient air. The workshop was held October 22-23, 1979, at the EPA facilities in the Research Triangle Park. Invited speakers and attendees were scientists and managers actively involved in research areas related to this topic.

The principal purposes of the workshop were to discuss ongoing research, to identify areas in which data are lacking or appear conflicting and to encourage the exchange of ideas on future experimental data base needs. An additional, but not unimportant, intent of the workshop was to allow EPA scientists and managers to learn of the ongoing viewpoints concerning nitrates as an environmental problem. For this reason no EPA research programs were formally presented at the workshop. Instead Dr. Basil Dimitriades, Director, Atmospheric Chemistry and Physics Division of the Environmental Sciences Research Laboratory began the meeting with the EPA overview of the nitrate question. He identified the existing information on nitrogen oxides as follows: (1) the species of concern are nitric acid, peroxyacetyl nitrate, ammonium nitrate, and particulate nitrates (alkali metal, etc., as cation); (2) nitrates result mainly from the gas phase photooxidation of NO_x; (3) NO_x reaction rates and stoichiometry have been established in smog chamber experiments. Areas in which experimental data are lacking or contradictory include: (1) experimental evidence for the heterogeneous oxidation of NO_2 in aqueous droplets; (2) field studies to demonstrate or refute the existence of NO_x conversion to nitrates on solid surfaces; (3) field study verification of NO_x reaction rate observations in smog chambers; (4) large uncertainties in deposition velocity measurements; (5) the contribution of particulate nitrates to fine particle mass as it relates to visibility impairment; (6) the contribution of nitrates to precipitation acidity.

Friedlander of UCLA discussed the equilibrium formation of NH_4NO_3 aerosols at low relative humidity and considered the effect of SO_2 oxidation as a competing process for available NH_3. He developed a relationship among NH_3, NO_2, SO_2, and OH radical to calculate the potential NH_4NO_3 aerosol that could be formed. A simple field test of the relationship is not possible, because OH radicals are difficult to measure, certainly within the 1 h time resolution called for by Friedlander's analysis.

Smog chamber studies have been used traditionally to study the pathways of potentially important atmospheric reactions leading to smog (ozone) formation. For the past 5 years, SRI International researchers have been analyzing data from the SAPRC chamber to elucidate NO_x loss mechanisms. Dale Hendry presented recent SRI results on their data analysis. Based on smog chamber data the major fate of NO_x is to react as NO_2 with the hydroxyl radical to form gas phase HNO_3. Some HNO_3 is formed from the hydrolysis of nitrogen pentoxide. The data support evidence for other pathways involving peroxynitrates and organic nitrates; direct NO_x hydrolysis and oxidation reactions, Hendry concludes, lead to N(V) formation--except the HNO_3 oxidation, which forms nitrous oxide as the major product. The lack of rate data for these reactions prevents quantitative evaluation of their importance in the atmosphere at this time.

Jeffries of UNC (Chapel Hill) addressed the problems involved in modeling smog chamber data using various available models. The study demonstrated the variabilities and unknowns in the different choices of NO_x transformation chemistry in currently used mechanisms. It was also shown that lack of knowledge in nitrogen transformation chemistry results in quite different distributions of the various species according to the modeler's mechanism, which is frequently based on educated guesses. The models Jeffries tested, except for the Dodge mechanism, predicted more nitric acid than PAN, usually by a factor of two or more. One of the models predicted more aromatic nitrate than any other nitrogen product. Clearly, more information on the mechanisms and specific reaction rates are needed to sort out these differences.

One of the more important conclusions of Jeffries' studies is the importance of nitrogen loss to the chamber walls, probably by some heterogeneous processes. Neglecting a wall loss mechanism leads to over-prediction of ozone concentrations in the calculations. The importance of such surface reactions in the real atmosphere, however, is not known. If it is unimportant there, then smog chambers underestimate ozone formation potential in the atmosphere, and currently used models need to be adjusted. In multiday smog chamber studies, heterogeneous processes seem to exist for HNO_3 reconverting to NO_2 and outgassing from the chamber walls. Again, there are no real atmospheric data to assess the importance of such processes in the ambient air. One may conclude the Jeffries' paper with a feeling that more is unknown than known in the modeling of smog chamber data for NO_x transformations.

C.W. Spicer presented results of ongoing work at Battelle Columbus Laboratories. Their studies involve work on the measurement, distribution, fate, and reaction rate of NO_x/NO_3^-. Battelle scientists have investigated the question of NO_3^- artifact formation on commonly used filter materials. All glass fiber filters (AE, AA, MSA) collected large quantities of gaseous nitrate, resulting in positive errors for historical nitrate data. More recently developed filters such as Teflon or certain quartz fiber filters tend to minimize the conversion of gaseous to particulate nitrates. Spicer concludes from his urban field measurements that, except for areas dominated by local ammonia sources, most of the atmospheric nitrate is in the gas phase. Both smog chamber and field studies were used to investigate NO_x transformation and fate processes and rates. Although the studies were in progress at the time of the meeting, some preliminary observations include the following: (1) Maximum HNO_3 apppears to vary linearly with initial NO_x for initial HC concentrations from 1 to 9 ppm C, (2) addition of SO_2 to the chamber mix retards HNO_3 formation, (3) the final PAN/HNO_3 ratio appears to increase rapidly up to 2 for NMHC/NO_x ratios up to 20. Observations in urban atmospheres give an afternoon value of PAN/HNO_3 averaging 1 to 2.

Transformation rates for NO_x were reported for studies in the Boston urban plume. Using a light aircraft to assist in acquiring data in the plume, Spicer and co-workers calculated a pseudo-first-order rate constant of 0.15 h^{-1} for the NO_x removal rate in the plume.

Appel and co-workers reported on sampling problems connected with nitrate measurements. As with the Spicer article, this discussion presented results on the artifact formation potential of glass fiber filters. Appel et al. conclude that these filters can be used as total inorganic nitrate samplers to collect quantitatively inorganic particulate nitrate and nitric acid. They also investigated the effect of heating samplers, as in the method of Okita et al., and concluded the technique increased measurement error. Even without heating, greater than 50 percent losses of particulate nitrate can occur from Teflon prefilters. They recommend studies in developing simple techniques for determining "true" particulate inorganic nitrates (e.g., total NO_3^- less HNO_3).

Stedman and Kelly (University of Michigan) presented their results for nitric acid measurements made in clean air. Using a specially constructed high sensitivity NO detector based on chemiluminescence they measured NO_x/HNO_3 ratios at a rural site (Erie, Colorado), a mountain ridge 20 km west of Boulder, Colorado, and in Claremont, California, the last site representing an urban area. Some atmospheric models predict HNO_3 concentrations greater than NO_x in both polluted and clean air. Data from both Colorado sites show HNO_3/NO_2 ratios less than 1 (0.1 to 0.3). Preliminary analyses of the Claremont data indicate NO_2/HNO_3 ratios larger than 1, as might be expected in an area dominated by local NO_x sources. The deviations from model calculations led Stedman and Kelly to conclude that NO_x sources have been overestimated or NO_x/HNO_3 sinks underestimated.

Two presentations concerned with the wet removal of NO_x were given. Gary Stensland (Illinois State Water Survey) discussed nitrate measurements from the MAP3S network and from a site operated by ISWS near Champaign, Illinois, since 1977. An historical data set was available from the same Illinois site for 1953-54; a fourth data set, based on the Junge network in operation in 1955-56 was compared with those data available from the National Atmospheric Deposition Program network, which began operation in 1978. Data analysis of these precipitation networks led Stensland to the following conclusions: (1) The spatial distribution of nitrate concentrations in rainwater has not changed significantly since 1955-56; (2) the nitrate temporal trend showed increased values in the 1970's compared to 1950's, and the amount of increase varies, depending on site and year compared; (3) For the one year of data at Champaign, Illinois, the particulate nitrate levels had the same seasonal variation as the precipitation nitrate, i.e., higher levels in the winter months than the summer months; (4) Sampling of convective rain cells demonstrated that NO_3^- and $SO_4^=$ values were less variable in space that Ca^{++}, Mg^{++}, and rainfall. This implies that gaseous and particulate scavenging are more important for the two anions than the cations, where one might expect particulate scavenging to predominate.

Miller and Everett reported on their analysis of historical trends of nitrate deposition for the eastern United States. The main conclusion the authors reached is that there is insufficient knowledge to confirm either the trends or the magnitude of the threat posed by acidity or nitrates to ecosystems. They cite the following arguments in reaching this conclusion. There is great difficulty in separating the influences of natural and anthropogenic nitrate sources. Anthropogenic sources are more localized than the natural sources, so the problem is to separate local man-made pertubations superimposed on natural contributions, which are varying. Problems exist also in analysis of the historical nitrate and acid data from precipitation. These include variability in sample collection (not excluding dry deposition of nitrates, different materials for collectors, automatic vs. manual collection devices, and spatial variability) and uncertainities in the analytical technique used for pH and nitrate measurements. The authors conclude that analysis of data from long-term studies, such as the VSGS Network, the Hubbard Brook Experimental station monitoring program, and the MAP3S results, are inconclusive or contradictory with regard to a nitrate-acidity relationship in precipitation. This presentation generated more discussion than any other at the workshop. Unfortunately, none of the ecologists currently involved in acidic rain studies in the northeastern U.S. were present to join in the discussion.

A short informal presentation was given by Stephen Schwartz of Brookhaven National Laboratory. The BNL group has been investigating aqueous phase NO_x processes and their importance in atmospheric rainout and washout phenomena.

After the formal and informal presentations, there was a discussion session moderated by William Wilson of the U.S. EPA. Word by word transcription was taken by a recorder, and salient comments were summarized under six broad categories--natural vs. anthropogenic sources, wet deposition measurements, dry deposition measurements, smog chamber studies, laboratory studies,and general observations. The most important and recurring observation throughout the discussion session was the lack of reliable measurement techniques for gas phase and particulate phase nitrates. Because of this problem, trend analysis of historical ambient nitrate data is difficult, and analysis of wet deposition values for nitrates and acidity over the past 20 years is equally difficult. Interpretation of smog chamber data has been deterred by wall deposition and outgassing of HNO_3 gas, expecially in multiday irradiation studies.

THE ISSUE OF NITRATES IN THE ATMOSPHERE

Basil Dimitriades

Environmental Sciences Research Laboratory
U. S. Environmental Protection Agency
Research Triangle Park, North Carolina 27711

INTRODUCTION

The Clean Air Act Amendments of 1977, sections 103, 108, 109, and 110, require that EPA: (a) study possible health and welfare problems arising from various air pollutants and (b) promulgate control policies when pollutants are found to have significant adverse effects. For any suspect pollutant, EPA first conducts an assessment study, and then decides whether the pollutant should be placed on the list of criteria pollutants (those pollutants for which maximum allowable atmospheric concentrations have been established). Following this determination, EPA must, in the following order, prepare a criteria document presenting its case against the pollutant, develop an ambient air quality standard for the new criteria-pollutant, and prepare and recommend emission control guidelines. In addition, EPA must also prepare and recommend guidelines for preparation of State Implementation Plans, that is, guidelines for development of pollutant control strategies. Thus, EPA must gather, develop, and analyze evidence pertaining to the formation, transport, and fate of the pollutant; and ultimately develop quantitative relations (a) between precursor emission rates and ambient concentrations, and (b) between source area and receptor areas.

At this time, EPA is in the process of assessing nitrates as an environmental problem. Within the scope of this activity, the Environmental Sciences Research Laboratory (ESRL) responsibility is (a) for characterizing nitrate pollution in ambient air, and (b) for developing the scientific bases for optimum nitrate control strategies. In the past several years, ESRL has been studying the nitrate question directly, and also indirectly while studying the photochemical oxidant pollution problem. In the course of these studies, substantial new information has been generated that answered some questions, e.g., (a) in the gaseous nitrate formation mechanism, thus correcting some fallacies, and (b) on the ambient concentrations of particulate nitrates. The same studies also raised new questions, some of which are controversial. The objectives of this discussion are:

- analyze the overall question of nitrates as an air pollution problem

- present the ESRL understanding and appreciation of the current relevant issues in terms of unanswered questions or questions with conflicting answers, and

- instigate a response--in terms of (a) alternative viewpoints regarding current issues and (b) recommendations for specific research projects addressed to such issues.

CONCLUSIONS

1. The nitrate species of concern are: nitric acid, mainly because of its effect on materials and some ecosystems; PAN because of its effect on vegetation; ammonium nitrate because it may contribute significantly to visibility reduction in the future; and nitrates because of the total, indirect effects on human health, and because of the nitrates role in the photochemidal ozone/oxidant problem.

2. It is unequivocally established that nitrates result in part and perhaps in toto from gas phase photooxidation of NO_x. There is some theoretical evidence that nitric acid can result from heterogeneous oxidation of NO_2 in aqueous solution droplets; conclusive experimental verification, however, is lacking. Likewise, laboratory observations of heterogeneous conversion of NO_x into nitrates on surface of solid materials have not been verified in real atmospheric systems.

3. The stoichiometry and rate of NO_x reaction have been determined in the smog chamber but not in the real atmosphere; this raises the need for field studies analogous to studies completed in the laboratory.

4. Measurements of deposition velocities have not been adequately validated, resulting in large uncertainties in the data available.

RECOMMENDATIONS

1. Field monitoring should be conducted to determine the contribution of particulate nitrate to fine particle mass that impairs visibility. Measurement methods that minimize positive or negative artifacts should be used.

2. Studies should be conducted to investigate the roles of NH_3 and H_2SO_4 in atmospheric formation of particulate nitrate. Studies should include (a) field investigation of causes of nitrate formation in areas with exceptionally high particulate nitrate levels, and (b) smog chamber testing of $HC/NO_x/NH_3/H_2SO_4$ to investigate the competition of H_2SO_4 and HNO_3 for NH_3 and the impact of sulfate control upon NH_4NO_3 formation.

3. Field studies should be conducted to determine adequacy of gas phase chemistry alone in accounting for observed ambient nitrate levels.

4. Experimental studies should be conducted to evaluate the theoretical evidence on nitrate formation from NO_2 in aqueous solution droplets.

5. Existing and (if needed) new data should be analyzed for applicability to the real atmosphere of laboratory evidence on NO_x oxidation on surface or solid materials.

6. Field studies should be conducted to determine the rate of loss and fate of NO_x in ambient air.

7. Existing methods for velocity deposition and washout ratio nmeasurements should be intercompared and validated.

THE ISSUES

The first, broad questions submitted here as constituting the nitrate issue are:

- What are the problems associated with ambient nitrates?
- Based on scientific grounds alone, what is the optimum strategy for nitrate control?

Nitrate-related problems have been examined by the National Academy of Sciences (National Research Council 1977) and by EPA (U. S. Environmental Protection Agency 1979). These judgments and our own current assessments are described.

Connection of Nitrates to Air Pollution Problems

Not much is known about and probably little direct toxicity is associated with nitrates at ordinary ambient concentrations. Indirectly, however, nitrates pose health hazards through conversion into nitrites, and subsequent reactions to oxidize blood iron and to form toxic nitrosamines (National Research Council 1978; U. S. Environmental Protection Agency 1979). Ambient air nitrates are not important in these reactions, since only ~5 percent of the total nitrate ingested by man comes from ambient air. Therefore, the health effects case made against total ambient nitrates is relatively weak. Individual nitrates, e.g., PAN or HNO_3, may pose health hazards but, again, it is not known whether current concentrations of these species constitute a health problem.

With respect to welfare effects, nitrates are known to cause damage to materials and to some ecosystems, directly and in the form of acid precipitation (National Research Council 1978; U. S. Environmental Protection Agency 1979). Furthermore, particulate nitrates could contribute somewhat to visibility reduction. These environmental effects, however, are not unquestionably established. The specific questions of interest here, some at issue and some not, are:

- Are nitrates contributing significantly to ambient air and precipitation acidity?

- Has precipitation acidity been increasing with increasing and changing human activities?

- Is particulate nitrate contributing significantly to visibility reduction?

In response to the ambient and precipitation acidity question, there is ample evidence to show that the predominant acidic air pollutants are H_2SO_4 (free or as acid salts) and HNO_3, and that the HNO_3 contribution is significant, according to Spicer (1979) and a recent, unpublished, EPA review (Shaw, R. W., personal communication 1979). In urban areas, HNO_3 is found to be the dominant acidic species with concentrations that can be much higher than 10 ppb. Away from urban areas, e.g., in the Smoky Mountains, the dominant acidic species appears to be acid ammonium sulfate.

The question regarding time trends of precipitation acidity is controversial and has been discussed (U. S. Environmental Protection Agency 1979). Likens (1976) has computed annual precipitation pH averages from cation/anion balances for years 1955-56 and 1972-73, for the northeast U. S. Examination of the Likens isopleths and those by the National Research Council (NRC) for 1965-66 shows a reduction in pH in the 1 to 2 decades preceding 1972. However, the NRC isopleths, unlike those of Likens, were derived from actual pH measurements; therefore, the pH differences may be the result of the different methods used to obtain the pH data. Likens' 10-year data for Hubbard Brook, New Hampshire, did not show a statistically significant trend. Finally, the 8-year data for several sites in the State of New York show considerable pH variation both within a year (±1.5) and from year-to-year (±1.0), but no systematic changes are indicated during the 1965-1973 period. Other data sets for individual sites either do not show trends or do not permit reliable quantification of the decreasing pH trends shown. A reasonable conclusion to be derived from this evidence is that the pH changed very little, if any, during the past 1 or 2 decades. Since the pH, however, is clearly below the natural minimum value of 5.6, it follows that precipitation acidity has increased, although not necessarily as a result of human activities alone in the last 20 years. To establish, therefore, any connection between precipitation acidity and emission, one should include pre-1950 data in the analysis. Alternatively, it is unlikely that a clear emissions-to-acidity correlation can be supported by the data available for the last two decades. Regarding this correlation, Rosenqvist (1978), interestingly, reported that acidification of river waters in Norway results mainly from humus acidity, and that such acidity has been changing because of changes in timber production practices and animal raising.

The final question regarding the connection of nitrates to air pollution concerns contribution of particulate nitrates to visibility reduction. Evidence in support of substantial contribution can be derived from past measurements of particulate nitrate and the Trijonis study results on visibility in the Southwest (Trijonis and Yuan 1978a). Early particulate nitrate measurements from the National Air Surveillance Network (NASN) showed occurrence at substantial ambient levels, in tens of micrograms per cubic meter. More recent data (Shaw, R. W., personal communication 1979), however, relatively free from positive artifact errors, show 24 h average particulate nitrate levels not exceeding, as a rule, 1 to 2 μg/m^3 in the fine particle size range (<2.5 μm), and comparable levels in the coarse particle range (2.5 to 15 μm), with rare excursions to higher levels. However, these data, in turn, may be erroneously low as a result of negative artifact sampling problems. At this time, the limited--and somewhat questionable--data available indicate that nitrate levels rarely exceed 5 percent of total fine--that is, optically active--particle mass for urban areas (e.g., in New York, Philadelphia, St. Louis, S. Charleston, Glendora; coarse particle concentrations may be exceeding that 5 percent in, e.g., parts of the Los Angeles basin). Such generally low nitrate levels are in rough agreement with Trijonis' results from his Northeast visibility study (Trijonis and Yuan 1978b), which show that only 0 to 8 percent of the visibility variation in Northeast cities can be accounted for by the nitrate fraction of the total suspended particulate.

Unlike his Northeast study, Trijonis' (Trijonis and Yuan 1978a) study of the Southwest showed the nitrate fraction to account for about 30 percent of total light extinction in southwest urban areas (Phoenix, Salt Lake City). Again, as Trijonis points out, the "nitrate" contribution does not represent nitrate alone; it represents other species such as HNO_3 or NO_2, or any species for which nitrate, as measured, can serve as a surrogate. Unfortunately, there are no reliable dichotomous sampler data available for southwest areas from which to compute the nitrate fraction in the fine particle mass. Likewise, there are no data or Trijonis-type visibility studies on the nitrate contribution to haze in southwest rural/remote areas.

In conclusion, the visibility-related evidence available (a) is incomplete, and (b) does not seem to support an important role for particulate nitrate in the visibility problem. If this issue is to be settled finally, additional evidence must be obtained. The specific need is additional valid measurements of total fine particle and nitrate masses in areas of visibility-related interest. To obtain valid data, the ongoing research on positive/negative nitrate artifact in ambient sampling should be completed and results used to achieve improved measurements. At this time, the ESRL viewpoint is that the only unanswered artifact-related question concerns the magnitude of negative artifact resulting from volatilization or acid-displacement of ammonium nitrate.

While particulate nitrate may not contribute significantly to haze at present, the possibility of a significant contribution in the future, nevertheless, does exist and merits some attention. This possibility is evidenced by the truly high levels of particulate nitrate (i.e., 18 μg/m^3 or higher) found on a few occasions (e.g., in Denver and Los Angeles) and by HNO_3 concentrations that are sufficiently high to form problem levels of NH_4NO_3. The determining factors in the latter case would be the NH_3 and H_2SO_4 concentrations. To explore the possibility of a significant contribution to haze in the future, the following studies are contemplated by ESRL:

- Investigation of the NH_3 and H_2SO_4 roles in geographical areas with exceptionally high particulate nitrate levels (Denver, Los Angeles, etc.)

- Smog chamber experiments with $HC/NO_x/SO_2/NH_3$ systems to investigate the competition of H_2SO_4 and HNO_3 for NH_3, and to explore the impact of H_2SO_4 control upon NH_4NO_3 formation.

Aside from their connection to the problems discussed above, nitrates have a role, directly and indirectly, in the photochemical O_3/oxidant problem. Some specific effects are: (a) nitrates can serve as sources of NO_x, an oxidant precursor, in areas where other sources may not exist, (b) nitrate formation constitutes a "sink" for NO_x and for radicals important to the oxidant formation process, and (c) nitrate-related emission controls are almost certain to impact the O_3/oxidant-related air quality.

To summarize the discussion and conclusions on the connection between nitrates and currently recognized air pollution problems, the nitrate species of concern are: nitric acid, mainly because of its effect on materials and some ecosystems; PAN because of its effect on vegetation; NH_4NO_3 because of the possibility that it might contribute significantly to visibility reduction in the future; total nitrates because of their indirect effects on human health and because of their role in the photochemical O_3/oxidant problem.

Control of Nitrates

Another major nitrate issue is the formation, transport, and fate, and, in general, the control of nitrates. The underlying need is for a predictive model capable of treating the processes of interest, namely, the dispersion of NO_x emissions, the atmospheric conversion of NO_x into secondary products, the transport of reacted and unreacted NO_x, and the sink processes for NO_x and secondary products. Of interest also is the distinction between tall stacks and ground level sources of NO_x.

With respect to the dispersion and transport processes, there are no modeling problems that are unique to NO_x. There is ample evidence now that long range transport of pollution occurs; the range of transport of specific NO_x and NO_x-derived products depends on NO_x chemistry and the sink process. The main questions unique to NO_x and nitrates concern the atmospheric chemistry and sink processes for these compounds, namely:

- Is heterogeneous oxidation of NO_x a significant pathway to nitrate formation relative to the gas phase oxidation pathway?

- What is the detailed mechanism of the nitrate formation process?

- What is the magnitude of the sink processes affecting ambient nitrate buildup?

Heterogeneous Oxidation of Nitrogen Oxides to Nitrates--

Whereas the homogeneous gas phase oxidation of NO_x into nitrates of interest (i.e., HNO_3, $RONO_2$, PAN) has been well documented, evidence on the heterogeneous oxidation pathways is sketchy, indirect, and somewhat conflicting. "Heterogeneous oxidation" is stressed here to avoid confusion with other heterogeneous HNO_3 formation processes that do not involve oxidation, e.g., $N_2O_5 + H_2 \overset{surface}{} 2HONO_2$. Indications that the heterogeneous NO_x oxidation process is important were first based on the generally high levels of particulate nitrate measured in the NASN network. These indications, however, are no longer valid, because the NASN measurements are now known to be erroneously high; the belief now--and until the nitrate sampling methods are perfected--is that only on rare occasions (as, e.g., in Denver and in parts of the Los Angeles basin) does particulate nitrate exceed 1 to 2 $\mu g/m^3$.

Orel and Seinfeld (1977) offered a theoretical derivation of the extent to which NO_2 in water solution droplets can be converted into nitrate (and NO). Their calculations showed that, without help from catalytic processes, liquid phase reactions could produce several micrograms per cubic meter of nitrate from ordinary ambient concentrations of NO_x. This same evidence also predicts that such nitrate formation is favored by NH_3 and inhibited by SO_2/H_2SO_4. Because this Orel/Seinfeld analysis now constitutes a major part of the theoretical evidence that is related to these processes, and because the value of their analysis depends on the degree to which it agrees with real-atmosphere data, such agreement is examined here in some detail.

Comparison of observed and predicted particulate nitrate levels does not give significant credence to the Orel/Seinfeld (1977) liquid-phase oxidation pathway, since their theoretical analysis vastly overpredicts (by one to two orders of magnitude) ambient concentrations, and since there is another, possible pathway, $HNO_3(g) + HN_3(g) \rightarrow NH_4SO_4(s)$, that can account for the observed concentrations. Another way of checking the Orel/Seinfeld theory is by comparing predicted and observed effects of H_2SO_4 and NH_3 on particulate nitrate formation. Observations on the effect of NH_3 do not exist (to the knowledge of this author), but observations on the H_2SO_4 effect do exist and consist of both ambient air data and smog chamber data. Ambient air data obtained during the ACHEX study in Los Angeles in 1973 showed patterns depicting an inverse relationship between the nitrate and sulfate components in the aerosol samples (Harker et al. 1977): Early morning samples contained high nitrate and low sulfate levels; the reverse was true in the afternoon. Such patterns can mean, of course, that H_2SO_4 inhibits particulate nitrate formation. A similar effect was suggested by smog chamber data obtained by Harker et al. (1977) in 1975, showing that inclusion of SO_2/H_2SO_4 in irradiated $HC/NO_x/NH_3$ mixtures inhibits particulate NH_4NO_3 formation. Thus, at first glance, this experimental evidence does not appear to corroborate the Orel/Seinfeld analysis--at least, qualitatively. Careful examination of this evidence, however, casts considerable doubt, as explained next.

The ACHEX data patterns can be explained by mechanisms other than the one offered by Orel and Seinfeld (1977). For example, the high nitrate/low sulfate pattern observed in the morning can be interpreted as reflecting HNO_3--rather than particulate nitrate--formed in the gas phase and retained in the particulate sampling filter (fiberglass), either directly or after conversion into NH_4NO_3. In the Los Angeles atmosphere, HNO_3 forms much faster than H_2SO_4, because the NO_2 + OH reaction rate and NO_2 concentration are much higher than the SO_2 + OH rate and SO_2 concentration; HNO_3, therefore, is expected to peak earlier in the day, before H_2SO_4. Later on in the day H_2SO_4 forms to substantial concentrations and displaces HNO_3 from NH_4NO_3 (in the air) or from the filter, resulting in a high sulfate/low nitrate pattern.

The smog chamber evidence of Harker et al. (1977) was obtained in irradiations of $HC/NO_x/SO_2$ $/NH_3$ mixtures in an outdoor smog chamber. Inclusion of SO_2 in the irradiated mixtures resulted in particulates with a reduced nitrate component. Again, however, the evidence does not necessarily support a liquid phase pathway to nitrate formation. In fact, the data could reflect gas phase formation of HNO_3 followed by reaction with NH_3 to form particulate NH_4NO_3. The SO_2/H_2SO_4 effect could be explained either in terms of NH_3 reacting preferentially with H_2SO_4 or in terms of H_2SO_4 displacing HNO_3 from NH_4NO_3. Unfortunately, the investigators did not conduct experiments with varying levels of NH_3 to further clarify this process; e.g., with an excess NH_3, H_2SO_4 should not exert its displacement effect, and a positive or no effect of NH_3 on particulate nitrate yield would then support or refute the Orel/Seinfeld (1977) liquid phase pathway.

In conclusion, liquid phase oxidation of NO_x, although qualitatively not inconsistent with the real atmosphere and laboratory data now available, may or may not constitute a significant pathway to nitrate formation; reliable experimental verification is lacking at present. ESRL is contemplating smog chamber studies of $HC/NO_x/SO_2/NH_3$ systems that should provide additional evidence on this question.

Another heterogeneous process oxidizing NO_x to particulate nitrate (and nitrite) was suggested by Judeikis and his coworkers (1974), based on their laboratory studies of NO_2 reactions on surfaces of solid materials known to exist in ambient aerosols. These studies provided laboratory evidence suggesting that: (1) ambient NO_2 deposits on the surface of ambient particles in the form of NO_x^-, and (2) that the rate of this process is such that NO_2 can be almost completely removed from the gas phase in 0.5 to 5 h (depending on the amount of particulate material and moisture). If this laboratory evidence is indeed valid for the real atmosphere, then this heterogeneous process constitutes a significant pathway to particulate NO_x^- formation, since the associated NO_2 conversion rate is comparable to that observed in smog-chamber-irradiated urban HC/NO_x mixtures. The main questions regarding this evidence are whether and to what degree the laboratory findings are applicable to the real atmosphere. For example, are the solid materials studied by Judeikis et al. present in significant amounts in ambient fine particles? Presuming those materials to be present in the coarse particles, are ambient concentrations of coarse particle nitrates and nitrites consistent with Judeikis et al. predictions? No research studies are planned at this time by ESRL that specifically address the validation of the pathway proposed by Judeikis et al.

One promising approach to examining the relative importance of the gas-phase and heterogeneous pathways to nitrate formation is based on comparison of observed ambient nitrate concentrations to concentrations predicted by theory assuming gas-phase chemistry alone. Assuming, in specific, that $OH + NO_2 \rightarrow HONO_2$ is the main gas-phase reaction to HNO_3 formation and that dry deposition losses are relatively slow, one could estimate (and then compare observed and predicted) nitrate formation from measurements of ambient HNO_3, fine particle nitrate, OH, and NO_2. ESRL is currently planning to use this approach in testing the adequacy of gas-phase chemistry alone in ambient sulfate formation; perhaps these planned studies should be expanded to include measurement of the nitrate-related species.

In conclusion, the evidence regarding the various pathways to ambient nitrate formation is not sufficient at this time. Additional studies are needed to better assess the importance of each pathway for daytime, nighttime, summer, winter, tall stack plumes, and urban plumes.

Mechanism of Nitrate Formation--

Another question of interest in development of nitrate models is the detailed mechanism of nitrate formation. One important mechanistic question, for example, is raised by the stoichiometric studies on NO_x. Results from early smog chamber studies indicated poor accounting of the NO_x reactant in terms of nitrogen products. Later work by Gay and Bufalini (1971) and Spicer and Miller (1976) more fully considered the HNO_3 and wall-adsorbed nitrates, and resulted in a considerably improved nitrogen mass balance. It is now generally accepted that NO_x is accounted for nearly completely in smog chamber irradiated HC/NO_x systems. This smog chamber information, however, is not necessarily valid for the real atmosphere. The uncertainty here arises from the general belief that, unless proved to be so, the smog chamber atmosphere is not necessarily a duplication of the real atmosphere in every respect. One significant difference, for example, pertains to the relative importance of the following HNO_3 formation processes:

$$NO_2 + OH \xrightarrow{M} HONO_2 \text{ (photochemical process)}$$

$$N_2O_5 + H_2O \xrightarrow{\text{surface}} 2HONO_2$$

Because of the higher suface-to-volume ratio conditions in smog chambers, one should expect the surface-induced process to be strongly favored in chambers. Real atmosphere studies are, therefore, needed in order to properly assess the importance of these two processes, and more generally, to determine the rate of NO_x conversion into HNO_3 and other products. Such studies should include: 1) measurements as needed to determine the fate and total rate of loss of NO_x, and 2) monitoring-type measurements in daytime and nighttime and during the different seasons, to assess the relative strengths of the photochemical and dark processes. ESRL has a study program under way addressed to these needs.

Sink Processes--

One final subject of interest is the magnitude of the sink processes for the reactant and product--gaseous and particulate--species related to nitrate pollution. One non-pollutant-specific issue is whether the existing methods (Hicks and Wesely 1978) for (dry/wet) deposition rate measurement have been or should be evaluated for accuracy, both absolutely and in relation to each other. If evidence on accuracy is not available, field studies to evaluate and intercompare deposition velocity and washout ratio measurent methods would appear strongly needed. A second question relates to the terrain, meteorological, etc., factors that affect the depostion rate of a given pollutant on a given surface. For example, are separate deposition velocity measurements necessary for areas that differ only in terrain? Also, in view of the multiplicity and strong effects of factors affecting such measurements (Wesely and Hicks 1977; McMahon 1979): How meaningful is comparison of data from different studies? Or, what is the confidence interval one can place around deposition velocity measurements made in a given locality under a given set of relevant conditions?

REFERENCES

Gay, W. B., and J. J. Bufalini. 1971. Nitric Acid and the Nitrogen Balance of Irradiated Hydrocarbons in the Presence of Oxides of Nitrogen. Environ. Sci. Technol., 5:422.

Harker, A. B., L. W. Richards, and W. E. Clark. 1977. The Effect of Atmospheric SO_2 Photochemistry upon Observed Nitrate Concentrations in Aerosols. Atmos. Environ., 11:87-91.

Hicks, B. B., and M. L. Wesely. 1978. An Examination of Some Micrometeorological Methods for Measuring Dry Deposition. EPA-600/7-78-116. U. S. Environmental Protection Agency, Research Triangle Park, North Carolina 27711.

Likens, G. E. 1976. Acid precipitation. Chem. Eng. News, 54(48):29-44.

Judeikis, H. S., S. Siegel, T. Stewart, and H. Hogpath. 1974. The Role of Gas-Solid Interactions in Air Pollution. Grant report submitted by the Aerospace Corporation (El Segundo, California) to EPA-ESRL-RTP. Grant No. R801340, EPA Project Officer: J. Durham.

McMahon, T. A. 1979. Empirical Atmospheric Deposition Parameters--A Survey. Atmos. Environ., 13:571-585.

National Research Council. 1977. Nitrates: An Environmental Assessment. National Academy of Sciences, Washington, D.C.

Orel, A. E., and J. H. Seinfeld. 1977. Nitrate Formation in Atmospheric Aerosols. Environ. Sci. Technol., 11:1000-1007.

Rosenqvist, I. Th. 1978. Alternative Sources for Acidification of River Water in Norway. Sci. Total Environ., 10:39-49.

Spicer, C. W. 1979. The Distribution, Fate and Reaction Rate of NO_x in the Atmosphere. Presented at an EPA-sponsored technical symposium, "Implications of a Low NO_x Vehicle Emissions Standard," Reston, Virginia, May 2-4, 1979.

Spicer, C. W., and D. F. Miller. 1976. Nitrogen Balance in Smog Chamber Studies. JAPCA, 26:45.

Trijonis, J., and K. Yuan. 1978a. Visibility in the Southwest. An Exploration of the Historical Data Base. EPA-600/3-78-039, U. S. Environmental Protection Agency, Research Triangle Park, North Carolina 27711.

Trijonis, J., and K. Yuan. 1978b. Visibility in the Northeast. EPA-600/3-78-075, U. S. Environmental Protection Agency, Research Triangle Park, North Carolina 27711.

U. S. Environmental Protection Agency. 1979. Air Quality Criteria for Oxides of Nitrogen (draft). U. S. Environmental Protection Agency, Office of Research and Development, Environmental Criteria and Assessment Office, Research Triangle Park, North Carolina 27711.

Wesley, M. L., and B. B. Hicks. 1977. Some Factors that Affect the Deposition Rates of Sulfur Dioxide and Similar Gases on Vegetation. JAPCA, 27:1110.

THERMODYNAMICS AND KINETICS OF AEROSOLS CONTAINING AMMONIUM NITRATE:
Preliminary Investigations

Sheldon K. Friedlander

School of Engineering and Applied Sciences
University of California
Los Angeles, California 90024

INTRODUCTION

This paper is concerned with the formation of ammonium nitrate (NH_4NO_3)-containing aerosols at relative humidities (RH's) less than ~60 percent. Under these conditions, NH_4NO_3 tends to remain in the solid phase; at higher RH's, a droplet phase tends to form (Dingemans 1941).

The cut-off in RH's that divides solid from droplet phases may not be sharp, because the presence of other salts may lead to a continuum of states over which the droplets may exist. However, in the Southwest, the RH's are frequently low enough for a low humidity analysis to be of interest.

In the first part of the paper, the thermodynamics of the NH_4NO_3 equilibrium are reviewed with its implications for atmospheric sampling. In the second part, the kinetics of NH_4NO_3 formation are discussed for the isothermal case when the equilibrium relationship holds. Applications to field data are also considered.

Effects on particle size distribution are under investigation and are not reported in this paper.

SUMMARY AND RECOMMENDATIONS

1. An extensive air monitoring program should be initiated to test the equilibrium hypothesis

$$K_c(T) = [NH_3]\ [HNO_3]$$

because of its usefulness in interpreting atmospheric field data. Measurements should be carried out using methods capable of short time resolution such as the long path, Fourier transform infrared (FTIR) technique.

2. More use should be made of impactor measurements with greased stages to determine aerosol nitrate concentrations. Sampling should be carried out

over short time periods to minimize evaporative losses. The accumulation of a deposit over a small surface element should reduce both positive and negative artifacts.

3. In air containing nitrogen dioxide (NO_2), ammonia (NH_3), and the hydroxyl radical (OH), the presence of sulfur dioxide (SO_2) tends to suppress NH_4NO_3 formation; when the equilibrium relation holds, the effect can be predicted quantitatively. A test of the prediction should be carried out in a field study.

THERMODYNAMIC CONSIDERATIONS

The vapor pressure (p) of $NH_4NO_3(s)$ has been measured by Brandner et al. (1962) by passing dry air or nitrogen over the solid at various temperatures in the range of 76 to 170°C. The authors explained their results by assuming that NH_4NO_3 dissociated on vaporizing:

$$NH_4NO_3(s) \rightarrow NH_3(g) + HNO_3(g) \tag{1}$$

The heat of vaporization calculated from the vaporization curve of the solid was 42.7 kcals/g mole. The heat of dissociation of $NH_4NO_3(s)$, calculated from the published heats of formation of the compounds appearing in Equation 1, is 42.1 kcals/g mole (Brandner et al. 1962). The agreement between these two values lends support to the assumption of complete dissociation, that is,

$$p_{NH_4NO_3} << p_{NH_3} \text{ or } p_{HNO_3}$$

This result is not conclusive because of inaccuracies resulting from the logarithmic dependence of the vapor pressure of the heat of dissociation.

The vaporization reaction of Equation 1 leads to equimolal concentrations of NH_3 and nitric acid (HNO_3) in the gas. The results of vapor pressure measurements can easily be generalized to the case when the molal concentrations of NH_3 and HNO_3 in the gas are unequal. Let μ_i be the chemical potential of species i. For Equation 1, the condition of chemical reaction equilibrium is:

$$\mu_{NH_4NO_3} = \mu_{NH_3} + \mu_{HNO_3} \tag{2}$$

The condition of phase equilibrium is

$$\mu_{NH_4NO_3}(g) = \mu_{NH_4NO_3}(s) \tag{3}$$

The gas phase can be assumed to be a perfect gas mixture, and we can write

$$\mu_{NH_4NO_3(g)} = \mu^{\circ}_{NH_4NO_3(g)} + RT \ln p_{NH_4NO_3}$$

where μ° = the chemical potential in the standard state

T = temperature in Kelvin units

Similar expressions can be written for the chemical potential (μ) of NH_3 and of HNO_3. Substituting these chemical potential expressions into Equation 2 gives

$$-RT \ln (p_{NH_3}\ p_{HNO_3})/p_{NH_4NO_3} = \mu^\circ_{NH_3} + \mu^\circ_{HNO_3} - \mu^\circ_{NH_4NO_3(g)} \quad (4)$$

Since

$$\Delta G^\circ = -RT \ln K_p \quad (5)$$

the equilibrium constant, K_p, is given by

$$K_p = p_{NH_3}\ p_{HNO_3}/p_{NH_4NO_3} \quad (6)$$

The value of the denominator, the vapor pressure of NH_4NO_3, is not known, but it is probably very small considering the experimental measurements discussed above. Moreover, the NH_4NO_3 vapor pressure is practically constant at any given temperature, because it represents the saturation vapor pressure over $NH_4NO_3(s)$. Thus, the vapor pressure of NH_4NO_3 can be combined with K_p to give:

$$K'_p = P_{NH_4NO_3}\ K_p = P_{NH_3} P_{HNO_3}$$

If the gas mixture results from the evaporation of $NH_4NO_3(s)$, the vapor pressures of NH_3 and HNO_3 are equal, and K_p can be determined by measuring the total pressure over the solid. Based on the data of Brandner et al. (1962) the equilibrium constant is given by

$$\ln K_c = 62.296 - 21510/T \quad (7)$$

where

$$K_c = [HNO_3]\ [NH_3] \quad (8)$$

with the concentration expressed in parts per million, and temperature T in Kelvin units.

Stelson et al. (1979) pointed out that if NH_4NO_3 is present in the aerosol as a separate solid phase, the product of the gas-phase concentrations of NH_3 and HNO_3 in ambient air should tend toward the equilibrium constant given by Equation 7. As shown in Figure 1 (Stelson et al. 1979), atmospheric data for West Covina, California, are in fair agreement with the equilibrium hypothesis. More recently, Doyle et al. (1979) compared the equilibrium theory with measurements in Riverside, California, that were made with an FTIR spectrometer.

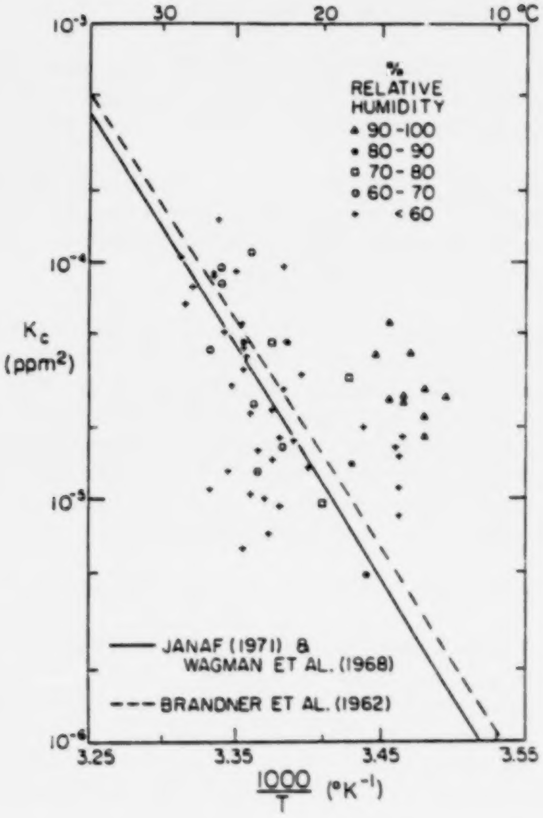

Figure 1. The product $[NH_3][HNO_3]$ calculated from the data of Spicer (1974) for West Covina, California, compared with equilibrium theory. The dashed line represents Equation 7, and the solid line is based on data from the JANAF (1971) Tables.

They concluded that the data supported the equilibrium hypothesis but noted that atmospheric measurements under more carefully controlled conditions would be needed for a complete confirmation.

These results show that great care must be taken in sampling for particulate NH_4NO_3 or for gas-phase NH_3 or HNO_3. Aerosol samples should be collected only when the air is saturated, with respect to NH_4NO_3. For this reason, simultaneous measurement of gas and aerosol phases would be desirable. It would be better not to filter the air before the gas-phase concentrations are measured, because aerosol deposited in the filter tends to evaporate if an unsaturated air parcel enters the system later.

Another alternative would be to sample the aerosol for relatively short durations, perhaps 30 min or less. Shorter time spans would be less likely to allow large changes in concentrations of the air parcel being sampled.

Sampling for NH_4NO_3 by filtration over long periods of time--days or weeks--will probably result in measured values that are lower than actual concentrations. This would be true, assuming no positive artifacts result from HNO_3 adsorption or reaction with the filter.

The cascade impactor provides a useful alternative to the filter for sampling aerosols containing NH_4NO_3. The use of the cascade impactor reduces positive artifacts, since the sample deposits over a very small area of limited adsorptive capacity. Loss of collected sample may still occur if the sampling period is very long and a clean air parcel passes through the impactor. However, the formation of a deposit "heap" may reduce evaporative losses, even at reduced pressures (low pressure impactor). Carefully testing the impactor for NH_4NO_3-containing aerosols would be desirable.

KINETICS OF NH_4NO_3 FORMATION: EFFECTS OF SO_2 OXIDATION

In plumes and polluted atmospheres, chemical reactions may result in the formation of HNO_3, H_2SO_4, and organic acids. If NH_3 is present, neutralization reactions occur and form condensable molecules such as NH_4NO_3, ammonium bisulfate (NH_4HSO_4), ammonium sulfate ($(NH_4)_2SO_4$), and ammonium formate ($HCOONH_4$). In the following discussion, only HNO_3 and H_2SO_4 are considered; however, a generalization of results to include organic acids should not be difficult.

The reaction of H_2SO_4 with NH_3 can be considered irreversible, because the vapor pressures of NH_3 and H_2SO_4 over their salts can be neglected. As H_2SO_4 is formed, it competes with HNO_3 for the available NH_3.

When the equilibrium relation, Equation 8, holds for the gas and aerosol phases, a considerable simplification is possible in analyzing the aerosol dynamics. Differentiating Equation 8 with respect to time, assuming the temperature is constant, gives:

$$[NH_3]d[HNO_3]/dt + [HNO_3]d[NH_3]/dt = 0 \tag{9}$$

The derivatives with respect to time represent changes in an elemental gas volume due to chemical processes.

The change in the concentration of NH_3, $d[NH_3]/dt$, results from conversion to the aerosol phase by reaction with HNO_3 and H_2SO_4:

$$d[NH_3]/dt = d([NH_3]/dt)_{NH_4NO_3} + (d[NH_3]/dt)_{(NH_4)_2SO_4} \tag{10}$$

The subscripts indicate the reaction products. The change in HNO_3 concentration, $d[HNO_3]/dt$, can be written as the sum of two terms:

$$d[HNO_3]/dt = (d[HNO_3]/dt)_f + (d[HNO_3]/dt)_{NH_4NO_3} \tag{11}$$

The first term on the right hand side represents the formation rate of $HNO_3(g)$; the second term is the loss rate of $HNO_3(g)$ to the aerosol phase by formation of $NH_4NO_3(s)$.

Stoichiometry requires that the rate of formation of $NH_4NO_3(s)$ be given by

$$d[NH_4NO_3]/dt = -(d[HNO_3]/dt)_{NH_4NO_3} = -(d[NH_3]/dt)_{NH_4NO_3} \tag{12}$$

Substituting the terms of Equations 10 and 11 in Equation 9, then rearranging, with Equation 12 gives:

$$\begin{aligned} d[NH_4NO_3]/dt = {} & \{[NH_3]/([NH_3] + [HNO_3])\}\{d[HNO_3]/dt\}_f \\ & + \{[HNO_3]/([NH_3] + [HNO_3])\}\ \{d[NH_3]/dt\}_{(NH_4)_2SO_4} \end{aligned} \tag{13}$$

Introducing the equilibrium constant gives:

$$\begin{aligned} d[NH_4NO_3]/dt = {} & \{[NH_3]^2/([NH_3]^2 + K_c)\}\{d[HNO_3]dt\}_f \\ & + \{K_c/([NH_3]^2 + K_c]))\}\ \{d[NH_3]/dt\}_{(NH_4)_2SO_4} \end{aligned} \tag{14}$$

The second term on the right hand side is negative, because

$$\{d[NH_3]/dt\}_{(NH_4)_2SO_4}$$

is the rate at which NH_3 is converted to $(NH_4)_2SO_4$. The first term on the right is always positive or zero.

Thus, the rate of formation of $NH_4NO_3(s)$ may be positive, negative, or zero, depending on the relative rates of formation of H_2SO_4 and HNO_3 by homogeneous gas-phase reactions. When the rate of H_2SO_4 formation is high, $NH_4NO_3(s)$ will evaporate. Formation of $NH_4NO_3(s)$ is favored by high concentrations of NH_3.

The rate of formation of $HNO_3(g)$ is assumed to be determined by the reaction:

$$NO_2 + OH + M \xrightarrow{k_1} HNO_3 + M \tag{15}$$

Thus

$$(d[HNO_3]/dt)_f = k_1 [OH] [NO_2] \tag{16}$$

The rate of formation of H_2SO_4 is assumed equal to the rate of reaction of SO_2 with OH:

$$HO + SO_2 + M \xrightarrow{k_2} HSO_3 + M \tag{17}$$

Thus

$$(d[NH_3]/dt)_{(NH_4)_2SO_4} = -2k_2 [OH] [SO_2] \tag{18}$$

The factor 2 appears, because two moles of NH_3 are assumed lost for each mole of HSO_3 (and H_2SO_4) formed.

Substituting Equations 16 and 18 in Equation 14 gives, with some rearrangement:

$$d[NH_4NO_3]/dt = \{k_1[OH] [NO_2]/(1+K_c/[NH_3]^2)\} \{1 - (2k_2K_c [SO_2]/k_1 [NO_2] [NH_3]^2)\} \tag{19}$$

According to Equation 19, the criterion for $NH_4NO_3(s)$ formation is

$$[NO_2] [NH_3]^2/[SO_2] > 2k_2K_c/k_1 \tag{20}$$

At 300K, $K_c = 5 \times 10^5$ (ppm)^2, $k_1 = 1.1 \times 10^{-11}$, and $k_2 = 9 \times 10^{-13}$ cm^3 molecule^{-1} sec^{-1} (Hampson and Garvin 1978). Thus

$$2k_2K_c/k_1 = (2) (9) (5) (10^{-5})/110 = 8 \text{ (ppb)}^2 \tag{21}$$

Equation 20 represents a dynamic condition for NH_4NO_3 formation, subject to the equilibrium constraint, Equation 8.

APPLICATION TO FIELD STUDIES

An experimental verification of Equation 19 would require detailed measurements of the chemical composition in the same parcel of air at two different times. Gases such as SO_2 and NO_2 can be measured on an essentially continuous real-time basis with commercial instrumentation, but NH_3 and HNO_3

are more difficult to determine. Aerosol nitrates are usually sampled over much longer periods of time (hours) by filtration. Measurements of OH are rarely made in field studies. The lack of good time resolution data for NH_4NO_3 and the lack of any OH data prevent a detailed test of Equation 19.

An approximate test of Equation 19 can be made for a box reactor model. For this purpose, short time resolution data should be obtained on the gas-phase concentrations of SO_2, NO_2 and NH_3, as well as aerosol-phase NH_4NO_3. The measurements can be made at a single point.

Integrating Equation 19 with the initial condition $[NH_4NO_3] = 0$ at $t = 0$, results in

$$[NH_4NO_3]/\theta = \overline{\{k_1[OH][NO_2]/(1+K_c/[NH_3]^2)\}\{1-(2k_2K_c[SO_2]/k_1[NO_2]\ [NH_3]^2)\}} \quad (22)$$

where $[NH_4NO_3]$ is the concentration at time θ, and the right-hand side is the average over the time range 0 to θ.

This result can be applied to the ambient data collected at a single monitoring site, given sufficient time resolution, say <1 h. The parameters most easily measured are $[NH_4NO_3]$ in the aerosol phase, $[NO_2]$, $[SO_2]$, and the temperature. It should also be possible to measure $[NH_3]$, but [OH] is rarely measured.

The quantities on the right-hand side are measured over a time interval around θ, while theory requires the average value from time $t = 0$ to $t = \theta$. Thus, only an approximate test of Equation 19 is possible. This test can be made by plotting $Y = [NH_4NO_3]/[NO_2]$ vs. $X = k_1[NO_2][NH_3]^2/k_2K_c[SO_2]$, with $Z = K_c/[NH_3]^2$ as a parameter. For values of $X < 2$, the formation of NH_4NO_3 as measured by the parameter Y should be slight. For values of $X > 2$, Y should increase significantly as X increases, with Z as a parameter. Variations in [OH] (usually not measured) will contribute to the scatter in the data.

REFERENCES

Brandner, J. D., N. M. Junk, J. W. Lawrence, and J. Robins. 1962. Vapor Pressure of Ammonium Nitrate. J. Chem. Eng. Data, 7:227-228.

Dingemans, P. 1941. Die Dampfspannung von Gesattighten NH_4NO_3 - losungen. Rec. Trav. Chim., 60:317-328.

Doyle, G. J., E. C. Tuazon, R. A. Graham, T. M. Mischke, A. M. Winer, and J. N. Pitts, Jr. 1979. Simultaneous Concentrations of Ammonia and Nitric Acid in a Polluted Atmosphere and Their Equilibrium Relationship to Particulate Ammonium Nitrate. Environ. Sci. Technol., in press.

Hampson, R. H., Jr., and D. Garvin. 1978. Reaction Rate and Photochemical Data for Atmospheric Chemistry -1977. NBS Special Publication 513.

JANAF Thermochemical Tables, 2nd Edn. 1971. NSRDS-NBS 37.

Spicer, C. W. 1974. The Fate of Nitrogen Oxides in the Atmosphere. Battelle Columbus Report to Coordinating Research Council and U.S. Environmental Protection Agency. EPA-600/3-76-030.

Stelson, A. W., S. K. Friedlander, and J. H. Seinfeld. 1979. A Note on the Equilibrium Relationship between Ammonia and Nitric Acid and Particulate Ammonium and Nitrate. Atmos. Environ., 13:369-371.

Wagman, D. D., W. H. Evans, V. B. Parker, I. Harlow, S. M. Baily, and R. H. Schumm. 1968. Selected Values of Chemical Thermodynamic Properties; tables for the first thirty-four elements in the standard order of arrangement. NBS Technical Note 270-3.

ATMOSPHERIC NITROGEN CHEMISTRY: NO_x LOSS REACTIONS

Dale G. Hendry

SRI International
333 Ravenswood Avenue
Menlo Park, California 94025

INTRODUCTION

The dominant fate of the large volumes of nitric oxide (NO) produced by stationary and mobile sources is conversion to pentavalent nitrogen, or nitrogen (V)--nitric acid ($HONO_2$ or HNO_3) and its salts. A number of processes contribute to this overall conversion, and the relative importance of these various pathways depends on the concentration of reactants, light intensity ($h\nu$), temperature, and other atmospheric conditions.

Table 1 summarizes the generally recognized atmospheric inorganic nitrogen chemistry, which is similar to that formulated by Robinson and Robbins (1971); in addition, a detailed discussion of tropospheric nitrogen chemistry has been presented by Cox (1979). Reactions 4 and 10 in Table 1 are the reactions

TABLE 1. INORGANIC NITROGEN CHEMISTRY

Atmospheric Reaction	Number
$NO + HOO\cdot \longrightarrow NO_2 + OH$	(1)
$NO + O_3 \longrightarrow NO_2 + O_2$	(2)
$NO + OH \longrightarrow HONO$	(3)
$NO_2 + OH \longrightarrow HONO_2$	(4)
$NO_2 + O_3 \longrightarrow NO_3 + O_2$	(5)
$NO_2 + h\nu \xrightarrow{O_2} NO + O_3$	(6)
$NO_2 + HOO\cdot \rightleftharpoons HOONO_2$	(7)
$NO_3 + NO \longrightarrow 2NO_2$	(8)
$NO_3 + NO_2 \rightleftharpoons N_2O_5$	(9)
$N_2O_5 + H_2O \longrightarrow 2HONO_2$	(10)

responsible for $HONO_2$ formation. Reaction 4 is believed to be solely a gas-phase reaction; whereas Reaction 10 is believed to require a heterogeneous surface, or an aqueous phase.

Other processes, especially those involving organic reaction intermediates, are suspected of contributing to nitrate (NO_3^-) formation. In this review, evidence will be examined from smog chamber experiments indicating the importance of additional nitrate-generating reactions, and important candidate processes will be considered. For all cases considered, rate data are needed to quantitatively evaluate the importance of these processes in the atmosphere.

CONCLUSIONS AND RECOMMENDATIONS

Based on smog chamber data, the major fate of the oxides of nitrogen (NO_x) in the atmosphere is to react as nitrogen dioxide (NO_2) with the hydroxyl radical (OH) to form $HONO_2$. Some $HONO_2$ is also formed by nitrogen pentoxide (N_2O_5) hydrolysis. However, the data support evidence for other pathways that can involve peroxynitrates, organic nitrates, direct NO_x hydrolysis, and oxidation reactions of nitrous acid (HONO). All these pathways lead to nitrogen (V) formation except the oxidation reactions of HONO, in which nitrous oxide (N_2O) may be a major product. Data on these alternative pathways are needed for verification and quantification of their role in atmospheric conversion of NO_x to stable products.

ANALYSIS OF SMOG CHAMBER NITROGEN BALANCE

One of the largest data bases of smog chamber data has been obtained by the Statewide Air Pollution Research Center (SAPRC) at the University of California, Riverside (Pitts et al. 1977). Researchers at SAPRC have investigated the effects of hydrocarbon (HC) type and structure; concentrations of HC, NO, and NO_2, and to a lesser degree, light intensity ($h\nu$) and temperature. Product analysis has been directed to obtaining organic carbon balances. Although extensive efforts were not made to determine the fate of the NO_x, sufficient information is available, when coupled with theoretical considerations, to point out the importance of alternative nitrate-forming pathways.

Propene

Figure 1 summarizes SAPRC propene run EC-314, accomplished in a 5800-liter evacuable chamber. The initial conditions included concentrations of 1.046 ppm propene, 0.684 ppm NO, and 0.246 ppm NO_2. The temperature of the run was 302 K, the relative humidity (RH) was 57 percent, and the NO_2 photolysis rate constant was 0.48 min^{-1}. It is clear from Figure 1 that the formation of peroxyacetyl nitrate (PAN) accounts for only a small portion of the NO_2 lost. The difference is generally assumed a result of $HONO_2$ formation by Reactions 4 and 10 (Table 1).

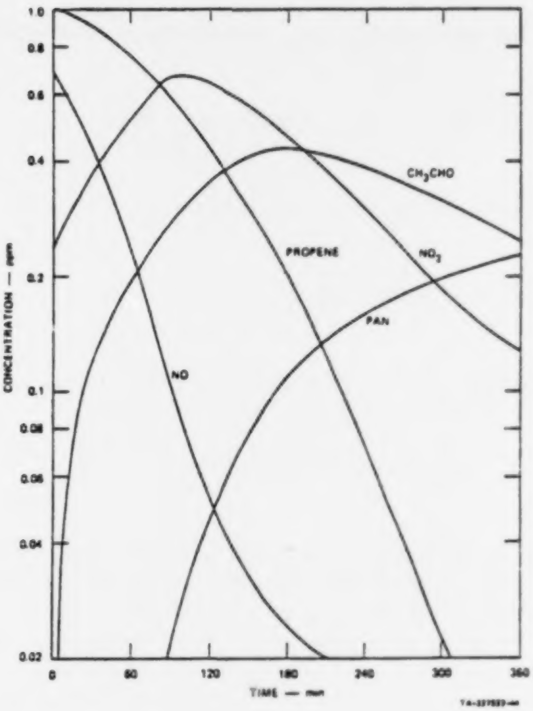

Figure 1. SAPRC propene run EC-314.

The contribution of Reaction 4 can be estimated by the expression

$$[HONO_2] = k_4 \sum [OH]_i \; [NO_2]_i \; (\Delta t_i)$$

where k_4 = rate constant for Reaction 4

Δt_i = time interval

$[OH]_i$ = average OH concentration over each Δt_i

$[NO_2]_i$ = average NO_2 concentration over each Δt_i

All values are known except $[OH]_i$, which may be established from the change in propene concentration, $[P]_t$, during each time interval

$$\text{In}[P]_t/[P]_{t+1} = k_{OH}[OH]_i + k_{O_3}\,[O_3]_i + k_O[O^3P]_i$$

where $[P]_t$, $[P]_{t+1}$, and $[O_3]_i$ = measured values

k_{OH}, k_{O_3}, and k_O = rate constants for reaction of propene with OH, ozone (O_3), and O^3P, respectively--all determined values

The value of $[O^3P]_i$ may be accurately estimated from the steady-state expression

$$[O^3P]_i = k_{NO_2} [NO_2]/k_{O_2} [O_2]$$

where k_{O_2} is the rate constant for the reaction

$$O^3P + O_2 \rightarrow O_3 \tag{11}$$

and k_{NO_2} is the rate constant for photolysis of NO_2

$$NO_2 + h\nu \rightarrow NO + O^3P \tag{12}$$

Figure 2 summarizes nitrogen balance as a function of time for SAPRC run EC-314; included is the calculated concentration of $HONO_2$ formed by Reaction 4. The figure shows that $HONO_2$ from Reaction 4 becomes a dominant fraction of the nitrogen as the chamber experiment proceeds. PAN accounts for a significant amount but is not a final product, because it dissociates to again form NO_2. At the end of the run, Figure 2 indicates that 17 percent of nitrogen is missing. This difference is made up of NO_x lost by dilution (~9 percent) and $HONO_2$ formation by Reaction 10, based on computer modeling of this run.

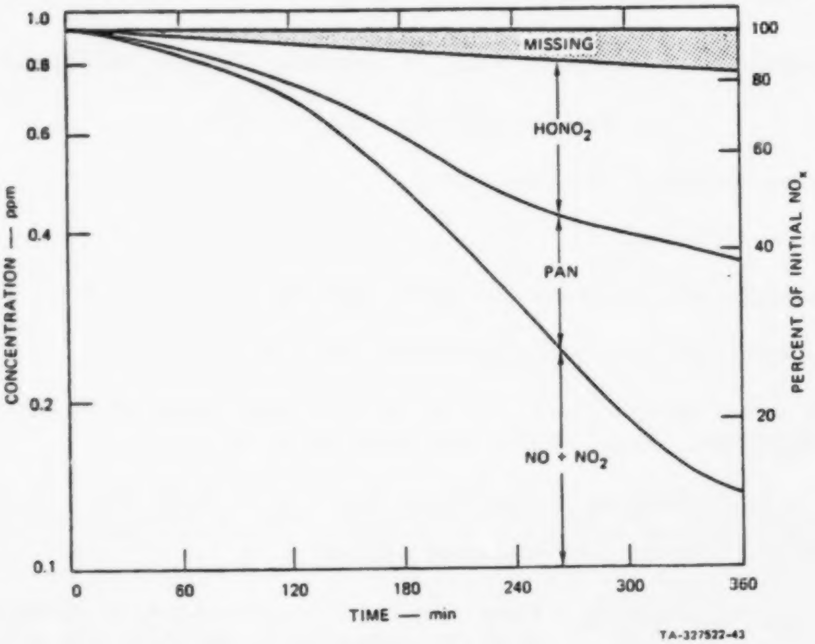

Figure 2. Nitrogen balance: propene.

n-Butane

SAPRC n-butane run EC-306 is summarized in Figure 3. Concentrations were 6.4 ppm n-butane, 0.147 ppm NO, and 0.04 ppm NO_2; other initial conditions were 303 K, 59 percent RH, and 0.43 min^{-1} NO_2 photolysis rate. In addition to PAN, the nitrates of 1- and 2-butanol are reported in this reaction. The nitrogen balance is shown in Figure 4. The $HONO_2$ formed by Reaction 4 has been computed as in the propene case and included in the figure.

The $HONO_2$ from Reaction 4 is relatively small in this case because of the generally low OH and NO_2 concentrations in n-butane chamber experiments. Unlike the propene case, a significant fraction (41 percent) of the initial NO_x is missing by the end of the reaction. Dilution accounts for a 9.40 percent NO_x loss, and computer simulation indicates that 16 percent is caused by N_2O_5 hydrolysis (Reaction 10). Thus, ~16 percent of the nitrogen is unaccounted for in this run.

Toluene

Figure 5 summarizes the data for SAPRC toluene run EC-266. Initially, concentrations were 1.20 ppm toluene, 0.43 ppm NO, and 0.06 ppm NO_2; the temperature was 302 K and the RH was 48 percent. In this experiment, as in other toluene chamber experiments, only about 25 percent of the consumed toluene is accounted for by the cresols, nitrocresols, and nitrotoluenes, as well as PAN and formaldehyde (HCHO), which are shown in Figure 5. The major nitrogen-containing product is PAN; trace amounts of nitrotoluene and nitrocresol are also detected, but the reported amounts are less than 1 percent of the initial NO_x.

The nitrogen balance is plotted in Figure 6. The $HONO_2$ values were computed by methods used for propene. At the end of the reaction, 48 percent of the nitrogen is missing. Dilution accounts for 9.3 percent of the total initial NO_x. Comparison with computer simulation results indicates that about 10 percent of the nitrogen should be converted to $HONO_2$ by N_2O_5 hydrolysis. These determinations therefore do not account for about 30 percent of the nitrogen.

ALTERNATIVE NO_X LOSS REACTIONS

From the analysis of the smog chamber experiments, we see the nitrogen balance is very good for propene (100 percent), moderate for n-butane (~84 percent), and only satisfactory for toluene (~70 percent). Thus, pathways other than Reactions 4 and 10 exist that allow NO_x conversion to $HONO_2$ or other nitrogen-containing compounds. Some possible pathways are discussed below.

Peroxynitrate Reactions

A careful study of the homogeneous atmospheric chemistry of peroxybenzoyl nitrate (PBzN) was completed (Kenley and Hendry 1979). Figure 7 shows the effect of NO and NO_2 on the decomposition rate. The high acceleration due to

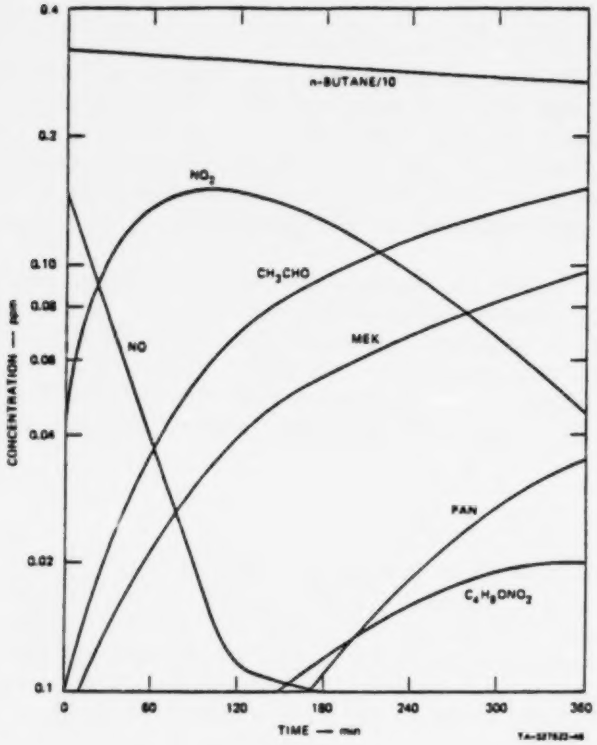

Figure 3. SAPRC n-butane run EC-306.

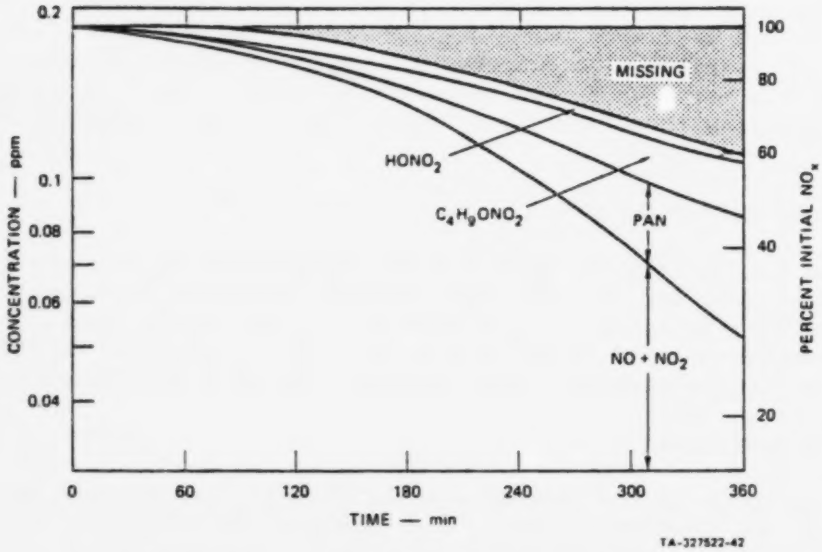

Figure 4. Nitrogen balance: n-butane.

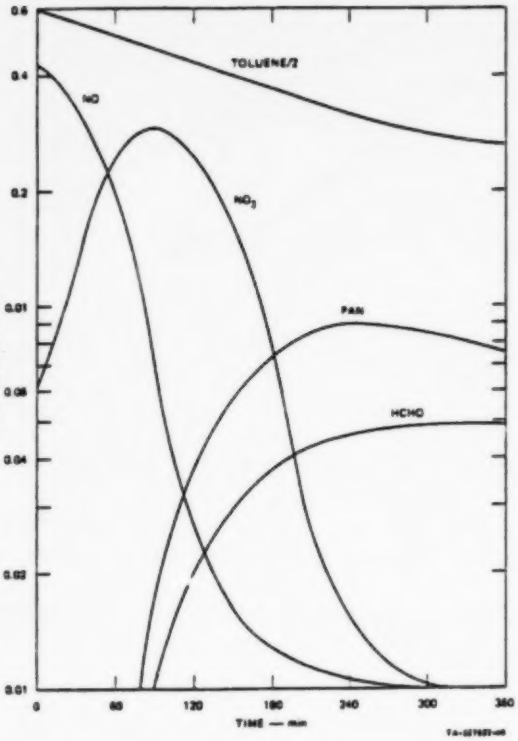

Figure 5. SAPRC toluene run EC-266.

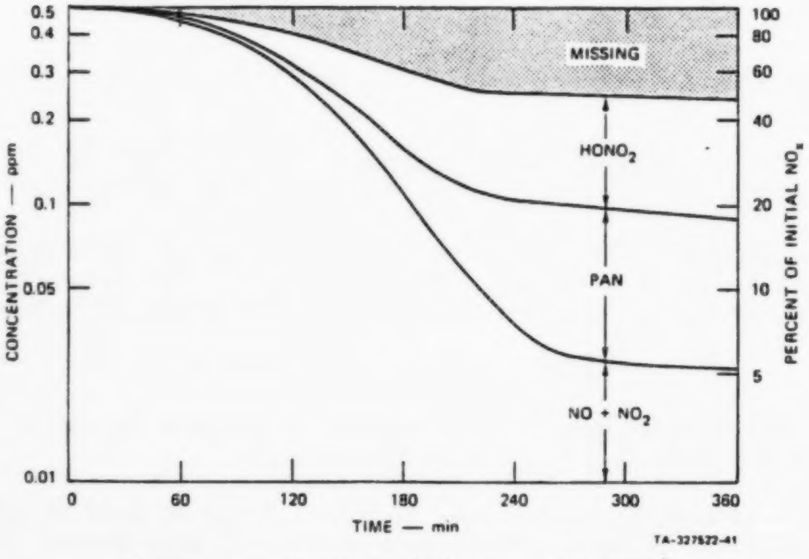

Figure 6. Nitrogen balance: toluene.

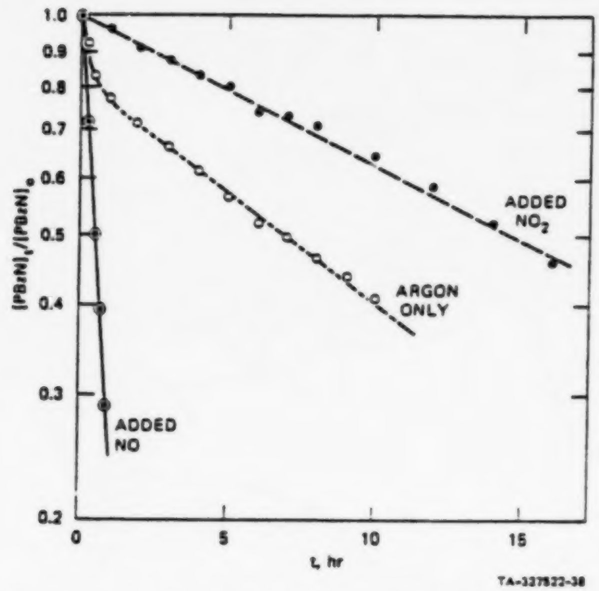

Figure 7. Decomposition of PBzN at 300 K.

NO is independent of the NO concentration, if [NO] > [PBzN]. The effect of NO, as well as the rapid exchange of $^{15}NO_2$, is consistent with the rapid equilibrium

$$PhC(O)O_2\cdot + NO_2 \qquad PhC(O)O_2NO_2(PBzN) \tag{13}$$

where PBzN is effectively destroyed upon rapid reaction of the peroxybenzoyl radical ($PhC(O)O_2$) with NO

$$PhC(O)O_2\cdot + NO \rightarrow PhC(O)O\cdot + NO_2 \tag{14}$$

The decomposition rate in the presence of added NO and NO_2 is

$$-d[PBzN]/dt = k_{-13}[PBzN] \quad 1 + \frac{k_{-13}[NO_2]}{k_{14}\ [NO]} \tag{15}$$

Thus, as long as [NO] >> [NO_2], the second term in parentheses is much less than 1 and the first-order decay of PBzN gives k_{-13}. The value of k_{-13} has been measured in this manner as a function of temperature and may be expressed

$$\log(k_{-13}/s^{-1}) = 15.2 - 5660/T$$

By measuring the loss of PBzN in the presence of varying ratios of [NO_2]/[NO], we have found the ratio k_{14}/k_{-13} to be 1.52 ± 0.12.

Once k_{13} and k_{-13}/K_{14} are known, Equation 15 may be used to estimate the atmospheric lifetime of PBzN, assuming no other reactions besides Reactions 13, -13, and 14 occur. At 300 K and a ratio of $NO_2/NO = 1$, the lifetime is

3.2 h; at a ratio of $NO_2/NO = 10$, the lifetime is 20.2 h. Thus, PBzN is expected to have a significant lifetime and should be present in the toluene smog chamber runs and also detectable in the atmosphere where benzaldehyde or HC's (such as toluene, reacting readily to give benzaldehyde) are present.

At toluene concentrations (0.02 ppm) reported for Los Angeles (Calvert 1976) and assuming an NO_2/NO ratio of 2.0, and that $[OH] = 1 \times 10^{-7}$ ppm, a PBzN formation rate equal to 1.4×10^{-6} ppm min^{-1} is computed. Thus, assuming a residence time of 5 h, a concentration of 0.4 ppb PBzN formed from toluene is expected. Other alkyl benzenes should also contribute to PBzN formation; although these compounds have low concentrations, as compared to toluene (Calvert 1976), they are more reactive than toluene and are expected to produce PBzN with high frequency (Heuss and Glasson 1968). Thus, including other HC's besides toluene, a concentration in the range of 0.4 to 0.8 ppb of PBzN is expected for the Los Angeles area late in the day.

In the San Francisco Bay area, where expected PBzN concentrations are lower (possibly in the range of 0.05 to 0.1 ppb), Appel (1973) has reported less than 0.07 ppb on a moderately smoggy day (O_3 max = 0.10 ppm). Meijer and Niebour (1977) have reported concentrations of PBzN from 0.03 to 4.6 ppb in the Netherlands, but the conditions were favorable for formation of this compound because of the presence of styrene, which is readily converted to benzaldehyde. The difficulty of detecting PBzN suggests alternative routes by which PBzN is lost in the atmosphere.

Heterogeneous or solution reactions of PBzN, as well as other peroxy nitrates of low volatility, may be important. Several groups (Nicksic et al. 1967; Steer et al. 1969) have reported the base hydrolysis of PAN, which is

$$CH_3C(O)OONO_2 + OH^- \rightarrow CH_3C(O)OH + O_2 + NO_2^- \qquad (16)$$

Under acidic conditions the following hydrolysis may be important

$$CH_3C(O)OONO_2 + H_2O \xrightarrow{H^+} CH_3C(O)OOH + HONO_2 \qquad (17)$$

Both of these reactions could be alternative and important NO_x loss reactions. Reaction 16 would be a source for NO_2^- that would have an expected stability in basic solution but would form HONO in acidic solution. The $HONO_2$ formed in Reaction 17 would either stay in solution or volatilize.

The analysis of products in the toluene chamber reactions suggests that aromatic ring cleavage is a major reaction pathway, even early in the reaction. We have suggested that the open ring fragments will form peroxyacyl radicals, which in turn form the corresponding PAN's (Hendry et al. 1980). These peroxynitrates are expected to have a variety of functional groups and to be significantly more nonvolatile than even PBzN. They should readily deposit on surface particulate or chamber walls, where they could react similarly to Reactions 16 and 17. The large NO_2 fraction that is unaccounted for in the toluene may result from these types of reactions.

To gain more insight into the NO_x loss in the toluene experiments, the NO_x/consumed-toluene ratio was computed as a function of reaction time, and the data are plotted in Figure 8. From this plot we see that a maximum of 1 to 1.5 in NO_x loss per toluene-molecule-reacted occurs between 120 and 180 min, somewhat after the point of the NO_2 maximum and where the maximum accumulation of peroxynitrates is expected. Hence, these data support the possibility that peroxynitrates of complex structure contribute to the NO_x loss.

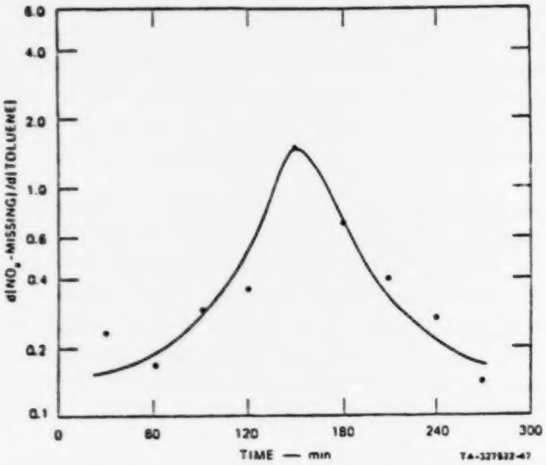

Figure 8. Missing nitrogen relative to toluene loss.

Organic Nitrate Reactions

As shown in the n-butane smog chamber experiment, organic nitrates can be important products. Darnall et al. (1976) have shown that the amounts of organic nitrates in smog chamber experiments increase with increasing molecular weight of the HC being studied. They have argued that this product type forms in the reaction

$$ROO\cdot + NO \rightarrow RONO_2 \qquad (18)$$

which competes with the important reaction

$$ROO\cdot + NO \rightarrow RO\cdot + NO_2 \qquad (19)$$

No matter how these compounds are formed, they are expected to slowly hydrolyze to $HONO_2$

$$RONO_2 \xrightarrow[H^+]{H_2O} ROH + HONO_2 \qquad (20)$$

The missing nitrogen in n-butane may be explained by other nitrates that were not detected or that have hydrolyzed. For example, since rearrangement of the n-butoxy radical is important, 1-butanol-4-nitrate could be an important product, being formed by the following reactions:

$$CH_3CH_2CH_2CH_2O\cdot \xrightarrow{O_2} \cdot O_2CH_2CH_2CH_2CH_2OH \tag{21}$$

$$\cdot O_2CH_2CH_2CH_2CH_2OH \xrightarrow{NO} NO_2\text{-}OCH_2CH_2CH_2CH_2OH \tag{22}$$

This product would be difficult to detect and would be expected to readily hydrolyze to $HONO_2$ and 1,4-butanediol.

NO_x Hydrolysis

Orel and Seinfeld (1977) have demonstrated that hydrolysis of NO_x might be the source of aerosol NO_3^- in the environment. However, NO_x hydrolysis is an extremely complex process. The reaction of NO_2 with aqueous phases has long been known to be rapid and to lead to the following initial equilibrium:

$$2NO_2 \rightleftharpoons HONO + HONO_2 \tag{23}$$

However, the ultimate fate of the HONO and $HONO_2$ depends first on the acidity of the medium and second on the presence of any substances with which they can react.

At low acidity, the HONO is expected to decompose as follows

$$2HONO \rightarrow H_2O + NO + NO_2 \tag{24}$$

so that the overall equilibrium is

$$3NO_2 \overset{H_2O}{\rightleftharpoons} 2HNO_3 + NO \tag{25}$$

However, the HONO decomposition rate is expected to be low, resulting in appreciable concentration; therefore, HONO participation in other reactions is predicted, as discussed below.

In the middle acidity range, the HONO is converted to nitrosonium ion

$$HONO + H^+ \rightarrow HOH + NO^+ \tag{26}$$

and the overall equilibrium of NO_2 is

$$2NO_2 \rightleftharpoons NO^+ + HNO_3 \tag{27}$$

At very high acidities, the $HONO_2$ is converted to nitronium ion

$$HONO_2 + H^+ \rightleftharpoons HOH + NO_2^+ \qquad (28)$$

and the overall equilibrium is

$$2NO_2 \overset{H^+}{\rightleftharpoons} NO^+ + NO_2^+ \qquad (29)$$

These three general equilibria (Expressions 25, 27, and 29) are possible in sulfuric acid aerosols, depending on the humidity. Therefore, each of these three processes may be important under different environmental conditions.

Even when the effect of acidity is recognized, the overall reaction is controlled by the kinetics of the competing reactions within the droplet. For example, at low acidity, if HONO disproportionates rapidly, $HONO_2$ (H^+, NO_3^-) and NO are the initial, volatilizable products. In this case, all NO_2 entering the droplet may return to the gas phase as NO and HNO_3 and thus may not form any NO_3^- particulate. However, if ammonia is present, ammonium nitrate can be formed in the aerosol, resulting in NO volatilization. On the other hand, if the HONO disporportionation is slow, then both HONO and $HONO_2$ may volatilize or react with ammonia to form ammonium nitrite as well as ammonium nitrate.

To determine how important these processes are, relative to other nitrate-forming processes, we need to study these equilibria and the rates at which they are obtained, as well as the rates of competing processes at various acidities.

HONO Chemistry

In the atmosphere, gas-phase HONO rapidly photolyzes ($\tau \approx 10$ min) and any other chemistry is generally considered insignificant. However, in view of the NO_x hydrolysis chemistry discussed above, aqueous HONO chemistry is also possible in the atmosphere. Oxidation of HONO to $HONO_2$ by O_2 or O_3 is probably too slow to be important. Reaction with sulfur dioxide (SO_2) is possible and is of extreme interest with regard to sulfate ($SO_4^=$) formation. Ross (1978) has shown that in dilute sulfuric acid, SO_2 and HONO react very rapidly, yielding both NO and N_2O with the following stoichiometry:

$$3HONO + 2SO_2 = 2SO_4^= + N_2O/2 + 2NO \qquad (30)$$

Thus, not only is SO_2 converted to $SO_4^=$, but also some of the NO_x ends up as N_2O. This is the first evidence that NO and NO_2 can be converted to a stable product other than $HONO_2$ or its salts. Further study of this reaction is needed to determine the importance of this atmospheric process, as is study of the HONO reaction with other components of the particulate phase.

REFERENCES

Appel, B. R. 1973. New and More Sensitive Procedure for Analysis of PBzN. J. Air Pollut. Control Ass., 23:1042-4.

Calvert, J. G. 1976. Hydrocarbon Involvement in Photochemical Smog Formation in Los Angeles Atmosphere. Environ. Sci. Technol., 10:256-262.

Cox, R. A. 1979. Tropospheric Chemistry of Nitrogen Oxides--A Summary of the Status of Chemical Kinetic Data. In: Chemical Kinetic Data Needs for Modeling the Lower Troposphere, J. T. Herron, R. E. Huie, and J. A. Hodgeson, eds. U.S. Department of Commerce, NBS Special Publication 557. pp. 71-81.

Darnall, K. R., W. P. L. Carter, A. M. Winer, and J. N. Pitts, Jr. 1976. Importance of RO_2 + NO in Alkyl Nitrate Formation. J. Phys. Chem., 80:1948-1950.

Hendry, D. G., A. C. Baldwin, and D. M. Golden. 1980. Computer Modeling of Simulated Photochemical Smog. EPA-600/3-80-029.

Heuss, J. M., and W. A. Glasson. 1968. Hydrocarbon Reactivity and Eye Irritation. Environ. Sci. Technol., 2:1109-1116.

Kenley, R. A., and D. G. Hendry. 1979. Chemistry of PBzN. In preparationn.

Meijer, G. M., and H. Niebour. 1977. Determination of PBzN in Ambient Air. Ver. Deutsch Ingen, 270:55-56.

Nicksic, S. W., J. Harkins, and P. K. Mueller. 1967. Some Analyses for PAN and Studies of its Structure. Atmos. Environ., 1:11-18.

Orel, A. E., and J. H. Seinfeld. 1977. Nitrate Formation in Atmospheric Aerosols. Environ. Sci. Technol., 11:1000-1007.

Pitts, J. N., Jr., K. R. Darnall, A. M. Winer, and J. M. McAfee. 1977. Mechanisms of Photochemical Reactions in Urban Air, II: Chamber Studies. EPA-600/3-77-14b, and subsequent quarterly reports. U.S. Environmental Protection Agency.

Robinson, E., and R. C. Robbins. 1971. Sources, Abundance and Fate of Gaseous Atmospheric Pollutant--Supplement. American Petroleum Institute Publication No. 4015.

Ross, D. S. 1978. Nitrate Formation in Atmospheric Aerosols. Environ. Sci. Technol., 12:726.

Steer, R. P., K. R. Darnall, and J. N. Pitts, Jr. 1969. The Base-Induced Decomposition of Peroxy Acetylnitrate. Tetrahedron Lett., 1969:3765-3767.

Stephens, E. R. 1967. The Formation of Molecular Oxygen by Alkaline Hydrolysis of Peroxyacetyl Nitrate. Atmos. Environ., 1:19-20.

HETEROGENEOUS NO_x REACTIONS IN THE ATMOSPHERE

Henry S. Judeikis

Chemistry and Physics Laboratory
The Ivan A. Getting Laboratories
The Aerospace Corporation
2350 East El Segundo Boulevard
El Segundo, California 90245

INTRODUCTION

Interest in the atmospheric chemistry of oxides of nitrogen (NO_x) has increased over the past several years, as evidenced by this workshop and a recent symposium on nitrogeneous air pollutants (Grosjean 1979). Most NO_x studies have emphasized gas phase NO_x reactions that lead to both gas phase and aerosol reaction products (Shuck and Stephens 1969; Demerjian et al. 1974; Hidy and Burton 1975). Studies of gas--solid interactions involving atmospheric aerosols or uptake by ground-level surfaces are more limited.

Several studies have demonstrated that nitrate (NO_3^-) and other nitrogen-containing adsorbed species are formed when particulate matter is exposed to NO_x (Chang and Novakov 1975; Harker et al. 1977; Judeikis et al. 1979). Recently, measurements have been made of gas--aerosol reaction rates involving NO_x with particulates generated by novel techniques (Clarke and Britton 1977; Ten Brink et al. 1978); Clarke and Britton examined the effects of NO_x on heterogeneous oxidation of sulfur dioxide (SO_2), while Ten Brink et al. found that selected metal oxide particles readily reacted with nitrogen dioxide (NO_2). Several measurements have also been made of deposition of nitric oxide (NO) and NO_2 onto ground-level surfaces such as selected soils and vegetation (Hill 1971; Abeles et al. 1971).

In this paper, a review is presented of measurements carried out in our laboratories of gas--solid NO_x interactions as they relate to gas--aerosol reactions (Judeikis et al. 1979) and to deposition at ground-level surfaces (Judeikis and Wren 1978). Comparison of these results with other literature data, as discussed in the cited references, indicates reasonable agreement. The results are then applied to representative atmospheric situations to estimate the contributions of gas--aerosol reactions to atmospheric NO_3^- aerosol burdens. Interactions with ground-level surfaces are also investigated for estimating ground-level NO_x sinks and for estimating the impact of these interactions on indoor air quality.

EXPERIMENTAL

Apparatus and Procedure

Several types of cylindrical flow reactors were used in our studies (Hedgpeth et al. 1974; Stewart and Judeikis 1974; Judeikis and Stewart 1976). The reactors were similar in that they contained an inner, concentric glass cylinder (in some cases a glass helix was used) that had been coated with the solid of interest. As indicated in the referenced material, the coatings were prepared from a water or water--alcohol slurry of the appropriate solid. The wet coatings were subsequently air dried and then generally dried overnight in the appropriate reactor in vacuum (10^{-4} torr) at room temperature.

During an experiment, an appropriately prepared reaction mixture (nitrogen or argon plus NO_x or oxygen) was caused to flow through the reactor under nonturbulent conditions (Reynolds numbers <100). As the reactive component of the mixture passed through the reactor, it diffused to the coated walls of the inner cylinder (or helix), where it was removed by heterogeneous reaction. This led to the development of concentration gradients for the reacting species in the radial and axial flow directions. These concentration gradients were related to heterogeneous reaction rates. Experimentally, we measured the concentration of the reacting species as a function of distance along the axial flow direction.

The three reactors differed principally in the particular method used for measuring concentrations. The first reactor (Hedgpeth et al. 1974) employed a chopped, dual beam, optical absorption technique that yielded NO_2 concentrations integrated over the length of the flow tube. Measurement of influent and effluent NO was carried out using chemiluminescent methods. The second reactor (Stewart and Judeikis 1974) employed laser induced fluorescence of NO_2 to measure NO_2 concentrations as a function of distance along the flow direction. The third reactor (Judeikis and Stewart 1976; Judeikis and Wren 1978) utilized multiple probes at various fixed positions along the cylinder axis. These probes were coupled, via a multiport rotary valve, to a mass spectrometer for NO and NO_2 determinations. In selected cases, surface reaction products were analyzed by wet chemical techniques or by using specific ion electrodes (Judeikis et al. 1979).

Data Analysis

Data were analyzed using models that accounted for mass transport by diffusion and flow (Walker 1961; Judeikis and Stewart 1976; Judeikis and Wun 1978; Judeikis 1979). In a few cases, small corrections for gas phase reactions were required (Judeikis et al. 1979). Application of these models to the experimental data yielded heterogeneous reactivities in terms of collision efficiencies (ϕ), i.e., the fraction of gas--solid collisions leading to removal of the reacting species (Judeikis and Stewart 1976). For interactions involving ground-level surfaces, the ϕ values are related to deposition velocites (Vg) by use of the expression $\phi = Vg\ k_r$, where k_r is the molecular velocity of the reacting species normal to the surface.

RESULTS

NO_2 Reactions

Experimental results for NO_2 are summarized in Table 1 and discussed in detail elsewhere (Judeikis and Wren 1978; Judeikis et al. 1979). In general, reactivities were found to be relatively insensitive to the NO_2 and oxygen content of the reaction mixture, as well as to the total pressure. However, water vapor was found to have pronounced effects on reaction rates, particularly for the more nonreactive solids. The most notable example of this from Table 1 is the case of ZnO, where the ϕ value increased by a factor of >300 when the zero percent relative humidity (RH) of the reaction mixture was increased to 40 to 50 percent. The results given in Table 1 were obtained from experiments in which the gas phase reactions between NO_2 and H_2 (Kaiser and Wu 1977) were minimal.

In several cases, the effects of simulated sunlight on reactivities were examined. These experiments were carried out at wavelengths >400 nm to avoid direct photolysis of NO_2. Although different solids gave evidence for both enhancement of reactivities in the presence of simulated sunlight as well as photodesorption of NO_2, overall effects on NO_2 reactivities were less than ~30 percent.

However, prolonged exposures to NO_2 were found to have significant effects on reaction rates, as well as reaction products. Initially, NO_2 removal led quantitatively to the formation of adsorbed nitrates and nitrites, as determined by analysis of surface reaction products, the dominant species depending upon the solid used. On continued exposure to NO_2, reactivities decreased. This was accomplished by a gradual change in reaction products from adsorbed nitrates and nitrites to gaseous NO. For prolonged exposures, the $NO_2 \rightarrow NO$ conversion became quantitative; however, reactivities ultimately approached zero. Overall, for the more reactive materials in Table 1, ~0.05 to 0.1 g NO_2 per gram of solid was removed from dry reaction mixtures and ~0.2 to >0.4 g NO_2 per gram of solid from humidified reaction mixtures (40 to 50 percent RH). Approximately one-third of the NO_2 removed was converted to adsorbed nitrates and nitrites, with the remainder being converted to gaseous NO.

The NO_2--solid reactions appeared to be of the capacity limited type, with reactions diminishing as surfaces became saturated with reaction products. For several solids, attempts to restore reactivities through removal of volatile surface reaction products by evacuation of saturated solids were largely unsuccessful. However, exposure of selected saturated surfaces to gaseous ammonia, or lightly rinsing such surfaces with distilled water to remove soluble surface reaction products, were found to be effective. Surfaces treated in either of these manners were found to be virtually as reactive as fresh surfaces of the same materials.

TABLE 1. EXPERIMENTAL REACTIVITIES FOR NO_2[*]

Material	Reactor	$\phi \times 10^5$	
		0% RH	40 to 50% RH
Charcoal	C[†‡]	160	-
MnO_2	C[†‡]	100	-
Al_2O_3[§]	C[†‡]	30	-
PbO	A[†]	>10[#]	>10[#]
Cement-II	A[†]	>10[#]	>10[#]
Fly ash	A[†]	>10[#]	>10[#]
CaO	A[†]	>10[#]	>10[#]
Al_2O_3[§]	A	>10[#]	>10[#]
ZnO	A	<0.03	>10[#]
Adobe clay soil	B[**]	8.4	8.4[††]
Sandy loam soil	B[**]	6.4	6.4[††]
Cement-I	B[**]	3.4	3.4[††]
Cu_2O	A	<0.03	3
Fe_2O_3	A	<0.03	3
Sand	A	<0.03	1
V_2O_5	A	<0.03	0.1
$(NH_4)_2SO_4$	A	<0.03	0.1
H_2SO_4	A[†]	<0.03	0.1

[*] Uncertainties are approximately ±50 percent.

[†] These experiments were conducted with nitrogen or argon mixtures containing trace amounts of NO_2. The remaining experiments were conducted with N_2--O_2 (~5:1) mixtures containing traces of NO_2 or NO + NO_2, except those in reactor B. (See below.[**])

[‡] Separate experiments with these materials in reactor A and with N_2--O_2 (~5:1) mixtures yielded ϕ values $>10 \times 10^{-5}$ at 0 and 40 to 50 percent RH.

[§] The two results for Al_2O_3 are for material from different sources.

[#] These results were obtained from earlier experiments in which NO_2 reactions were limited by diffusion to the walls. Consequently, only minimum reactivities could be assigned for these materials.

[**] Experiments conducted with 0 or ~10 percent oxygen gave essentially identical results.

[††] Here only, 95 percent RH. Blank runs in this system at 95 percent RH gave negligible NO_2 losses.

NO Reactions

Reactions of NO with the materials listed in Table 1 were generally much less extensive than those of NO_2. Typically, ϕ values for NO removal were less than those for NO_2 removal by about an order of magnitude or more. One notable exception to this general conclusion was the case of MnO_2, where the ϕ value for NO removal was $> 10 \times 10^{-5}$. Although the soils and cement indicated some activity toward NO removal ($\phi \approx 1$ to 2×10^{-5}), most of the materials in Table 1 gave $\phi < 0.01 \times 10^{-5}$ for NO. Where reactions did occur, the same type of saturation behavior noted for NO_2 was also observed for NO.

In contrast to the case of NO_2, water vapor was found to have no effect on reactivities. Although exposure to simulated sunlight did appear to enhance reactivities to some degree for a few materials, the magnitude of the resulting ϕ values were still considerably less than those of NO_2 for the corresponding materials. In the case of materials saturated by exposure to NO, it was found that reactivity toward NO could be restored by the water rinse treatment, but not by treatment with gaseous ammonia.

DISCUSSION

Nitrate Aerosol Production

Nitrate produced in atmospheric particles by NO_2--aerosol reactions can be estimated using the ϕ values in Table 1 and a gas--aerosol reaction model (Judeikis and Siegel 1973; Preining 1973). Thus

$$d[NO_3^-]/dt = 1.35\ \phi\ k_c\ A[NO_2] \qquad (1)$$

where k_c = molecular velocity of NO_2 normal to the particle surface (92 m/sec at 20°C)

A = surface area per unit volume of atmospheric aerosol particles ($\sim 1.2 \times 10^{-3}$ m^2/m^3 for an aerosol burden M of 80 $\mu g/m^3$; Judeikis et al. 1978)

$[NO_2]$ = atmospheric concentration of gaseous NO_2, taken as 100 $\mu g/m^3$

1.35 = molecular weight ratio of NO_3^- to NO_2

For purposes of this calculation, the assumption has been made that NO_3^- is the only surface reaction product. The product $k_cA\ [NO_2]$ is the NO_2--aerosol collision rate. Consequently, since ϕ is the fraction of effective collisions, Equation 1 gives the NO_3^- production rate.

From Table 1, we note that measured ϕ values range from $<3 \times 10^{-7}$ to 1.6×10^{-3}. For ϕ values of 10^{-3}, 10^{-4}, 10^{-5}, and 10^{-6}, Equation 1 yields NO_3^- aerosol production rates of 54, 5.4, 0.54 and 0.054 $\mu g/m^3/h$, respectively; e.g., if all of the atmospheric aerosol of 80 $\mu g/m^3$ had a reactivity of 10^{-3}, the NO_3^- aerosol production rate would be 54 $\mu g/m^3/h$.

Of course, the values given above do not take into account saturation effects or conversion of NO_2 to gaseous NO when the reaction proceeds as described in the previous section. While the above rates would be applicable to freshly emitted aerosol particles, the latter effects would reduce NO_3^- production from NO_2--aerosol reactions. These effects will now be considered.

Consider an emission of fresh particles of $M_i\,\mu g/m^3$, in a time increment Δt, having a surface area A_i. It will be assumed that these particles can remove 0.3 g of NO_2 per gram of solid, but that only one-third of the NO_2 removed will be converted to NO_3^- aerosol. Thus, the capacity (C) of the particles to produce NO_3^- aerosol will be $1.35 \times (1/3) \times 0.3 = 0.135$ g NO_3^- per gram of particles. It will further be assumed that

$$\phi = \phi_o\,(1 - [NO_3^-]_i/C\,M_i) \qquad (2)$$

where ϕ = the reactivity of freshly emitted particulate matter.

This type of expression is a reasonable description of the observed changes in reactivity toward NO_2 as saturation sets in; it has previously been used to describe similar changes observed for SO_2--solid reactions (Liberti et al. 1978; Judeikis et al. 1978). Also, consider that the freshly emitted particles will be removed from the atmosphere within a lifetime τ. Thus, the surface area available for NO_2 aerosol reactions will be $A_i\,e^{-t/\tau}$. Substitution of this expression and Equation 2 into Equation 1 and integrating yields

$$[NO_3^-]_i = C\,M_i\,\left\{1 - \exp\left[\,-\,\alpha(1 - e^{t/\tau})\right]\right\} \qquad (3)$$

where, using $A/M = A_i/M_i$,

$$\alpha = 1.35\,\tau\,\phi_o k_c A[NO_2]/(CM) \qquad (4)$$

Note that the NO_3^- given by Equation 3 is the total NO_3^- on the M_i particles. Since the aerosols have an atmospheric lifetime τ, the airborne particulate nitrate $[NO_3^-]_{ia}$ will be given by

$$[NO_3^-]_{ia} = [NO_3^-]_i\,e^{-t/\tau} \qquad (5)$$

In Equation 3, M_i is equal to $\beta\Delta t$, where β is the total particle emission rate. At equilibrium, β is equal to the total particle loss rate of $(1/\tau)M$. Thus, $\beta = (1/\tau)M$, and $M_i = (\Delta t/\tau)M$. Using this expression and Equation 3, the total atmospheric NO_3^- burden resulting from NO_2--aerosol reactions, $[NO_3^-]_a$, can be obtained by a summation of Equation 5 over i, or as $\Delta t \rightarrow 0$, by

$$[NO_3^-]_a = \int_0^\infty CM/\tau \left\{1 - \exp\left[-\alpha(1 - e^{-\tau/t})\right]\right\} e^{-t/\tau}\, dt \qquad (6)$$

This expression can be integrated, making use of the substitution, $X = \exp(-t/\tau)$, with the result that

$$[NO_3^-]_a = CM\ [1-1/\alpha\ (1 - e^{-\alpha})] \qquad (7)$$

where, for τ in days, and making use of values previously given for the quantities in Equation 4, $\alpha = 1.2 \times 10^5\ \phi_o\tau$, and $CM = 10.8\ \mu g/m^3$. Table 2 gives resulting atmospheric NO_3^- burdens for various values of ϕ_o and τ.

TABLE 2. ATMOSPHERIC NITRATE BURDENS FROM NO_2--AEROSOL REACTIONS[a]

	Number of Days (τ)		
ϕ_o	3	10	30
10^{-3}	10.8	10.8	10.8
10^{-4}	10.5	10.7	10.8
10^{-5}	7.9	9.9	10.5
10^{-6}	1.7	4.5	7.9
10^{-7}	0.2	0.6	1.7
10^{-8}	0.0	0.1	0.2

[a] Calculated from Equation 7.

It will be noted from Table 2 that for ϕ_o values greater than ~10^{-5}, $[NO_2]_a$ will be limited by saturation effects, e.g., by the capacity of aerosol particles to transform gaseous NO_2 into particulate NO_3^-. As indicated in Table 1, a number of solids studied had ϕ values in this range. Coupled with the high transformation rates found for freshly emitted aerosols (indicated at the start of this section), the results suggest that NO_2--aerosol reactions will be most important at or near emission sources. Moreover, since the gaseous concentration of NO_2 in the atmosphere is generally much greater than the $[NO_2]_a$ values in Table 2, the results further suggest that NO_2--aerosol reactions will be limited by particle emissions and not NO_x emissions. Interactions with atmospheric ammonia could lead to some reactivation of saturated particles, based on results described in the preceding section. At present, the quantitative data available are insufficient to estimate the degree of reactivation.

Of course, other potential pathways to NO_3^- aerosol formation exist, such as thermal or photochemical formation from gas phase reactions and reactions in aqueous aerosols. The results obtained here indicate that NO_2--solid aerosol reactions could make important contributions to total atmospheric NO_3^- aerosol burdens.

NO_x Deposition on Ground-Level Surfaces

The ϕ values given in Table 1 for NO_2 interactions with the clay and loam soils and cement (I and II) translate into deposition velocities, V_g, of 0.77, 0.60, 0.32, and >0.93 cm/sec, respectively. For NO, corresponding values for the first three materials were 0.13, 0.19, and 0.21 cm/sec; these values agree reasonably well with earlier literature results (Judeikis and Wren 1978). For atmospheric concentrations of 100 $\mu g/m^3$, the deposition velocities cited here translate to fluxes to ground-level surfaces of 0.32 to 0.93 $\mu g/m^2/sec$ for NO_2, and 0.13 to 0.21 $\mu g/m^2/sec$ for NO. Of course, because of the saturation effects noted in the Results section, these fluxes would diminish with time (NO_x exposure). The results do suggest environmental processes for regeneration of saturated surfaces, such as interaction with atmospheric ammonia and precipitation washing away soluble surface reaction products.

An interesting feature of the NO_2--solid reactions is the interaction with cement. A similar result was previously observed for SO_2 (Judeikis and Stewart 1976). The latter observation was subsequently expanded upon to demonstrate the potential passive reduction of indoor SO_2 levels through the use of reactive building materials such as cement (Judeikis 1979a). A similar exercise will now be carried out for NO_2.

The rate of change of NO_2 concentrations in a room $[NO_2]r$ can be expressed by

$$d[NO_2]_r/dt = 1/V\left\{(1 - f)F[NO_2]_o + fF[NO_2]_r - F[NO_2]_r - V_g A_r [NO_2]_r\right\} \qquad (8)$$

where V = room volume (900 ft^3 for a room 10 x 12 ft, and 7.5 ft in height)

F = ventilation rate (taken as 300 ft^3/min)

f = fraction of exhaust air recirculated (typically 0.7)

A_r = room surface area effective in removing NO_2 with a deposition velocity V_g

Here we will consider a room with unpainted cement walls and ceiling with A_r = 410 ft^2 and V_g = 0.32 or 0.93 cm/sec. The remaining 160 ft^2 of surface area in the room, as well as any additional surface area from furnishings, will be considered nonreactive (V_g = 0). Further, the room air is assumed sufficiently well mixed that interaction with the surfaces is not limited by transport of NO_2 to those surfaces. No indoor sources of NO_2 are assumed, and gas phase chemistry is neglected.

The first term on the right side of Equation 8, $(1 - f)F[NO_2]_\sigma$, expresses the NO_2 flow into the room from outdoor air; $[NO_2]_\sigma$ is the outdoor NO_2 concentration, taken as 100 $\mu g/m^3$. The second and third terms on the right side of Equation 8 express the influx and efflux of NO_2 into and out of the room by recirculated and exhausted room air. The last term accounts for deposition on the unpainted cement surfaces in the room.

At steady-state ($d[NO_2]_r/dt = 0$), Equation 8 may be solved, using the parameters given above, for the room concentrations of NO_2. The results are $[NO_2]_r = 26$ and 10 $\mu g/m^3$, respectively, for $V_g = 0.32$ and 0.93 cm/sec, factors of 4 and 10 reductions from the outdoor level of 100 $\mu g/m^3$. Here, as in the case of NO_2--aerosol reactions, saturation effects would diminish the effective ness of active surfaces to remove NO_2 upon prolonged exposures. Similarly as in Equation 2, we may write

$$V_g = V_{go} \left[1 - [NO_2]_{ads}/[NO_2]_\infty\right]$$

where V_{go} = initial deposition velocity (0.32 or 0.93 cm/sec)

$[NO_2]_{ads}$ = total NO_2 removed from the room air by the cement surfaces at any given time

$[NO_2]_\infty$ = amount removed as $t \to \infty$.

For $[NO_2]_\infty$, our experimental results suggest a value of ~2 g/m^2. Thus, the value of NO_2 removed at $t = 0$ can be calculated from the last term in Equation 8, starting with the equilibrium values for $[NO_2]_r$ of 26 or 10 $\mu g/m^3$. These values can then be used for Equation 9 to calculate the decrease in V_g, and the results can be used with Equation 8 to determine changes in $[NO_2]_r$. The time can then be increased by Δt and the process repeated (i.e., numerical integration) to determine saturation effects. The results of this exercise indicated $[NO_2]_r$ increased to 40, 60, 80, and 100 $\mu g/m^3$, respectively, after 91, 167, 231, and 520 days for the case of $V_g = 0.32$ cm/sec; and after 135, 158, 175, and 270 days for $V_g = 0.93$ cm/sec.

The results discussed earlier suggest that as the active surfaces become saturated by NO_2 exposure (after ~3 to 6 mo for the example give here), surface activity could be restored simply by washing the surfaces with water. In view of the results obtained with ammonia exposure, common ammonical household cleaners would probably be even more beneficial.

Of course, unpainted cement has obvious esthetic problems associated with its use. However, other alkaline surfaces, such as decorative brick, might be as effective or perhaps even more effective in removing acidic NO_2 than the two cements studied here. Use of these materials in schools, nursing homes, hospitals, and other areas housing sensitive individuals might be particularly advantageous. One final advantage in employing these materials is that no energy expenditure is required in terms of air scrubbing or filtration.

REFERENCES

Abeles, F. B., L. E. Craker, L. E. Florence, and G. R. Leather. 1971. Fate of Air Pollutants: Removal of Ethylene, Sulfur Dioxide, and Nitrogen Dioxide by Soil. Science, 173:914-916.

Chang, S. G., and T. Novakov. 1975. Formation of Pollution Particulate Nitrogen Compounds by NO--soot and NH_3--soot Gas--Particle Surface Reactions. Atmos. Environ., 9:495-504.

Clarke, A. G., and L. G. Britton. 1977. Heterogeneous Reactions of Sulfur Dioxide and Nitrogen Dioxide. Proceedings of the 4th International Clean Air Congress, Tokyo. pp. 469-471.

Demerjian, K. L., J. A. Kerr, and J. G. Calvert. 1974. The Mechanism of Photochemical Smog Formation. In: Advances in Environmental Sciences and Technology, Vol. 4, J. N. Pitts and R. L. Metcalf, eds. John Wiley and Sons, New York. pp. 1-262.

Grosjean, D. 1979. Nitrogeneous Air Pollutants: Chemical and Biological Implications. Symposium at the 175th National Meeting, American Chemical Society, Anaheim, California, March 12-17, 1978. Ann Arbor Science, Ann Arbor, Michigan.

Harker, A. B., L. W. Richards, and W. E. Clark. 1977. The Effect of Atmospheric SO_2 Photochemistry upon Observed Nitrate Concentrations in Aerosols. Atmos. Environ., 11:87-91.

Hedgpeth, H., S. Siegel, T. B. Stewart, and H. S. Judeikis. 1974. Cylindrical Flow Reactor for the Study of Heterogeneous Reactions of Possible Importance in Polluted Atmospheres. Rev. Sci. Instrum., 45:344-347.

Hidy, G. M., and C. S. Burton. 1975. Atmospheric Aerosol Formation by Chemical Reactions. Int. J. Chem. Kin., Symp. No. 1:509-541.

Hill, C. A. 1971. Vegetation: A Sink for Atmospheric Pollutants. J. Air Pollut. Control Ass., 21:341-346.

Judeikis, H. S. 1979. Mass Transport and Chemical Reaction in Cylindrical and Annular Flow Tubes. Submitted to J. Phys. Chem.

Judeikis, H. S. 1979a. Use of Building Surfaces in the Passive Abatement of Gaseous Air Pollutants. J. Architect. Res., 7:28-33.

Judeikis, H. S., and S. Siegel. 1973. Particle-Catalyzed Oxidation of Atmospheric Pollutants. Atmos. Environ., 7:619-631.

Judeikis, H. S., and T. B. Stewart. 1976. Laboratory Measurement of SO_2 Deposition Velocities on Selected Building Materials and Soils. Atmos. Environ., 10:769-776, and references therein.

Judeikis, H. S., and A. G. Wren. 1978. Laboratory Measurements of NO and NO_2 Depositions onto Soil and Cement Surfaces. Atmos. Environ., 12:2315-2319.

Judeikis, H. S., and M. Wun. 1978. Measurement of Chlorine Atom Diffusion. J. Chem. Phys. 68:4123-4127.

Judeikis, H. S., T. B. Stewart, and A. G. Wren. 1978. Laboratory Studies of Heterogeneous Reactions of SO_2. Atmos. Environ., 12:1633-1641.

Judeikis, H. S., S. Siegel, T. B. Stewart, H. R. Hedgpeth, and A. G. Wren. 1979. Laboratory Studies of Heterogeneous Reactions of Oxides of Nitrogen. Symposium at the 175th National Meeting, American Chemical Society, Anaheim, California, March 12-17, 1978. Ann Arbor Science, Ann Arbor, Michigan. pp. 83-109.

Kaiser, E. W., and C. H. Wu. 1977. A Kinetic Study of the Gas Phase Formation and Decomposition Reactions of Nitrous Acid. J. Phys. Chem., 81:1701-1706.

Liberti, A., D. Brocco, and M. Possanzini. 1978. Adsorption and Oxidation of Sulfur Dioxide on Particles. Atmos. Environ., 12:255-261.

Preining, O. 1973. Discussion: Particle-Catalyzed Oxidation of Atmospheric Pollutants. Atmos. Environ., 7:925.

Shuck, E. A., and E. R. Stephens. 1969. Oxides of Nitrogen. In: Advances in Environmental Sciences, Vol. I, J. N. Pitts and R. L. Metcalf, eds. Wiley-Interscience, New York. pp. 73-118.

Stewart, T. B., and H. S. Judeikis. 1974. Measurements of Spatial Reactant and Product Concentrations in a Flow Reactor Using Laser Induced Fluorescence. Rev. Sci. Instrum., 45:1542-1545.

Ten Brink, H. M., J. A. Bontje, H. Spoelstra, and J. F. van de Vate. 1978. The Interaction Between NO_x, O_3 and Airborne Particles. In: Atmospheric Pollution 1978, Proceedings of the 13th International Colloquium, Paris, France, April 25-28, 1978. Studies in Environmental Science, Vol. 1, M.M. Benarie, ed. Elsevier, Amsterdam. pp. 239-244.

Walker, R. E. 1961. Chemical Reaction and Diffusion in a Catalytic Tubular Reactor. Phys. Fluids, 4:1211-1216.

MODELING ASPECTS OF NITROGEN OXIDES USING SMOG CHAMBER DATA

Harvey E. Jeffries
Ken Sexton

Department of Environmental Sciences and Engineering
School of Public Health
University of North Carolina
Chapel Hill, North Carolina 27514

INTRODUCTION

The definitions of aspect can be interpreted to mean what we see, what we reason, and what we believe. These describe well the concerns for modelers of oxides of nitrogen (NO_x) or hydrocarbon (HC) chemistry. Smog chamber and atmospheric data are what we see. Since these data do not include enough information, the modeler has to reason, on the basis of other laboratory data, that processes not actually observed in the smog chamber are occurring, and therefore he includes these processes in his model. Sometimes it is clear that what we can prove is happening and what we think is happening are not enough to explain what we see happening. So to predict what is seen but for which he has no proof, the modeler often must include processes that he believes are happening.

Numerical models require a value for every part of the model, so modelers must make choices; these choices involve uncertainties. It is this range of uncertainties about NO_x transformation processes that will be explored in this study. The technique will be to: 1) simulate a range of conditions in the UNC outdoor smog chamber with different models, and 2) compare the various model predictions of nitrogen species distribution to each other and to the chamber data. The object is to show the variability in choices of NO_x transformation chemistry in current mechanisms.

CONCLUSIONS AND RECOMMENDATIONS

The first conclusion is that it is relatively difficult to know that the various models used in this study were implemented correctly. The models generally appear as listings of chemical reactions and their rate constants. In the original formatting and printing of these listings, in reading and rekeypunching the mechanism, in choosing the rate constants for the reactions marked "experimental" or "k varying," errors can easily occur. Few mechanisms appear with a test simulation or example for comparison. Publications of mechanisms almost never include a listing of all species concentrations at a given time in a sample simulation. Few explicit details are given for time-varying photolysis rates. These uncertainties often cannot be resolved except by the exchange of computer printouts. This was done for several models included herein.

Secondly, current knowledge of nitrogen transformation processes allows a relatively wide range of choices in distribution of nitrogen in models. Because ozone (O_3) concentration is primarily dependent upon a ratio of nitrogen dioxide (NO_2) to nitric oxide (NO), the various models can simulate O_3 reasonably well, but with different NO_x chemistries. Thus, the use of these mechanisms to predict species other than O_3 may be a questionable practice.

Third, except for the DODGE mechanism, in which the peroxyacetyl nitrate (PAN) chemistry is known to be incorrect, all mechanisms, for all conditions simulated herein, predict more total nitric acid (HNO_3 or $HONO_2$) than PAN, usually by a factor of 2 or more. In addition, for auto-exhaust conditions one mechanism predicts more aromatic nitrate (ANO_3) than any other nitrogen product. Propylene--toluene experiments do suggest a unique aromatic nitrogen loss mechanism. Except for this ANO_3, all mechanisms predict very small concentrations of organic nitrates (RNO_3 or $RONO_2$).

Fourth, substantial nitrogen loss to the walls appears possible by a heterogeneous process, even in large chambers like those at the Univeristy of North Carolina at Chapel Hill. Without this nitrogen-loss process, models overpredict ozone. The extent to which this process occurs in the open atmosphere is not known. If it is an unimportant process, then smog chambers underestimate atmospheric ozone potential, and models used in air shed simulations must be adjusted accordingly.

Processes, probably heterogeneous, clearly exist for reconverting HNO_3 to NO_2 in the large Teflon chamber; thus, O_3 can form in conditions in which it otherwise might not (second day). The conditions for which this recycle occurs are not clearly understood; the results of 2-day (or overnight) experiments must be viewed with suspicion. The degree to which these recycle processes may occur on ambient surfaces adds an uncertainty to the gas-phase nitrogen removal rates in the environment. Clearly, further research is needed in this area.

Finally, NO_x behavior in smog chambers must be studied further if reliable models of nitrogen chemistry, and of ozone chemistry, are desired.

NITROGEN TRANSFORMATION PROCESS

Figure 1 illustrates the NO_x transformation processes thought to occur in smog chambers, including some speculative heterogeneous processes (Cox 1979; Jeffries 1980). Typically seen in smog chamber experiments is conversion of NO to NO_2, and the subsequent disappearance of NO_2. The extent of this conversion and disappearance is a function of both absolute concentrations of NO_x and HC, and the HC/NO_x ratio. Nitrogen species with long chemical lifetimes in smog chambers are $RONO_2$, $HONO_2$, and, to a lesser extent, PAN. The other nitrogen species have more or less transitory existences. It appears in most smog chambers that the nitrogen pentoxide (N_2O_5) + water (H_2O) reaction is an important nitrogen-loss mechanism, that this reaction is surface mediated, and that the

$HONO_2$ is formed on the walls. The consequences of this reaction occurring at significant rates are important and will be discussed later. Details of most nitrogen chemistry are discussed in other sections of this Proceedings.

MECHANISM CHARACTERISTICS

The primary goal in the development of all these mechanisms was to simulate chamber O_3 behavior. Table 1 lists key characteristics of the mechanisms used in the simulations of this study.

Two of the mechanisms, CARTER (Carter et al. 1979) and JEFFRIES (Jeffries 1980), are for propylene only. (The n-butane chemistry of Carter et al. was not implemented in this version.) The DODGE mechanism (Dodge 1977) is for a mixture of propylene and n-butane. It is an explicit mechanism, but is used to model the O_3 formation in complex mixtures. In its development, a 25/75-percent propylene/butane carbon split was used to represent auto exhaust in the Bureau of Mines (BOM) smog chamber. The last three mechanisms--CBII, DERMJ, and LLOYD--are "lumped" mechanisms, intended to model complex mixtures. The CBII, or carbon bond II, mechanism (Whitten et al. 1980) is a "model of a model" mechanism; it models carbon bonds rather than lumped species. The DERMJ mechanism (Demerjian 1979, personal communication) is a simple, lumped species mechanism used in the Photochemical Box Model (PBM). The (LLOYD) mechanism (Lloyd et al. 1979) is a more complex, lumped species mechanism and is used in ELSTAR, a Lagrangian atmospheric model.

The CARTER mechanism is the most explicit propylene mechanism in recent literature, accounting for more nitrogen species than does any other mechanism. The JEFFRIES mechanism simulates well the large seasonal effects caused by changes in temperature, humidity (H_2O) , and light intensity ($h\nu$) for propylene systems. The DODGE mechanism is the default mechanism for OZIPP/EKMA, the EPA oxidant control strategy calculation tool (Whitten and Hogo 1978). The CBII mechanism is used in the SAI airshed simulation model and therefore will be used in the EPA control strategy calculations. The DERMJ mechanism, in the PBM, will also be used in some EPA control strategy calculations. The LLOYD mechanism is part of a five-level Lagrangian model, initially used to simulate LARPP runs, and representing a somewhat more complex, lumped species mechanism.

The mechanisms were obtained either from the literature or directly from the authors. Where rate constants were specified, these rate constants were used directly. Since much uncertainty is associated with photolysis rate constants for aldehydes, a relatively wide range of choices of rates are allowed for this specie. These rate constants were expressed as a ratio to the NO_2 photolysis rate constant and are listed in Table 2. In addition, some mechanisms have a single, lumped species to represent all aldehydes; fractional stoichiometric coefficients were used to represent the fraction that is formaldehyde (HCHO). These coefficients are also indicated in the table of rate constants (Table 2).

Another area where the mechanisms differ significantly is the N_2O_5 chemistry. The rate constants for several nitrogen trioxide (NO_3) reactions have recently been reevaluated (Demore et al. 1979); in the CBII and DERMJ

TABLE 1. CHARACTERISTICS OF SIMULATION MECHANISMS USED IN THIS STUDY

	Mechanism					
Characteristic	CARTER	JEFFRIES	DODGE	CBII	DERM	LLOYD
Reactions:						
total no.	75	61	76	75	36	58
i/o*	32/43	30/31	23/53	14/61	19/17	17/41
temp†	0	17	0	6	0	4
H_2O†	1	5	3	1	1	2
light†	9	7	12	4	3	4
Species:						
total	38	30	36	30	23	40
i/o	14/24	15/15	12/24	9/21	12/11	14/26
organic	C_3H_6 C_1–C_2 ald	C_3H_6 C_1–C_2 ald MEK	C_3H_6, C_4H_8 C_1–C_4 ald.	PAR, OLE ETH, CARB ARO	HC_1, HC_2 HC_3, HC_4	PA, ALKE C_2H_4, AR RCHO, HCHO
N-species	NO_x, HNO_3 PAN, HO_2NO_2 RO_2NO_2, RNO_3 (HONO)	NO_x, HNO_3 PAN, HO_2NO_2 O_2NO_2, (HONO)	NO_x, HNO_3 PAN, (HONO)	NO_x, HNO_3 PAN, RNO_3 $ARONO_3$	NO_x, HNO_3 PAN, HO_2NO_2 RNO_3, (HONO)	NO_x, HNO_3 PAN, HO_2NO_2 RNO_3, $ARNO_3$ (HONO)
Chamber verification:	UCR	UNC	BOM	UCR, UNC	BOM	UCR
Comments:	most explicit C_3H_6 mechanism	simulates well the seasonal changes in temp, H_2O, and hν	EKMA mechanism	SAI airshed model mechanism	PBM mechanism	

*Number of inorganic/number of organic.

†Number of reactions with rate constants dependent on temperature, water vapor, or light intensity.

TABLE 2. RATE CONSTANTS (AT 298K) FOR SELECTED REACTIONS IN MECHANISMS

	Mechanism					
Reaction	CARTER	JEFFRIES	DODGE	CBII	DERM	LLOYD
$O_3+NO_2 \rightarrow NO_3+O_2$	5.47(-2)	4.80(-2)	4.50(-2)	4.80(-2)	5.5(-2)	5.0(-2)
$NO_3+NO \rightarrow 2NO_2$	2.80(+4)	2.80(+4)	1.30(+4)	2.80(+4)	1.1(+4)	2.7(+4)
$NO_3+NO_2 \rightarrow N_2O_5$	6.80(+3)	3.93(+3)	5.60(+3)	-	-	9.3(+2)
$N_2O_5 \rightarrow NO_3+NO_2$	22.2	6.85	22.0	-	-	91.3
$H_2O+N_2O_5 \rightarrow 2HNO_3$	1.5(-5)	1.5(-5)	2.50(-6)	[1.50(-5)]	[1.1(-5)]	1.0(-6)
$H_2O+NO_3+NO_2 \rightarrow 2HNO_3$	-	-	-	4.8(-3)	3.4(-3)	-
HCHO→radicals*	1.5(-3)	2.90(-3)	2.40(-3)	(1/2) 4.10(-3)†	(1/2) 1.65(-3)†	2.0(-3)
HCHO→stable*	-0-	7.10(-3)	2.00(-3)	3.80(-3)*	-0-	2.0(-3)
RCHO→radicals*	8.40(-4)	1.0(-3)	1.0(-3)	(1/2) 4.10(-3)†	(1/2) 1.65(-3)†	8.0(-4)
OH+HCHO→	1.39(+4)	1.40(+4)	1.50(+4)	1.90(+4)	2.2(+4)	1.60(+4)
OH+RCHO→	2.36(+4)	2.40(+4)	1.50(+4)	-	-	2.20(+4)

*Ratio of photolysis rate to the photolysis rate of NO_2.

†A single lumped species represented HCHO and higher aldehydes; the fraction that was HCHO was 1/2.

mechanisms, N_2O_5 was assumed to be in steady state and, therefore, was not represented in either mechanism. Thus, the following three reactions:

$$NO_3 + NO_2 \rightarrow N_2O_5 \qquad k_1 \qquad (1)$$

$$N_2O_5 \rightarrow NO_3 + NO_2 \qquad k_2 \qquad (2)$$

$$H_2O + N_2O_5 \rightarrow 2\ HONO_2 \qquad k_3 \qquad (3)$$

were lumped into

$$H_2O + NO_3 + NO_2 \rightarrow 2HNO_3 \qquad k_{eff} = k_3(k_1/k_2) \qquad (4)$$

For CBII, the reaction rate used for Equation 4 was 4.8×10^{-3} ppm^{-2} min^{-1} at 298 K, which corresponds to a reaction rate of 1.5×10^{-5} ppm^{-1} min^{-1} for Equation 3, the same as the CARTER and JEFFRIES rate. For DERMJ, the reaction rate used for Equation 4 was 3.4×10^{-3} ppm^{-2} min^{-1}, which corresponds to a rate of 1.1×10^{-5} ppm^{-1} min^{-1} for Equation 3, about 25 percent lower than the CARTER, JEFFRIES, or CBII rate. In addition to the older rate constants for Equations 1 and 2, the DODGE mechanism has a lower reaction rate for Equation 3. The LLOYD mechanism uses a very low rate for Reaction 1, a very high rate for Reaction 2, and the lowest rate for Reaction 3, resulting in the formation of significantly less HNO_3 by this path.

As will be shown later, the rate of Reaction 3, or its equivalent in Reaction 4, is an important factor in the various models. Because the rate is important, and because it may be heterogeneously controlled, the nitric acid formed--presumably on the walls, by the N_2O_5 pathway (N_2O_5 + H_2O)--will be labeled as $WHNO_3$ in the model results presented here.

Other areas of differences in the nitrogen chemistry of the models include: whether the chemistry of peroxynitric acid (HO_2NO_2) was in the model and what rates were used; whether the chemistry of nitrous acid (HONO or HNO_2) was in the model; and whether $RONO_2$ formation was included and what pathways of formation were used.

In the CARTER and JEFFRIES mechanism, the formation of HO_2NO_2 has the potential to "store" hydroperoxide (HO_2) radicals, as nitric oxide (NO) is being converted to NO_2; and then to "release" these radicals and NO_2, as NO_2 is being removed and O_3 is forming. This process may be important at high HC concentrations or at cooler temperatures where the HO_2NO_2 is more stable. In the DERMJ mechanism, the rate constants used for the formation and decomposition of HO_2NO_2 are such that significant amounts of HO_2NO_2 remain at the end of the simulation. Current knowledge would suggest that this does not occur in the real world (Graham et al. 1978). In such a short mechanism, however, it is necessary to limit the O_3 production. The DODGE and CBII mechanisms do not include HO_2NO_2 chemistry.

Whitten et al. (1980) demonstrated that for many explicit simulations it makes little difference if HONO chemistry is included in the model; the CBII mechanism therefore excludes HONO chemistry for the sake of compactness.

Although the other mechanisms under study include HONO chemistry, the relative importance of this chemistry to predictions of these mechanisms was not tested.

Since the JEFFRIES mechanism was only for propylene, the formation of RNO_3 was omitted. In this system, the expected formation path for RNO_3 would be

$$RO + NO_2 \rightarrow RNO_3 \tag{5}$$

and the reactions

$$RO \rightarrow Ald + H \tag{6}$$

and

$$RO + O_2 \rightarrow Ald + HO_2 \tag{7}$$

compete very effectively with Reaction 5. In the JEFFRIES and DODGE models, pathways like Reactions 6 and 7 were considered to be the exclusive pathways. Therefore, no RNO_3 species are in these mechanisms. On the other hand, the CARTER mechanism included every possible RNO_3 formation pathway for propylene. The model predictions for these species will be shown later. Since the CBII, DERMJ, and LLOYD mechanisms were intended to model mixtures, they included

$$RO_2 + NO \rightarrow RNO_3, \quad R > C_4 \tag{8}$$

as a pathway for RNO_3 formation (Darnall et al. 1976), and the rates were adjusted to represent the fraction of RO_2's that were "long chain." In addition, the CBII and LLOYD mechanisms included a pathway for aromatic organic nitrate ($ARONO_2$ or $ARNO_3$) formation. These pathways are currently speculative, and typically the rates are adjusted to obtain good agreement with smog chamber observations of O_3 and NO_x.

CHAMBER EXPERIMENTS AND SIMULATIONS

Although the intent of this study is to compare each mechanism to all others under the same input conditions, it is helpful to have some external reference. Therefore, several experiments in the UNC chamber were selected to provide the set of inputs and serve as references for the models. Table 3 gives the initial conditions and HC types for these experiments.

The August 8, 1977, propylene run (Figures 2, 3, and 4) had good nitrogen (Figure 5) and carbon balances (Figure 6); the results of this run also illustrate the strong effects of temperature on O_3 formation. Propylene is the simplest HC that exhibits all the major smog chemistry and is a significant atmospheric olefin. It has also been the most studied and the most modeled. Most mechanisms should do well for propylene: all mechanisms were run for the August 8 conditions.

The June 19, 1978, experiment (Figure 22) was a direct test of the reactivity of a 25-percent propylene/75-percent butane mixture, compared to a

TABLE 3. CHAMBER EXPERIMENTS AND SIMULATIONS

Experimental Characteristic	August 8, 1977	June 19, 1978		September 18, 1978		June 13, 1979	
		Red	Blue	Red	Blue	Red	Blue
HC type:	propylene	UNC Mix	propylene butane	auto exhaust	UNC Mix	propylene	propylene toluene
ppmC	1.68	2.14	2.07	3.1	3.1	2.7	5.5
NO_x, ppm	0.495	0.35	0.35	0.34	0.34	0.45	0.45
Mechanism and simulation studied:	CARTER JEFFRIES DODGE CBII/CT CBII/VT DERMJ	CBII DERMJ LLOYD	DODGE CBII/VT	DODGE DERMJ LLOYD CBII/VT		CBII/TOL	CBII/TOL

TABLE 4. 1978 UNC SIMULATED URBAN HYDROCARBON MIX

Class/Compound	Carbon Fraction		Mole Factor
	UNC* Analysis	Matheson Analysis	UNC* Analysis
Paraffins			
isopentane	0.1484	0.1270	0.1273
n-pentane	0.2531	0.2535	0.2411
2-methy-pentane	0.0996	0.1027	0.0712
2,4-dimethyl-pentane	0.0864	0.0791	0.0528
2,2,4-dimethyl-pentane	0.1202	0.1111	0.0644
Subtotal	0.7077	0.6734	0.5568
UNC Average Carbon Number = 5.89			
Olefins			
1-butane	0.0254	0.0301	0.0272
C15-2-butane	0.0313	0.0297	0.0335
2-methyl-butane	0.0347	0.0393	0.0298
2-methyl-2-butane	0.0317	0.0393	0.0272
ethylene	0.1167	0.1343	0.2504
propylene	0.0524	0.0539	0.0750
Subtotal	0.2922	0.3266	0.4431
UNC Average Carbon Number = 2.78			
TOTAL	0.9999	1.0000	0.9999

*UNC analysis is based on an average of many determinations of what actually appears in the chamber.

more complex urban type mixture. Table 4 lists the compounds and the distribution for the UNC mix. The BLUE side of this run is a good direct test of the DODGE mechanism, which was only verified for the indoor BOM chamber. Simulating the RED mix side of this run exercises the paraffin/olefin portion of the lumped mechanisms.

The September 18, 1978, experiment (Figure 30) was a direct comparison of the reactivity of automobile exhaust and the UNC mix. The auto exhaust was from a fast-idle, uncontrolled car and was probably more reactive than, for instance, the BOM auto exhaust. Simulating this run provided for exercising the aromatics portion of the mechanisms and allowed for including initial aldehydes.

The June 13, 1979, run (Figure 35) illustrates the special nature of aromatics. Adding more carbon, but in the form of toluene, resulted in the formation of less O_3 and PAN. This phenomenon is thought to result from a nitrogen removal process unique to aromatics chemistry. This run and its simulation by one mechanism is included to show how this process might occur.

In addition to the basic simulations shown in Table 2, other simulations were performed to illustrate certain mechanism responses to changes in input conditions. These simulations will be discussed later.

RESULTS AND DISCUSSION

August 8, 1977, (Propylene) Experiment

The experimental results for nitrogen species and O_3 are shown in Figure 2, and those for the organic species are shown in Figure 3. This was a matched dual run. Only the RED side of the chamber is shown in Figure 2, but both RED and BLUE results are shown in Figure 3. The two sides were essentially identical. Figure 4 shows the total solar radiation (TSR), chamber temperature, and dew point for the run. It is clear that the variations in O_3 in Figure 2 are correlated with the occurrence of clouds, as shown by the TSR curve. The chamber temperature also fluctuated with TSR.

Figure 5 presents a nitrogen balance (N-BAL) for August 8. Significantly, between 20 and 25 percent of the original nitrogen was not measured as NO, NO_2, PAN, nor gas-phase NO_3. Figure 6 presents a carbon balance for August 8. Since carbon dioxide (CO_2) is not measured in the chamber, the amount of unmeasured carbon in the form of CO_2 is not known. Models suggest that about 0.15 ppmC could be CO_2, resulting in a nearly perfect carbon balance.

Table 5 gives the initial conditions for each of the simulations. For ease of simulation, a smooth light profile--following the shape of the TSR curve in Figure 3 up to about 12 noon, but smoothed through the high points of the TSR curve after 12--was used to derive the photolysis rates for each simulation of August 8. The actual temperature data in Figure 4 were used in the simulations. Thus, all simulations would be expected to form more O_3 than is shown in Figure 2. Since all models used the same light profile, however, relative comparisons are valid. The DATA column of Table 6 gives the N-BAL at O_3 maximum for the experimental data.

TABLE 5. INPUT DATA AND PARAMETERS FOR MODELS FOR AUGUST 8, 1977

Compound	CARTER1	CARTER2	JEFFRIES	DODGE[†]	CBII/CT[‡§]	CBII/VT[‡§]	LLOYD/UNC	DERMJ[§]
HNO (ppb)	2.5	0	0	2.5	-	-	0	0
HC (ppm by vol)	C_3H_6: 0.56	C_3H_6: 0.56	C_3H_6: 0.56	C_3H_6: 0.56	PAR: 0.56 OLE: 0.56	PAR: 0.56 OLE: 0.56	ALKE: 0.56	HC1 0.56

[*] Except as noted, all models had: $[NO]_0$ = 0.395 ppm, $[NO_2]_0$ = 0.100 ppm, $[CO]_0$ = 0.4 ppm, $[O_3]_0$ = 0.1 ppb, $[H_2O]_0 = 2 \times 10^4$ ppm; photolysis rates were scaled to TSR for August 8. Models with temperature dependence used chamber temperature data for August 8, 1977.

[†] DODGE model did not have initial CO.

[‡] CT = constant temperature, VT = variable temperature.

[§] CBII and DERMJ models did not have initial O_3.

TABLE 6. N-BAL (PERCENT) AT O_3 MAXIMUM FOR MODELS AND DATA, AUGUST 8, 1977[*]

Species	DATA[†]	CARTER1	CARTER2	JEFFRIES	DODGE	CBII/CT	CBII/VT	LLOYD/UNC	DERMJ
NO_2	8.2	32.73	0.32	9.31	0.00	1.50	5.42	0.90	5.24
NO	0.4	0.95	0.000	0.13	0.00	0.03	0.07	0.01	0.11
$WHNO_3$[‡]	(24.4)	21.25	29.08	25.96	4.60	31.63	25.75	49.23	18.22
HNO_3	39.3	26.95	35.32	44.78	35.84	32.72	40.15	28.78	24.07
HO_2NO_2	-	0.18	0.01	1.23	-	-	-	0.02	17.77
RNO_3	-	3.37	3.80	-	-	2.33	3.08	0.15	3.57
PAN	27.6	14.47	31.49	18.44	60.04	31.86	25.54	20.68	30.95
TOTAL	100.0	99.90	100.02	99.92	100.00	100.04	100.01	99.76	99.93
O_3 max (ppm)	>0.90	0.458	0.696	0.953	0.584	0.783	0.949	0.991	0.784

[*] Initial conditions: 0.495 ppm NO_2, 1.5 ppmC propylene.

[†] This value is the N-BAL at O_3 maximum for experimental data.

[‡] $WHNO_3$ is formed from $N_2O_5 + H_2O$.

CARTER Simulation--

The initial CARTER1 simulation of August 8 is shown in Figure 7. As indicated in Table 5, this simulation included 2.5 ppb of HONO as an initial radical source, because inspection of the mechanism indicated that it would probably be necessary. Even with this initial HONO, the simulation is slow and is less reactive than the actual data. In the original development of the mechanism, Carter noted the slowness of his mechanism and therefore included an artificial source of radicals (? + hν → OH) at rates that varied from 0.12 to 0.71 ppb/min. Several simulations of August 8 which included this reaction were performed. The simulation that used an OH input of 0.12 ppb/min is shown in Figure 8. The several speculative aspects of the CARTER mechanism include $RONO_2$ production, which is discussed above. The mechanism predictions for $RONO_2$ for the two simulations are shown in Figure 9 and 10. In Table 6, the N-BAL for the CARTER simulations at O_3 maximum is given.

A prime reason for the slowness or low reactivity of the CARTER mechanism is the production of large amounts of 2-hydroxy propanol as opposed to acetaldehyde (RCHO) and formaldehyde (HCHO). The species has not been measured in smog chambers. (It would be a difficult measurement to make.) One reason for the production of 2-hydroxy propanol in the CARTER mechanism is to improve consistency with RCHO and HCHO measurements in the UCR chamber. The latter are generally lower than measurements in similar UNC chamber runs (Pitts et al. 1979). Because hydroxyaldehyde instead of RCHO and HCHO is produced, a substantial source of "maintenance" radicals from the aldehyde photolysis reactions is initially lost. It should be noted that the mechanism included only HCHO photolysis to radicals (Table 2); this is one way to maximize photolysis-generated radicals, but it could also suggest that not enough HCHO is being produced to allow inclusion of both pathways. The decrease in RCHO and HCHO production and therefore the necessity to include another radical source (? + hν → OH) at high rates means that the CARTER propylene mechanism is almost totally dominated by the magnitude of this artifical reaction.

JEFFRIES Simulation--

Figure 11 shows a comparison between the model predictions (solid lines) and the experimental measurement (dashed lines and symbols) for the JEFFRIES mechanism. This simulation was originally performed as part of another study to investigate mechanisms for simulating large temperature and water vapor effects of summer, fall, and winter conditions. The mechanism was not adjusted between simulations.

One result of this study was that all experimental chamber data were consistent with a single, relatively large rate constant (1.5×10^{-5} ppm^{-1} min^{-1}) for $N_2O_5 + H_2O \rightarrow 2HNO_3$. That is, when the appropriate H_2O concentration and temperature for the $N_2O_5 \rightarrow NO_2 + NO_3$ reaction (as well as others) were used in the simulation, good agreement was obtained for all measured species, provided the HNO_2 formed above was not included in HNO_3 formed by other pathways (mainly $OH + NO_2 \rightarrow HNO_3$). This result is consistent with the occurrence of the N_2O_5 reaction as a surface process. The nitric acid formed by N_2O_5 reaction with H_2O was called $WHNO_3$, and it was assumed to be on the walls.

The predicted N-BAL for the JEFFRIES simulation is shown in Figure 12, and it is to be compared with the experimental N-BAL shown in Figure 5. The $WHNO_3$

prediction agrees very well with the missing nitrogen in Figure 5. The N-BAL at O_3 max for the JEFFRIES mechanism is given in Table 6.

DODGE Simulation--

The DODGE simulation of August 8 is shown in Figure 13. This simulation exercises only the propylene portions of the mechanism. Because the DODGE mechanism was formulated in 1976, it contains several areas now known to be incorrect. Nevertheless, it is well known and still the major mechanism for EKMA. The PAN portion of the DODGE mechanism is one area for which new data are available (Hendry and Kenley 1977). New kinetics data for PAN are included in all the other mechanisms, resulting in significantly lower PAN predictions in comparison to the DODGE mechanism. Because the DODGE mechanism removes nitrogen into PAN as a stable product, NO_2 is not available for continued O_3 formation, and thus much less O_3 is predicted. The high temperature of the August 8 run further enhances the PAN recycle process, resulting in a strong temperature effect on O_3 formation that is not captured in the constant temperature DODGE (and CARTER) mechanism. The N-BAL at O_3 max for the DODGE simulation is given in Table 6.

CBII Simulation--

This simulation exercises the olefin and some of the paraffin portion of the mechanism. Since the CBII mechanism is designed for variable temperature (VT) simulations, two simulations--one at constant temperature (CBII/CT) and one using the temperature profile for August 8 (CBII/VT)--were performed; these are shown in Figures 14 and 15. At constant temperature, equal amounts of PAN and gaseous HNO_3 and a lower amount of O_3 are produced (Figure 14). At the actual temperature of the run, significantly less PAN and more O_3 are produced (Figure 15). The CBII mechanism has been used with different rates for the $N_2O_5 + H_2O \rightarrow WHNO_3$ reaction. For the purposes of this series of comparisons, the rates in Table 2 were used. The sensitivity to this choice will be discussed below. Table 6 gives the N-BAL at O_3 maximum for the two CBII simulations of August 8, 1977.

LLOYD Simulation--

This simulation exercises only the alkene portion of the lumped mechanism. Because some difficulties were encountered in simulating August 8 data using the LLOYD mechanism and the rate constants given in Table 2, a LLOYD simulation using the JEFFRIES rate constants for the N_2O_5 reactions was performed; results are shown in Figure 16. The difficulties and the simulation using the LLOYD values in Table 2 will be discussed later. Table 6 gives the N-BAL at O_3 maximum for the August 8 simulation with the LLOYD mechanism and the UNC, or JEFFRIES, N_2O_5 rate constants.

DERMJ Simulation--

This simulation exercises only the HC1 (olefin) portion of the mechanism. Figure 17 shows the August 8 simulation using the DERMJ mechanism. The mechanism predicts more PAN than gaseous HNO_3 and a larger amount of HO_2NO_2 (17 percent of the nitrogen ends up as HO_2NO_2). This is a consequence of the rate constants used for formation and decomposition of HO_2NO_2. Table 6 gives the N-BAL at O_3 maximum for the August 8 DERMJ simulation.

August 8 Simulations Discussion--

Table 6 illustrates, for a system as simple as propylene, the wide range of choices in modern photochemical kinetics mechanisms. Predictions of percent nitrogen, by species, range as follows (excluding CARTER 1): NO_2, 0.0 to 9.3; NO, 0.0 to 0.13; PAN, 18.44 to 60.0; HNO_3, 24.1 to 44.8; $WHNO_3$, 4.6 to 49.2; HO_2NO_2, 0 to 17.7; RNO_3, 0 to 3.8; and for O_3 max, the predicted range was 0.584 to 0.991 ppm.

Five simulations predict more gaseous HNO_3 than PAN, some by nearly a factor of 2. In only one mechanism (DODGE with incorrect PAN chemistry) does PAN exceed total HNO_3 (i.e., $WHNO_3$ + HNO_3); total HNO_3 accounts for about 60 percent of the nitrogen in the majority of the simulations, even in this propylene system which should have a high yield of PAN.

The O_3 maximum data shown in Table 6 indicate that only three mechanisms were close to the observed O_3 maximum: JEFFRIES, CBII/VT, and LLOYD/UNC. Of these three, CBII/VT agrees most closely in N-BAL with the observed data. Comparison of the CBII/CT simulation to the CBII/VT simulation shows that temperature can be a significant factor in N-BAL and O_3 production. On the other hand, comparison of Figures 11 and 15 shows that the CBII/VT simulation is substantially faster (>60 min) than the JEFFRIES simulation and the actual data for August 8.

Heterogeneous Chemistry Discussion--

Since it appears from Table 6 that N_2O_5 heterogeneous chemistry has a significant effect on N-BAL and O_3 production, three simulations were performed using different rates for this chemistry. The JEFF/N (Figure 18) and CBII/N (Figure 19) mechanism simulations for August 8 omitted the $N_2O_5 + H_2O \rightarrow 2HNO_3$ reaction. Without this nitrogen loss, more NO_2 is available for O_3 production, and the models predict values of 1.05 and 1.16 ppm O_3. The shifts in N-BAL and the values of the original simulations are given in Table 7. In both simulations, NO_2 and HNO_2 increase more than PAN; this is in part caused by the short lifetime of PAN at the run conditions. It is clear that the importance of the N_2O_5 process in the ambient urban environment must be assessed if kinetic models are to be used in control strategy calculations. In some mechanisms, like DODGE and LLOYD, this process is assigned a low value (Table 2), and in others, like the CBII or DERMJ, it is assigned values similar to those used in smog chambers or intermediate values.

Included in this group of simulations is the original LLOYD simulation of August 8 (Figure 20) using rate constants (Table 2 values) specified by Lloyd et al. (1979). The N-BAL's for this simulation and the simulation using UNC N_2O_5 rates are included in Table 7 for comparison. The simulation revealed a significant problem with the LLOYD mechanism: it does not conserve mass (Figure 21).

Thus, as long as nitrogen is available, the mechanism can make aldehydes, which in turn generate more radicals, which generate more aldehydes. By this process, the mechanism produces more aldehydes than carbon available in the initial propylene. The LLOYD mechanism includes a low loss rate for NO_2 by the N_2O_5 pathway; this, coupled with the above sequence, results in an artificially high reactivity for O_3 formation. Adding NO_2 losses, such as in Figure 16, decreases the amount of aldehydes formed and thus lowers the number of radicals and consequently the number of NO oxidations (and therefore O_3 formation).

TABLE 7. N-BAL (PERCENT) AT O_3 MAXIMUM FOR MODELS AND DATA, AUGUST 8, 1977*

SPECIES	DATA	JEFF	JEFF/N	CBII/VT	CBII/N	LLOYD/N_2O_5	LLOYD/VT
NO_2	8.2	9.31	13.0	5.42	10.85	0.90	39.52
NO	0.4	0.13	0.13	0.07	0.10	0.01	0.41
$WHNO_3$	(24.4)	25.96	-	25.75	-	49.23	0.15
HNO_3	39.3	44.78	56.89	40.15	55.62	28.78	36.13
HO_2NO_2	-	1.23	1.78	-	-	0.02	0.30
RNO_3	-	-	-	3.08	3.50	0.15	0.20
PAN	27.6	18.44	26.85	25.54	29.83	20.68	23.20
TOTAL	100.0	99.92	98.66	100.01	99.89	99.76	99.90
O_3 max (ppm)	>0.90	0.953	1.049	0.949	1.159	0.991	1.154

*Initial conditions: 0.495 ppm NO_x, 1.5 ppmC propylene.

The CBII mechanism has a unique way of incorporating the exact carbon mass and has a way to deplete the carbon mass. Some difficulties remain when all the PAR (paraffin) carbons are gone, since oxidation can continue; this process is obvious, however.

June 19, 1978, (Paraffin/Olefin) Experiment

The June 19, 1978, experimental results for NO, chemiluminescent NO_2 (includes PAN), and O_3 are shown in Figure 22; the solid lines are for the 11-component UNC mix (Table 4), and the dashed lines are for a 25-percent-propylene/75-percent-n-butane mixture. The UNC mix side had slightly more initial HC and produced slightly more O_3.

Table 8 gives initial conditions and physical parameters used in the simulation. For the mix simulations, the carbon fractions given in Table 4 were used to calculate HC species initial conditions.

Dodge Simulations--

Two simulations of June 19, propylene/butane side, were performed with the DODGE mechanism; the second simulation used initial HONO as a radical source to speed up the initial portion of the simulation. The simulations are shown in Figures 23 and 24. The DODGE mechanism is an explicit mechanism for propylene/ /butane, and it predicts the O_3 on June 19 reasonably. It overpredicts PAN. Table 9 gives the N-BAL at O_3 maximum for the DODGE simulation of June 19.

TABLE 8. INPUT DATA AND PARAMETERS FOR MODELS FOR JUNE 19, 1978*

	PROPYLENE/BUTANE			MIX			
Compound	DODGE†	DODGE†	CBII/VT‡	DERMJ	CBII/VT‡	LLOYD	LLOYD
HONO (ppb)	0	3.0	-	0	-	0	0
HC (ppm by vol)	PROP: 0.164	PROP: 0.164	OLE: 0.164	HC1: 0.214	OLE: 0.124	ALKE: 0.101	ALKE: 0.101
	BUT: 0.395	BUT: 0.395	PAR: 1.744	HC2: 0.2497	ETH: 0.152	C_2H_4: 0.13	C_2H_4: 0.13
					PAR: 1.608	PA: 0.251	PA: 0.251
							RCHO: 0.05
							HCHO: 0.09

*Except as noted, all models had: $[NO]_0 = 0.261$ ppm, $[NO_2]_0 = 0.091$ ppm, $[CO]_0 = 0.4$ ppm, $[O_3]_0 = 0.1$ ppb, $[H_2O]_0 = 2\times10^4$ ppm; photolysis rates scaled to TSR for June 19, 1978. Models with temperature dependence used chamber temperature data for June 19.

†DODGE model did not have initial CO.

‡CBII model did not have initial O_3.

TABLE 9. N-BAL (PERCENT) AT O_3 MAX FOR JUNE 19, 1978*

Species	DATA	DODGE	DODGE	CBII/VT	DERMJ	LLOYD	CBII/VT	DATA
NO_2	<19	2.086	16.27	17.01	9.13	9.17	13.45	<18
NO		0.59	0.45	0.23	0.19	0.11	0.16	
$WHNO_3$		3.07	3.27	17.87	20.72	35.36	19.20	
HNO_3		42.93	45.18	47.98	38.12	32.32	47.04	
HO_2NO_2					14.22	1.14		
RNO_3				4.86	2.30	0.11	4.68	
PAN	<24	31.93	35.17	12.07	15.78	21.34	15.55	<25
TOTAL		99.39	100.34	100.02	100.45	99.54	100.07	
O_3 max (ppm)	0.435	0.463	0.476	0.645	0.626	0.850	0.692	0.500

*Initial conditions: 0.352 ppm NO_x, 2.07 ppmC propylene/butane; 0.352 ppm NO_x, 2.14 ppmC UNC mix.

CBII/VT Simulations--

Two CBII simulations were performed using variable temperature. In the results shown in Figure 25, the initial conditions were for the propylene/butane side of June 19. Figure 26 shows the simulation of the mix side. Although the CBII mechanism correctly predicts more O_3 on the mix side, both simulations overpredict O_3 by 150 percent. Several other mix days were simulated with CBII, and O_3 was overpredicted in all cases tested.

Interestingly, more PAN is predicted in the mix simulation than in the propylene/butane simulation; since the HNO_3 and NO_3 predictions are almost identical, more NO_2 was converted into PAN. Table 9 gives the N-BAL at O_3 maximum for the CBII simulations of June 19.

DERMJ Simulation--

The simulation results are shown in Figure 27. A comparison of Figure 26, the CBII mechanism, and Figure 27, the DERMJ mechanism, shows that the predictions are almost identical for NO, NO_2, and PAN. Like the CBII mechanism, the DERMJ mechanism also overpredicts the O_3 (125 percent) for the paraffin/olefin mixture. Less HNO_3 is predicted by the DERMJ mechanism, because formation of a large quantity (14 percent of the initial nitrogen) of HO_2NO_2 is predicted. Table 9 gives the N-BAL at O_3 maximum for this June 19 simulation.

LLOYD Simulation--

Two simulations were performed using initial conditions slightly different than those indicated in Table 8. In the first, shown in Figure 28, only initial paraffins and olefins were used as the HC. The mechanism exhibited very low reactivity, in contrast to its behavior for the August 8 propylene simulations. Since the auto exhaust simulation discussed below (Figure 33) was more reasonable, a second June 19 simulation was performed, but the initial aldehydes of the auto exhaust simulation were added to the paraffin/olefin mixture (Table 8). The results of this simulation are shown in Figure 29. This simulation exhibited a great overprediction of O_3 and higher reactivity for NO_x. This sensitivity of predictions is due, in part, to the aldehyde-peroxy radical chemistry of this mechanism, that is, the nonconservation of carbon mass, which was discussed earlier. Table 9 gives the N-BAL at O_3 maximum for the second LLOYD simulation of June 19, 1978.

June 19 Simulations Discussion--

Of the four mechanisms used to simulate the two systems of June 19, only the DODGE simulation gave a reasonable prediction of O_3 maximum; the other mechanisms overpredicted O_3 by 125 to 170 percent. All mechanisms predicted more gas-phase HNO_3 than PAN, with ratios between nearly 4 to 1 and about 1.5 to 1. All but the DODGE mechanism predicted that total nitric acid (HNO_3 + $WHNO_3$) is nearly 60 percent of the initial nitrogen, a figure similar to that for the propylene simulation.

September 18, 1978 (Auto Exhaust) Experiment

Results of this auto exhaust--mix comparison experiment are shown in Figure 30. The auto exhaust was from a 1969 fast-idle automobile, and for the simulations, the HC concentrations given in Table 10 were used. These concentrations were obtained from applying each author's HC fractionation for auto exhaust to the total carbon injected into the chamber.

TABLE 10. INITIAL HC CONCENTRATIONS (ppm BY VOL) USED IN SIMULATION MODELS FOR SEPTEMBER 18, 1978*

DODGE†	CBII/VT	DERMJ‡	LLOYD
PROP: 0.258	OLE: 0.051	HC1: 0.2155	ALKE: 0.16
BUT: 0.581	ETH: 0.051	HC2: 0.1789	C_2H_4: 0.05
HCHO: 0.100	PAR: 1.953	HC3: 0.1643	PA: 0.215
	ARO: 0.124	HC4: 0.1113	AR: 0.12
	HCHO: 0.115		RCHO: 0.05
			HCHO: 0.09

*Except as noted, all models had: $[NO]_0 = 0.255$ ppm, $[NO_2]_0 = 0.085$ ppm, $[CO]_0 = 0.4$ ppm, $[O_3]_0 = 0.1$ ppb, $[H_2O]_0 = 2 \times 10^4$; photolysis rates were scaled to TSR for September 18, 1978. Models with temperature dependence used chamber temperature data for September 18, 1976.

†DODGE model did not have initial CO.

‡DERMJ model did not have initial O_3.

DODGE Simulation--

The simulation results are shown in Figure 31. For the auto exhaust run, the simulation predicts too much PAN, and thus O_3 generation is substantially curtailed. The maximum O_3 predicted, however, agrees quite well with that of the mix. The mix composition was that of Table 4, except that acetylene was included, resulting in about 5 percent unreactive carbon. The mix composition, 70 percent paraffin/30 percent olefin, was therefore close to the DODGE mix of 75 percent paraffin/25 percent olefin. Table 11 gives the N-BAL for the DODGE simulation.

CBII/VT Simulation--

The CBII/VT simulation (Figure 32) is very close to the experiment, except for the O_3 maximum. It appears that the simulation simply ran out of NO_2 a little early. Comparison of the predicted PAN with the later afternoon chemiluminescent NO_2 values (which include PAN) suggests that the simulation did not make enough PAN. The aromatics chemistry of the CBII mechanism includes the formation of an ANO_3 (Figure 32). In the simulation, the formation of this compound accounted for 34 percent of the nitrogen, and PAN formation accounted for 12 percent of the nitrogen. It appears that if the

ANO_3 production rate were reduced somewhat, more PAN would have formed, and O_3 production could have continued slightly longer, providing a much better prediction of the auto exhaust experiment. Table 11 gives the N-BAL for the CBII simulation for September 18, 1978.

TABLE 11. N-BAL (PERCENT) AT O_3 MAX FOR MODELS, SEPTEMBER 18, 1976*

Species	DATA	DODGE	CBII/VT	DERMJ	LLOYD
NO_2	10	3.35	2.30	5.52	6.80
NO		0.05	0.03	0.07	0.07
$WHNO_3$		6.06	12.24	29.80	47.31
HNO_3		33.90	33.68	26.39	26.03
HO_2NO_2				12.29	0.10
RNO_3			5.15	2.18	0.08
ANO_3			34.23		2.08
PAN	<25	56.41	12.41	23.59	16.35
TOTAL	35	99.77	100.04	99.84	98.82
O_3 MAX (ppm)	0.78	0.501	0.598	0.584	0.652

*Initial conditions: 0.340 ppm NO_x, 3.1 ppmC auto exhaust.

DERMJ Simulation--

The DERMJ simulation (Figure 33) resulted in NO, NO_2, and O_2 predictions nearly identical to the CBII/VT simulation (Figure 32). The nitrogen balance for the DERMJ simulation, however, differs significantly from that of the CBII simulation (Table 11). The DERMJ mechanism lumped organic nitrates in the aromatic chemistry with paraffin nitrates as RNO_3 and thus had no ANO_3. Without the extra nitrogen loss as ANO_3, the DERMJ mechanism predicts more PAN (in approximate agreement with the experimental data). The mechanism also predicts that 12 percent of the nitrogen is converted to HO_2NO_2, however, which almost certainly does not occur. It is clear that similar NO, NO_2, and O_3 predictions can be achieved in many ways in current mechanisms.

LLOYD Simulation--

The LLOYD simulation results are shown in Figure 34. The simulation more closely agrees with the paraffin/olefin mix run (Figure 30, dashed lines) than with the auto exhaust run. The simulation included aromatics and initial aldehydes, however (Table 10). Table 11 gives the N-BAL for the LLOYD simulation of September 18, 1978.

September 18, 1978, Simulation Discussion--

Again only the DODGE mechanism predicted more PAN than HNO_3. Total nitric acid ($WHNO_3$ + HNO_3) predictions ranged from 45 to 73 percent of the initial nitrogen, while PAN predictions ranged form 12 to 23 percent (excluding the DODGE simulation). The CBII mechanism uniquely predicted a significant ANO_3 formation (34 percent of initial nitrogen). This aspect of aromatic nitrate will be further discussed below.

June 13, 1979 (Propylene/Toluene) Experiment

Experimental results for the propylene--propylene/toluene dual run are shown in Figure 35. This experiment was first suggested by Whitten et al. (1980), who predicted that even though more HC was present with the propylene/toluene mixture, less O_3 would be produced because of a postulated nitrogen-loss mechanism uniquely associated with aromatics chemistry. As shown in Figure 35, the toluene side did form O_3 earlier and slightly faster; it lost NO_2 faster and stopped producing O_3 earlier than the propylene-only side. The nitrogen product formed did not respond on the chemiluminescent NO_2 analyzer, nevertheless. The response after 1200 h was characterized entirely by PAN. Even though both sides initially had the same amount of propylene, the side containing toluene formed less PAN.

CBII/TOL Simulation--

To simulate the results of this experiment, Whitten et al. (1980) replaced the aromatics chemistry of the CBII mechanism with a semiempirical, semiexplicit mechanism for toluene; the olefin--paraffin chemistry remained the same as that used in the other simulations herein. Whitten's simulation results for the propylene-only side of June 13 are shown in Figures 36a, b, and c; the results for the propylene/toluene side are shown in Figures 37a, b, and c. The mechanism correctly predicts the experimental results. Figures 38a, b, and c show the predictions for a case where the unique reaction between NO_3 and a toluene intermediate is omitted.

No other simulations of this experiment were performed, although it is expected that the DERMJ and LLOYD mechanisms would give results similar to those shown in Figures 38a, b, and c, since these mechanisms do not include significant aromatics nitrogen loss pathways.

The Whitten toluene mechanism predicts that dinitrates are formed in this system. The success of the mechanism would suggest that special analysis should be performed for these compounds in experimental nitrogen balances.

NITRIC ACID SPECIAL EXPERIMENTS

August 5, 1979, Experiment

Because of the apparent importance of the $N_2O_5 + H_2O \rightarrow 2HNO_3$ reaction, an experiment to investigate this reaction was performed in the UNC chamber. The results for this nighttime experiment are shown in Figure 39. In one side of the dual chamber, NO_2 was injected. The other chamber side had clean background air only. An O_3 generator was used to slowly inject O_3 into both chambers by alternating the O_3 stream between the two chamber sides every 2 sec. Thus, the dashed O_3 line in Figure 39 shows the O_3 concentration when the O_3--NO_2 reaction is absent. The solid O_3 line in Figure 39 is the O_3 in the side with NO_2. After about 52 min, the O_3 injection was stopped. Ozone decayed very slowly in the clean side by reacting with the walls. Both O_3 and NO_2 decayed in the other side. Measurements were performed for gaseous HNO_3, and none was detected. The temperature was nearly constant throughout the experiment and the dew point was 68°F.

The mechanism shown in Table 12 was used to simulate the August 5 experiment. The results are shown in Figure 40. The predicted O_3 and NO_2 curves are identical to those in Figure 39, the experimental data. The nitrogen loss from the system agrees perfectly with the predicted wall nitric acid.

TABLE 12. NIGHTTIME OZONE/NITROGEN DIOXIDE MECHANISM

1)	$\rightarrow 1.00\ O_3$		3.55×10^{-3}*
2)	$O_3 \rightarrow$		1.17×10^{-4}
3)	$O_3 + NO_2 \rightarrow 1.00\ NO_3$		$1.77 \times 10^{2} \exp(-2.45 \times 10^{3}/T)$
4)	$NO_3 + NO_2 \rightarrow 1.00\ N_2O_5$		$2.19 \times 10^{2} \exp(8.61 \times 10^{2}/T)$
5)	$N_2O_5 \rightarrow 1.00\ NO_3 + 1.00\ NO_2$		$7.44 \times 10^{15} \exp(-1.03 \times 10^{4}/T)$
6)	$N_2O_5 \rightarrow 2.00\ WHNO_3$	$[H_2O]$*	1.5×10^{-5}

*Zeroth order rate for 0 to 51 min; after 51 min rate = 0.0.

The simulation was repeated but without any H_2O, that is, without the $N_2O_5 + H_2O \rightarrow 2HNO_3$ reaction. The simulation results for NO_2 and O_3 without H_2O are nearly identical to those with H_2O (Figure 41). The NO_2 final concentrations differ by 2.9 ppb and the O_3 final concentrations by 3.1 ppb. Thus, O_3 and NO_2 measurements can not distinguish between the mechanisms and hence can not provide a rate constant for the $N_2O_5 + H_2O$ reaction. The simulation without H_2O does, however, predict 131 ppb gas-phase N_2O_5. The high temperature, total NO_x converter in the gas-phase HNO_3 chemiluminescent monitor should certainly respond to N_2O_5; no response other than to NO_2 was obtained, however, suggesting the $N_2O_5 + H_2O \rightarrow 2HNO_3$ reaction has a significant rate in the UNC chamber. The lack of measured gas-phase HNO_3 further suggests that the process is heterogeneous. In future experiments, NO will be injected at the end of the experiment to titrate any gas-phase N_2O_5 as a check, and daytime experiments similar to the August 5 test will be performed.

November 3 to 4, 1978, Experiment

As part of another series of experiments to investigate nitrogen balances, the November 3, 1978, experiment was performed. The HC used was ethylene, and the only predicted nitrogen products were NO_2 and HNO_3, since PAN can not form in this system. There was broken sky cover on this day (Figure 42), and not much O_3 was formed. The rapid changes in slope for the NO and NO_2 data shown in Figure 43 are associated with this solar radiation condition.

The chemiluminescent NO_x analyzer used for the data shown in Figure 43 does not respond to HNO_3; thus, the NO_2 measured is only NO_2, which was almost totally reacted from the system by 1900 h on the first day. The chamber was not vented at the end of the first day, and, as shown in the figure, O_3 reacted with NO_2 and ethylene overnight. The night was overcast and the temperature was essentially uniform (Figure 42 and climatic data). The next morning was also heavily overcast. The O_3 concentration began to rise rapidly as the solar radiation increased on the morning of the second day. The rise was terminated at about 1100 h by increased cloud cover and decreasing solar radiation.

A second chemiluminescent NO_x analyzer, equipped to measure NO_x + HNO_3 alternately with NO_x only, was also used to monitor the November 3 experiment. The analyzer response is shown in Figure 44.

Trace HNO_3 was observed in the chamber at 0600 h on November 3, presumably because HNO_3 was off-gassing from the walls after the chamber was closed for injection. All HNO_3 formed during the run, however, disappeared from the gas phase. That is, the NO_x + HNO_3 trace followed only the NO_2 trace in Figure 43 after NO was oxidized. This suggests that all HNO_3 was lost to the walls.

At night, after about 1900 h, HNO_3 began to reappear in the gas phase. At 0200 h on November 4, HNO_3 off-gassing rate began to increase, and NO_x (NO_2) began to appear as well. At about 0830 hours on November 4, NO_x began to increase rapidly. A rise in O_3 concentration at about the same time is highly correlated to the solar radiation curve in Figure 42. Temperature was slowly decreasing during this period. Shortly after sunrise, the dewpoint--previously ~38° to 41°F--increased rapidly to 48°F, with a few readings as high as 52° F; later in the day, the dewpoint decreased again. Overnight, total nitrogen (NO_x + HNO_3) slowly decreased to about 35 ppb, and NO_x decreased to zero at 0200 h on November 5.

The whole process was repeated on November 5, with 0.085 ppm NO_x appearing in the gas phase, O_3 formation occurring, and NO_x disappearing again. The chamber was vented on the evening of November 5.

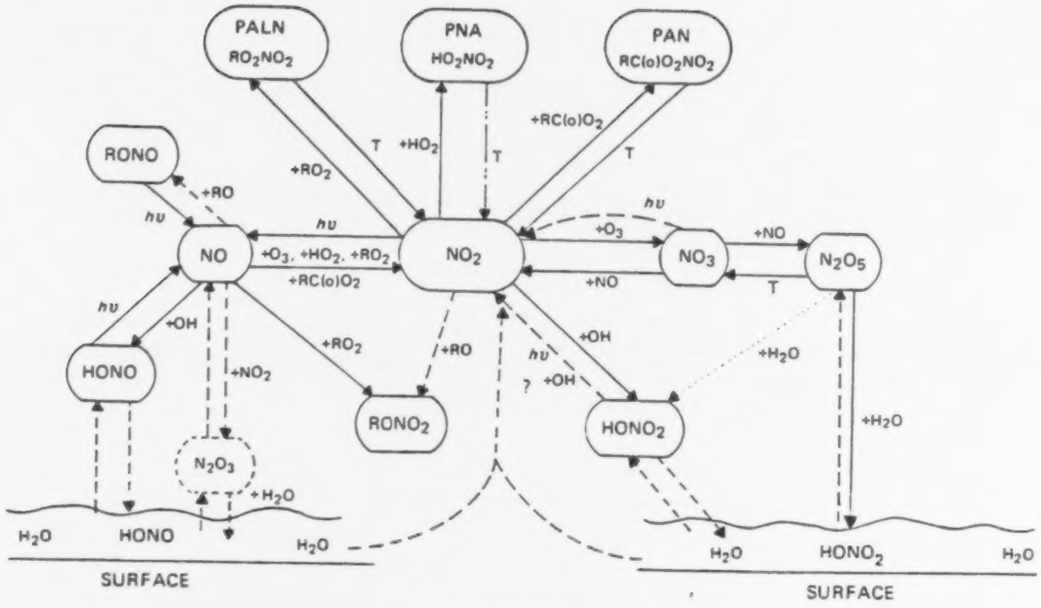
PALN
RO2NO2
PNA
HO2NO2
PAN
RC(o)O2NO2
RONO
+RO2
T
+HO2
T
+RC(o)O2
T
+RO
hυ
hυ
hυ
NO
+O3, +HO2, +RO2
+RC(o)O2
NO2
+O3
NO3
+NO
+NO
N2O5
T
hυ
+OH
HONO
+NO2
+RO2
/+RO
RONO2
hυ
? +OH
+OH
HONO2
+H2O
+H2O
N2O3
+H2O
H2O
HONO
H2O
SURFACE
H2O
HONO2
H2O
SURFACE

Figure 1. Nitrogen transformation processes.

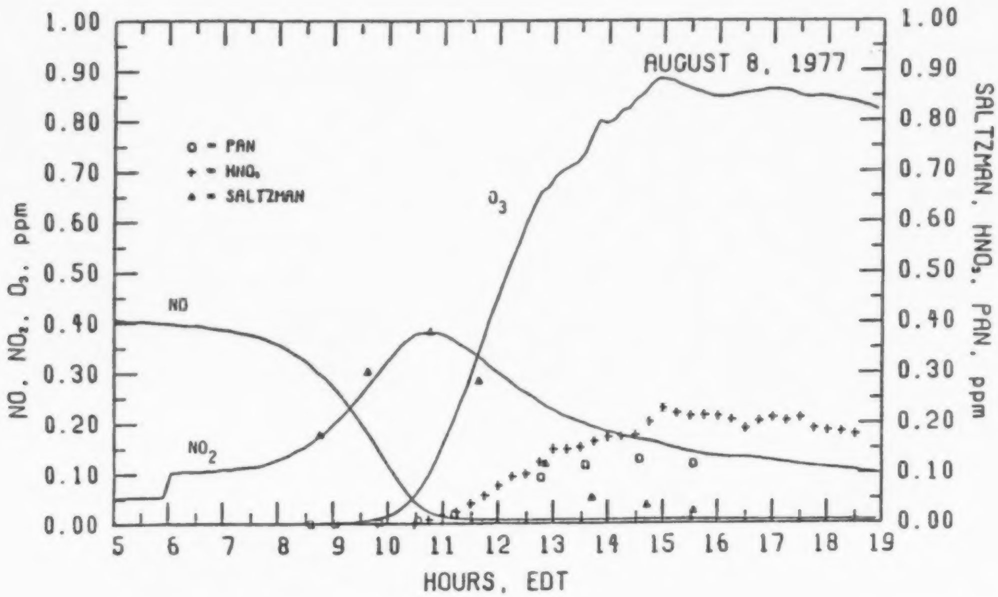

Figure 2. Experimental data from UNC outdoor smog chamber. Initial conditions: NO 0.395 ppm, NO_2 0.100 ppm, propylene 1.5 ppmC.

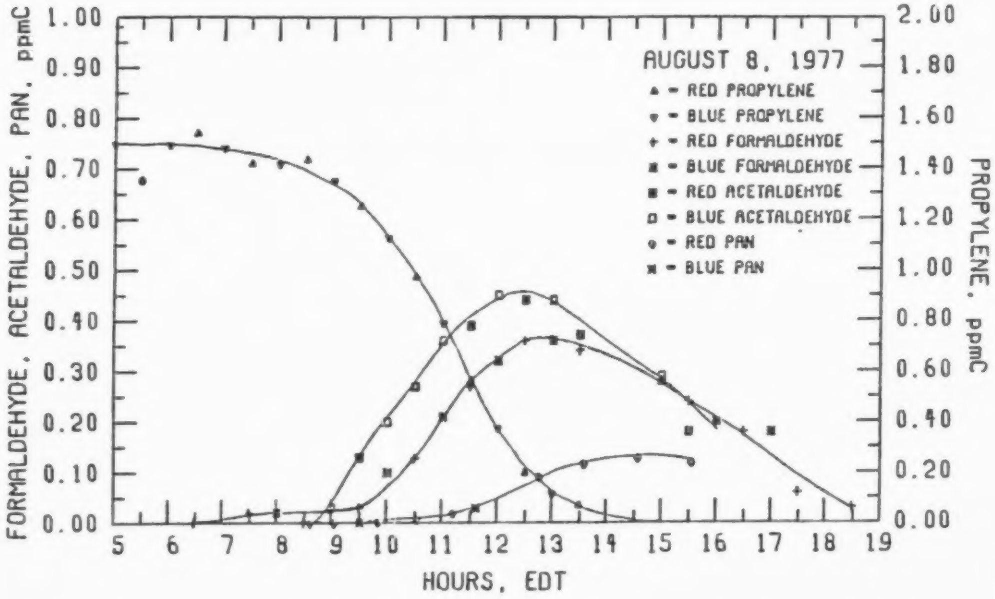

Figure 3. Experimental data from UNC outdoor smog chamber. Initial conditions: NO 0.395 ppm, NO_2 0.100 ppm, propylene 1.5 ppmC.

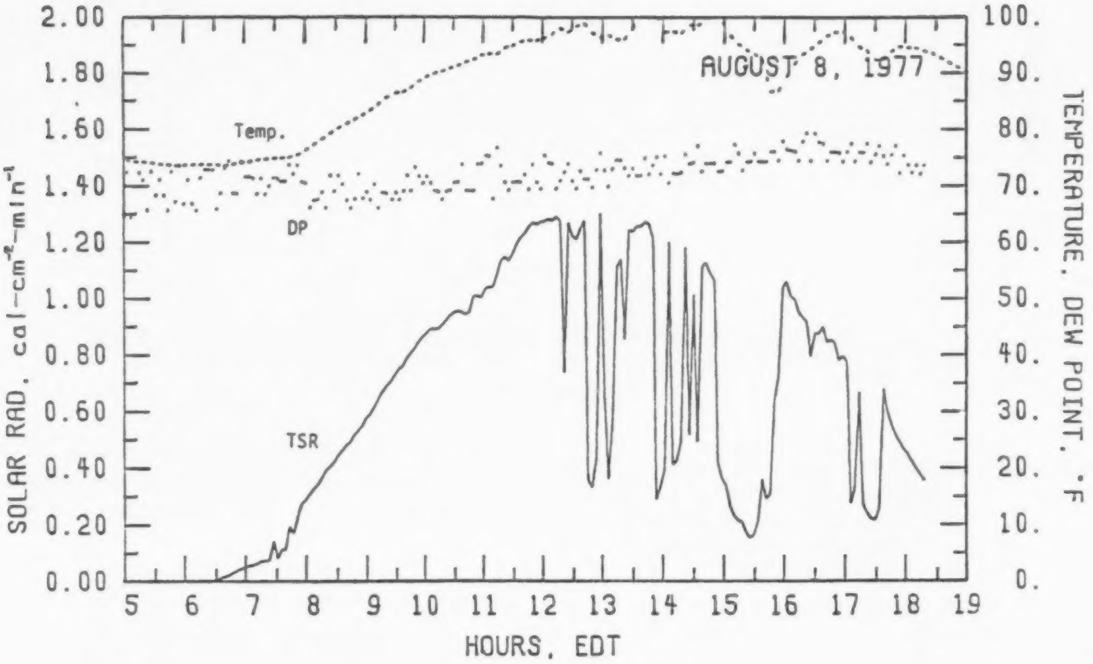

Figure 4. Experimental data from UNC outdoor smog chamber.

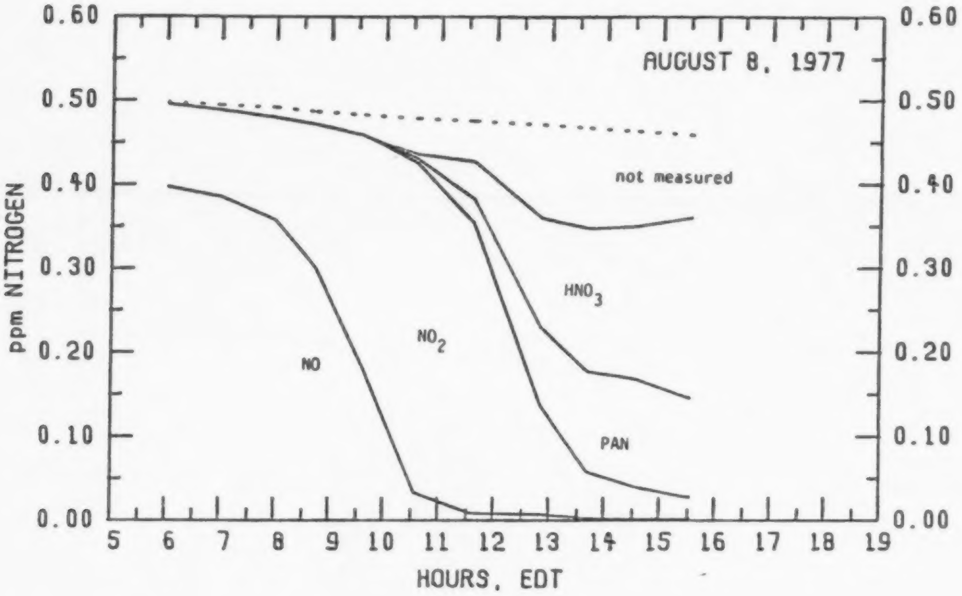

Figure 5. Experimental nitrogen balance. Each line represents the sum of all species below it. Dashed line represents the initial concentration corrected for dilution. Initial conditions: NO 0.395 ppm, NO_2 0.100 ppm, propylene 1.5 ppmC.

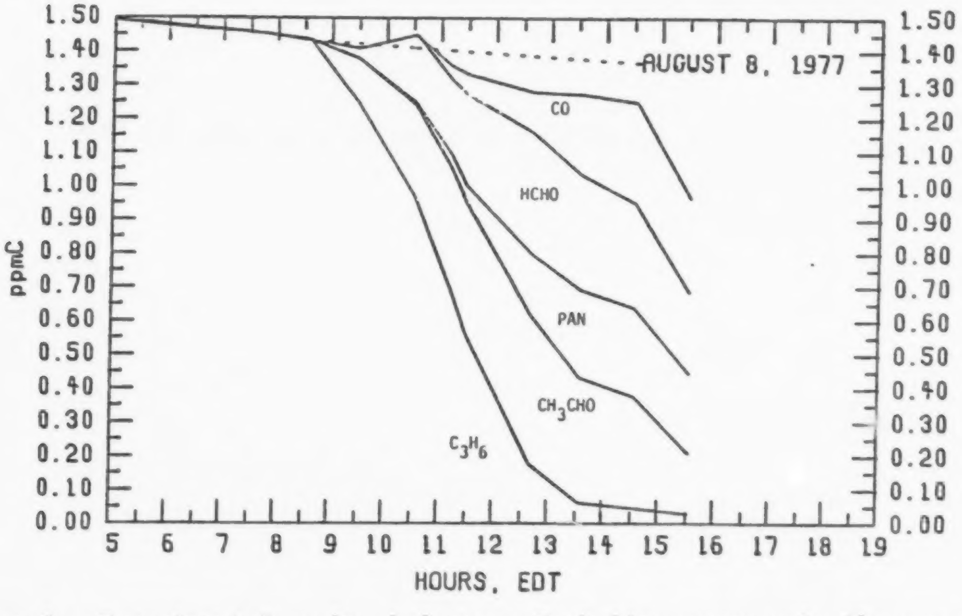

Figure 6. Experimental carbon balance. Each line represents the sum of all species below it. Dashed line represents initial concentration corrected for dilution. Initial conditions: NO 0.395 ppm, NO_2 0.100 ppm, propylene 1.5 ppm C.

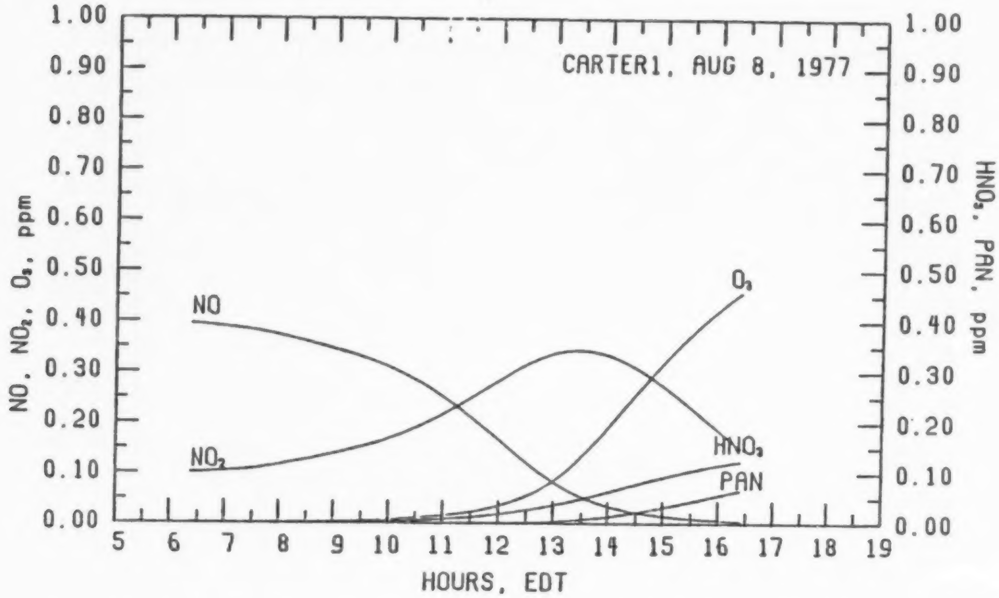

Figure 7. Simulation with CARTER mechanism. Initial conditions: NO 0.395 ppm, CO 0.4 ppm, O_3 0.1 ppb, H_2O 2×10^4 ppm, HONO 2.5 ppb, propylene 0.56 ppmV; photolysis rates scaled to TSR for August 8.

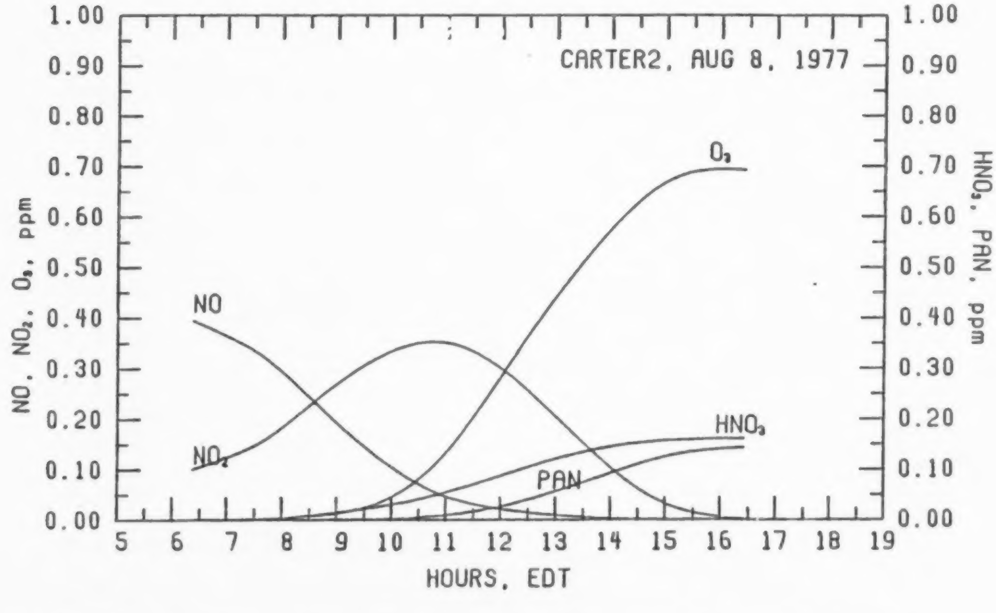

Figure 8. Simulation with CARTER mechanism. Initial conditions: NO 0.395 ppm, NO_2 0.100 ppm, CO 0.4 ppm, O_3 0.1 ppb, H_2O 2×10^4 ppm, HONO 0.0 ppb, propylene 0.56 ppmV; photolysis rates scaled to TSR for August 8. Simulation includes artificial OH source.

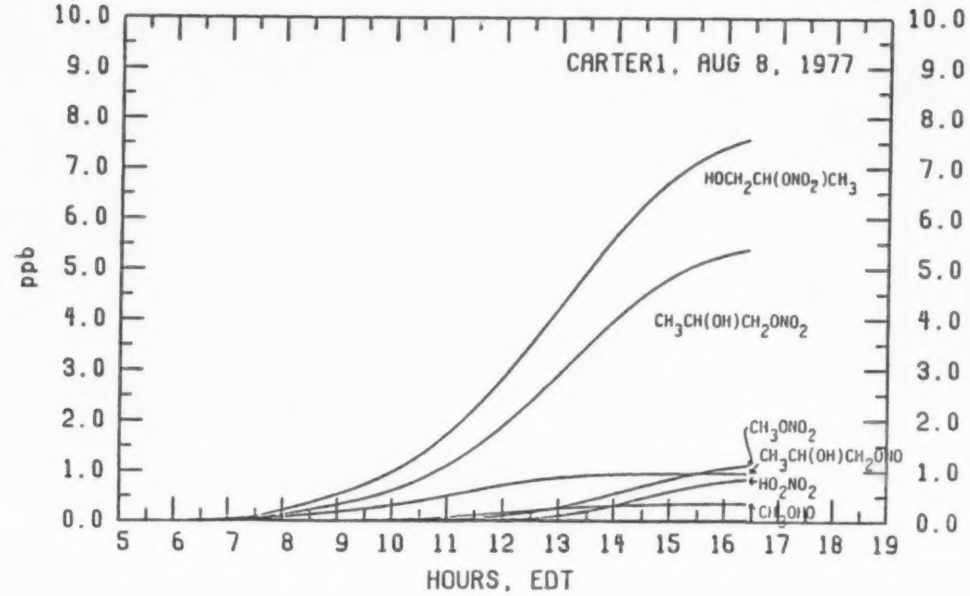

Figure 9. Minor nitrogen species in CARTER mechanism.

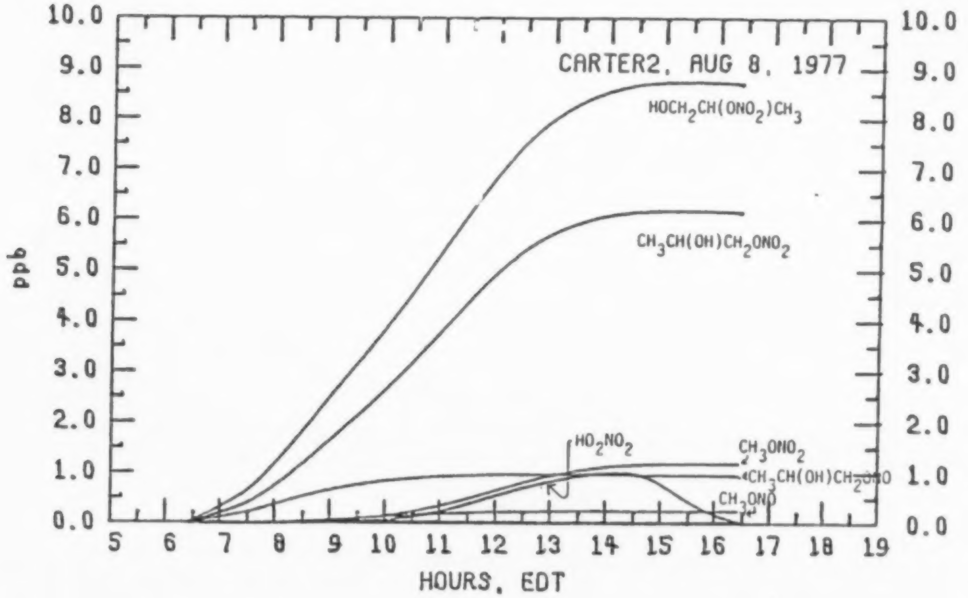

Figure 10. Minor nitrogen species in CARTER mechanism.

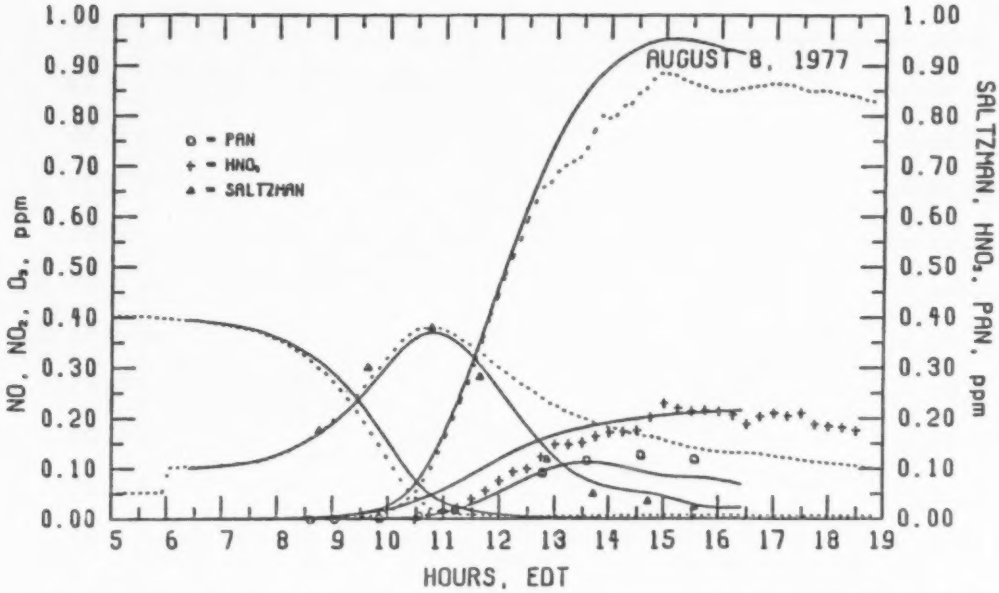

Figure 11. Experimental data from UNC outdoor smog chamber as dashed lines and symbols. Solid lines are simulation with JEFFRIES mechanism. Initial conditions: NO 0.395 ppm, NO_2 0.100 ppm; CO 0.4 ppm, O_3 0.1 ppb, H_2O 2×10^4 ppm, propylene 1.5 ppmC; photolysis rates scaled to TSR for August 8.

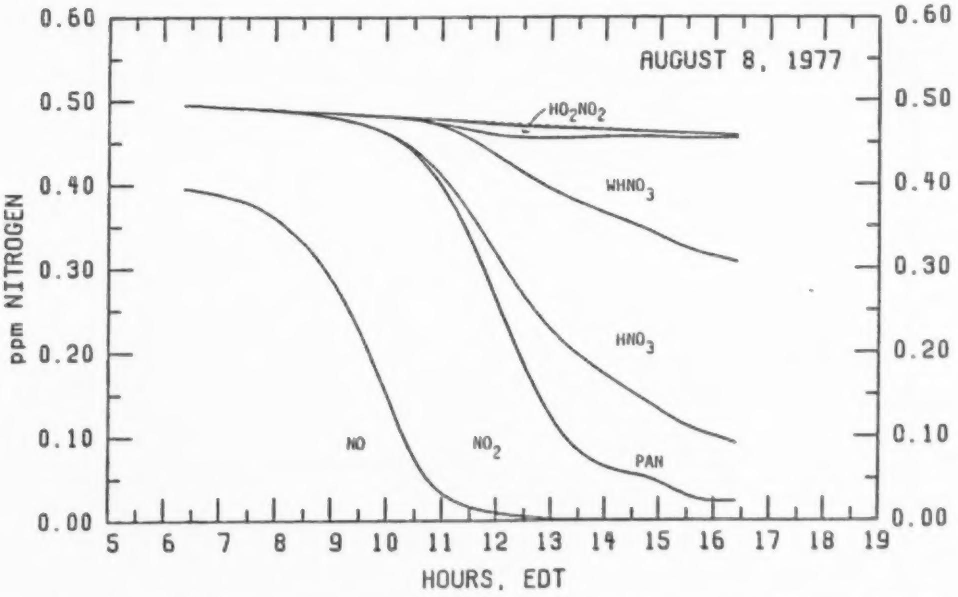

Figure 12. Simulation nitrogen balance. Each line represents the sum of all species below it. Dashed line represents the initial concentration corrected for dilution. Initial conditions: NO 0.395 ppm, NO_2 0.100 ppm, propylene 1.5 ppmC.

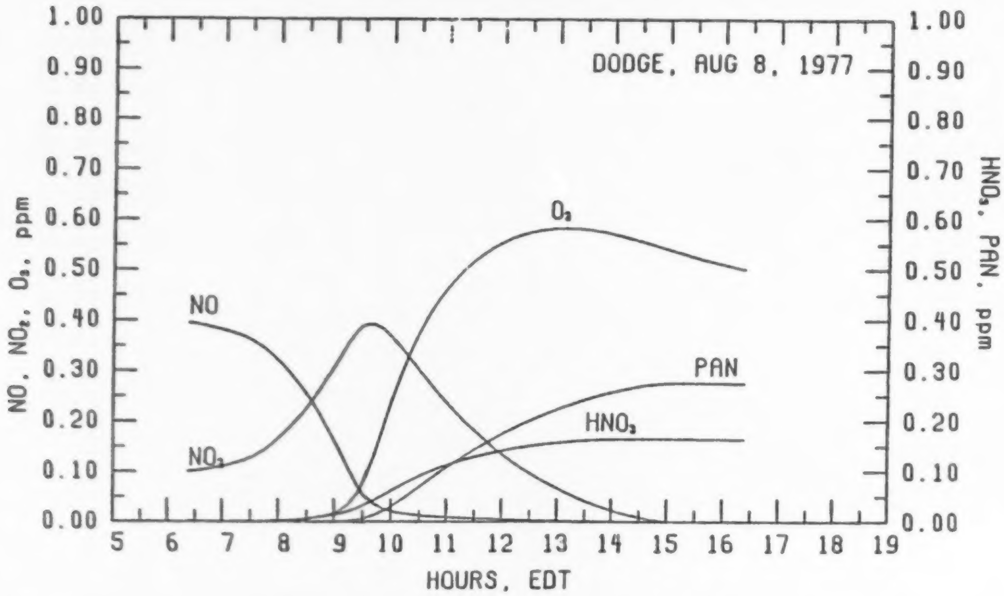

Figure 13. Simulation with DODGE mechanism. Initial conditions: NO 0.395 ppm, NO_2 0.100 ppm, O_3 0.1 ppb, H_2O 2×10^4 ppm, HONO 2.5 ppb, propylene 0.56 ppmV; photolysis rates scaled to TSR for August 8.

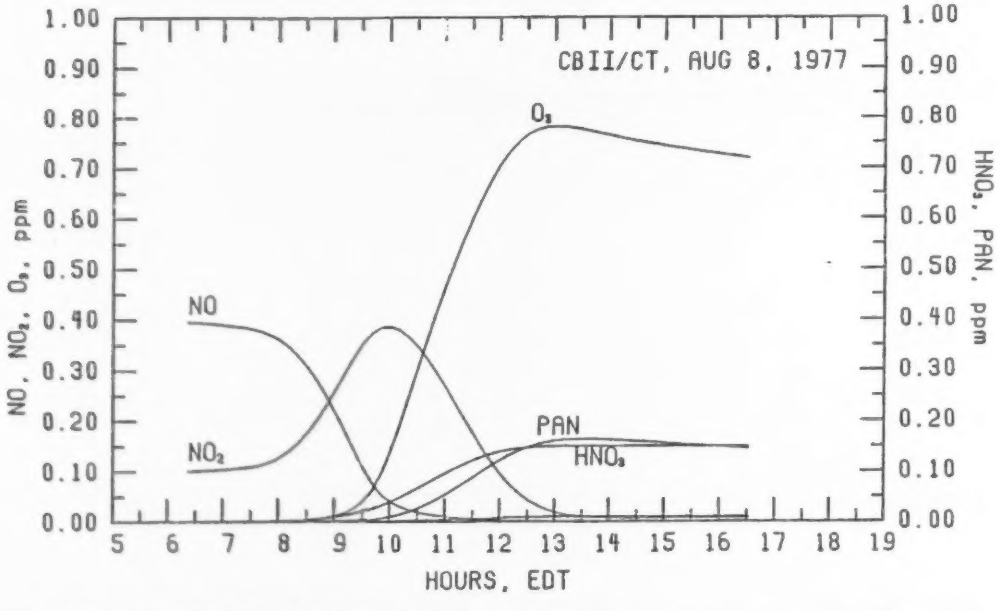

Figure 14. Simulation with CBII mechanism using constant temperature. Initial conditions: NO 0.395 ppm, NO_2 0.100 ppm, CO 0.4 ppm, H_2O 2×10^4 ppm, paraffin 0.56 ppmV, olefin 0.56 ppmV; photolysis rates scaled to TSR for August 8.

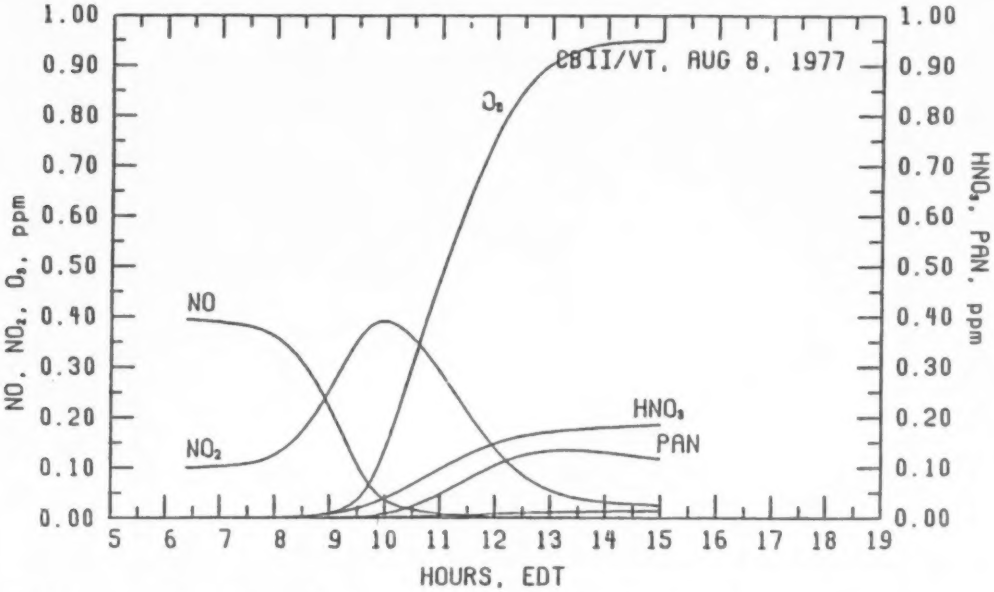

Figure 15. Simulation with CBII mechanism using variable temperature. Initial conditions: NO 0.395 ppm, NO_2 0.100 ppm, CO 0.4 ppm, H_2O 2×10^4 ppm, paraffin 0.56 ppmV, olefin 0.56 ppmV; photolysis rates scales to TSR for August 8.

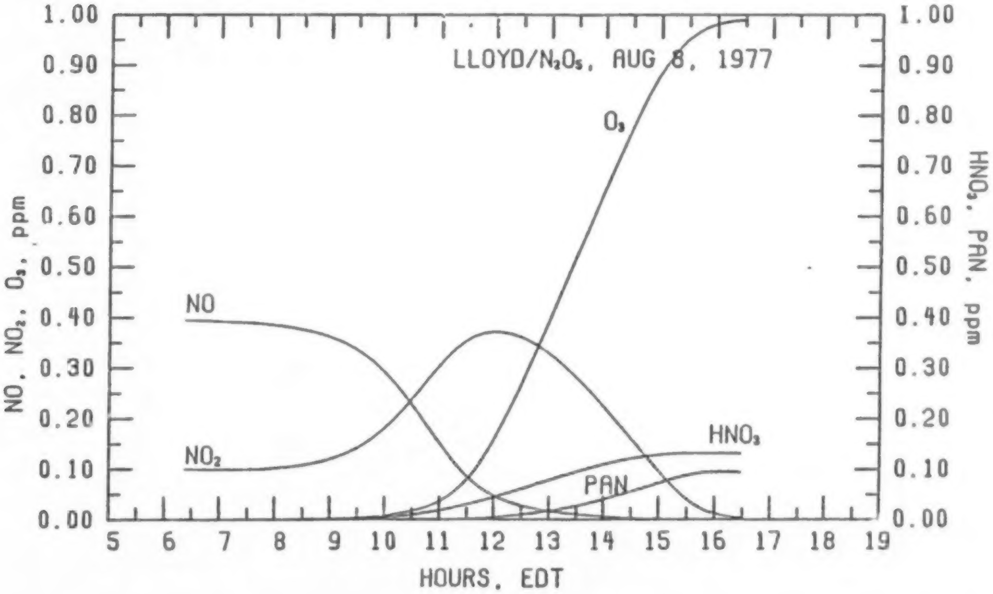

Figure 16. Simulation with LLOYD mechanism using UNC N_2O_5 rates. Initial conditions: NO 0.395 ppm, NO_2 0.100 ppm, CO 0.4 ppm, O_3 0.1 ppb, H_2O 2×10^4 ppm, HONO 0.0 ppb, alkenes 0.56 ppmV; O_3 maximum 0.991 ppm; photolysis rates scaled to TSR for August 8.

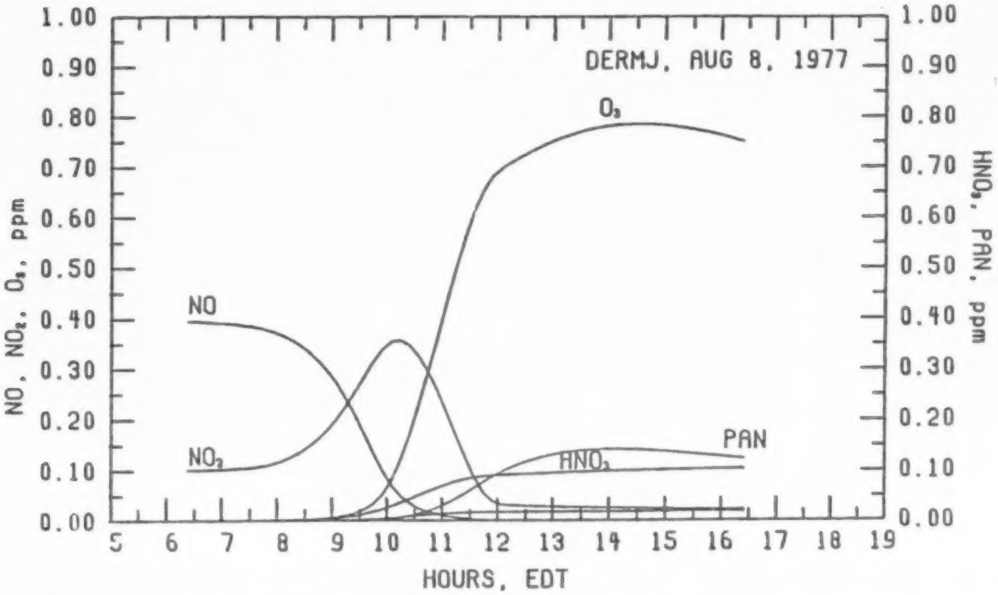

Figure 17. Simulation with DERMJ mechanism. Initial conditions: NO 0.395 ppm, NO_2 0.100 ppm, CO 0.4 ppm, H_2O 2×10^4 ppm, HCl 0.56 ppmV; photolysis rates scaled to TSR for August 8.

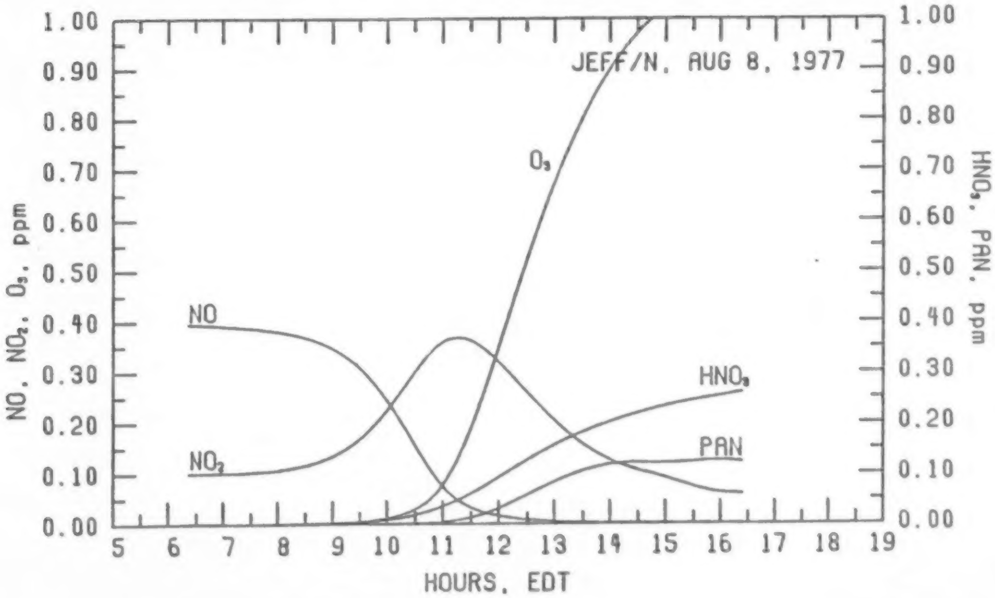

Figure 18. Simulation with JEFFRIES mechanism. $N_2O_5 + H_2O + 2HNO_3$ omitted. Initial conditions: NO 0.395 ppm, NO_2 0.100 ppm, CO 0.4 ppm, O_3 0.1 ppb, H_2O 2×10^4 ppm, propylene 0.56 ppmV; O_3 maximum 1.049 ppm; photolysis rates scaled to TSR for August 8.

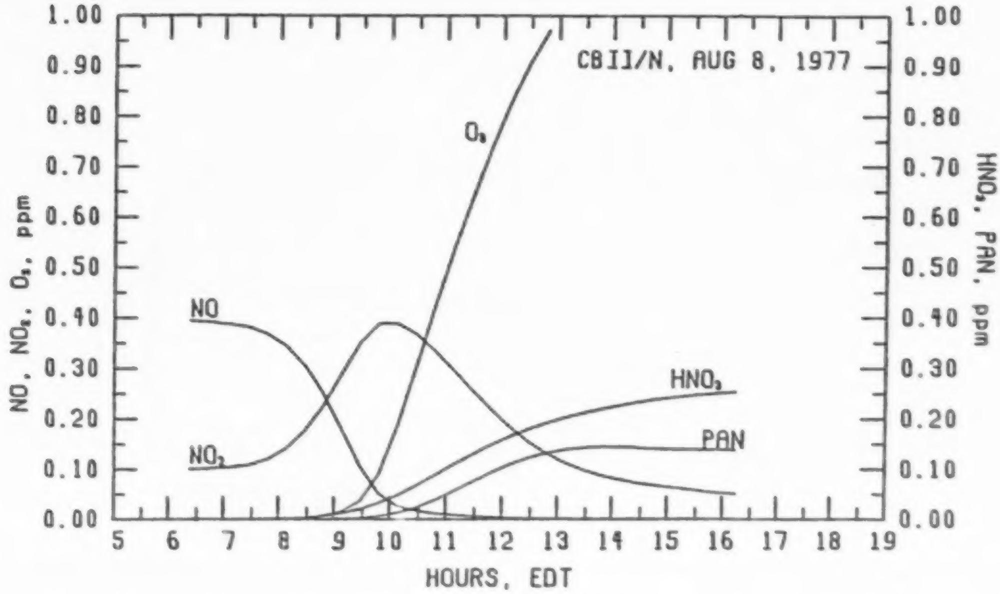

Figure 19. Simulation with CBII mechanism using variable temperature. $N_2O_5 + H_2O \rightarrow 2HNO_3$ omitted. Initial conditions: NO 0.395 ppm, NO_2 0.100 ppm, CO 0.4 ppm, H_2O 2×10^4 ppm, paraffin 0.56 ppmV, olefin 0.56 ppmV; O_3 maximum 1.159 ppm; photolysis rates scaled to TSR for August 8.

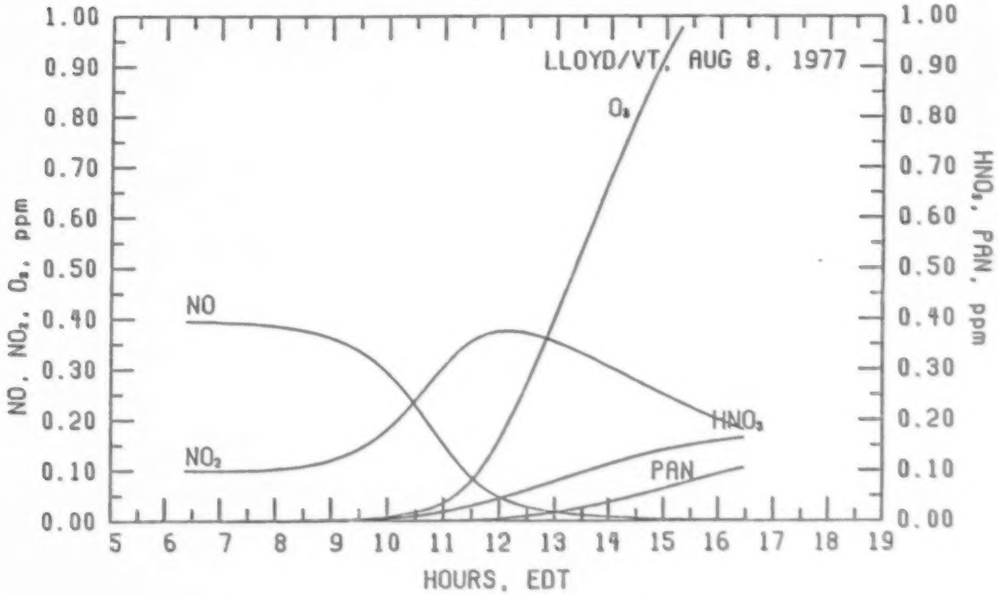

Figure 20. Simulation with LLOYD mechanism using variable temperature and Lloyd's rates for N_2O_5 chemistry. Initial conditions: NO 0.395 ppm, NO_2 0.100 ppm, CO 0.4 ppm, O_3 0.1 ppb, H_2O 2×10^4 ppm, alkenes 0.56 ppmV; O_3 maximum 1.154 ppm; photolysis rates scaled as above.

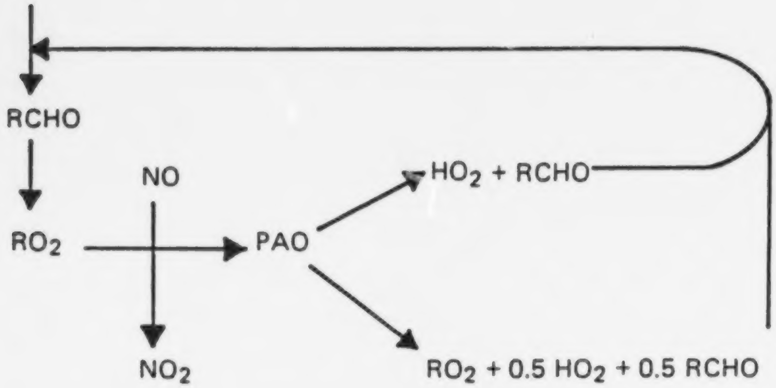
RCHO
NO
HO$_2$ + RCHO
RO$_2$
PAO
NO$_2$
RO$_2$ + 0.5 HO$_2$ + 0.5 RCHO

Figure 21. Reaction sequence from LLOYD mechanism showing nonconservation of carbon mass.

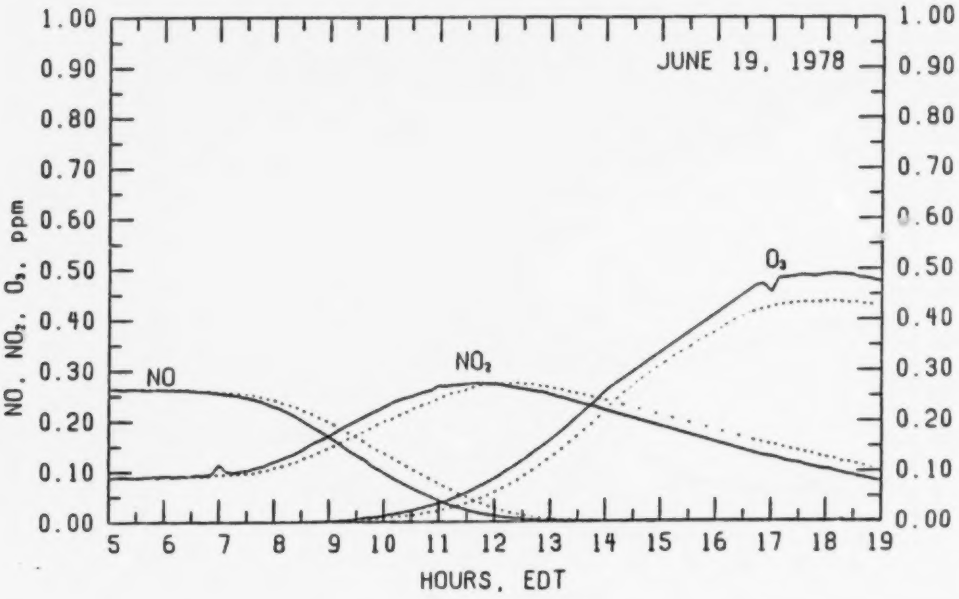

Figure 22. Experimental data from UNC outdoor smog chamber. Comparison of 25% propylene/75% n-butane mixture (---), with 11 component mix (____). Initial conditions: NO 0.261 ppm, NO_2 0.091 ppm, HC 2.07 ppmC (---), HC 2.14 ppmC (____).

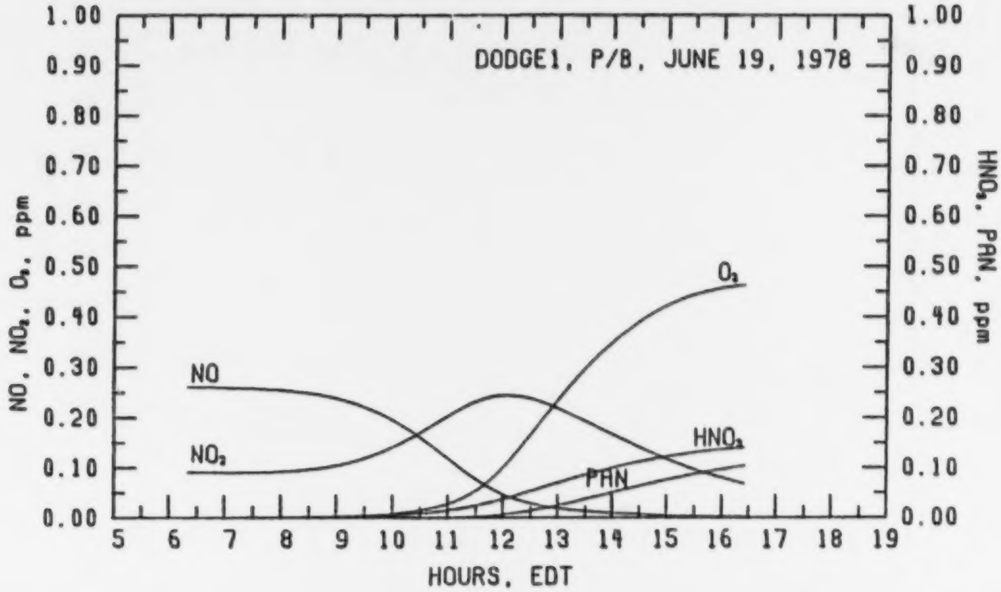

Figure 23. Simulation of propylene-butane experiment using DODGE mechanism. Initial conditions: NO 0.261 ppm, NO_2 0.091 ppm, CO 0.4 ppm, H_2O 2×10^4 ppm, HONO 0.0 ppb, propylene 0.164 ppmV, butane 0.395 ppmV; photolysis rates scaled to TSR for June 19.

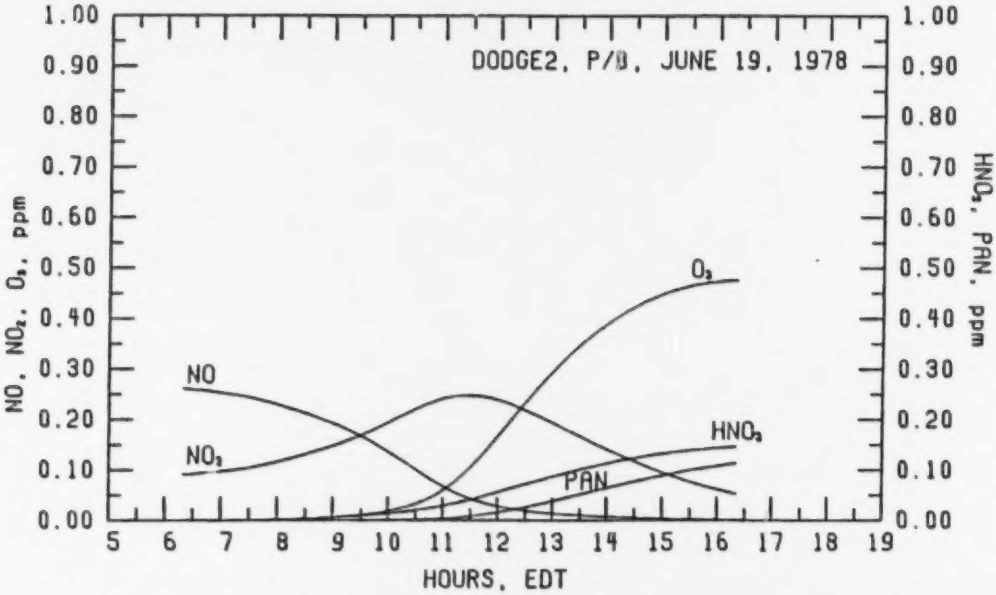

Figure 24. Simulation of propylene-butane experiment using DODGE mechanism. Initial conditions: NO 0.261 ppm, NO_2 0.091 ppm, CO 0.4 ppm, H_2O 2×10^4 ppm, HONO 3.0 ppb, propylene 0.164 ppmV, butane 0.395 ppmV; photolysis rates scaled to TSR for June 19.

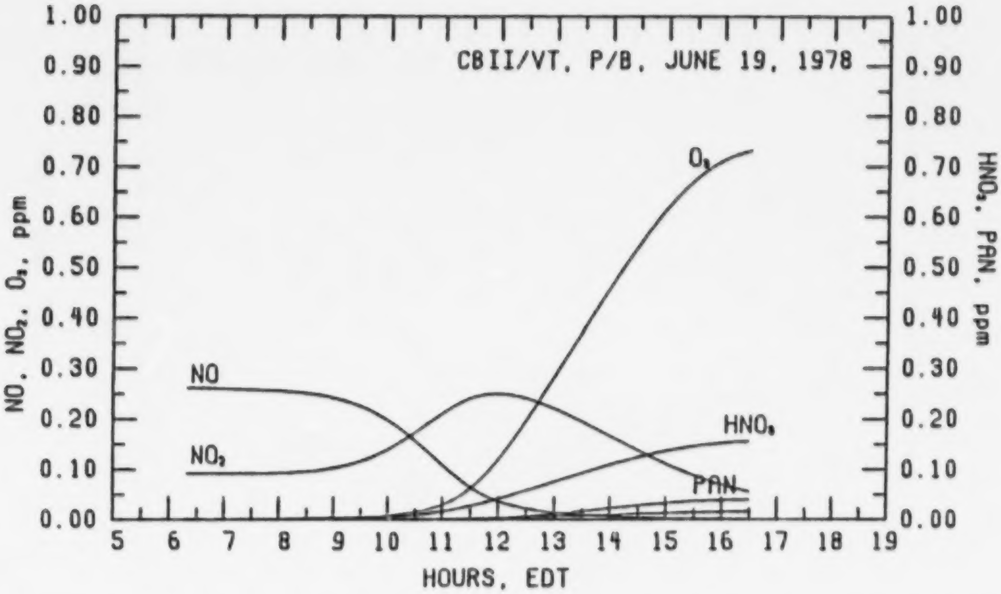

Figure 25. Simulation of propylene-butane experiment using CBII mechanism with variable temperature. Initial conditions: NO 0.261 ppm, NO_2 0.091 ppm, CO 0.4 ppm, H_2O 2×10^4 ppm, olefin 0.164 ppmV, paraffin 1.744 ppmV; photolysis rates scaled to TSR for June 19.

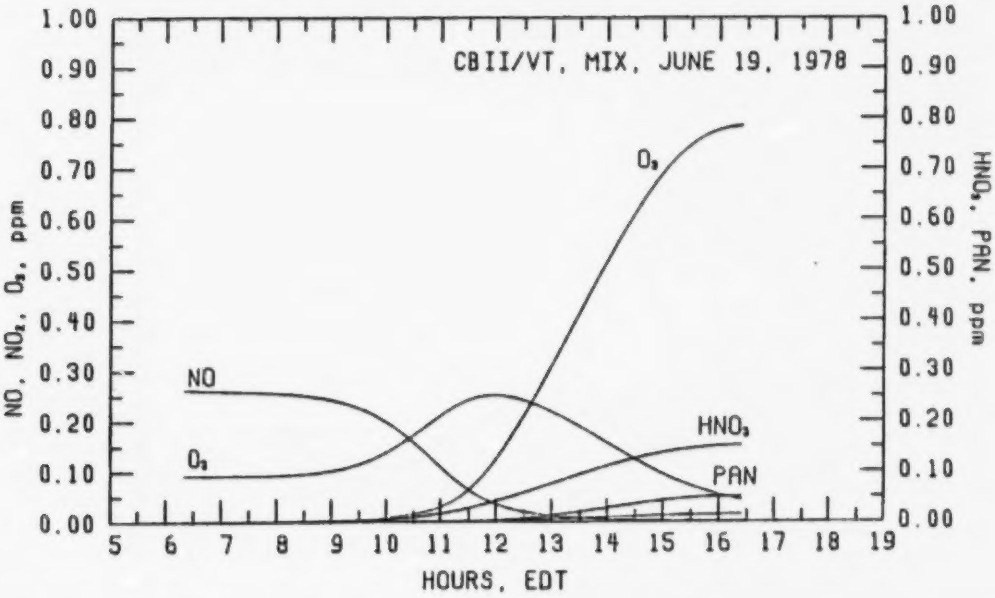

Figure 26. Simulation of mix experiment using CBII mechanism with variable temperature. Initial conditions: NO 0.261 ppm, NO_2 0.091 ppm, CO 0.4 ppm, H_2O 2×10^4 ppm, olefin 0.124 ppmV, ethylene 0.152 ppmV, paraffin 1.608 ppmV; photolysis rates scaled to TSR for June 19.

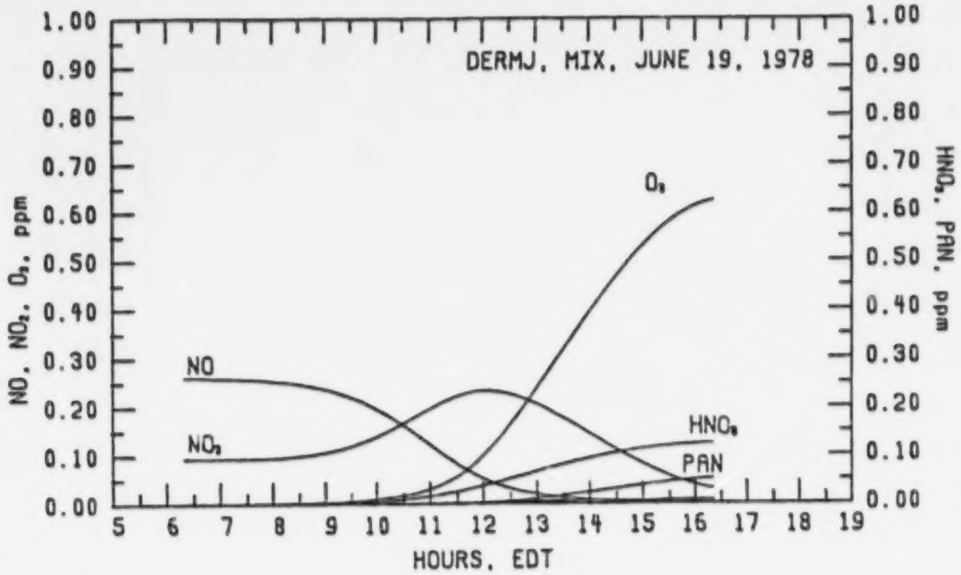

Figure 27. Simulation of mix experiment using DERMJ mechanism. Initial conditions: NO 0.261 ppm, NO_2 0.091 ppm, CO 0.4 ppm, O_3 0.1 ppb, H_2O $2x10^4$ ppm, HCl 0.214 ppmV, HC2 0.2497 ppmV, HONO 0.0 ppb; photolysis rates scaled to TSR for June 19.

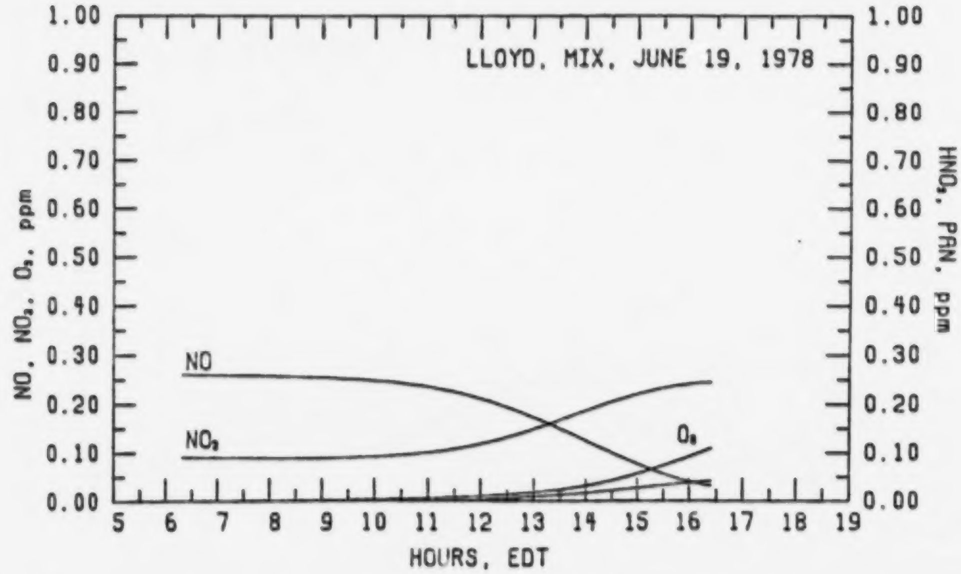

Figure 28. Simulation of mix experiment using LLOYD mechanism. Initial conditions: NO 0.261 ppm, NO_2 0.091 ppm, CO 0.4 ppm, O_3 0.1 ppb, H_2O $2x10^4$ ppm, HONO 0.0 ppb, alkene 0.101 ppmV, C_2H_4 0.13 ppmV, paraffin 0.251 ppmV; photolysis rates scaled to TSR for June 19.

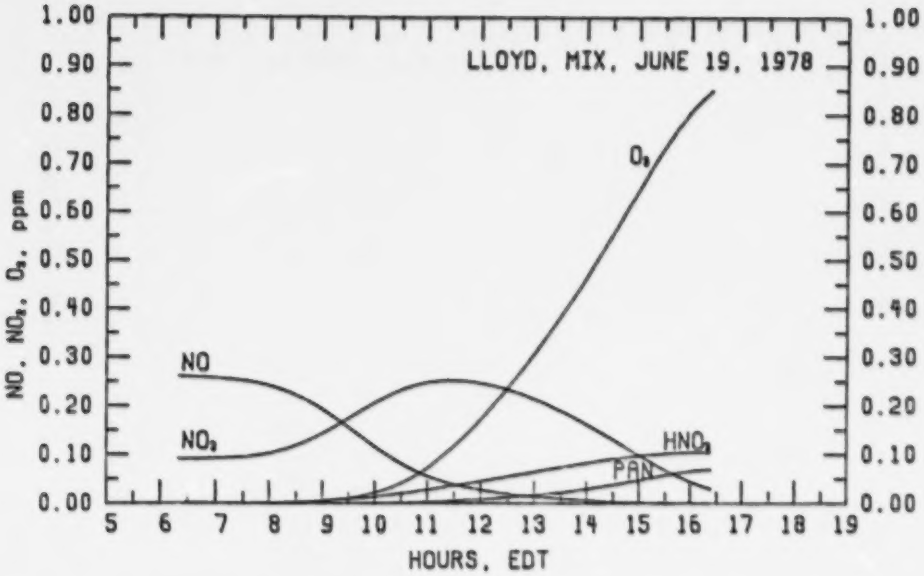

Figure 29. Simulation of mix experiment using LLOYD mechanism. Initial conditions: NO 0.261 ppm, NO_2 0.091 ppm, CO 0.4 ppm, O_3 0.01 ppb, H_2O 2×10^4 ppm, HONO 0.0 ppb, alkene 0.101 ppmV, C_2H_4 0.13 ppmV, paraffin 0.251 ppmV, RCHO 0.05 ppmV, HCHO 0.09 ppmV; photolysis rates scaled to TSR for June 19.

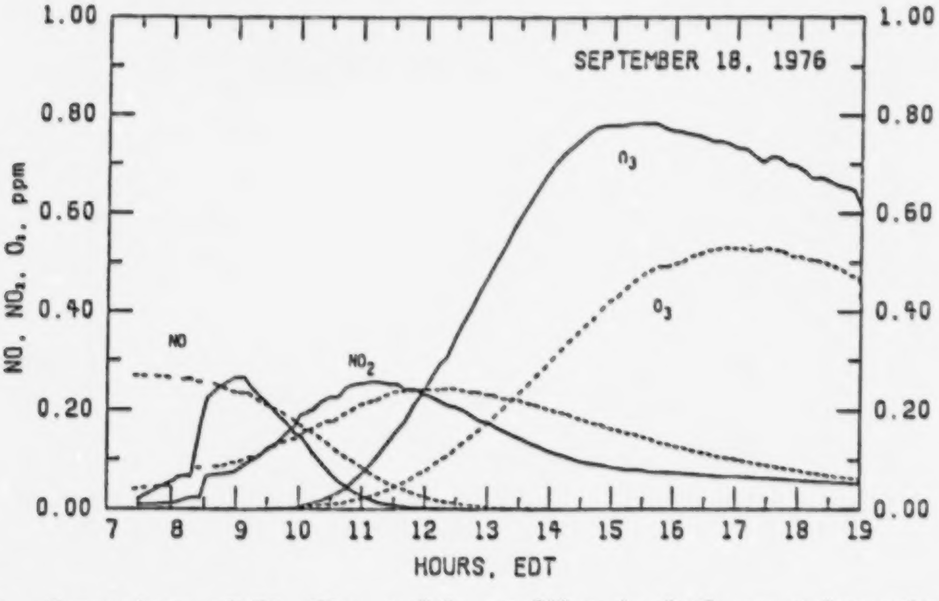

Figure 30. Comparison of NO, NO_2, and O_3 profiles in dual run using auto exhaust as NMHC (___) and UNC as NMHC (---). Initial conditions: (___), NO_x: 0.34 ppm; NMHC 3.1 ppmC; (---), NO_x: 0.33 ppm; NMHC: 3.1 ppmC.

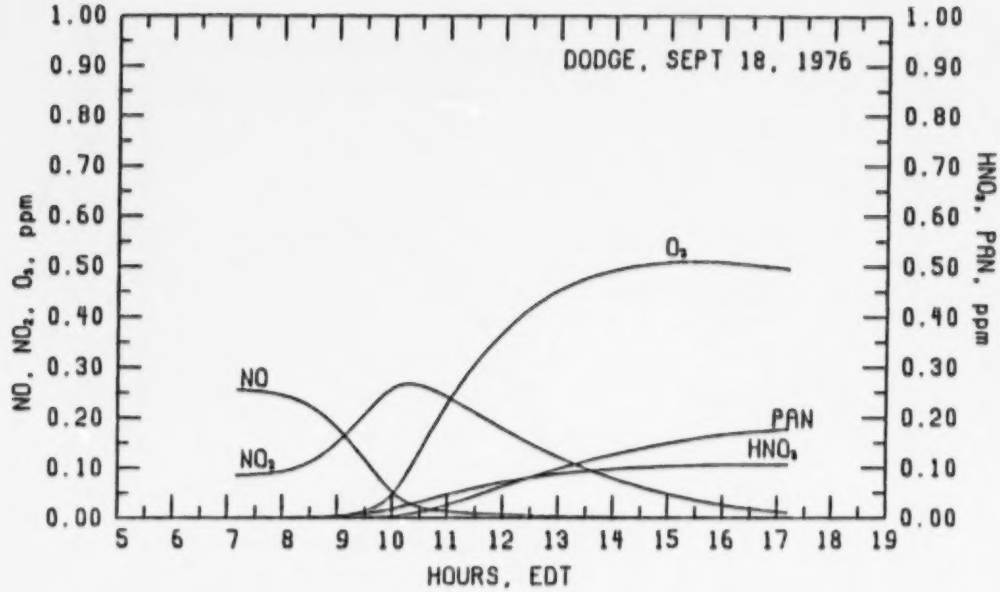

Figure 31. Simulation with DODGE mechanism. Initial conditions: NO 0.255 ppm, NO_2 0.085 ppm, O_3 0.1 ppb, H_2O 2×10^4 ppm, propylene 0.258 ppmV, butane 0.581 ppmV, HCHO 0.100 ppmV; photolysis rates scaled to TSR for September 18.

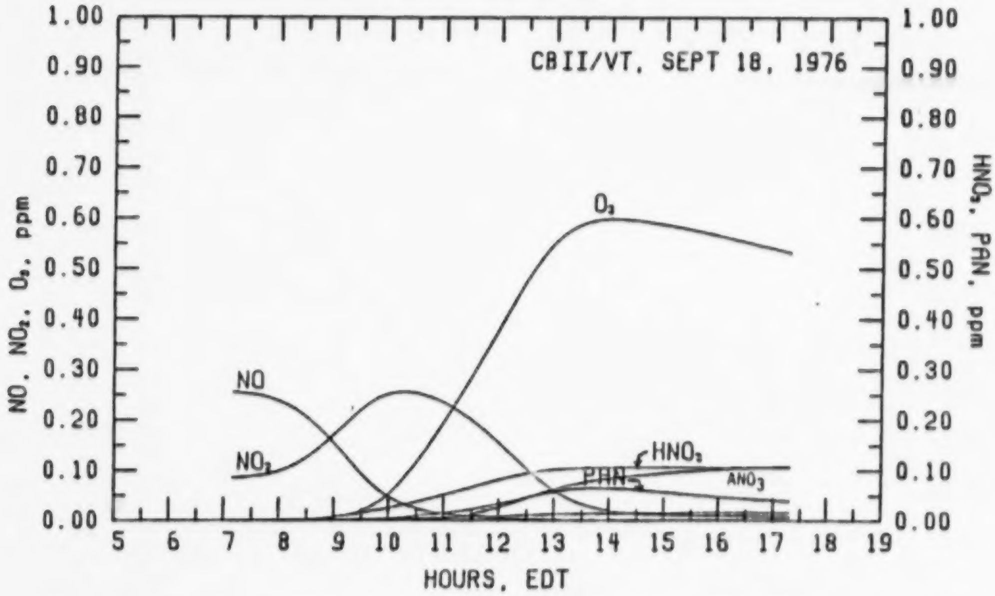

Figure 32. Simulation with CBII using variable temperatures. Initial conditions: NO 0.255 ppm, NO_2 0.085 ppm, CO 0.04 ppm, O_3 0.1 ppb, H_2O 2×10^4 ppm, olefin 0.051 ppmV, ethylene 0.051 ppmV, paraffin 1.973 ppmV, aromatic 0.124 ppmV, HCHO 0.115 ppmV; photolysis rates scaled to TSR for September 18.

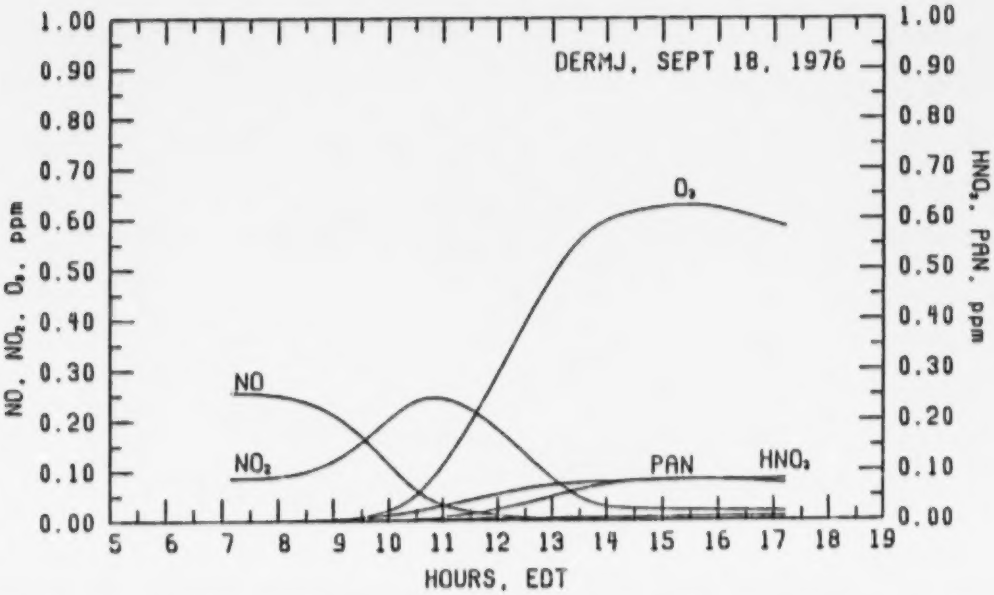

Figure 33. Simulation with DERMJ mechanism. Initial conditions: NO 0.255 ppm, NO_2 0.085 ppm, CO 0.4 ppm, H_2O 2×10^4 ppm, HC1 0.2155 ppmV, HC2 0.1789 ppmV, HC3 0.1643 ppmV, HC4 0.1113 ppmV; photolysis rates scaled to TSR for September 18.

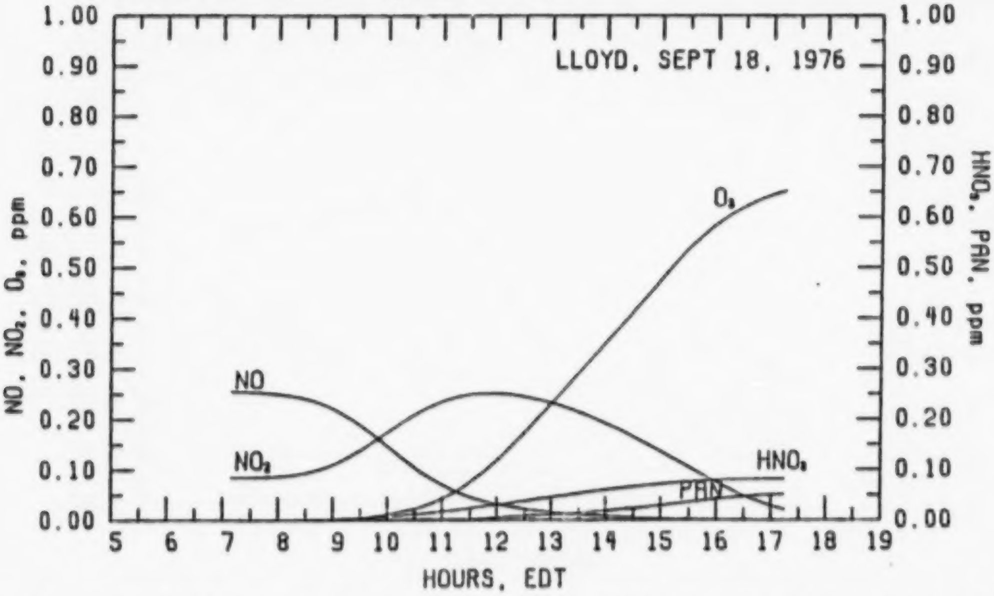

Figure 34. Simulation with LLOYD mechanism. Initial conditions: NO 0.255 ppm, NO_2 0.085 ppm, CO 0.4 ppm, O_3 0.1 ppb, H_2O 2×10^4 ppm, alkenes 0.16 ppmV, C_2H_4 0.05 ppmV, paraffin 0.215 ppmV, aromatic 0.12 ppmV, RCHO 0.05 ppmV, HCHO 0.09 ppmV, photolysis rates scaled to TSR for September 18.

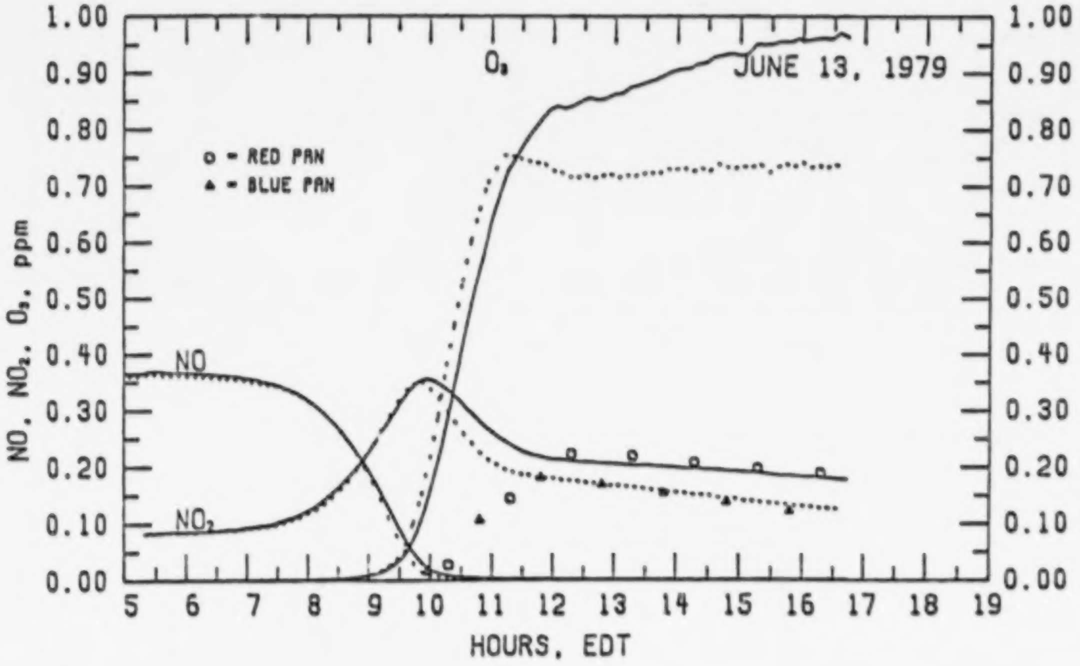

Figure 35. Experimental data from UNC outdoor smog chamber comparing propylene (___) with propylene and toluene (---). Initial conditions: (___), NO_x 0.45 ppm, propylene 2.7 ppmC; (---), NO_x 0.45 ppm, propylene 2.7 ppmC, toluene 2.8 ppmC.

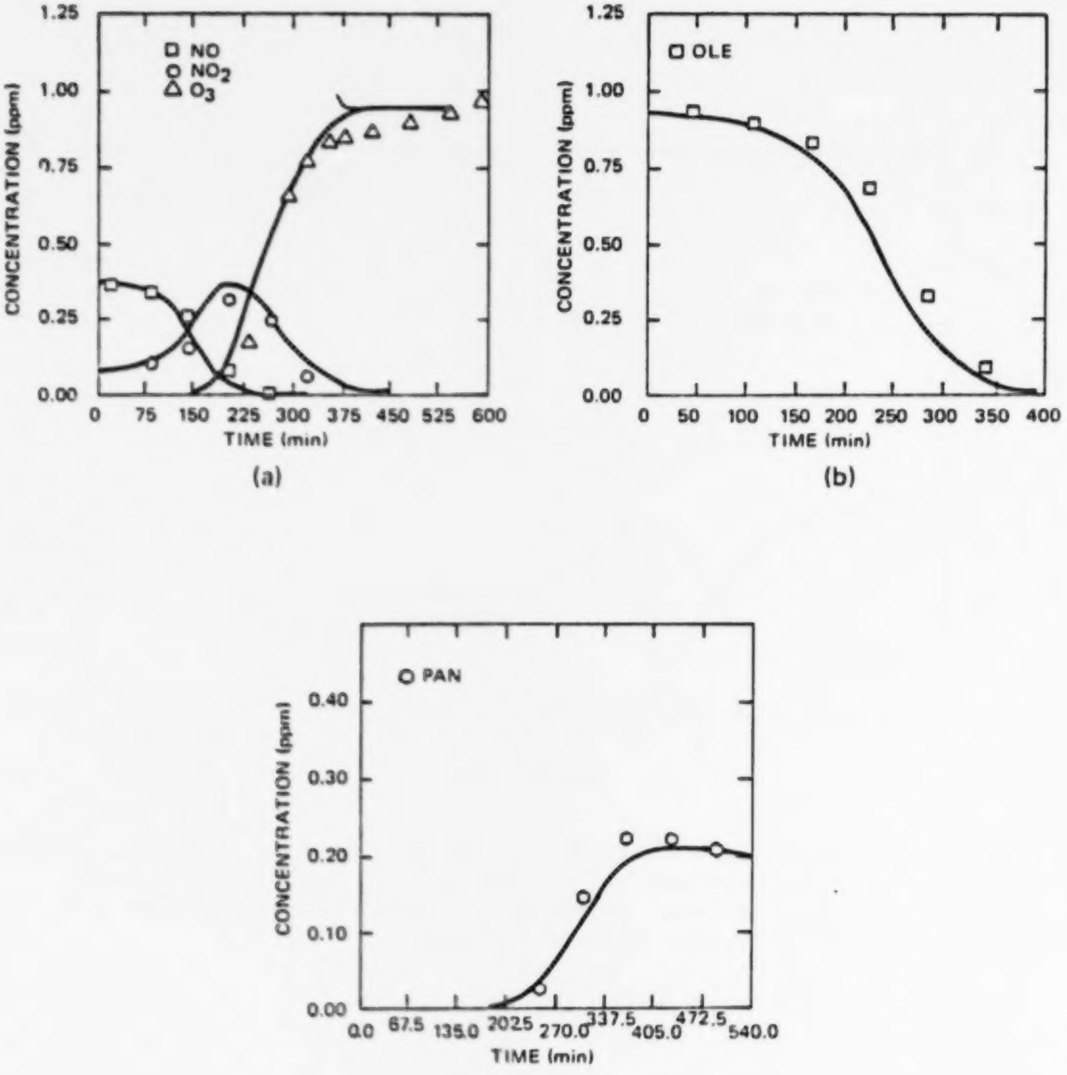

(a) (b)

(c)

Figure 36. Simulation results for UNCR propylene, June 13, 1979.

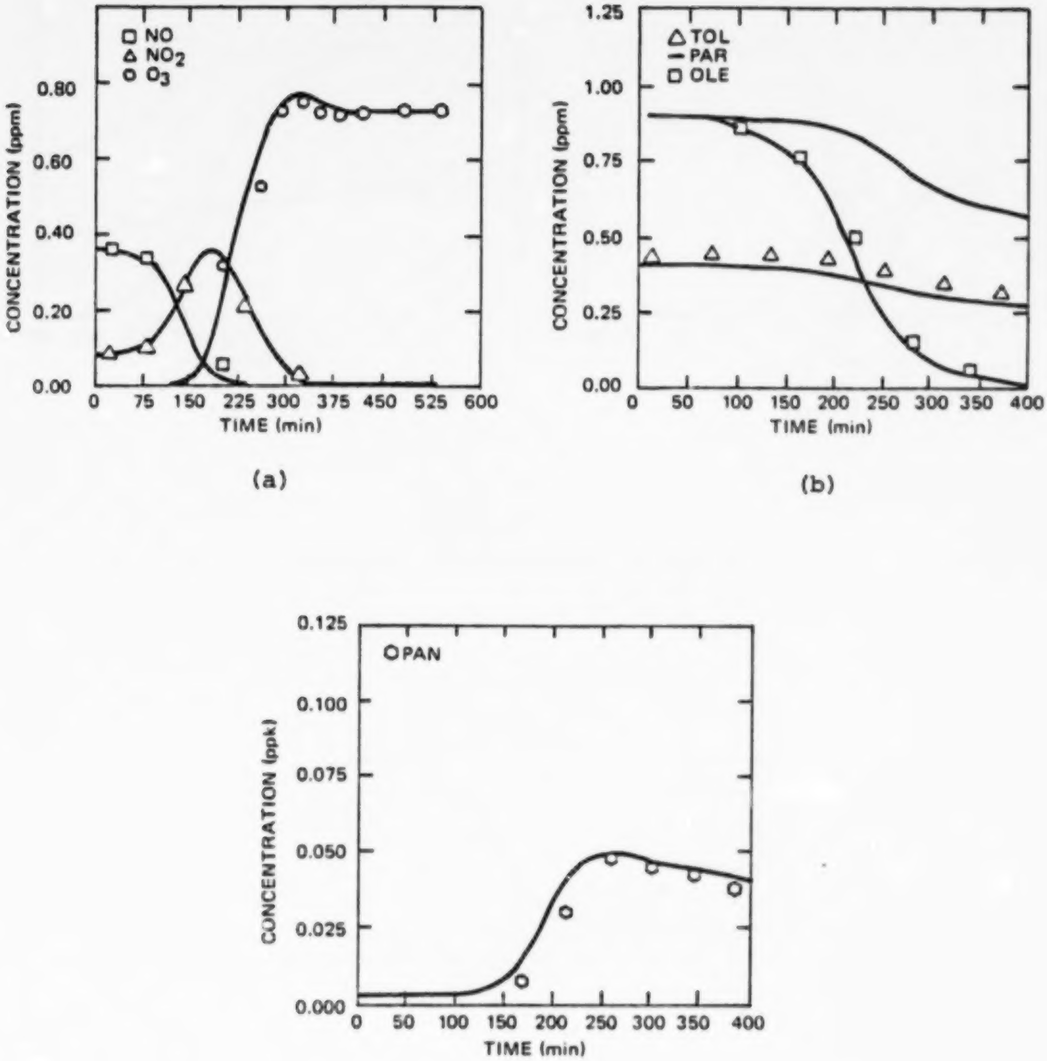

(a)

(b)

(c)

Figure 37. Simulation results for UNCB toluene-propylene, June 13, 1979.

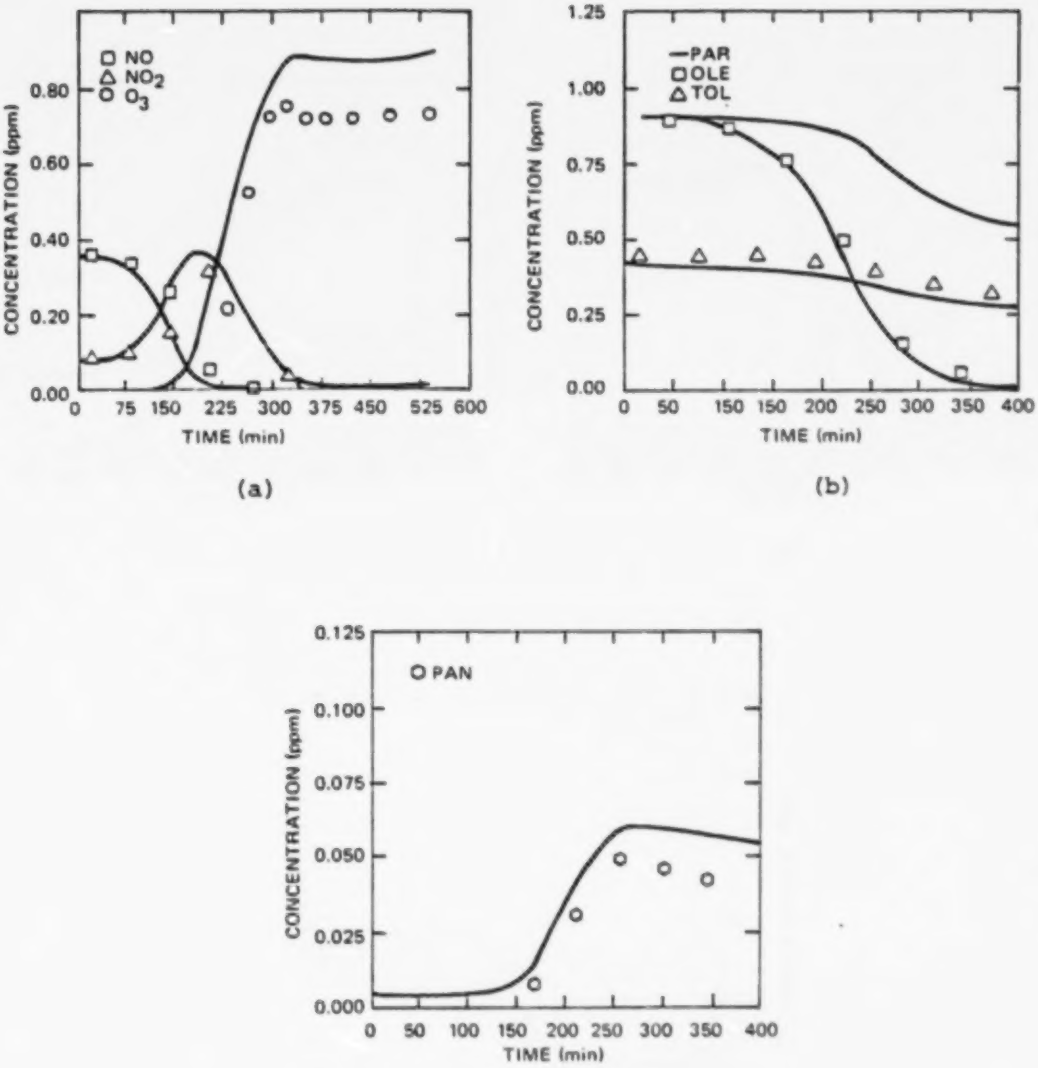

(a)

(b)

(c)

Figure 38. Simulation results for UNCB toluene-propylene, June 13, 1979, without NO_x loss.

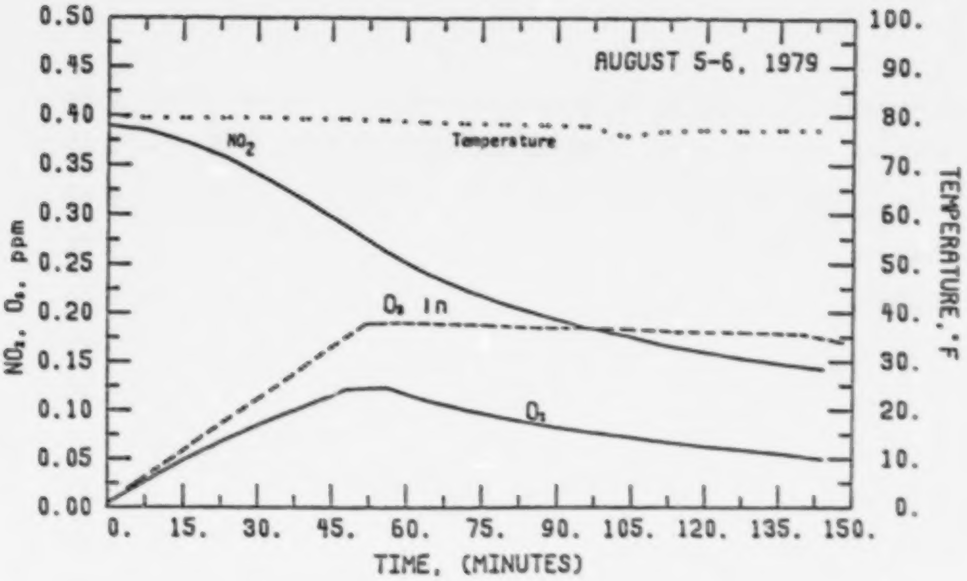

Figure 39. Experimental data from UNC outdoor smog chamber at night.

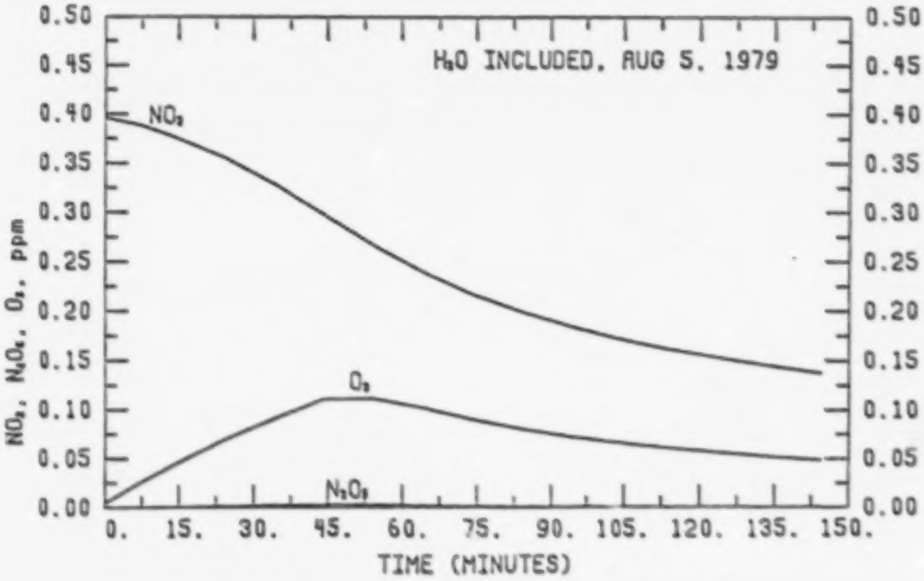

Figure 40. Simulation including heterogeneous N_2O_5 chemistry.

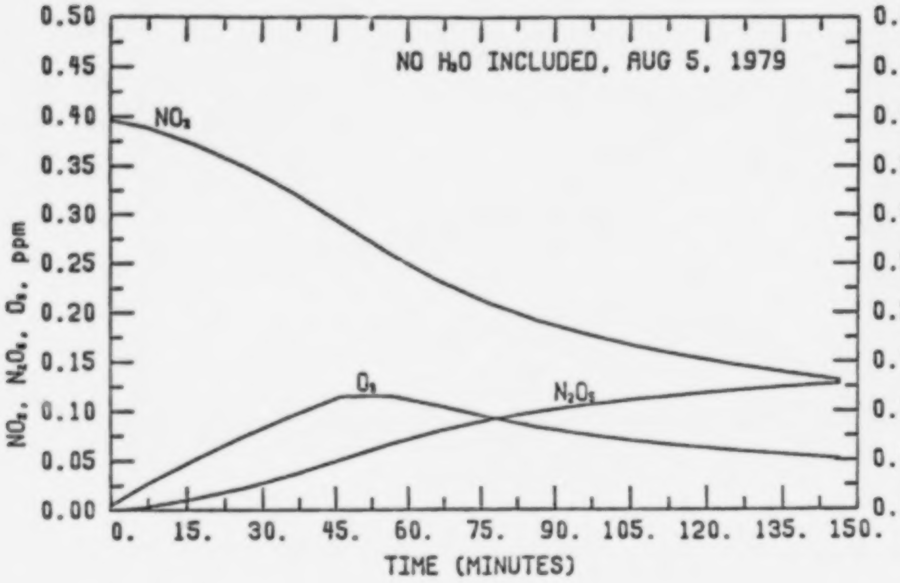

Figure 41. Simulation omitting heterogeneous N_2O_5 chemistry.

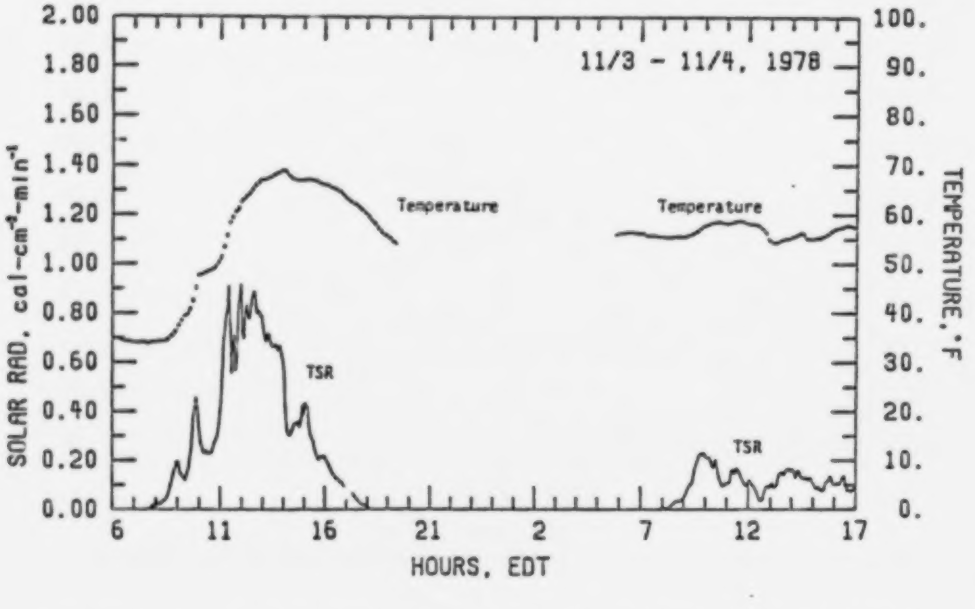

Figure 42. Experimental data from UNC outdoor smog chamber.

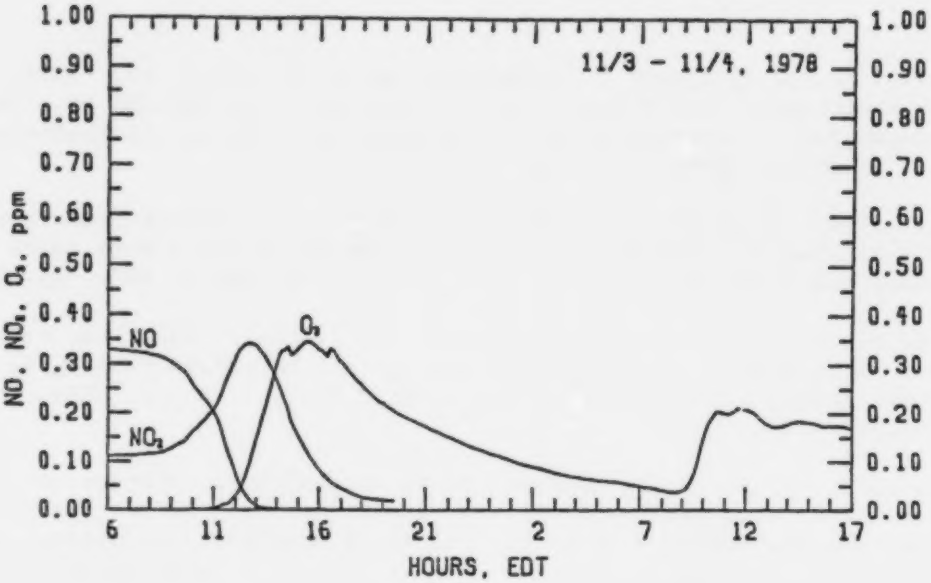

Figure 43. Experimental data from UNC outdoor smog chamber. Initial conditions: NO 0.321 ppm, NO_2 0.107 ppm, ethylene 3.29 ppmC.

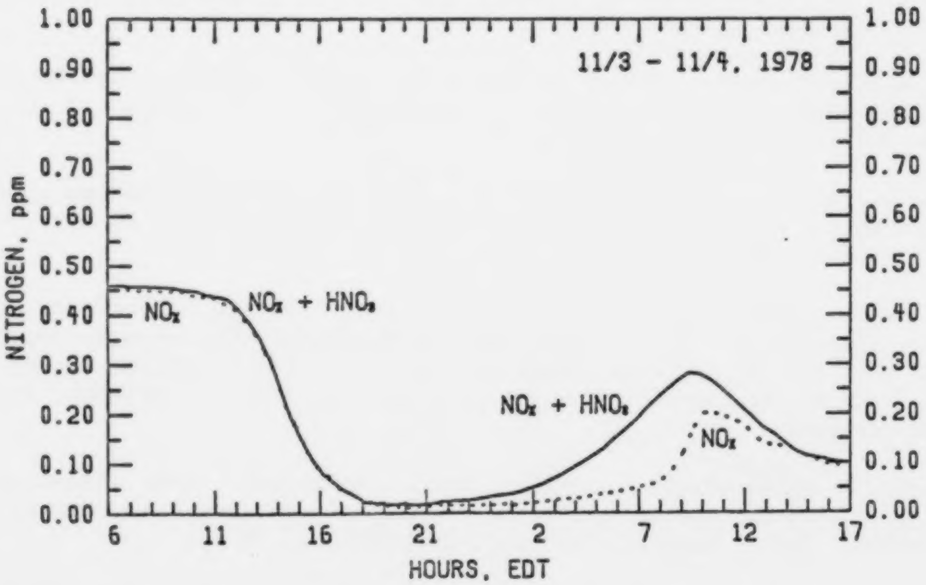

Figure 44. Experimental data from UNC outdoor smog chamber using chemiluminescent nitric acid analyzer.

REFERENCES

Carter, W. P. L., A. C. Lloyd, J. L. Sprung, and J. N. Pitts, Jr. 1979. Computer Modeling of Smog Chamber Data: Progress in Validation of a Detailed Mechanism for the Photooxidation of Propene and n-Butane in Photochemical Smog. Inter. J. Chem. Kinetics, 11:45-101.

Cox, R. A. 1979. Tropospheric Chemistry of Nitrogen Oxides--A Summary of the Status of Chemical Kinetics Data. In: Chemical Kinetic Data Needs for Modeling the Lower Troposphere. NBS Special Publication 557. pp. 71-84.

Darnall, K. R., W. P. L. Carter, A. M. Winer, A. C. Lloyd, and J. N. Pitts, Jr. 1976. Importance of RO_2 + NO in Alkyl Nitrate Formation from C_4/C_6 Alkane Photooxidations under Simulated Atmospheric Conditions. J. Phys. Chem., 80(17):1948-1950.

Demore, W. B., L. J. Sties, S. Kaufman, D. M. Golden, R. S. Hampson, M. J. Kurylo, J. J. Margitan, M. J. Molina, and T. Watson. 1979. Chemical Kinetic and Photochemical Data for Use in Stratospheric Modelling, Evaluation No. 2. JPL Publication 79-27. California Institute of Technology, Jet Propulsion Laboratory, Pasadena, California.

Dodge, M. 1977. Combined Use of Modeling Techniques and Smog Chamber Data to Derive Ozone-Precursor Relationships. In: Proceedings of International Conference on Photochemical Oxidant Pollution and Its Control. EPA-600/3-77-001b. U.S. Environmenal Protection Agency, Research Triangle Park, North Carolina, pp. 881-890.

Graham R. A., A. M. Winer, and J. N. Pitts, Jr. 1978. Pressure and Temperature Dependence of the Unimolecular Decomposition of HO_2NO_2. J. Chem. Phys., 68:4505-4510.

Hendry, D. G., and R. A. Kenley. 1977. Generation of Peroxy Radicals from Pernitrates (RO_2NO_2). Decomposition of Peracylnitrates. J. Amer. Chem. Soc., 99(9):3198-3199.

Jeffries, H. E. 1980. Use of Laboratory Data to Describe the Fate of NO_x in the Atmosphere. In: Proceedings of Technical Symposium on Implications of a Low NO_x Vehicle Emission Standard. EPA Technical Report, in press. U. S. Environmental Protection Agency, Research Triangle Park, North Carolina.

Lloyd, A. C., F. Lurmann, D. M. Golden, and J. Hutchins. 1979. Development, Testing, and Possible Applications of ELSTAR. Environmental Research and Technology, Inc., Westlake Village, California. 18 pp.

Pitts, J. N., Jr., K. Darnall, W. P. L. Carter, A. M. Winer, and R. Atkinson. 1979. Mechanisms of Photochemical Reactions in Urban Air. Smog Chamber Studies. EPA-600/3-79-110. U. S. Environmental Protection Agency. 569 pp.

Whitten, G. Z., and H. Hogo. 1978. User's Manual for Kinetics Model and Ozone Isopleth Plotting Package. EPA-600/8-78-041a. U. S. Environmental Protection Agency, Research Triangle Park, North Carolina. pp. 1-238.

Whitten, G. Z., J. P. Killus, and H. Hogo. 1980. Modeling of Simulated Photochemical Smog with Kinetic Mechanisms. EPA-600/3-80-028a, Vol. 1. U.S. Environmental Protection Agency, Research Triangle Park, North Carolina. 347 pp.

NITRATE MEASUREMENTS IN PRECIPITATION FOR THE STUDY OF TRENDS, PATTERNS, AND SCAVENGING PROCESSES

Gary J. Stensland

Atmospheric Sciences Section
Illinois State Water Survey
Urbana, Illinois 61801

INTRODUCTION

Nitrate (NO_3^-) is one of the major ions in precipitation samples, and the study of this ion is important for understanding the acid precipitation phenomenon (Likens 1976). In this discussion, the spatial patterns and time trends of NO_3^- in precipitation will be examined using data from studies carried out in the United States in the mid 1950's and the late 1970's. For temporal trends, data from the northeastern United States will be emphasized. An annual cycle of the NO_3^- concentrations in precipitation for Champaign, Illinois, will be compared to ambient aerosol data for the same location.

Scavenging by rain and snow is one of the major pathways for the removal of anthropogenic nitrogen compounds from the atmosphere. The relative importance of the various scavenging mechanisms which produce NO_3^- in precipitation is not yet well established. A basic question to be answered regarding NO_3^- and sulfate ($SO_4^=$) is whether these ions are found in precipitation as a result of gaseous or particulate scavenging mechanisms. In this paper, the spatial variation of NO_3^- in samples from single, convective, rain cells will be used to suggest that gaseous removal mechanisms are probably important.

CONCLUSIONS

1. With respect to the spatial pattern of NO_3^- concentrations in precipitation, the limited data available show that the current distribution in the eastern United States is similar to that observed in 1955/56. The highest values occur north of the Ohio River, from Wisconsin to New York. The values are generally higher in the northeast than in the southeast. The current data for the western United States are too limited to compare to the 1955/56 data.

2. With respect to the temporal trend of NO_3^- in precipitation, all data show increased concentrations in the late 1970's compared to the mid-1950's. The amount of increase varies, depending on which sites and which years are compared, ranging from a factor of ~1.3 to a factor of 3. This is in general agreement with the rise in nitrogen oxide (NO_x)

emissions for the United States, which increased by a factor of ~2.1 from 1955 to 1976.

3. For 1 year of data at Champaign, Illinois, the ambient aerosol NO_3^- levels had the same seasonal trend as for the NO_3^- in precipitation, namely, higher levels in the winter months than in the summer months.

4. For rain samples from six convective rain cells, NO_3^- and $SO_4^=$ concentrations were observed to be less variable in space than calcium (Ca^{++}), magnesium (Mg^{++}), and rainfall. This characteristic suggests that both gaseous and particulate scavenging are probably important for NO_3^- and $SO_4^=$, as compared to calcium and magnesium, where only particulate scavenging would be occurring.

Conclusions regarding temporal and spatial patterns of NO_3^- concentrations in precipitation can not be more specific at this time because of the lack of an adequate data base.

PATTERNS AND TRENDS FOR NITRATE IN PRECIPITATION

To assess the effect of air pollution emissions on air quality and human health, a large national ambient air monitoring network has operated continuously for about 20 years. A shortage of precipitation quality data for the United States persists, however, and only recently have the adverse effects of altered precipitation quality aroused national and international concern. As a result, a national precipitation chemistry network for the United States, the National Atmospheric Deposition Program (NADP), began operation in October 1978. This program, which has established both monitoring and research objectives, currently (as of October 1980) includes 74 collection sites distributed across the United States, and utilizes standardized collection and analysis methods.

Nitrate patterns and trends in precipitation will be examined with five data sets; site locations for four of these data sets are shown in Figure 1. The first data set is from the Multistate Atmosphere Power Production Pollution Study (MAP3S) network (Battelle Pacific Northwest Laboratories 1977), still in operation and now consisting of eight sites in the Northeast. Beginning in September 1977, the samples from this project were analyzed for all the major cations and anions, as described by Dana et al. (1978); data collected for about 1 year from 3 MAP3S sites were used for this analysis. Second, the Atmospheric Sciences Section of the Illinois State Water Survey (ISWS) began a precipitation chemistry collection program at a site near Champaign, Illinois, in May 1977 (Stensland 1979a). The third data set, taken from an ISWS study conducted by Larson and Hettick (1956) at the same site from October 1953 to August 1954, provided historical data for this present analysis. The fourth data set, based on the Junge network, which was in operation from July 1955 to June 1956, provided the remainder of the historical data (Junge and Gustafson 1956; Junge 1963). The Junge network, shown in Figure 1, consisted of 63 sites distributed across the continental United States. The Junge sites in Bermuda and Newfoundland were not included in this analysis. The fifth data set, from the NADP network, will be compared with the Junge data set.

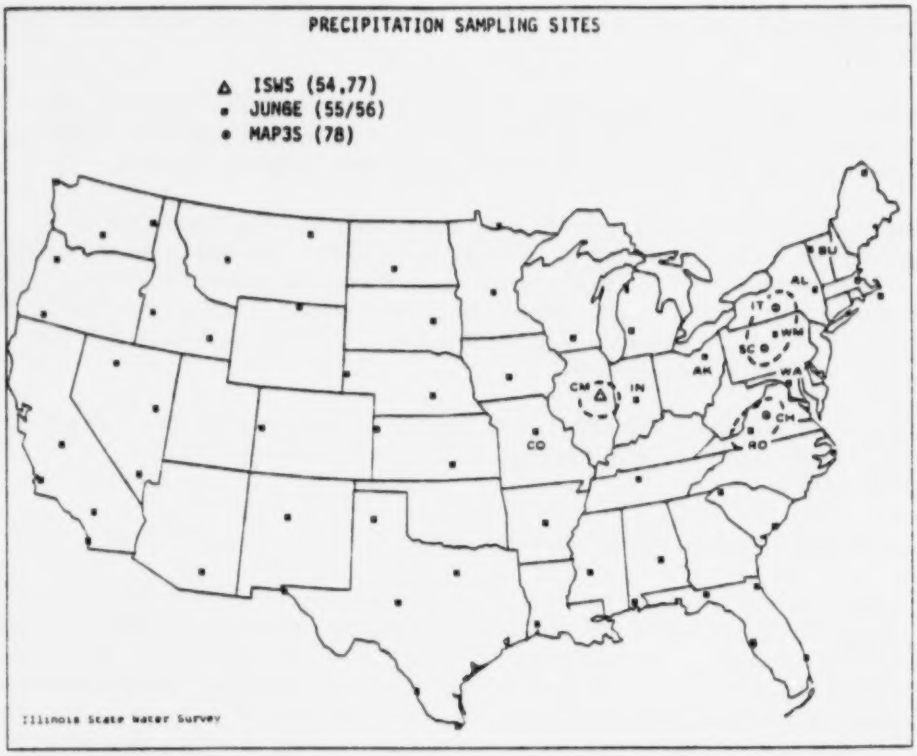

Figure 1. Precipitation chemistry sampling sites. The dashed contours enclose sites which are to be compared with each other.

Collection Methods and Procedures

For the MAP3S sites, an automatic wet-only sampler is used to collect event samples, where event refers basically to a daily sample. The collecting funnel is thoroughly rinsed after each sample is removed. The MAP3S sites are all located at least several kilometers away from the nearest urban areas. The 1977 ISWS samples were obtained with a HASL-type collector (Volchok and Graveson 1975). The 1954 ISWS samples were collected manually during precipitation events using a stainless steel funnel (1.2 m diameter), which was uncovered and rinsed at the beginning of the events. The 1955/1956 Junge samples were collected with a Plexiglas funnel and polyethylene bottle, which were exposed only during precipitation events. The event samples were composited to provide one sample per site per month. The samplers were located at Weather Bureau facilities so that personnel would be available to expose the collecting funnels during the precipitation events. Some of the Junge sites were closer to cities and industrial areas than desirable, but the consistent data patterns produced by the study indicated that most of the sites produced data representative of their region. Finally, the NADP sites are located such that regionally representative samples are obtained. A commercial version of the HASL collector is used at each site. The samples are collected on Tuesday of each week and sent to a central laboratory for chemical analysis.

The automatic samplers being used at the MAP3S, ISWS, and NADP sites minimize the potential for evaporation or dry deposition, two processes which can cause erroneous ion concentration data. It also appears that these potential problems were avoided in the Larson and Hettick (1956) study. The Junge data may have been affected somewhat by these two processes, although the event collection mode would have helped minimize these effects.

Discussion

The strong relationship between the ion concentrations in rain and snow events and the precipitation amounts is well known; when the amount is less than about 5 mm, the concentrations are usually very high. To compensate for this effect, many researchers use the sample volume-weighted averages for data interpretation; other researchers use median values.

Nitrate concentration data from the five projects are shown in Table 1 and in Figures 2 and 3. A mixture of median and sample-volume-weighted concentrations are presented for the following reasons. Since accurate sample volumes were not available for the 1954 ISWS data, for all ISWS data in Table 1 the median concentrations are given. For the Junge data, the monthly compositing procedure produced sample-volume-weighted concentrations. However, the Junge NO_3^- data were reported only as quarterly-weighted averages (Junge 1958). Therefore, the Weather Bureau precipitation data for the Junge sites were used to calculate the annual weighted average NO_3^- data given in Table 1 and Figure 2. Since the Junge data and the MAP3S data are to be compared, the MAP3S sample-volume-weighted averages are listed in Table 1 instead of the median values. For the NADP data in Figure 3, median values are presented, since the data set is small and median values should reach a stable value more quickly than weighted average concentrations.

TABLE 1. NO_3^- CONCENTRATIONS IN PRECIPITATION (mg/liter)
AND RATIOS OF RECENT VALUES TO HISTORICAL VALUES

Recent Values	Historical Values		Ratio*
Column 1	Column 2	Column 3	Column 4
Midwest Sites†			
CM (1977): 1.85	CM (1954): 1.25	CO (1955/56): 0.58 IN (1955/56): 0.53	1.5
Eastern Sites†			
IT (1978): 1.71	WM (1955/56): 1.31	BU (1955/56): 1.12	1.3
SC (1978): 1.67	WM (1955/56): 1.31	AL (1955/56): 0.77	1.3
CH (1978): 1.54	RO (1955/56): 0.84	WA (1955/56): 0.54	1.8

*Ratio of Column 1 to Column 2.
†CM is an ISWS site; CO, IN, WM, RO, BU, AL, and WA are Junge sites; IT, SC, and CH are MAP3S sites.

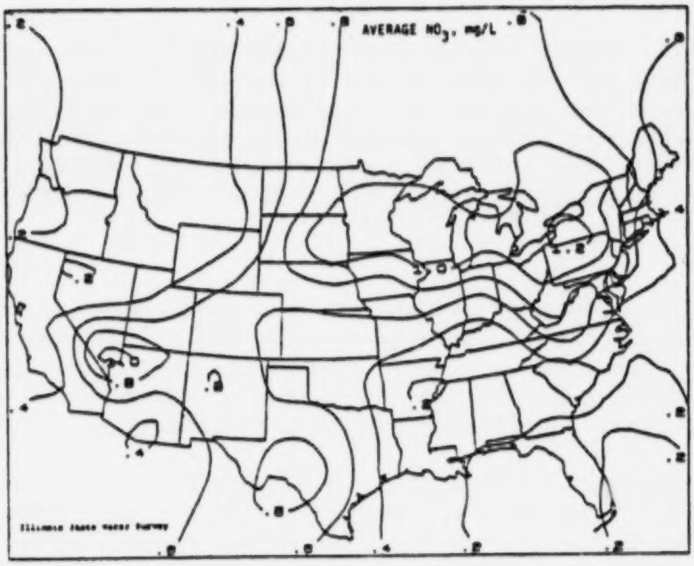
AVERAGE NO_3, mg/L
.2
.4
Illinois State Water Survey

Figure 2. Contours of the sample-volume-weighted NO_3^- concentrations for the Junge network, in operation from July 1955 to June 1956 (Junge 1958; Stensland 1979c).

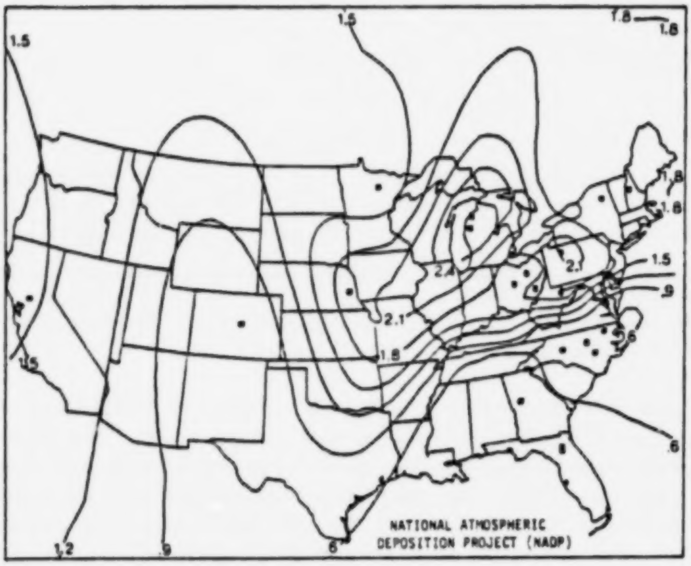
1.5
1.5
1.8
1.8
1.8
1.8
1.8
2.4
2.1
1.5
.9
2.1
1.8
.6
1.5
.6
1.2
.9
.6
NATIONAL ATMOSPHERIC DEPOSITION PROJECT (NADP)

Figure 3. Contours of the median NO_3^- concentrations from the initial NADP (1979) results.

The spatial distribution pattern of NO_3^- in precipitation in the eastern United States in 1955/56 (Figure 2) is generally similar to that for 1978/79 (Figure 3). In particular, the relatively large region of elevated NO_3^- values in the northeast is present in both data sets. From this area of high concentrations the values clearly decrease toward the southeastern United States, and values are also lower in the New England states. At this time the sparcity of NADP sites in the West does not allow any detailed comparison with the Junge data. For Figure 3, most of the sites had data for 5 months, from October 1978 through February 1979. The remaining sites had data for time intervals varying from 1 to 8 months. Because of the short sampling time span, the NADP data presented in Figure 3 should be considered preliminary.

The data in Figures 2 and 3 for the northeastern United States demonstrate that recent NO_3^- concentrations are higher than those for 1955/56, by a factor of about two. This general time trend is also followed for the sites from North Carolina to Florida. The time trend can be questioned for at least three reasons: 1) weighted averages are plotted on Figure 2 and medians are plotted on Figure 3, 2) data shown in each figure represent sampling periods <1 year in duration, and 3) the NADP data in Figure 3 are generally for only the winter months. To at least partially overcome these three deficiencies, additional time trend data are presented in Table 1. The primary sites in Table 1 (Columns 1 and 2) are enclosed by dashed contours in Figure 1. They include CM (Champaign, Illinois), IT (Ithaca, New York), SC (State College, Pennsylvania), WM (Williamsport, Pennsylvania), CH (Charlottesville, Virginia), and RO (Roanoke, Virginia). The 1954 (Larson and Hettick) data in Table 1 provide a data point 1 year prior to the 1955/56 Junge data. Likewise, the MAP3S data, denoted as 1978 in Table 1, are actually for the 1-year period from September 1977 to August 1978 and thus do not coincide in time with the NADP data.

The upper portion of Table 1 displays the nitrate data for the midwestern sites and the lower portion presents the data for the eastern sites. Broken lines connect sites which are located close to each other. The basic feature to note is that the NO_3^- ratios for each site are greater than 1 but less than 2. The third column provides additional sites to compare to those in the first column (these additional sites are also indicated on Figure 1); the comparison produces ratios larger than those listed in Column 4 of the table. In general, the conclusions from Table 1 agree with those formulated after comparing Figures 2 and 3.

For comparison to the NO_3^- trend in precipitation, the NO_x emissions for the United States are shown in Figure 4, along with the sulfur oxide (SO_x) emissions. The data for this plot were tabulated from several government reports (summarized in Stensland 1979b). The emissions data are values for the entire United States; trends represented by these data are assumed to reflect patterns of emissions produced by sources contributing to the air and precipitation quality sites in the eastern United States. A study of the geographical distribution of the 1972 emissions data does show that the EPA air quality regions I through VI (basically the eastern United States) contributed 80 percent of the total NO_x emissions (National Research Council 1973). The same study showed that six states (New York, Pennsylvania, Ohio, Michigan, Indiana, and Illinois) contributed 45 percent of the total.

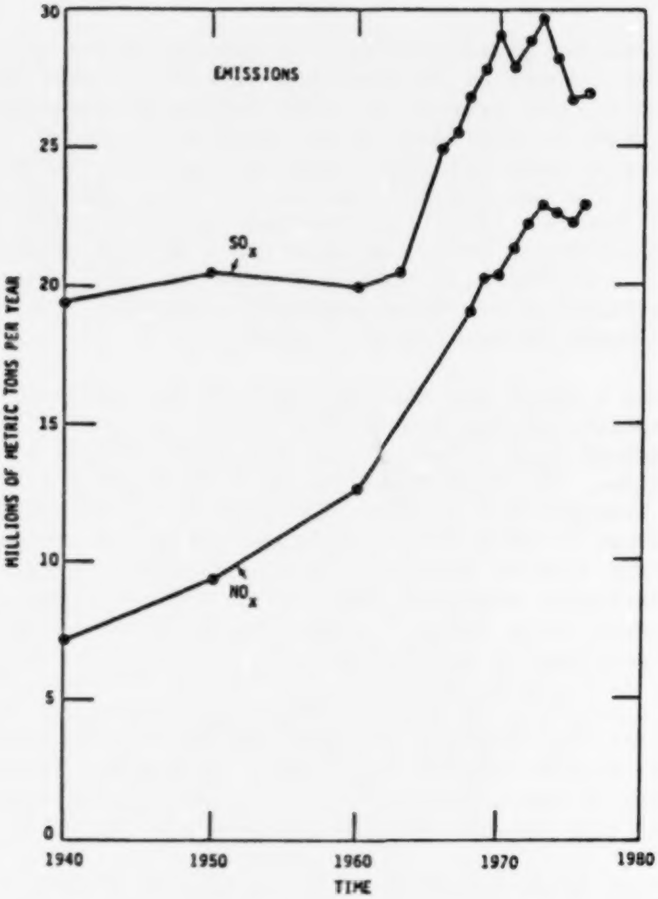

Figure 4. Emission trends for NO$_x$ and SO$_x$ from the data in various government reports, as tabulated by Stensland (1979b).

With respect to sources, Cavender et al. (1973) reported that gasoline combustion in motor vehicles accounted for 34 percent of the NO$_x$ emissions in 1970, while coal, fuel oil, and natural gas combustion in stationary sources accounted for 44 percent of the total.

From Figure 4 it is seen that from mid-1950 to 1976, NO$_x$ emissions increased from about 11 to 23 million metric tons per year, or by a factor of 2.1. At the same time, the SO$_x$ emissions increased from about 20 to 27 million metric tons per year, or a factor of 1.3. Cook (1971) explained that the relatively small increase in SO$_x$ emissions could be traced to heavier use of natural gas and low-sulfur-oil and -coal since the mid-1950's. The larger growth rate in NO$_x$ emissions results from the large increase in energy consumption for electric power generation and for transportation. Cook showed that between 1955 and 1979, electric power consumption increased by a factor of 2.6 and energy consumption for transportation increased by a factor of 1.6.

In general, the increased NO_3^- levels in precipitation seem to be consistent with the anthropogenic emission increases. This point is supported by the following rough estimates for the United States. From Figures 2 and 3 a typical area average NO_3^- value for precipitation is chosen to be 0.6 mg/liter for 1955 and 1.5 mg/liter for 1979. Using an areal average value of precipitation for the United States of 75 cm, the annual wet deposition of NO_3^- expressed as nitrogen is 0.8 Tg-N in 1955 and 2.0 Tg-N in 1979, or an increase of 1.2 Tg-N (1 Tg-N = 1 million metric tons expressed as nitrogen). The NO_x emissions in the previous paragraph translate to annual emissions of 3.4 Tg-N in 1955 and 7.1 Tg-N in 1976, or an increase of 3.7 Tg-N. Some of the emitted NO_x will be removed by dry deposition and some transported beyond U.S. boundaries. Thus, the rough estimate suggests that the fossil fuel combustion emissions can reasonably account for the increased NO_3^- in precipitation.

Another large flux of nitrogen in the environment is from fertilizers. The annual United States nitrogen fertilizer consumption increased from 1.8 Tg-N in 1955 to 9.4 Tg-N in 1976 (Hargett 1976), with the percent anhydrous ammonia consequently rising from 18 percent to 47 percent in 1976. If one third of the airborne NO_x is removed as wet deposition, then approximately one half of the increased fertilizer application would have to be lost to the atmosphere to explain the observed NO_3^- trend in precipitation. Soderlund (1977) used measured NO_x release rates from the soil to make a rough estimate that fertilizer applied in Western Europe contributed 0.03 to 0.3 Tg-N to the atmosphere versus 3.8 to 9.5 Tg-N from fossil fuel combustion. Fertilizer thus does not seem to be important in explaining increased NO_3^- levels in precipitation.

In order to account for the pH levels found in the current precipitation for the northeastern United States, a significant NO_3^- fraction must be assumed to be in the form of nitric acid (HNO_3). If this formation also occurred in 1955, one can assume the trend of increased NO_3^- levels led to greater levels of HNO_3 in precipitation. However, the actual trend of the pH of the precipitation depends on several chemical constituents. Recent work suggests that the major reason for the apparent decreasing precipitation pH is the current low levels of basic constituents (Stensland 1979c; Stensland and Semonin, unpublished data).

DAILY PRECIPITATION AND AEROSOL DATA FOR ILLINOIS

Particles in the ambient air are incorporated into raindrops and snowflakes. Therefore, interesting and useful data should result if the same chemicals are monitored in both air and precipitation at a site. A reasonable short sampling interval, such as daily sampling, is desirable. Also, because of the complexity of the scavenging processes, it is necessary to obtain a large number of samples in order to identify persistent features. This type of sampling was carried out at the site 8 km south of Champaign, Illinois, from June 1977 to May 1978.

In Figure 5 are plotted the NO_3^- concentrations for the daily precipitation samples, collected with the modified HASL collector. Since the NO_3^- is always high for cases with slight precipitation, these cases were excluded in comparing the precipitation concentrations to air concentrations. For Figure 5, the cases with daily precipitation <1 mm have not been included.

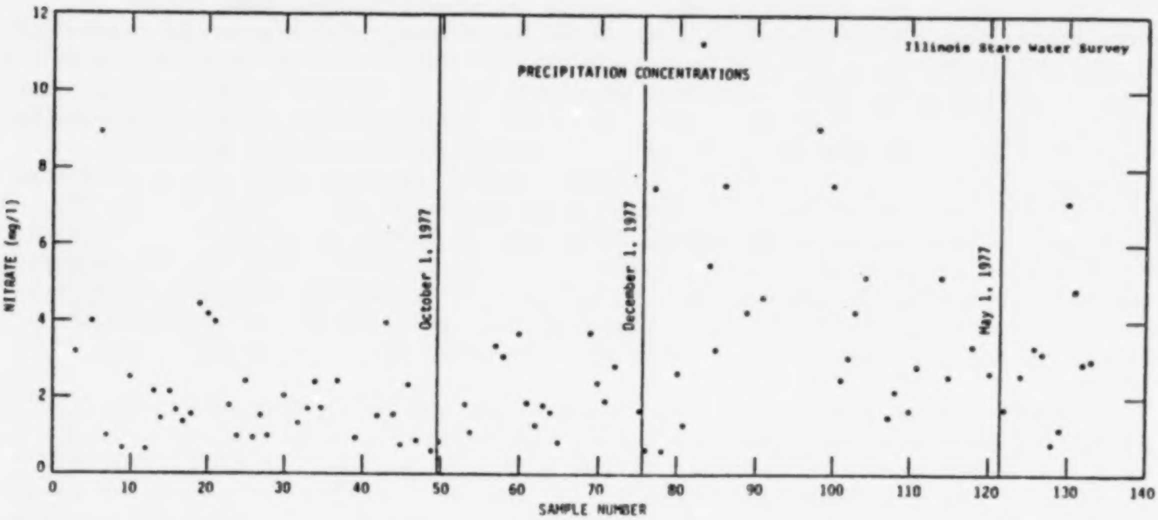

Figure 5. Nitrate concentrations in daily precipitation samples, collected at Willard Airport, Champaign, Illinois, from June 1977 to May 1978.

Method

The ambient air data from Nuclepore filter samples collected at the same site are shown in Figure 6. From 21 to 29 daily samples were available to calculate the statistics for each month, except for June 1977 when only 16 were available. The lines on Figure 6 connect the maximum, minimum, mean, and median values for each month. The standard deviation from the mean is also

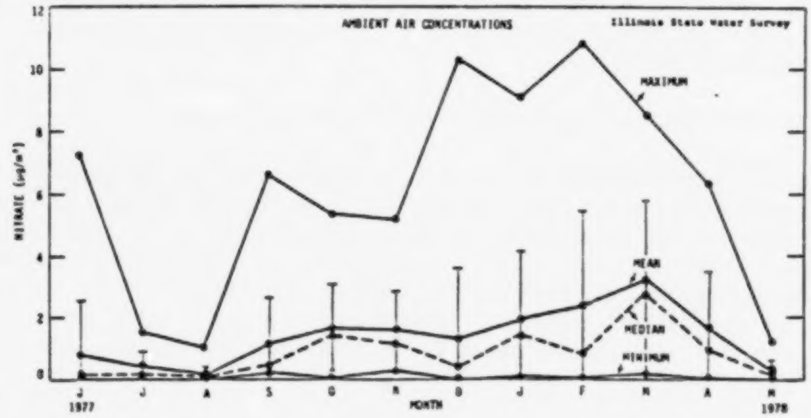

Figure 6. Monthly averages for ambient aerosol nitrate concentrations for daily samples collected at Willard Airport, Champaign, Illinois.

shown. Figure 7 presents the concurrent data for $SO_4^=$. The sampling procedure consisted of drawing air through filters at about 30 liters/min for either 30 or 45 min/h for the 24-h sampling interval, so that about 20 m^3 of air were sampled. However, in June, July, and part of August, the procedure was instead to sample continuously for 12 h, usually from noon to midnight. The aerosol collection media were Nuclepore filters, 37 mm in diameter and with 0.8 μm pore diameters. For the extraction procedure, the filters were placed in 25 ml of deionized water and shaken for 20 min with a wrist action shaker. The anions were then determined by standard colorimetric procedures with a Technicon Auto Analyzer II system.

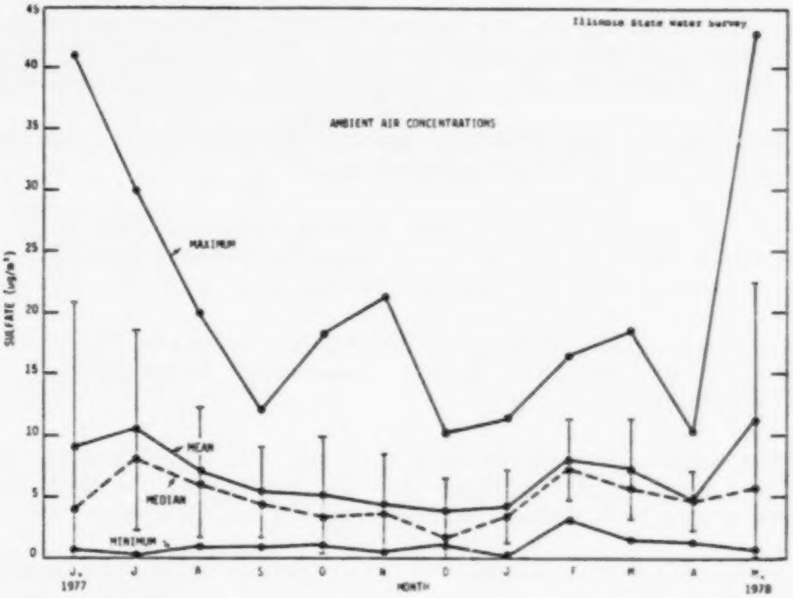

Figure 7. Monthly averages for ambient aerosol sulfate concentrations for daily samples collected at Willard Airport, Champaign, Illinois.

Discussion

In Figure 6 the mean and median NO_3^- curves are seen to peak in March, while the four largest NO_3^- maximum values extend from December through March. In Figure 7, the median $SO_4^=$ curve peaks in February and in July. In the $SO_4^=$ data can be seen the dramatically large maximum monthly values in May and June.

In Table 2 are presented the median precipitation and aerosol values for NO_3^- and $SO_4^=$ for two 5-month periods selected to coincide with the NO_3^- aerosol peak and valley trend in Figure 6. The May-September interval is basically a summer interval, while the December-April interval is basically a winter interval. The median data in Table 2 suggest that $SO_4^=$ is not significantly different in the summer versus the winter period for either the aerosols or the precipitation. However, for NO_3^-, the median precipitation

TABLE 2. MEDIAN NO_3^- AND $SO_4^=$ CONCENTRATIONS IN AMBIENT AEROSOLS ($\mu g/m^3$) AND IN PRECIPITATION (mg/liter) FOR 1 YEAR AT CHAMPAIGN, ILLINOIS

Ion/Season	Ambient Aerosol	Precipitation
(NO_3^-) May-Sept	0.1	1.8
(NO_3^-) Dec-Apr	1.1	3.3
($SO_4^=$) May-Sept	5.9	3.8
($SO_4^=$) Dec-Apr	5.0	4.1

concentrations are a factor of 1.8 higher in the winter than the summer and a factor of 11 higher for the ambient aerosol. It does therefore seem that in a general sense the trends for NO_3^- in aerosols and precipitation are consistent.

Two of the possible explanations for the differences in the magnitude of the NO_3^- aerosol and precipitation trends are:

a) the NO_3^- in precipitation results from scavenging of both gaseous and particulate species, and the gaseous species have a seasonal trend opposite that of NO_3^- aerosol, or

b) the Nuclepore filters were not providing accurate NO_3^- aerosol values, and perhaps the measurement error had a seasonal trend.

The Table 2 data also demonstrate that the $SO_4^=/NO_3^-$ ratios in precipitation are much different than for the aerosols. An explanation for this difference could be based on circumstance a or b, above.

It is strange that NO_3^- aerosol concentrations should have the strong seasonal trend shown in Table 2, while $SO_4^=$ does not. The transportation source emissions, which are very important for NO_x but not for SO_x, should not have such a seasonal trend.

While the NO_3^- aerosol data in Figure 5 were being collected, a series of short-term field experiments were carried out to intercompare various filter setups (Stensland and Bartlett 1979). The results from an 8-day study in April 1978, intercomparing four setups, are shown in Figure 8. Filters were either Whatman 41 (WHAT 41) or Nuclepore (NUCL); numbers in parentheses are filter diameters in centimeters, followed by filter pore diameters in micrometers. For the dual (stacked) Nuclepore (DUAL NUCL) setup, the two filters were analyzed separately, and results were added together to produce the data in Figure 8. Ambient air was drawn through the filter samplers for 45 min of each hour during the 24-h sampling periods. The NUCL (37,0.8) and DUAL NUCL (47,0.8,0.8) flow rates were set at 30 and 50 liters/min, respectively, to produce a face velocity of about 40 cm/sec for both setups.

The agreement between $SO_4^=$ and Ca^{++} for the four filter setups was good, except for the large Ca^{++} value on Day 102. This extraordinary value can be

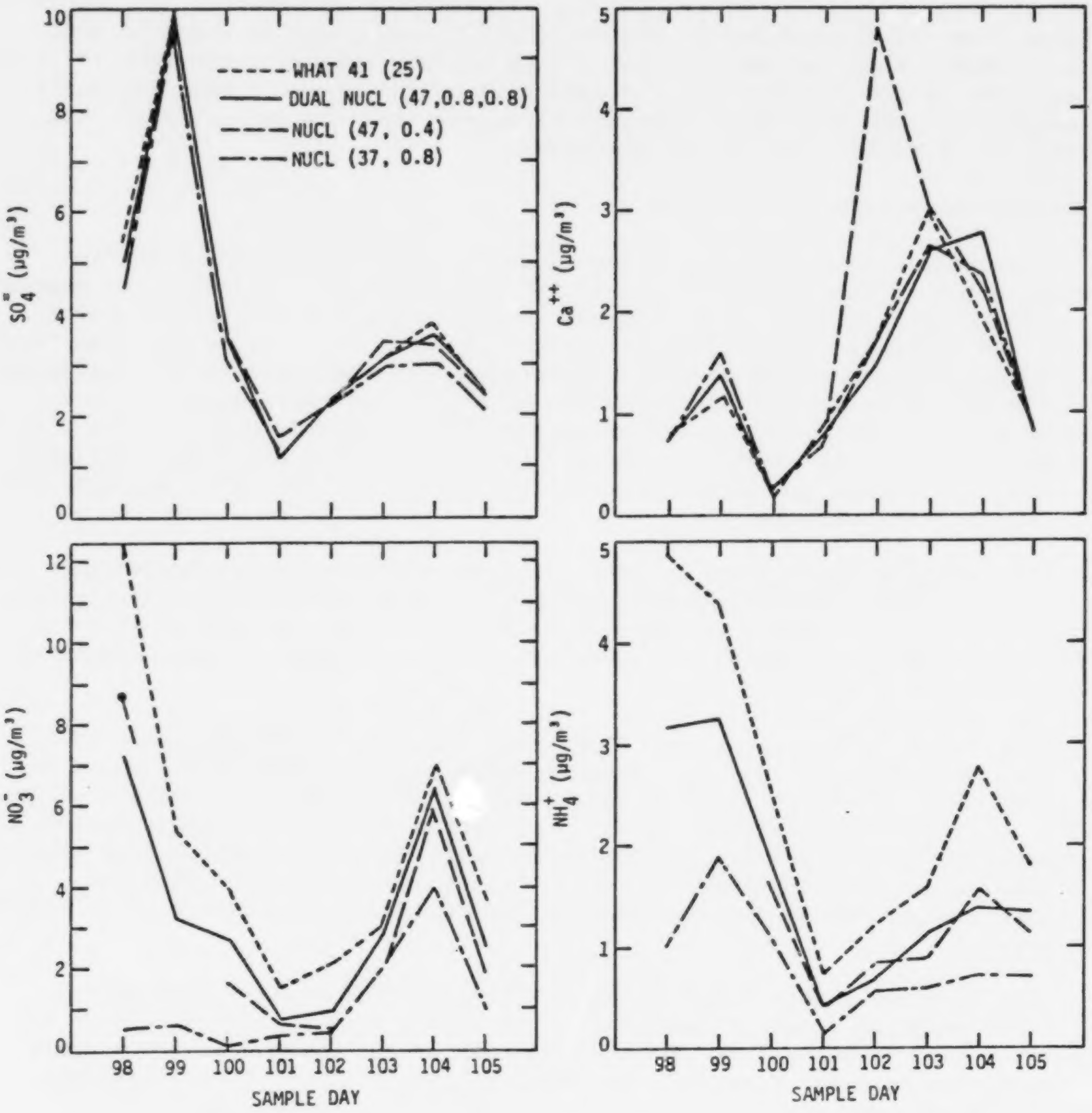

Figure 8. Daily aerosol concentrations of water soluble sulfate, calcium, nitrate, and ammonium for four filter setups.

partially explained by the site locations; the NUCL (47,0.4) filter was at ground level, in contrast with the other three filter setups, on a tower about 10 m off the ground and about 50 m southwest of the ground site. Vehicular traffic may have produced the large Ca^{++} value at the ground site on Day 102. For NO_3^- and ammonium (NH_4^+), agreement among the four filter setups was not good. The high values for the Whatman 41 samples are not unexpected, but the differences among the three Nuclepore setups is surprising; duplicate results, however, were produced in a second 8-day experiment (not shown). For the 16 samples from the 2 experiments, the median NO_3^- concentration with the DUAL NUCL (47,0.8,0.8) setup was a factor of 6.2 greater than with the NUCL (37,0.8) setup. The factor for NH_4^+ was 1.5, which is better than for NO_3^- but still unacceptable. The NO_3^- data in Figure 8 suggest that the aerosol NO_3^- data summarized in Table 2 may not be accurate.

PRECIPITATION SCAVENGING OF NITRATE

A general scenario for the scavenging processes which produce NO_3^-in precipitation is the following. Particles containing NO_3^- and $SO_4^=$ are carried by updrafts into the base of a cloud and serve as cloud condensation nuclei (CCN). The droplets typically reside in the cloud 30 min, and during this time gaseous nitrogen compounds may be incorporated into the droplets and converted to nitrates. A raindrop which falls out of this cloud represents a volume equivalent to a collection of something like 10^6 cloud droplets. In the 2 to 3 min fall time from cloud base to ground, the raindrop can scavenge additional NO_3^- via particulate and gaseous removal processes. This general scenario does not consider the ice phase.

One possible way to gain insight into this complicated wet scavenging system is to obtain rain samples from a single cloud passing over fixed ground sites, and then to compare the spatial variation for the various ions. This field experiment was carried out recently, and results for one case are being presented now.

The Summer Chemistry of Rain Experiment for 1978 (SCORE-78) began on 6/1/78. Precipitation chemistry sampler sites, separated by about 1.5 km and serviced after individual rain showers, were in operation until the end of July 1978. The rapid servicing of the sites protected against ion concentration increases due to evaporation and dry deposition. The rain samples were usually filtered or refrigerated within 6 to 24 h after the rainfall to minimize chemical changes due to the slow dissolution of particulate matter or to other phenomena.

The 23 sites in the SCORE-78 network (Figure 9) basically were set up along two sampling lines, oriented north to south, with a site separation of about 1.5 km. Weighing type of recording rain gages, located at the airport site (AT) and at sites 1 through 12, were equipped with 6-h chart rotation gears that provided excellent time resolution of rain accumulation rate. Similar rain gages were located at sites 13 through 21, except that 24-h chart rotation gears were used. Bulk rain chemistry samplers were located at sites 4, 9, and 13 through 21. Wet/dry samplers of the HASL type were located at sites 1 through 9, BT, and AT.

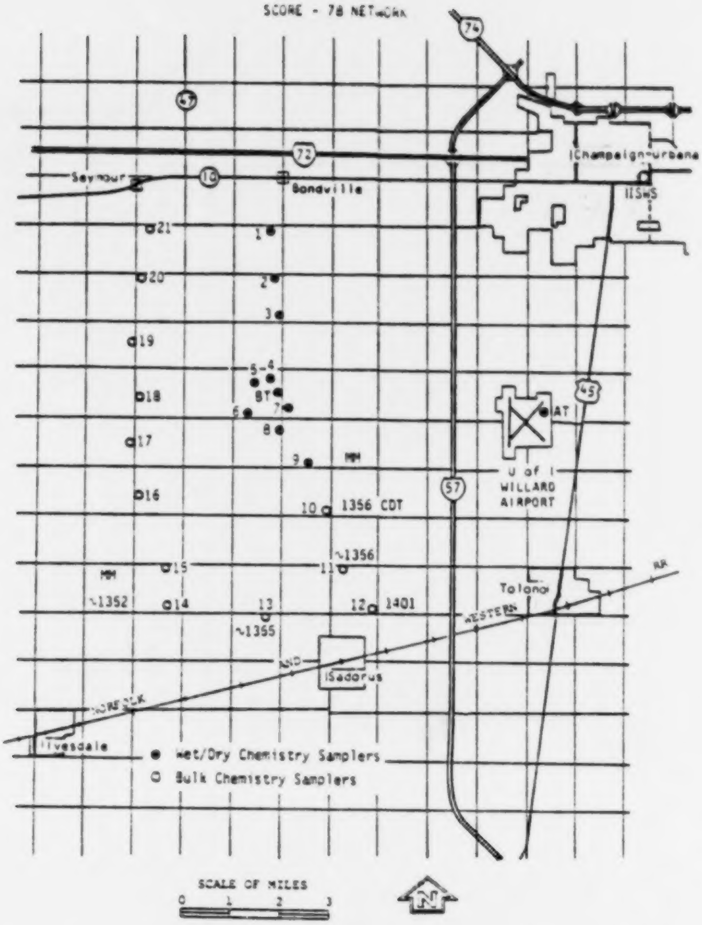
SCORE - 78 NETWORK
74
47
72
10
Seymour
Bondville
Champaign-Urbana
ISWS
1
2
3
4
5
BT
6
7
8
9
MM
10
1356 CDT
~1356
11
12
1401
13
~1355
14
15
16
17
18
19
20
21
MM
~1352
AT
45
57
U of I
WILLARD
AIRPORT
Tolono
Sadorus
Ivesdale
NORFOLK AND WESTERN RR
● Wet/Dry Chemistry Samplers
○ Bulk Chemistry Samplers
SCALE OF MILES
0
1
2
3
N

Figure 9. The SCORE-78 network; the times that the rainfall began on the afternoon of 7/1/78 are indicated.

On 6/30/78, a hailstorm moved across the network between 1503 and 1550 CDT, and additional rainshowers followed during the night. The total rainfall across the network from this storm system varied from 7 to 30 mm. On the following day a small shower formed in the southeastern portion of the network, giving rainwater samples at sites 9 through 15. The rainfall start and end times (Figure 9 and 10) indicate that the shower, lasting only 5 to 10 min at any site, formed on the network and then moved southeastward off the network. Figure 11 presents the sample volume and pH contours for the shower, with the asterisks denoting the locations of sites 9 through 15. The isopleths on Figures 11 through 13 were produced by a computer program. The program used an objective map analysis technique based on a successive corrections scheme developed by Barnes (1964; 1973) and modified by Achtemeier et al. (1978). The sample volume pattern in Figure 11 shows that the strongest portion of the rain cell affected the southeastern sites. The 1345 CDT surface weather observations for Willard Airport were T = 88°F, TD = 74°F; the wind was 10 knots from 240°; there was 7/10 sky cover, 3/10 opaque; haze reduced visibility to 4 mi.

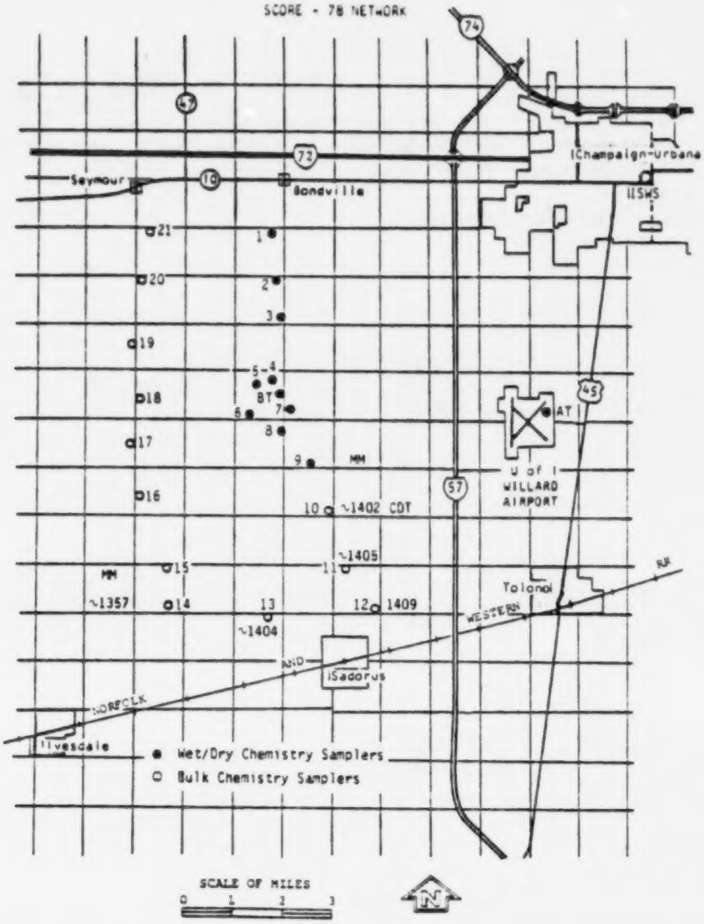
SCORE - 78 NETWORK
74
47
72
10
Seymour
Bondville
Champaign-Urbana
ISWS
21
20
19
18
17
16
15
14
1
2
3
5
4
BT
6
7
8
9
MM
10
~1402 CDT
~1405
11
12
1409
13
~1404
MM
~1357
45
AT
57
U of I
WILLARD
AIRPORT
Tolono
RR
WESTERN
AND
NORFOLK
Sadorus
Ivesdale
● Wet/Dry Chemistry Samplers
○ Bulk Chemistry Samplers
SCALE OF MILES
0
1
2
3
N

Figure 10. The ending time of the rainfall for the 7/1/78 single shower.

Table 3A contains the actual parameter values for the rainshower. Since 0.25 mm (0.01) in of rainfall was equivalent to a sample volume of about 8 ml, the sample volume values in Table 3A indicate that the rainfall for the shower varied from about 1 to 4.2 mm (0.04 to 0.17 in). The on and off times indicate when the precipitation chemistry containers were installed and removed at each site. Since the exposure time was short and since rain in substantial amounts had fallen in the previous 24 h, evaporation should have been negligible and dry deposition effects should have been small for the bulk samplers. By comparing the sample volume for sampler 9W (the wet/dry sampler at Site 9) and the volume for sampler 9 (the bulk collector at Site 9), an approximate 3-ml difference is seen, possibly reflecting an evaporation loss; and a 10-percent correction would bring the ion concentrations (Table 3B) for 9W into better agreement with those for 9. However, somewhat different collection efficiencies for the two rainwater chemistry samplers could also account for the different sample volumes and ion concentrations in samplers 9W and 9. For Figures 11 through 13, the data for sampler 9 were used, since samplers 10 through 15 were also bulk collectors.

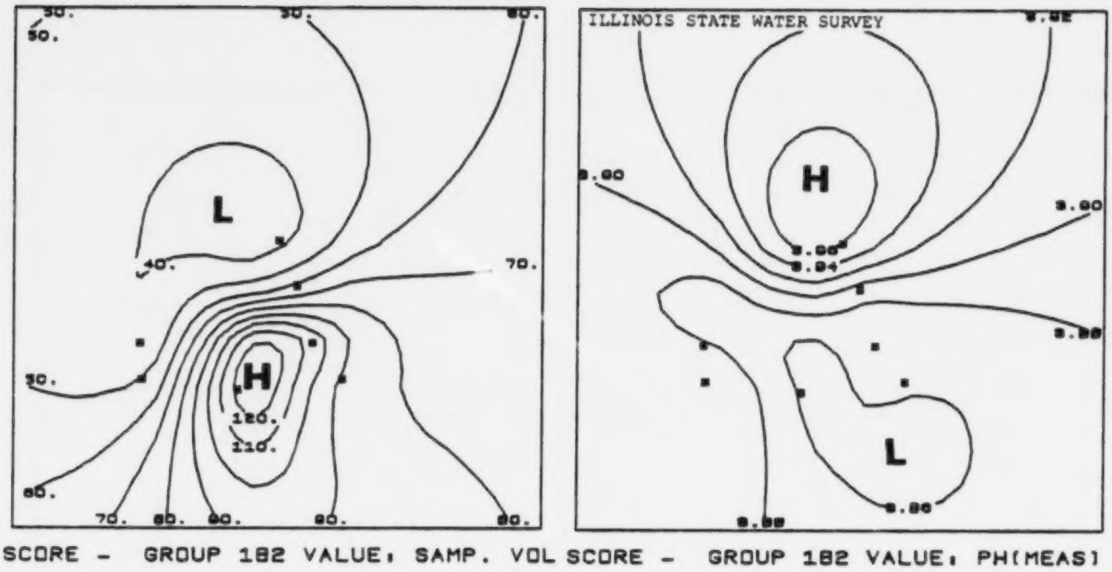

SCORE - GROUP 182 VALUE, SAMP. VOL SCORE - GROUP 182 VALUE, PH(MEAS)

Figure 11. The spatial variation of sample volume (ml) and pH for the rainshower of 7/1/78.

It is important to determine which ions produce similar spatial patterns for the single rainshowers. A useful tool to qualitatively examine the patterns are the computer-produced contours in Figures 12 and 13. In many portions of the contours, no real ion concentrations exist, since rain did not fall over the entire network. Contours in these nonrain areas are mathematical impressions resulting from the spatial variation among the seven discrete data points.

In Figure 12, the spatial patterns for $SO_4^=$ and NO_3^- are observed to be almost identical. Likewise, the spatial patterns for Ca^{++} and Mg^{++} are essentially identical to each other but somewhat different than those for $SO_4^=$ and NO_3^-. This might be a reflection of the difference in the scavenging of calcium or magnesium particles versus sulfur and nitrogen, which have both particulate and gaseous components in the ambient air.

The magnitude of the spatial variations is also noteworthy. Data on the spatial variations for samples from six single rain cells are presented in Table 4. Ratios of the second highest to the second lowest observed values are listed. (Rain cell 182 was already considered for Figures 11 through 13.) The median ratio values for the six cases, listed in the last line of Table 4, indicate that NO_3^- and $SO_4^=$ are more uniform than Ca^{++}, Mg^{++}, or sample volume. The data may reflect the scavenging of Ca/Mg particles as CCN particles and the subsequent dilution in the rain cell. On the contrary, as this dilution of

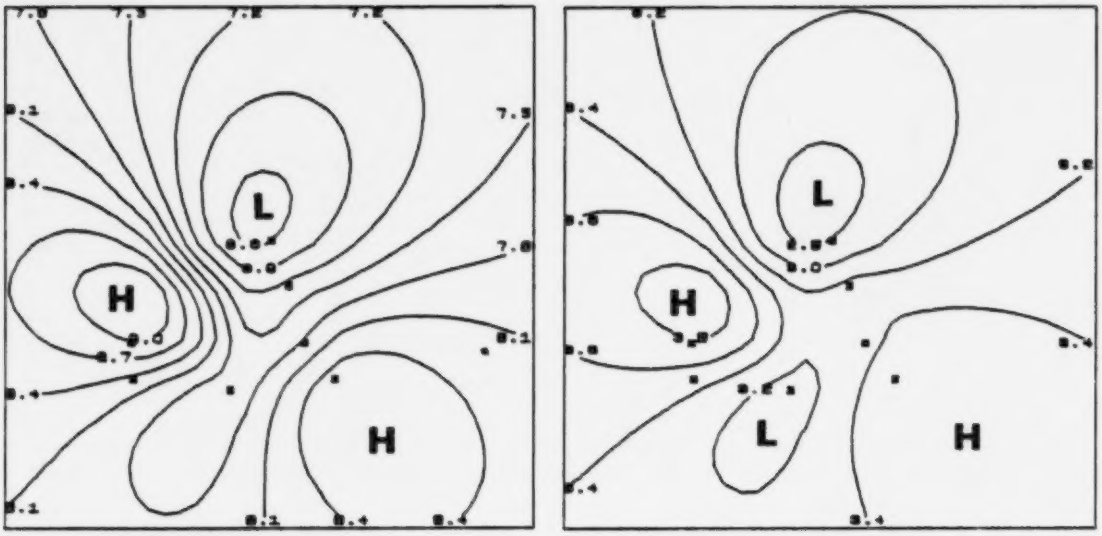
7.9
7.3
7.2
7.2
7.5
7.8
L
H
H
L
L
H
H

SCORE - GROUP 182 VALUE: SO4(PPM) SCORE - GROUP 182 VALUE: NO3(PPM)

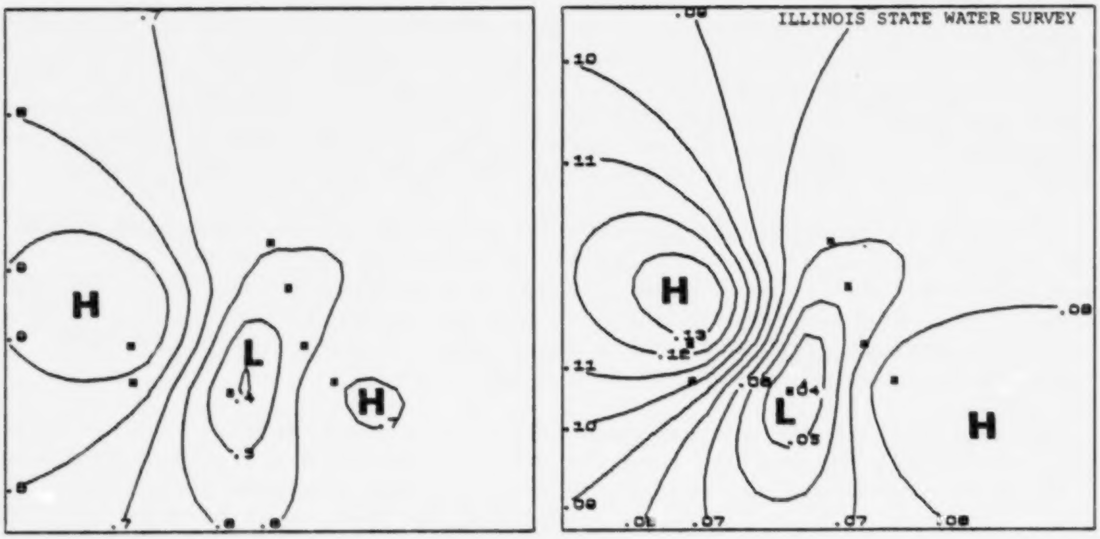
ILLINOIS STATE WATER SURVEY
.7
.7
H
L
H
.10
.11
.13
.12
.11
.10
.08
.04
.05
.07
.07
.08
.08
H
L
H

SCORE - GROUP 182 VALUE: CA(PPM) SCORE - GROUP 182 VALUE: MG(PPM)

Figure 12. The spatial variation of sulfate, nitrate, calcium, and magnesium in the rainwater from the shower of 7/1/78.

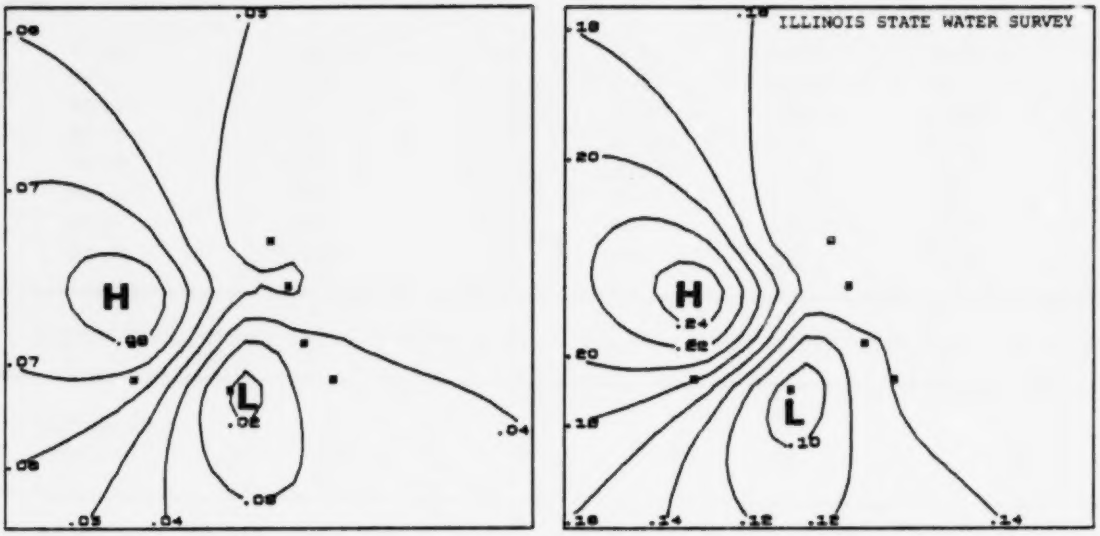
.06
.05
.07
H
.08
.07
L
.02
.04
.06
.03
.04
.03
ILLINOIS STATE WATER SURVEY
.18
.18
.20
H
.24
.22
.20
L
.10
.18
.16
.14
.12
.12
.14

SCORE - GROUP 182 VALUE: K(PPM) SCORE - GROUP 182 VALUE: CL(PPM)

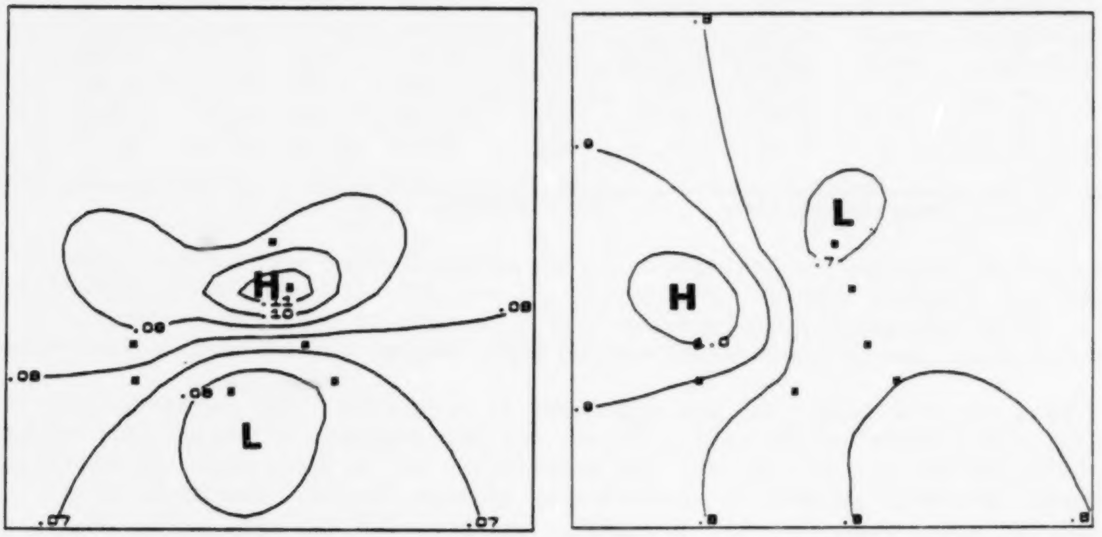
H
.11
.10
.09
.09
.08
.06
L
.07
.07
.8
.9
L
.7
H
1.0
.9
.8
.8
.8

SCORE - GROUP 182 VALUE: NA(PPM) SCORE - GROUP 182 VALUE: NH4(PPM)

Figure 13. The spatial variation of potassium, chloride, sodium, and ammonium in the rainwater from the shower of 7/1/78.

TABLE 3A. NUMERICAL DATA FOR THE 7/1/78 EVENT IN SCORE-78

Gage*	Time On (CDT)	Time Off (CDT)	Sample Volume (ml)	Measured pH	Measured Conductivity (µmhos/cm	Calculated pH
9W	1216	1534	36.6	4.01	53.4	4.01
9	1217	1532	33.7	4.02	52.5	4.05
10	1210	1418	50.9	3.83	77.8	3.83
11	1205	1427	136.9	3.90	70.8	3.88
12	1158	1444	58.5	3.85	78.9	3.81
13	1151	1501	124.9	3.85	76.6	3.84
14	1145	1509	54.5	3.94	65.0	3.96
15	1139	1516	35.8	3.84	86.9	3.68

TABLE 3B. ION CONCENTRATIONS FOR THE 7/1/78 EVENT, MICROEQUIVALENTS/LITER

Gage	$SO_4^=$	NO_3^-	Cl^-	Ca^{++}	Mg^{++}	K^+	Na^+	NH_4^+	Cations/ Anions
9W	114.5	39.4	2.54	23.4	4.6	0.77	1.78	28.8	1.00
9	124.3	37.9	3.38	30.4	6.3	1.02	2.57	36.0	1.04
10	168.0	61.1	5.36	30.4	5.2	1.59	6.92	43.8	1.00
11	146.8	47.9	3.10	23.0	4.8	0.74	2.13	36.0	0.97
12	192.6	60.8	4.51	40.9	8.6	1.07	3.04	48.2	0.94
13	161.4	51.1	2.54	19.5	3.1	0.46	2.44	43.8	0.98
14	141.6	45.5	2.54	36.4	4.4	1.05	2.35	36.0	1.03
15	218.0	71.6	9.03	55.9	14.6	2.71	4.74	85.2	0.97

*9W = wet/dry sampler at Site 9; 9 = bulk sampler at Site 9.

Ca/Mg is taking place in the cloud, a more continuous removal of the gaseous sulfur and nitrogen species would produce a smaller dilution effect of $SO_4^=$ and NO_3^-. This very general explanation will be made more specific in future research which models cloud microphysics and chemical transformation processes.

Data for four more ions are presented in Figure 13. The patterns for potassium and chloride are very similar, and are somewhat different than those for Ca^{++} and Mg^{++} in Figure 12. The pattern for Na^+ differs from any other ion pattern. The NH_4^+ pattern is very similar to that for $SO_4^=$ and NO_3^-; this similarity would indicate: 1) the source was ammonium sulfate, ammonium bisulfate, or ammonium nitrate particles, but 2) the precipitation solutions were not at equilibrium with a spatially uniform concentration for ground-level ammonia.

TABLE 4. RATIOS OF THE SECOND HIGHEST TO THE SECOND LOWEST ION CONCENTRATION FOR SAMPLES FROM SINGLE RAIN CELLS FROM SCORE-78 (WITH CONCENTRATIONS IN mg/liter)

Rain cell	Number of Samples	Ratios for: NO_3^-	$SO_4^=$	Ca^{++}	Mg^{++}	Volume
171	14	1.6	1.8	3.0	2.5	1.9
181	18	2.0	1.8	2.5	3.7	5.2
182	8	1.6	1.6	1.8	1.9	3.5
183	20	3.4	2.1	6.3	7.0	20.2
193	20	2.0	2.5	3.0	3.4	2.3
194	23	1.8	1.6	2.4	2.5	5.2
Median		1.9	1.8	2.8	3.0	4.4

ACKNOWLEDGMENTS

The author wishes to thank R. G. Semonin for reviewing this manuscript and providing many useful suggestions. The author also acknowledges the skill and dedication of B. Komadina, R. Stahlhut, M. Peden, F. McGurk, and L. Skowron in the field work, chemical analysis, and data processing. This research was sponsored by the U.S. Department of Energy under contract EY-76-S-02-1199.

REFERENCES

Achtemeier, G. L., P. H. Hildebrand, P. T. Schickedanz, B. Ackerman, S. A. Changnon, Jr., and R. G. Semonin. 1977. Illinois Precipitation Enhancement Program and Evaluation Techniques for High Plains Cooperative Program. Illinois State Water Survey, Final Report on Contract 14-06-D-7197.

Barnes, S. L. 1964. A Technique for Maximizing Details in Numerical Weather Map Analysis. J. Appl. Meteorol., 3:396-409.

_______. 1973. Mesoscale Objective Map Analysis Using Weighted Time-Series Observations. NOAA Tech. Memo. 62, NSSL. 60 pp.

Battelle Pacific Northwest Laboratories. 1977. The MAP3S Precipitation Chemistry Network: First Periodic Summary Report (September 1976-June 1977). Report No. PNL-2402, Richland, Washington.

Cavender, J. H., D. S. Kircher, and A. J. Hoffman. 1973. Nationwide Air Pollutant Emission Trends, 1940-1970. Publication No. AP-115, Office of Air Quality Planning and Standards, U.S. Environmental Protection Agency, Research Triangle Park, North Carolina.

Cooke, E. 1971. The Flow of Energy in an Industrial Society. Sci. Amer., 225:137.

Dana, T., D. Drewes, S. Harris, and J. Rothert. 1978. Monthly Data Summaries of MAP3S Precipitation Chemistry Data. Battelle Pacific Northwest Laboratories, Richland, Washington.

Hargett, N. L. 1976. 1976 Fertilizer Summary Data. National Fertilizer Development Center, Tennessee Valley Authority, Muscle Shoals, Alabama.

Junge, C. E. 1958. The Distribution of Ammonia and Nitrate in Rain Water over the United States. Trans. Amer. Geophys. Union, 39:241-248.

_____. 1963. Air Chemistry and Radioactivity. Academic Press, New York.

_____, and P. E. Gustafson. 1956. Precipitation Sampling for Chemical Analysis. Bull. Amer. Meteorol. Soc., 37:244-245.

Larson, T. E., and I. Hettick. 1956. Mineral Composition of Rainwater. Tellus, 8:191-201.

Likens, G. E. 1976. Acid Precipitation. Chem. Eng. News, 54(48):29-44.

NADP. 1979. NADP First Data Report. Available from NADP Coordinator's Office, Natural Resource Ecology Laboratory, Colorado State University, Fort Collins, Colorado.

National Research Council. 1973. Air Quality and Stationary Source Emission Control. Prepared for the U.S. Senate Committee on Public Works. ______ pp.

Soderlund, R. 1977. NO_x Pollutants and Ammonia Emissions--A Mass Balance for the Atmosphere over NW Europe. Ambio, 6:118-122.

Stensland, G. J. 1979a. A Comparison of Precipitation Chemistry Data at Illinois in 1954 and in 1977. In: Study of Atmospheric Pollution Scavenging, R. G. Semonin, D. F. Gatz, M. E. Peden, and G. J. Stensland, eds. 16th Progress Report to the Department of Energy, Pollution Characterization and Safety Research Division, Contract EY-76-S-02-1199. pp. 32-40.

_____. 1979b. A Comparison of Sulfate and Nitrate in Precipitation in 1955 and 1977 to Emissions and Air Quality Trends. In: Study of Atmospheric Pollution Scavenging, R. G. Semonin, J. Bartlett, D. F. Gatz, M. E. Peden, L. M. Skowron, and G. J. Stensland, eds. COO-119-58, 17th Progress Report to the Department of Energy, Pollution Characterization and Safety Research Division, Contract EY-76-S-02-1199. pp. 1-15.

____. 1979c. Calculating Precipitation pH, with Application to the Junge Data. In: Study of Atmospheric Pollution Scavenging, R. G. Semonin, D. F. Gatz, M. E. Peden, and G. J. Stensland, eds. COO-1199-58, 17th Progress Report to Department of Energy, Pollution Characterization and Safety Research Division, Contract EY-76-S-02-108.

Stensland, G. T., and J. D. Bartlett. 1979. Measurements of Atmospheric Nitrate, Sulfate, Ammonium, and Calcium Using Various Filter Setups. Presentation (Paper No. 79-32-4) before the 72nd Annual Meeting of the Air Pollution Control Association, Cincinnati, Ohio.

Volchok, H. L., and R. T. Graveson. 1975. Wet/Dry Fallout Collection. Proceedings, 2nd Federal Conference on the Great Lakes, Argonne, Illinois, March 25-27, 259-264.

REACTION OF NO_x IN SMOG CHAMBERS AND URBAN ATMOSPHERES

Chester W. Spicer

Battelle
Columbus Laboratories
505 King Avenue
Columbus, Ohio 43201

INTRODUCTION

Since the beginning of the last decade, interest in atmospheric reactions of sulfur and nitrogen pollutants has continually increased. To date, sulfur compounds have been studied more thoroughly than nitrogen compounds, especially for transformation rate in ambient air; this is partly because sulfate ($SO_4^=$) health data became available first and partly because the sulfur reaction path is less complex than the nitrogen path. Also, sensitive analytical methods for studying many important nitrogen species have only recently been developed. As a consequence, knowledge has lagged on the ambient air reactions of nitrogen oxides (NO_x), NO_x comprising the total available nitric oxide (NO) and the total available nitrogen dioxide (NO_2).

Beginning in 1973, the atmospheric chemistry group at Battelle-Columbus has maintained a continuous investigation of NO_x atmospheric chemistry; this program has involved analytical methods development, smog chamber studies, kinetic modeling, and ground-level and airborne field experiments in urban atmospheres. This presentation describes the results of our studies to date. It should be emphasized, however, that experiments now in progress and future studies may significantly alter our current perceptions of atmospheric NO_x/nitrate (NO_3^-) chemistry. To better understand (and model) atmospheric NO_x reactions and to assess their impact on health, visibility, and precipitation chemistry, much work remains to be done.

RESULTS AND DISCUSSION

The presentation will be divided into discussions of the measurement, distribution, fate, and reaction rate of NO_x/NO_3^-. In some areas the discussions necessarily overlap.

Nitrate Measurement

Atmospheric nitrates may be classified as gases or particles, depending on their physical state in the air prior to sampling. Unfortunately, the distinction between the states after sampling is not as well-defined. Interconversions and mutual interferences of gaseous and particulate nitrates are now widely recognized, and research aimed at understanding and resolving these problems has been undertaken. The gaseous nitrates of greatest interest are peroxyacyl nitrates (PAN's) and nitric acid ($HONO_2$ or HNO_3). Analytical methods and detection limits for these species are listed in Table 1.

TABLE 1. GASEOUS NITRATE MEASUREMENT METHODS

Specie	Detection Limit	Method
peroxyacyl nitrates	0.1 ppb	electron capture GC
nitric acid		
continuous	1 ppb (0.1 ppb)	modified chemiluminescence
integrated	0.1 ppb	differential filtration

Although the electron capture gas chromatographic (ECGC) method for PAN's is satisfactory for most current applications, methodology for HNO_3 determination is still being evaluated. Modified commercial chemiluminescence instruments have been used in airborne, ground-level, and smog chamber studies and have a detection limit of ~1 ppb. Larger homemade versions attain detection limits of ~0.1 ppb, using essentially the same principles. Nitric acid can also be collected on a filter (after first removing particulate nitrate on a prefilter) and determined by any one of a number of analytical procedures. Quartz or Teflon has been used as the prefilter material; and nylon, cotton, and NaCl-impregnated quartz filters have all been employed to trap gaseous HNO_3. We use a Teflon/nylon filter combination and ion chromatographic analysis for integrated HNO_3 analysis. This procedure has been tested in the laboratory and in the field.

All HNO_3 collection methods currently in use were recently subjected to a collaborative test in Claremont, California. The protocol for this experiment has been reported by Howes et al. (1979). The results of the collaborative study should do much to alleviate the uncertainty in selecting HNO_3 and particulate NO_3^- measurement methods.

For particulate NO_3^-, several reports document the severity of artifact collection (Spicer and Schumacher 1977; Appel et al. 1979; Spicer and Schumacher 1979). The main, unresolved issue is the importance of nitrate loss due to the volatility of ammonium nitrate (NH_4NO_3) or to the reaction and volatilization of other NO_3^- salts. These topics were extensively investigated during the recent Claremont study (Howes et al. 1979), and conclusive results should be available by mid-1980.

Examples of laboratory and field evidence for artifact NO_3^- collection are presented in Figure 1 and Table 2. Figure 1 shows the NO_3^- mass retained by different glass and quartz fiber filters exposed to gaseous HNO_3 in particle-free air. Clearly, all three glass fiber filters (AE, AA, MSA) collect large quantities of gaseous NO_3^-. The quartz filters show much lower levels of interference, although Gelman microquartz still collects an unsatisfactorily large amount of gaseous NO_3^-. Teflon and Nuclepore filters were shown by Spicer and Schumacher (1979) to be essentially free from positive interference due to artifact collection. The two exposure levels in Figure 1 and the curves in Figure 2 indicate that the filters eventually saturate with respect to artifact collection. Different filters display different capacities for gaseous NO_3^- collection, and these capacities have been used to estimate the impact of artifact collection on hi-vol sampling (Spicer and Schumacher 1979).

TABLE 2. AVERAGE PAIR-WISE NO_3^- DIFFERENCES (8-h DAYLIGHT COLLECTION)

Filter Pair	Average NO_3^- Difference ($\mu g/m^3$)
Pallflex Quartz - Pallflex Quartz	0.1
Pallflex Quartz - ADL Quartz	0.5
Pallflex Quartz - Gelman A Glass	-7.0
Pallflex Quartz - Gelman AA Glass	-15.4

Table 2 lists the average pair-wise NO_3^- differences for duplicate hi-vol samplers using different filter materials. The NO_3^- difference for each filter pair is the average of several days of sampling (8-h daylight collections) in Upland, California. The quartz filters consistently collect much less NO_3^- than the glass fiber filters.

The conclusions to be drawn from our studies of particulate NO_3^- sampling and analysis methods are:

(1) Most historical nitrate data are in error

(2) Positive nitrate artifacts can be minimized by using Teflon, Nuclepore, or certain quartz fiber filters

(3) In most U.S. locations, true particulate nitrate concentrations rarely exceed 1 to 2 $\mu g/m^3$

(4) Most atmospheric nitrate is in the gas phase.

Distribution and Diurnal Behavior of Atmospheric Oxidized Nitrogen

Distribution data for oxidized nitrogen are available for a number of locations throughout the U.S. Such data are reported for five locations as percentages of the total measured oxidized nitrogen in Table 3. The contribution of each compound to the total oxidized nitrogen burden is tabulated.

TABLE 3. OXIDIZED NITROGEN DISTRIBUTION (PERCENT OF TOTAL)

Specie	West Covina (1973)	Phoenix (1977)	Temple City (1976)	Upland (1976)	Rubidoux (1976)
NO	23	45	19	10	--
NO_2	57	51	78	66	78
PAN	13	2	3	22	10
$HONO_2$	6	--	--	--	--
NO_3^-	0.5	2	1	1	12

Data from the same 8-h daylight period were used for each location in the table except the particulate NO_3^- entry for West Covina, where only 24-h values were available. Data from each location were averages over at least 4 weeks of sampling. Since results for all locations were obtained during daylight hours in the summer and fall smog seasons, the contribution of NO_2 always exceeded that of NO. The greatest PAN contributions were observed in the south coast air basin downwind of Los Angeles. The contribution by particulate NO_3^- was generally slight, except for Rubidoux, California, where a strong ammonia (NH_3) source just upwind is suspected of converting gaseous nitrates to particulate NH_4NO_3.

The diurnal behavior of several trace nitrogen compounds, O_3, and certain meteorological variables is shown in Figure 3. These data represent composite profiles generated from 5 weeks of sampling in West Covina, approximately 25 miles east of Los Angeles.

In the upper portion of the figure, profiles of four trace nitrogen species are plotted. The PAN concentration is low during the night and early morning, rising during the later morning and early afternoon, and peaking at about 2 p.m.--coincident with the O_3 maximum. Individual hourly average PAN concentrations frequently approach 50 ppb during midafternoon, although the composite profile reaches a maximum of only 20 ppb. After 2 p.m., the PAN concentration drops rapidly.

The composite HNO_3 concentration is also rather low during the night and morning hours. Similarly to O_3 and PAN, HNO_3 rises to its peak at about 2 p.m. Single hour averages occasionally reach values in excess of 30 ppb. The 5-week composite profile peaks at 10 ppb. After 2 p.m., the HNO_3 concentration decreases rapidly.

The fraction of the measured trace nitrogen species consisting of the reaction products PAN and HNO_3 (i.e., PAN + HNO_3/NO + NO_2 + PAN + HNO_3) averaged about 7 percent at night and 21 percent during midafternoon. During some individual hours, this fraction was as high as 54 percent.

As mentioned earlier, PAN, HNO_3, and O_3 maxima generally occur at about the same time. During the 5-week study in Los Angeles, the correlation coefficients among PAN, HNO_3, and O_3 were all in the range of 0.7 to 0.8. The HNO_3 concentration decreases more rapidly than PAN during the later afternoon, suggesting that some sink or scavenging mechanism is removing HNO_3 more rapidly than PAN. Formation of particulate NO_3^- may account for this removal.

Analysis of the results of recent field investigations suggest that, as observed in smog chamber studies, PAN and HNO_3 are the major initial products of NO_x reactions in urban atmospheres. The contribution of PAN and HNO_3 to the oxidized nitrogen burden may be defined as a distribution ratio, $F_n = PAN + HNO_3/NO + NO_2 + PAN + HNO_3$. Plots of this ratio composited over 5-week sampling periods in St. Louis, Missouri, and West Covina, California, are shown in Figure 4. The contribution of PAN and HNO_3 to the total oxidized nitrogen burden is very similar for the two cities. F_n reaches a peak at ~25 percent during midafternoon in both cities. The shape of the F_n curve is very similar to the O_3 profile for each city. Indeed, F_n and C_3 are highly correlated. This is not surprising, since both O_3 and F_n should vary in the same manner with photochemical smog intensity.

Another view of the diurnal pattern of oxidized nitrogen distribution is included as Figure 5. In this figure, hourly average concentrations of NO, NO_2, $HONO_2$, and PAN are plotted versus time of day for a rural site in the New Jersey pine barrens, about 45 miles downwind of Philadelphia. All gas-phase species were monitored with the most specific and sensitive techniques available. Integrated HNO_3 and particulate NO_3^- samples were collected, but the results are not yet available.

The concentrations of NO and NO_2 on July 22, 1979, maximized in the early morning, probably because of a restriction in mixing that resulted from a nocturnal inversion. By 10 a.m. EDT, PAN formation was evident; and by noon EDT, both PAN and $HONO_2$ were present in significant concentrations. In upcoming interpretive work, the oxidized nitrogen distribution and trends at this site will be compared with smog chamber and modeling results simulating transported urban air.

Another perspective on the distribution of oxidized nitrogen compounds was obtained by monitoring the appropriate species in a moving air parcel during several hours of reaction. For this experiment, the Boston urban plume was monitored in a Lagrangian fashion, as it was transported eastward over the ocean. Under these conditions, fresh emissions of NO_x and other species to the air parcel are negligible. The behavior of F_n with time in the Boston plume is shown in Figure 6. The initial time, T = 0, corresponds to the initial aircraft cross-section through the plume in midmorning just east of the coast. After 7 h of reaction and transport, F_n increased from about 0.15 to 0.70. If we consider that total oxidized nitrogen is conserved, then the change in F_n can serve as an indicator of the average rate of conversion. Figure 6 shows that the average conversion rate is about 8 percent per hour. The slope of a logarithmic plot of the F_n data should represent the pseudo-first-order conversion rate constant. For the data from August 18, 1978, such a plot yields a rate constant of $0.19\ h^{-1}$. Further discussion of transformation rates in relation to the Boston plume experiments is presented later in this paper.

A final aspect of this discussion of atmospheric oxidized nitrogen distribution concerns the NO_3^- distribution between the gas and particulate phases. Perhaps the most significant change in our perception of atmospheric NO_3^- which has resulted from the discovery of artifact NO_3^- concerns the atmospheric NO_3^- distribution. Contrary to our earlier understanding, atmospheric NO_3^- (PAN + HNO_3) is much more abundant in the gaseous than in the particulate state. This is shown in Table 4, where the ratio of gaseous/total NO_3^- is tabulated for eight locations. In all locations except Rubidoux, gaseous NO_3^- equals or exceeds 50 percent of the total atmospheric NO_3^-; gaseous NO_3^- makes up over 80 percent of the total. Because health effects and other potentially important effects of nitrates likely depend on the physical state of the nitrates, this new view on the problem is significant.

TABLE 4. ATMOSPHERIC NITRATE DISTRIBUTION

Location	Gaseous/Total NO_3^-
St. Louis, Mo. (1973)	0.95
West Covina, Calif. (1973)	0.98
Phoenix, Ariz. (1977)	0.50
Temple City, Calif. (1976)	0.75
Upland, Calif. (1976)	0.96
Rubidoux, Calif. (1976)	0.45
Beverly, Mass. (1978)	>0.95
Remote troposphere (above boundary layer)	~0.80

The larger percentage of gaseous NO_3^- also explains why the observed $NO_3^-/SO_4^=$ ratio is larger in precipitation samples than in aerosol collections. Much more NO_3^- is available for scavenging by precipitation than would be indicated by aerosol collection data, since the major fraction of atmospheric NO_3^- is gaseous.

NOx Transformation and Fate

One means of gathering data on NO_x reactions under controlled conditions is through the use of a smog chamber. We are currently investigating various aspects of NO_x reactions and NO_3^- formation using Battelle's 17.3-m^3 smog chamber in a Teflon-lined configuration. Simulations of both urban and rural atmospheric conditions are being carried out. The main objective of these experiments is to define the relationships among nitrates and between nitrates and their precursors. Results of one recent simulation are shown in Figure 7

(Spicer, unpublished data). In this experiment, a 17-component hydrocarbon (HC) mixture was used to simulate a typical urban atmosphere.

In this 10-h irradiation, the nonmethane hydrocarbon (NMHC)/NO_x ratio was 7.4, with 4.52 ppmC of the urban HC mixture and 0.610 ppm of NO_x. The top portion of the figure shows the time profiles of the pertinent nitrogen species along with O_3. The maximum values of other reaction products measured during the experiment are 0.51 ppm total aldehyde, 0.161 ppm formaldehyde, and 0.0266 ppm hydrogen peroxide. Data on particulate NO_3^- concentrations are not yet available.

The middle portion of Figure 7 depicts dynamically the contribution of the various nitrogen species to the overall nitrogen balance. The upper curve, labeled "A" in the figure, represents the amount of oxidized nitrogen which should remain in the chamber at any given time. It is based only on the measured chamber dilution rate. The concentration profiles for PAN and the sum of PAN + $HONO_2$ are labeled as B and C, respectively. Finally, curve D represents the sum of all the specifically measured nitrogen compounds and includes PAN, $HONO_2$, NO, and NO_2. The contribution of each specie is represented by the shaded area below the appropriate curve. The difference between the expected N_{total} and the measured sum of all the nitrogen species, i.e., A through D, must represent either (1) conversion of NO_x to an unmeasured product or (2) loss of nitrogen species to the walls. Particulate NO_3^- will undoubtedly account for a portion of the difference; however the NO_3^- data are not yet available. Species such as nitrogen pentoxide and nitric acid are known to be removed by the chamber surface, and their loss may account for the remainder of the discrepancy. We have recently determined the wall removal rates of these species in the chamber at different humidities and will soon begin modeling the smog chamber data, incorporating the measured surface removal rates into the kinetic code. The modeling results should be very valuable in interpreting the large body of data we are accumulating.

The lower segment of Figure 7 shows the time behavior of the nitrogen distribution ratio, F_n, defined above. Also shown is the PAN/$HONO_2$ ratio, which was unstable during the first 3 h, because the concentrations were low and changing rapidly. From the third hour on, the PAN/$HONO_2$ ratio gradually increased from 1 to 2. This is similar to the maximum ratio shown in Figure 1 for West Covina.

The matrix of smog chamber experiments designed to define NO_3^- precursor relationships is not yet complete. Nevertheless, some preliminary observations are warranted.

(1) The maximum $HONO_2$ concentration appears to vary linearly with initial NO_x at all HC loadings for experiments already completed (Figure 8). The slopes of the lines are nearly identical at all HC loadings.

(2) Comparison of these experiments with duplicate runs in the presence of SO_2 (conducted recently on another project) demonstrates a lower $HONO_2$ yield with SO_2 present. This may result from the competition of SO_2 and NO_2 for hydroxyl.

(3) The final PAN/$HONO_2$ ratio appears to increase rapidly with NMHC/NO_x up to a NMHC/NO_x ratio of 20, where PAN/$HONO_2$ is about 2. Above 20, the PAN/$HONO_2$ ratio remains constant or decreases slightly. During the afternoons in urban atmospheres we have observed PAN/$HONO_2$ ratios averaging 1 to 2.

Nitrogen balance in the atmosphere was investigated at the three locations shown in Table 5. Results are averages from 4 to 5 weeks of sampling at each location. The expected oxidized nitrogen concentration is determined using low-reactivity in-situ tracers such as carbon monoxide (CO), acetylene (C_2H_2), and fluorocarbon-11 (F-11). Details of the calculations, assumptions, and potential errors in this determination are presented elsewhere (Spicer 1977; Spicer et al. 1979a).

TABLE 5. ATMOSPHERIC NITROGEN BALANCE

City	Expected Oxidized Nitrogen (ppm)	Measured Oxidized Nitrogen (ppm)	Accountability (%)
West Covina	0.151	0.149	99
Upland	0.058	0.050	86
Rubidoux	0.057	0.052	91

The measured oxidized nitrogen values in Table 5 are the sum of all the measured nitrogen compounds, including NO, NO_2, PAN, HNO_3, and NO_3^-. Good agreement between the predicted and measured values at all three sites demonstrates a close nitrogen balance. Since much uncertainty is inherent in predicting total oxidized nitrogen, however, the agreement between predicted and measured values should be viewed with some caution. Nevertheless, a close, atmospheric nitrogen balance is clearly seen.

Transformation Rate - The Boston Plume

The area in which our understanding of atmospheric NO_x chemistry is most deficient is the NO_x-to-product transformation rate. Few atmospheric studies have approached this problem because of the technical difficulties involved. Breeding and coworkers (1976) investigated the transformations of several pollutants around St. Louis. Their results suggest a 2- to 4-h half-life for NO in the St. Louis plume, but their data for NO_2 are inconclusive. Thus, little was learned about the important conversion of NO_x to products.

Our group investigated the fate of NO_x in the St. Louis and Los Angeles urban areas in 1973 (Spicer 1977). Study goals were to identify the major NO_x reaction products and, to the extent possible, define the nitrogen mass balance. The experiment was not designed to obtain data on conversion rates, but if certain assumptions are accepted, a transformation rate of $0.10 \pm 0.05\ h^{-1}$ is consistent with the Los Angeles data.

A recent study in Boston made use of a Cessna 411 research aircraft in tracking the Boston urban plume as it moved eastward. For most study days a specific air parcel--e.g., the 8 a.m. EDT Boston air mass--was sampled just east of the coast at midmorning and then periodically throughout the day by successive flights. The concentrations of NO_x, in-situ inert tracers (CO, C_2H_2, F-11), PAN, $HONO_2$, C_1-C_5 HC's, O_3, and several other variables were determined shortly after the air parcel left the city and subsequently throughout the day. The concentrations of these same species were also determined in background air outside the plume to correct for plume dilution. The ratios of NO_x to the inert tracers were then used (after correction for background air dilution) in conjunction with reaction times to derive NO_x removal rates. The removal rates include both physical removal and chemical transformation.

During the study, air mass trajectory analysis was used to predict the position of the selected air parcel in order to vector the aircraft to the area. The plane then bracketed the predicted position with plume traverses. Subsequent, more detailed, trajectory analysis--based on wind data from 10 eastern Massachusetts stations--was used to determine the air parcel position more exactly and to select the plume traverse data that most closely matched the time and position of the specified air parcel.

An example of the Boston Plume trajectory for August 23, 1978, is shown in Figure 9. Air parcel positions are indicated for each hour (EDT). Sampling patterns are indicated in the figure by solid lines, representing the sampling intervals. These intervals were chosen after initial "scouting" traverses through the plume, because they yielded the highest concentrations of pollutants and tracers, thereby minimizing analytical imprecision. Only those sampling intervals which matched the time and position of the selected air parcel are shown in the figure. Further details of the experimental protocol may be found in the report by Spicer et al. (1979b).

For data interpretation, the tracer/NO_x ratios just downwind of Boston were used with tracer data from later downwind plume traverses to calculate the expected NO_x concentration for each downwind traverse. This value is then used in Equation 1 to define the NO_x removal rate. The first-order rate equation used to describe these experiments is

$$\ln \frac{(NO_x)_e}{(NO_x)_t} = kt \qquad (1)$$

where $(NO_x)_e$ = expected concentration of NO_x, or the concentration which should be present in the air parcel at time t after dilution is taken into account

$(NO_x)_t$ = actual amount of NO_x (i.e., NO + NO_2) measured at time t.

For the flights of August 23, 1978, represented in Figure 9, the first-order plot is shown in Figure 10. Interestingly, the data conform reasonably well to the first-order form. The slope of the line yields a pseudo-first-order rate constant of 0.15 h^{-1}.

The dates and rate constants for the four case study days resulting from the Boston Plume Study are listed in Table 6.

TABLE 6. NO_x REMOVAL RATE DATA FROM BOSTON URBAN PLUME STUDY, AUGUST 1978

Date	Reaction Interval (h)	Maximum Transport Distance Observed (km)	Hourly Rate Constant for NO_x Removal
14	3	83	0.20
18	7	122	0.24
23	7.5	142	0.15
30	5.5	95	0.14

The conversion (or 1/e) lifetime of NO_x in urban air--under the moderate photochemical smog conditions which existed during this study (maximum O_3 in the plume on these 4 days ranged from 90 to 140 ppb)--falls in the range of 4.2 to 7.1 h. The average lifetime is about 6 h. The average NO_x half-life under these conditions is found to be 4.1 h.

These data are apparently the first measured NO_x removal rates and lifetimes in urban air. They obviously should be validated and extended by further studies under similar as well as different environmental conditions. Such data should prove very valuable in assessing the impact of nitrogen oxides and their reaction products on our air environment.

ACKNOWLEDGMENT

The work reported here has been supported by the U.S. Environmental Protection Agency under several contracts and a grant, and the Coordinating Research Council. I am very grateful for the support of these organizations.

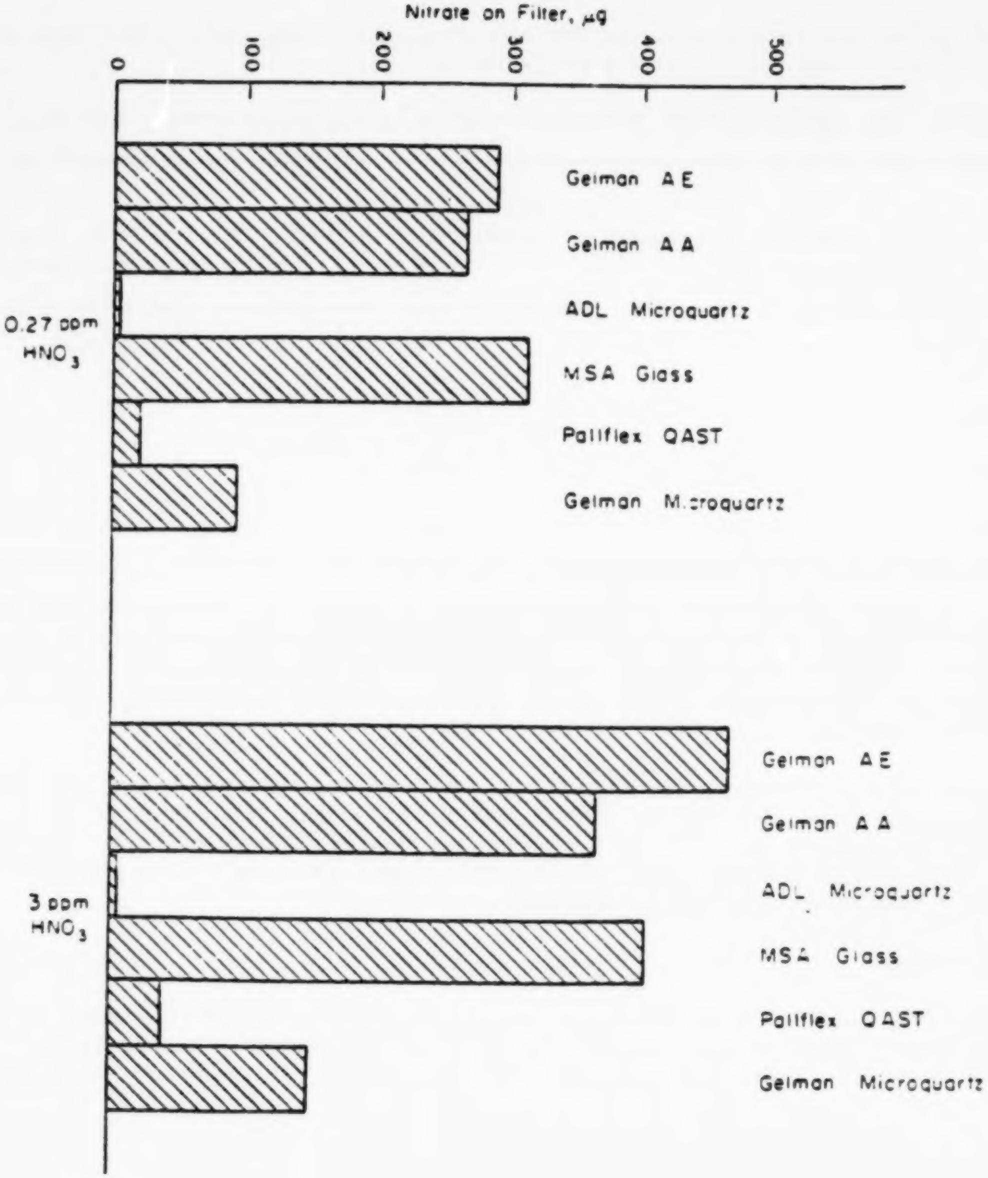

Figure 1. Comparison of nitrate mass collected on various filters exposed to $HONO_2$ (1.2 m^3 exposures).

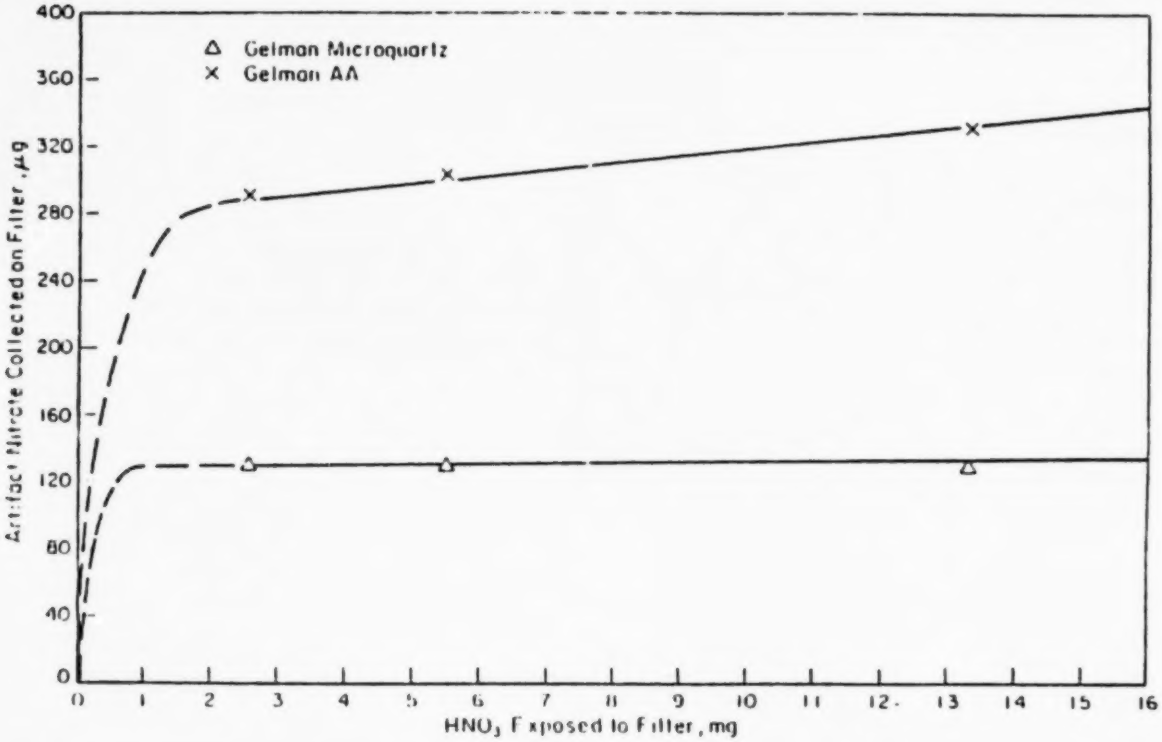

Figure 2. Artifact nitrate as a function of $HONO_2$ exposure.

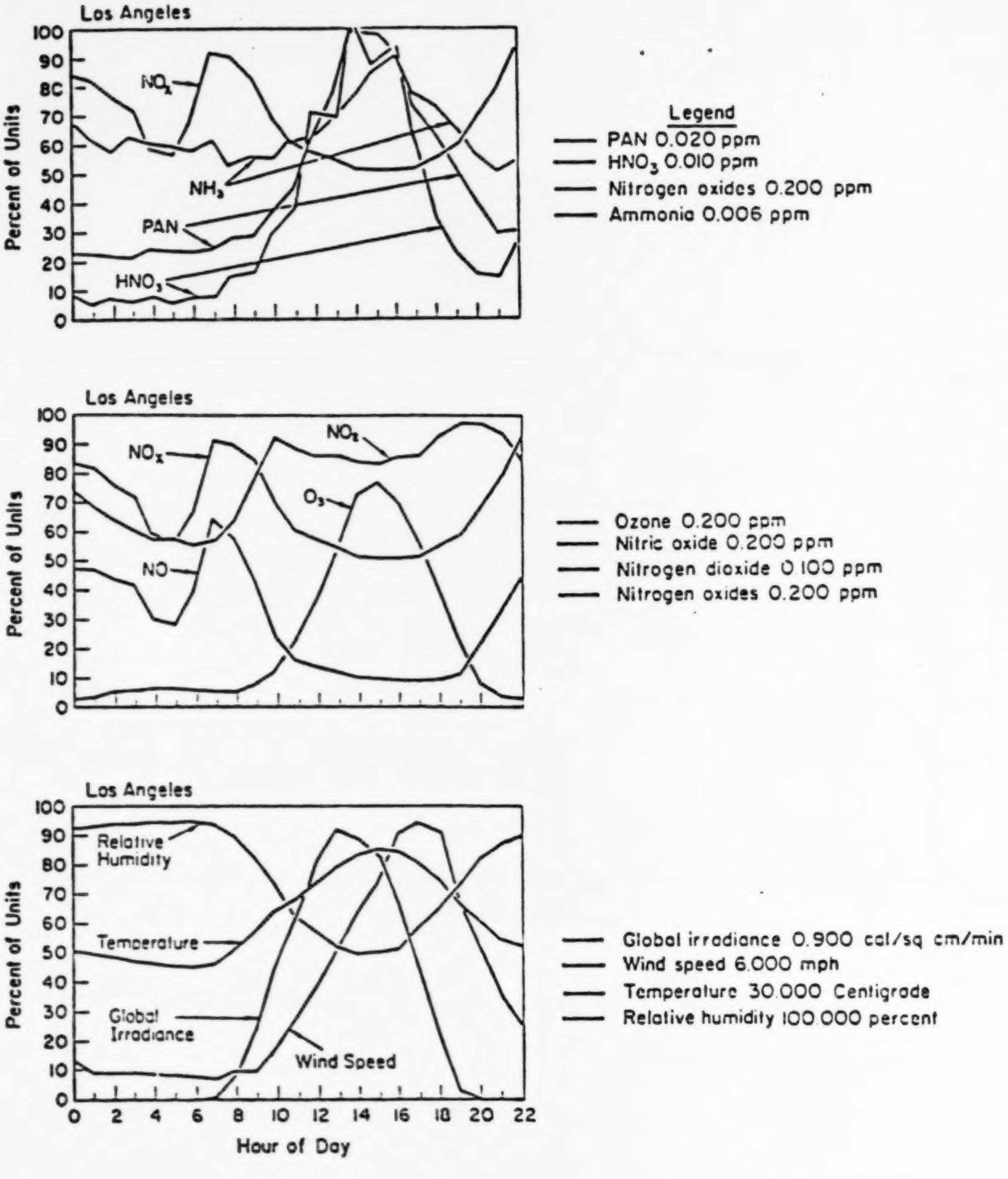

Figure 3. Average diurnal air quality and meteorological profile, West Covina.

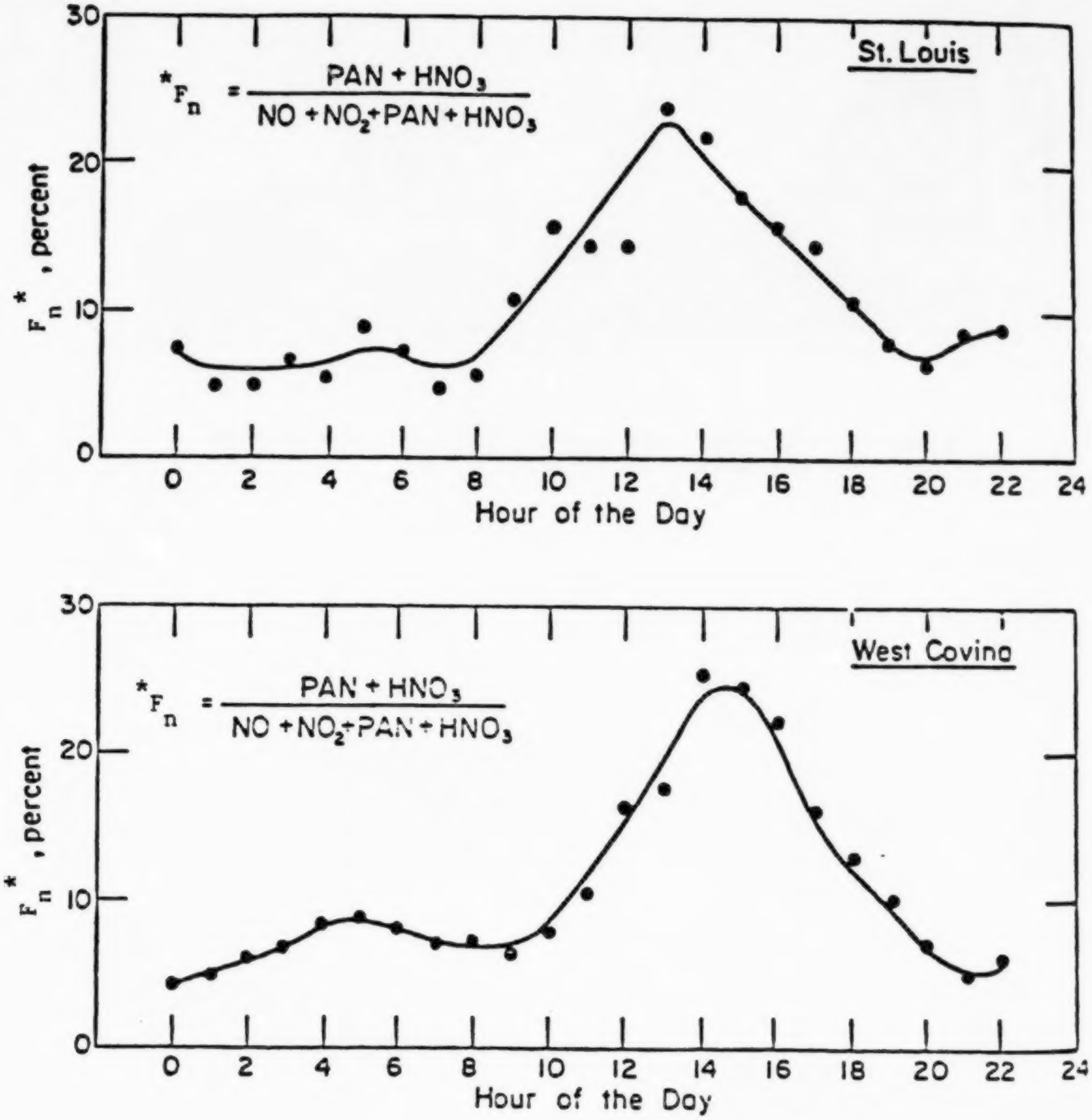

Figure 4. Composite profiles of F_n^* in St. Louis and West Covina.

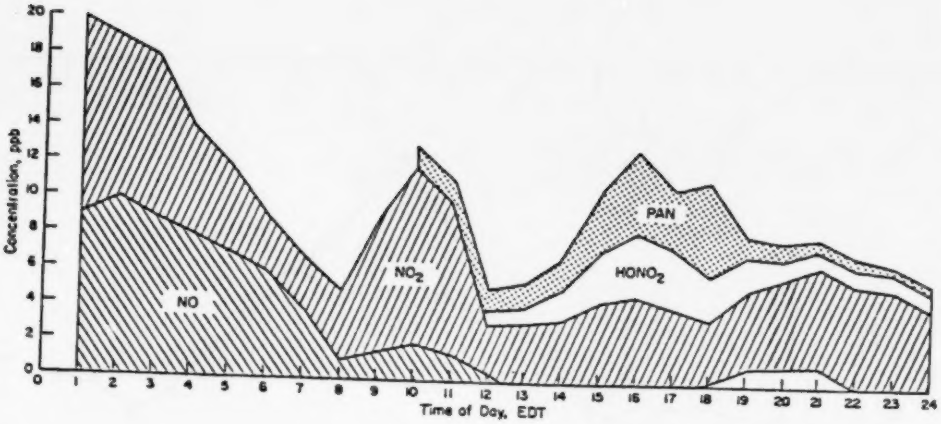

Figure 5. Oxidized nitrogen distribution downwind of Philadelphia, 7/22/79.

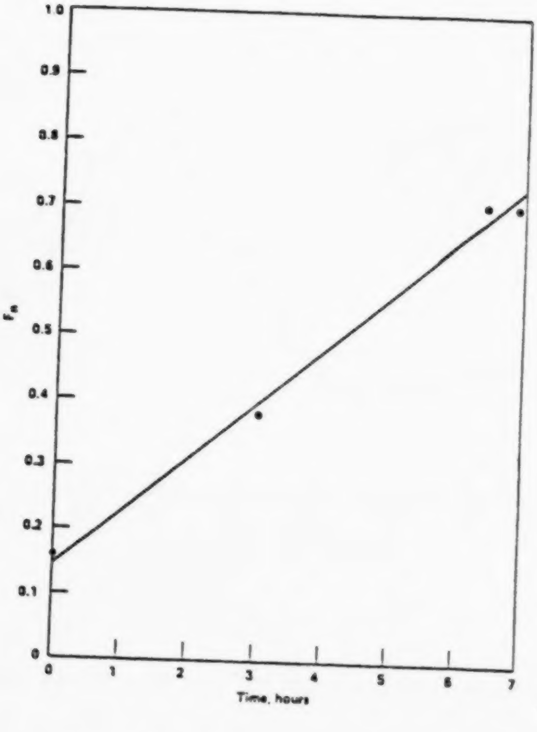

Figure 6. F_n vs. reaction time, 8/18/78.

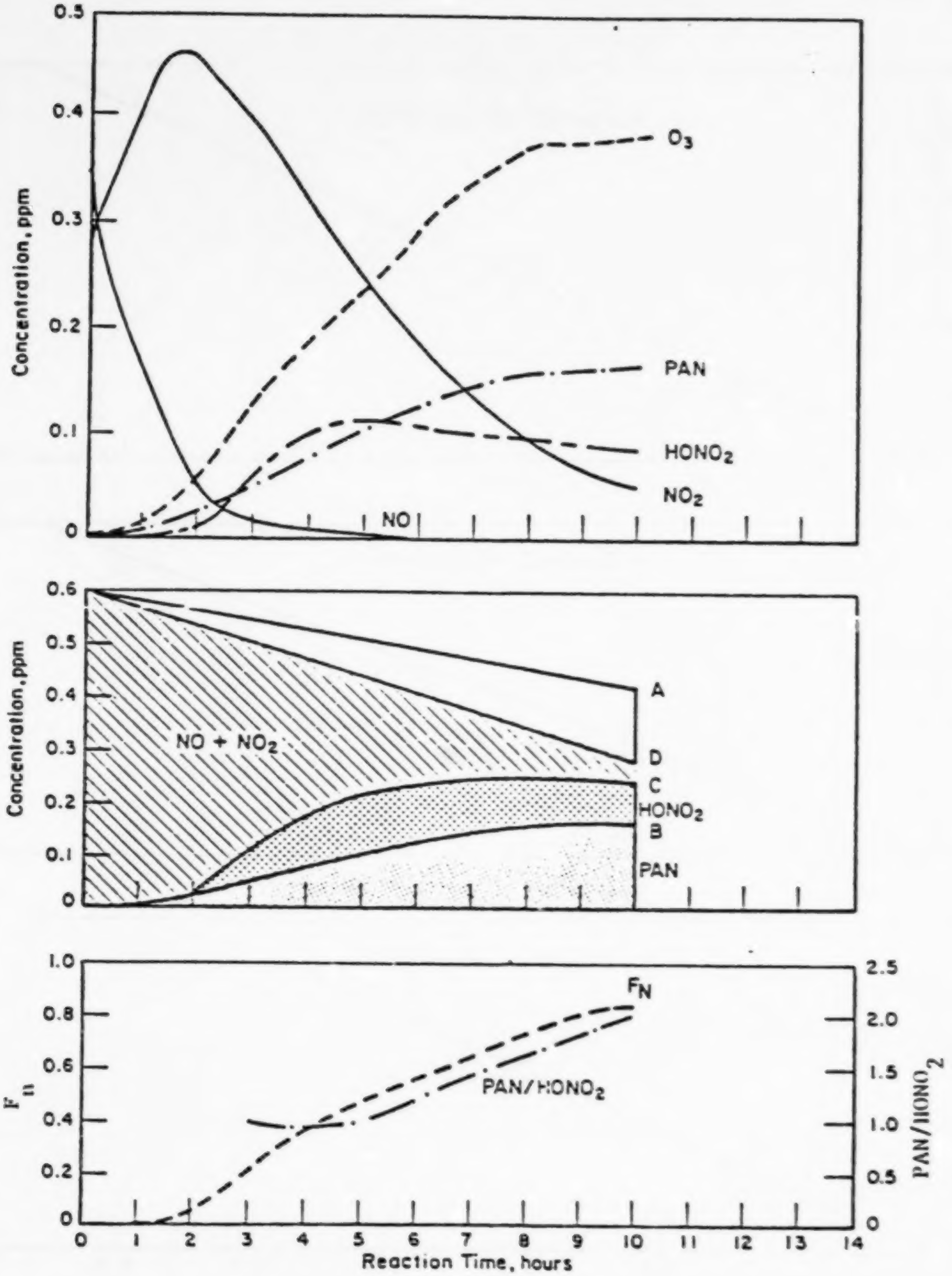

Figure 7. Results of irradiation of 4.52 ppmC urban HC mix and 0.61 ppm NO_x, 4/4/79.

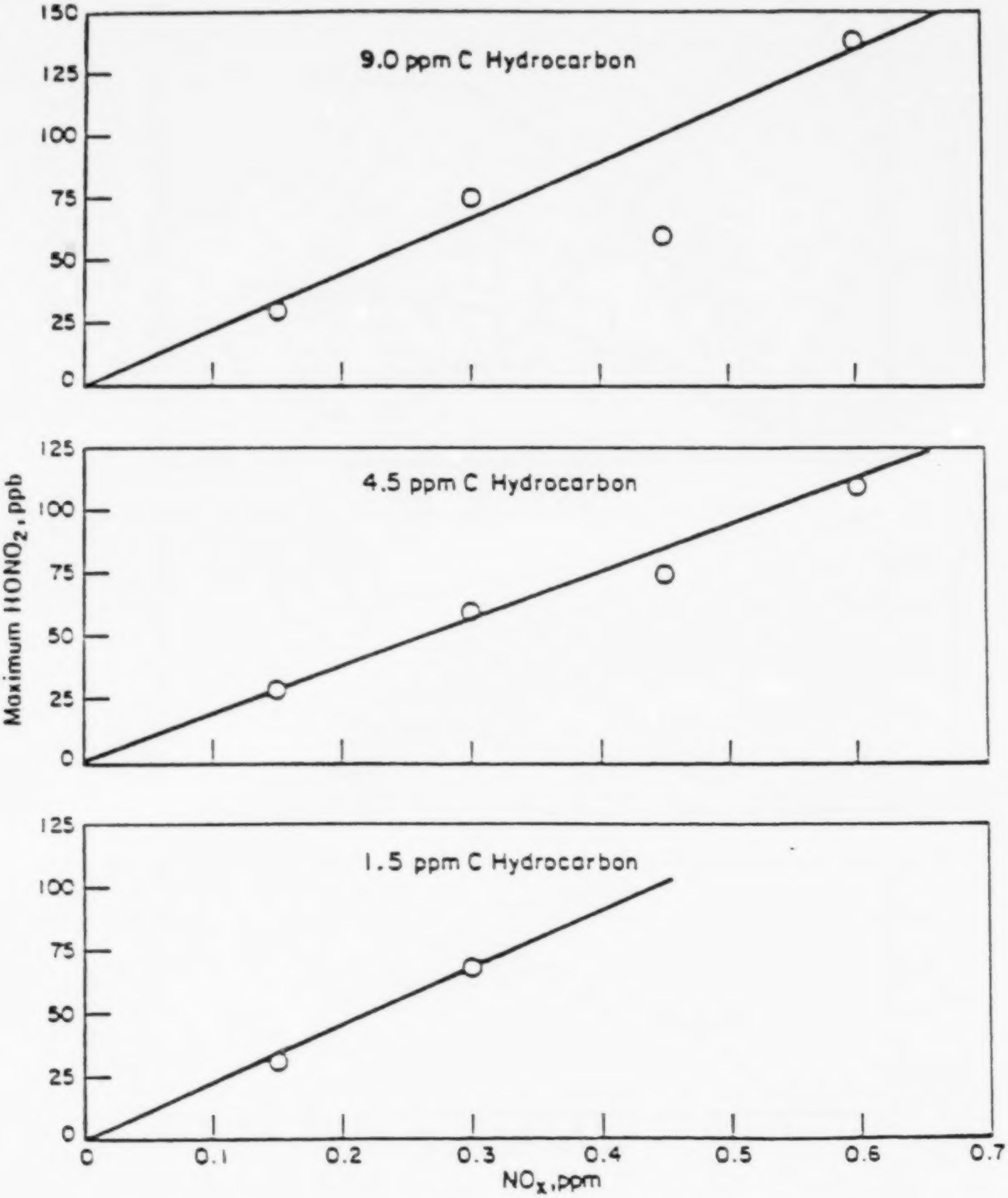

Figure 8. HONO$_2$ yield vs initial NO$_x$.

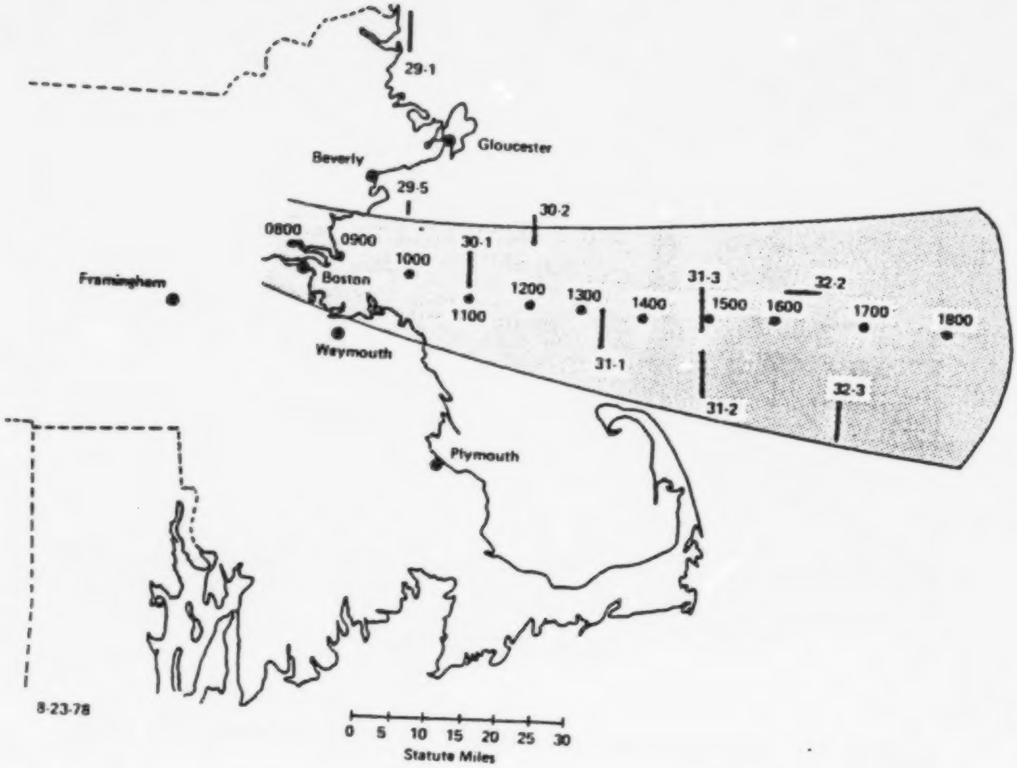
29-1
Gloucester
Beverly
29-5
30-2
0800
0900
30-1
1000
Framingham
Boston
1200
1300
1400
31-3
1500
1600
32-2
1700
1800
1100
Weymouth
31-1
31-2
32-3
Plymouth
8-23-78
0 5 10 15 20 25 30
Statute Miles

Figure 9. Air parcel trajectory and aircraft sample positions for August 23, 1978.

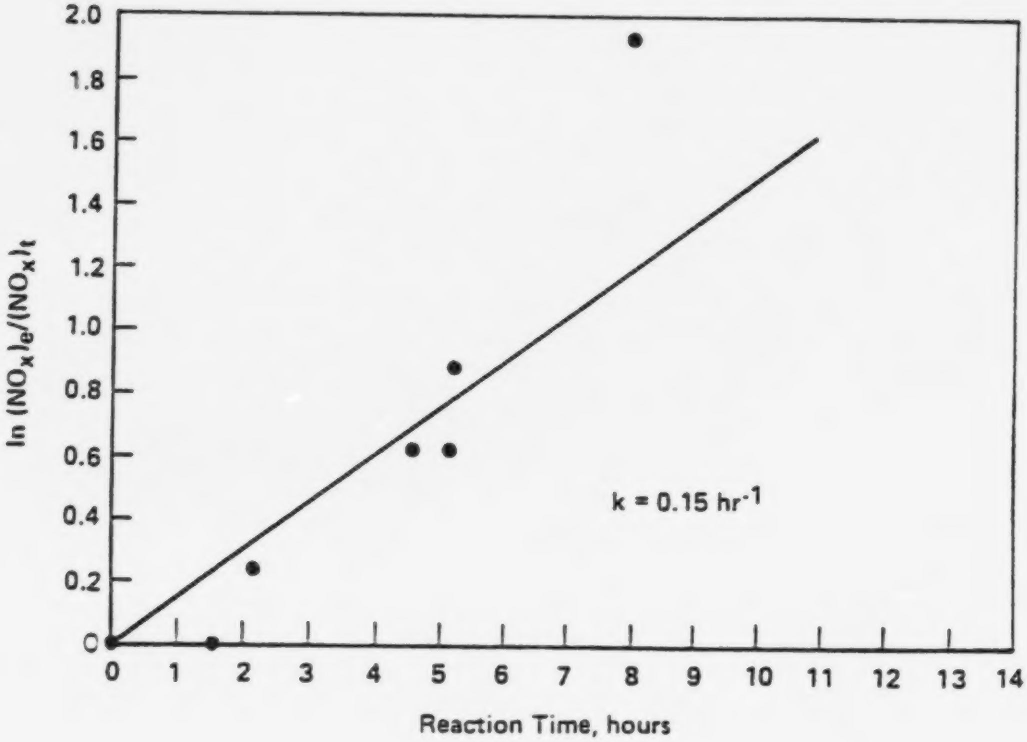

Figure 10. First order plot for flights of August 23, 1978.

REFERENCES

Appel, B. R., S. M. Wall, Y. Tokiwa, and M. Haik. 1979. Interference Effects in Sampling Particulate Nitrate in Ambient Air. Atmos. Environ., 13:319.

Breeding, R. J., H. B. Klonis, J. P. Lodge, Jr., J. B. Pate, D. C. Sheesley, T. R. Englert, and D. R. Sears. 1976. Atmos. Environ., 10:181.

Howes, J. E., C. W. Spicer, and B. P. Price. 1979. Protocol For a Field Study to Intercompare Methods for Measurement of Nitric Acid and Aerosol Nitrate. Battelle-Columbus report to EPA, Contract 68-02-3228.

Spicer, C. W. 1977. The Fate of Nitrogen Oxides in the Atmosphere. Adv. Environ. Sci and Tech.,. Vol. 7, J. N. Pitts and R. L. Metcalf, eds. J. Wiley, New York.

Spicer, C. W., and P. M. Schumacher. 1977. Interferences in Sampling Atmospheric Particulate Nitrate. Atmos. Environ., 11:873.

Spicer, C. W., and P. M. Schumacher. 1979. Particulate Nitrate: Laboratory and Field Studies of Major Sampling Interferences. Atmos. Environ., 13:543.

Spicer C. W., D. W. Joseph, P. R. Sticksel, G. M. Sverdrup, and G. F. Ward. 1979a. Reactions and Transport of Nitrogen Oxides and Ozone in the Atmosphere. Battelle-Columbus draft report to EPA, Contract 68-02-2439.

Spicer, C. W., J. R. Koetz, G. W. Keigley, G. M. Sverdrup, and G. F. Ward. 1979b. A Study of Nitrogen Oxides Within Urban Plumes Transported over the Ocean. Battelle-Columbus draft report to EPA, Contract 68-02-2957.

SAMPLING OF NITRATES IN AMBIENT AIR

B. R. Appel
Y. Tokiwa
M. Haik

Air and Industrial Hygiene Laboratory
Laboratory Services Branch
California Department of Health Services
2151 Berkeley Way
Berkeley, California 94704

INTRODUCTION

Several recent studies have clearly shown that the measurement of atmospheric particulate nitrate is subject to substantial error (Witz and MacPhee 1977; Spicer and Schumacher 1977; Spicer 1977; Appel et al. 1979a, Appel et al. 1979b). Errors arise, in part, because of the presence of gaseous nitric acid (HNO_3) in the troposphere. Collection of gaseous nitrogen oxides on filter media with subsequent measurement as nitrate (NO_3^-) is referred to as artifact particulate NO_3^- formation. Negative errors in particulate NO_3^- measurements can result when particulate NO_3^- reacts with strong acids (e.g. ammonium bisulfate, NH_4HSO_4), liberating HNO_3 (Harker et al. 1977) as well as by volatilization of NO_3^- salts.

In this paper is discussed: 1) positive and negative errors in particulate nitrate measurement, 2) measurement of nitric acid and true particulate nitrate, 3) composition of atmospheric particulate nitrates, and 4) research needs related to nitrates.

CONCLUSIONS

1. Glass fiber filters can serve as total inorganic nitrate samplers, quantitatively collecting both atmospheric inorganic particulate nitrates and nitric acid.

2. Nitric acid is the only observable contributor to artifact particulate nitrate formation in atmospheric sampling.

3. Particulate nitrate includes moderately volatile ammonium nitrate (NH_4NO_3) and possibly a more volatile nitrate (e.g., weakly bound HNO_3).

4. Heating of samplers for particulate nitrate and HNO_3 measurement by filter collection, as recommended by Okita and coworkers (1976), causes increased error. Even without heating, >50 percent losses of particulate nitrate from the Teflon prefilter can occur with corresponding positive errors in HNO_3 measurement.

5. Nitric acid values obtained by difference between total nitrate and total particulate nitrate measurements may be in error because of particulate nitrate losses in the acid gas denuder.

RECOMMENDATIONS

We believe the following should be studied to improve sampling techniques as well as to interpret possible adverse health effects of particulate nitrates:

- The composition of particulate nitrates (possible components include NH_4NO_3, sodium nitrate ($NaNO_3$), HNO_3 absorbed on particulate matter or as an addition compounds with NH_4NO_3);
- The contribution of adsorbed HNO_3 to particulate acidity in ambient air and as a sampling artifact;
- A simple technique for monitoring "true" particulate inorganic NO_3^- (e.g. total NO_3^- with a glass fiber filter less HNO_3 by the chemiluminescence technique (Joseph and Spicer 1978).

EXPERIMENTAL

The techniques employed for laboratory measurements of artifact particulate nitrate formation have been described elsewhere (Appel et al. 1979a). Nitric acid was sampled at 20 liters/min with 47-mm, NaCl-impregnated, Whatman 41 (W41) cellulose filters (Okita et al. 1976) and Duralon and Ghia Corp. nylon filters (Spicer 1979). Teflon prefilters, 2 µm pore size, Zefluor (Ghia Corp.), or 1 µm pore size Fluoropore (Millipore Corp.) were used to remove particulate nitrates. Prefilters and collection filters were mounted in series in Nuclepore multiple filter holders with polycarbonate inlet tubes (3.2 cm I.D., 15 cm length). The efficiency of the prefilters for collection of particulate matter is >99.9 percent, as measured with room air dust and a condensation nuclei counter (John and Reischl 1978). In some cases following each sampling period, ambient air, heated to a temperature which produced a relative humidity (RH) of <15 percent (typically 45 to 50 °C), was sampled for 3 min at 20 liters/min to desorb HNO_3 possibly retained on the prefilter and/or walls of the sampler.

Nitric acid was extracted from nylon filters with 0.1 N sodium hydroxide (NaOH) (Lazrus 1979) and from sodium chloride (NaCl)-impregnated filters, in distilled water with agitation by an Eberbach Model 6000 shaker for 60 min. Nitric acid was determined as nitrate by an automated copper--cadmium (Cu--Cd) reduction procedure (Technicon Industrial Systems 1973) after neutralization with 0.1 N hydrochloric acid (HCl) where necessary. This procedure had a median coefficient of variation of <3 percent with atmospheric samples, and accuracy of 98 percent with EPA audit filter strips spiked with known amounts of nitrate. The sum of particulate nitrate on the Teflon prefilter plus nitric acid (as NO_3^-) on the nylon or NaCl-impregnated afterfilter equalled the total nitrate (i.e., gaseous plus particulate nitrate) sampled.

In addition, total particulate nitrates were sampled following passage of the atmospheric sample through a diffusion denuder (Stevens et al. 1978) coated with magnesium oxide (MgO) (Shaw et al. 1979) as shown in Figure 1. The denuder was intended to remove gaseous HNO_3 while permitting nearly complete penetration of particulate nitrates to a Teflon prefilter and nylon (or NaCl/W41) afterfilter. Assuming no loss of particulate nitrate in the denuder, total nitrate less total particulate nitrate should equal the gaseous nitrate (i.e., HNO_3).

Atmospheric sampling was conducted at Harvey Mudd College, Claremont, California; at the Los Alamitos (California) Naval Air Station; at the Lennox, California, station of the South Coast Air Quality Management District; and at the San Jose station of the Bay Area Air Quality Management District.

RESULTS AND DISCUSSION

Artifact Particulate Nitrate Formation

A series of filter media (Table 1) were evaluated for their ability to form artifact particulate nitrate. Using the pH of an aqueous slurry to characterize filter alkalinity, the seven filter types ranged from weakly acidic (pH = 4.6) to relatively alkaline (pH = 9.4). Table 2 compares the collection of NO_2 alone, NO_2 plus O_3, and HNO_3 on these filters expressed in $\mu g/m^3$ as nitrate. NO_2 showed relatively little collection, with the highest levels for the alkaline filters. In the presence of O_3, artifact nitrate was substantially enhanced with the high pH glass fiber filters. However, collection of HNO_3 was 1 to 2 orders of magnitude higher than with NO_2. Filters showing the highest levels with HNO_3 include the low pH Spectrograde and the cellulose acetate filters. The levels of artifact particulate nitrate from

TABLE 1. FILTER MEDIA STUDIED FOR ARTIFACT PARTICULATE NITRATE FORMATION

Filter	pH
Fluoropore FALP, 1-µm pore size (Teflon)	5.8
Gelman GA-1, 5-µm pore size (cellulose acetate)	5.5
Whatman 41 (cellulose)	4.6
Gelman A (binder free glass fiber)	7.6
Gelman Spectrograde (silicone-treated glass fiber)	6.2
MSA 1106BH (binder free glass fiber)	9.4
Gelman "EPA Grade" (binder free glass fiber)	9.3

HNO_3 are compared to atmospheric nitrate results from simultaneous sampling at San Jose and Los Alamitos, California in Table 3. In both cases, Fluoropore showed the lowest, while the high-pH glass fiber, Spectrograde, and cellulose acetate filters showed the highest levels. We conclude from this that HNO_3 rather than NO_2 was the dominant source of artifact particulate nitrate.

TABLE 2. ARTIFACT NO_3^- FORMATION ($\mu g/m^3$) AT 50 PERCENT RH[a]

Filter	0.5 ppm NO_2	0.5 ppm NO_2[b] 0.5 ppm O_3	0.2 ppm HNO_3
Fluoropore	0.0	~0	2.4 (13)
Gelman A	2.2	2.5	38
Whatman 41	2.0	2.0	55
MSA 1106BH	2.3	9.1	91
Gelman EPA Grade	2.3	5.8	110
Spectrograde	1.4	1.4	125
Gelman GA-1	1.9	2.2	54 (186)

[a] Face velocity 47 cm/sec except for values in parentheses, which are for face value velocity 20 cm/sec, as used in atmospheric sampling.
[b] Estimated from results at 90 percent RH.

TABLE 3. COMPARISON OF ATMOSPHERIC NO_3^- AND ARTIFACT NO_3^- RESULTS FROM HNO_3[a]

Filter	Artifact NO_3^- from HNO_3[b]	24-h Ambient Nitrates
Fluoropore	0.34	0.6 ± 0.06
Gelman A	1.00	1.00
Whatman 41	1.44	1.14 ± 0.06
MSA 1106BH	2.37	1.29 ± 0.14
Gelman EPA Grade	2.86	---
Spectrograde	3.26	1.27 ± 0.06
Gelman GA-1	4.86	1.29 ± 0.2

[a] Expressed relative to results on Gelman A filters in simultaneous sampling.
[b] Six-hour exposures, 0.2 ppm HNO_3, 50 percent RH., 22° C.

An additional evaluation of artifact nitrate formation with a glass fiber filter was made in sampling at Claremont, California. Figure 2 compares NO_3^- concentrations obtained with 47-mm Gelman A glass fiber filters sampling for 2 to 8 h at 25 liters/min, with total NO_3^- values (i.e., the sum of the

NO_3^- on a Teflon prefilter and HNO_3 on a nylon NaCl/W41 afterfilter). To a good approximation, the results are equal, demonstrating that glass fiber filters can serve as total NO_3^- samplers; this held true under conditions in which total NO_3^- was 80 μg/m^3, and about 50 μg/m^3 of the total was HNO_3. Furthermore, since NO_2 is not collected on nylon or NaCl/W41 (Spicer 1979; Appel et al. 1979, unpublished studies for California Air Resources Board Contract A8-111-31), these findings confirm that HNO_3 is the principal source of artifact particulate nitrate on glass fiber filters.

Measurement of Nitric Acid

Duralon nylon and NaCl-impregnated cellulose filters are compared for efficiency of collecting laboratory-generated HNO_3 in Figure 3. Except for the nylon filter sample at ~20 μg NO_3^- loading, filters were heated in all cases. Under these conditions, nylon filters showed decreased efficiency at higher loadings. However, at the levels encountered in ambient air (<500 μg) efficiencies with nylon are expected to be >80 percent. The field study was conducted both with and without filter heating.

Figure 4 compares HNO_3 results on NaCl-impregnated and nylon filters obtained in side-by-side sampling at Claremont, California. For this comparison, all filters were post heated 3 min, since laboratory studies indicated this procedure minimized HNO_3 losses on prefilters. Consistent with the laboratory study, results on the NaCl/W41 filters are, in general, slightly higher than on nylon.

Both Okita's (1976) and Spicer's (1979) techniques for measuring HNO_3 by filter collection are subject to positive errors if any particulate NO_3^- is lost from the Teflon prefilter by dissociation to HNO_3. However, HNO_3 measured as the difference between total NO_3^- and total particulate NO_3^- ("HNO_3 by difference") should be independent of such errors. Figure 5 compares "HNO_3 by difference" and HNO_3 by filter collection for Claremont samples. No filters were heated for this comparison. Aside from three outliers, the results show reasonable correlation but are consistently higher by filter collection. This is consistent with NO_3^- loss from the prefilter. The same comparison, but with filter heating, is shown in Figure 6. Again, results are higher by filter collection, and Claremont results with heating show greater deviations from "HNO_3 by difference," compared to results without heating. Better agreement between the two techniques is seen with Lennox samples compared to those from Claremont.

In Figure 7, "HNO_3 by difference" is compared to simultaneous HNO_3 measurements by a long-path infrared technique performed by Tuazon at the State Air pollution Research Center in California (Tuazon et al. 1978). The results show substantial difference between the techniques even with relatively high HNO_3 concentrations. The difference may reflect loss of particulate NO_3^- passing through the acid gas denuder. Accordingly, only lower limit estimates of error in the HNO_3 values by filter collection can be inferred from comparison with "HNO_3 by difference" as in Figure 5.

Negative Errors in Particulate Nitrate Sampling

While Teflon filters show the lowest levels of artifact particulate NO_3^- formation, NO_3^- sampling with such inert filters is subject to negative error because of volatilization of NH_4NO_3. Table 4 describes an experiment in which NH_3- and HNO_3-free air was passed through Teflon filters loaded with <0.3 μm NH_4NO_3 particles. At 50 and 80 percent RH, the observed NO_3^- loss was about 50 percent. On the assumption that NH_4NO_3 dissociation is the source of loss, a lower limit value of 21 (ppb)^2 can be determined for the dissociation constant.

TABLE 4. LOSS OF NH_4NO_3 FROM TEFLON FILTER

Parameter	Value
Initial loading:	200 μg <0.3-μm NH_4NO_3
Purified air:	7 m^3 at 20 liters/min
Temperature:	21° C
RH:	50 and 80 percent
Loss of NO_3^-:	46 ± 8 percent
Possible mechanism:	$NH_4NO_3 - HNO_3 + NH_3$
Dissociation constant, K:	>21 (ppb)^2

Loss of particulate nitrate from Teflon filters during atmospheric sampling can be estimated by comparing the NO_3^- results on prefilters with the total particulate NO_3^-sampled, as shown in Figure 1. The comparison was made without filter heating (Figure 8). The data points fall into two groups--one showing reasonable agreement between techniques; and the second, much higher results by the total particulate NO_3^- sampler. The first group corresponds to samples collected during night and morning hours. The samples deviating badly were collected during ambient temperatures in the range 29 to 35 °C and RH's about 30 percent. More than 50 percent of the NO_3^- is lost from the Teflon prefilters under these conditions. Figure 9 makes the same comparison but with filter heating. The results for all samples are similar to those when the ambient temperature was high. Most of NO_3^- on the prefilter has been lost. Since the total particulate NO_3^- values may be low because of losses in the acid gas denuder, NO_3^- losses from the Teflon prefilters inferred from these comparisons represent minimum values.

Figure 10 compares the diurnal variations of particulate NO_3^-, as measured by the total particulate NO_3^- sampler, with those for HNO_3 and O_3 for 3 of the 8 days sampled in Claremont. HNO_3 and O_3 show similar diurnal patterns, while the diurnal maximum for particulate NO_3^- occurs earlier in the day. These are consistent with earlier results employing cellulose acetate filters (Appel et al. 1978).

The Composition of Atmospheric Particulate Nitrate

Employing temperature-programmed Electron Spectroscopy for Chemical Analysis (ESCA) on Los Angeles Basin samples, loss rate measurements for the NO_3^- and NH_4^+ bands were greatly in excess of those from pure NH_4NO_3 (Appel et al. 1976). It was concluded that absorbed NH_3 and HNO_3, or other volatile NO_3^-, were important contributors to those bands, with adsorbed NH_3 in large molar excess, relative to NO_3^-.

On the assumption that changes in gas-phase HNO_3 concentrations would produce proportionate changes in adsorbed HNO_3, the significance of HNO_3 as a contributor to total particulate acidity was examined, as measured by microtitration of aqueous extracts (Brosset and Ferm 1978; Appel et al. 1979c). Figure 11 compares the diurnal variations for HNO_3, H^+ in aqueous extracts expressed as H_2SO_4, and H_2SO_4 measured by the benzaldehyde extraction technique (Leahy et al. 1975; Appel et al. 1979c). Although the correlation between H_2SO_4 and H^+ as H_2SO_4 is poor, the correlation between total H^+ and gas-phase HNO_3 is also poor. Neutralization of H^+ by alkaline materials in the aqueous extract may be influencing these results.

We next consider the particulate NO_3^- sampled following passage through the acid gas denuder. If particulate NO_3^- were nonvolatile, all would be retained on the prefilter (except the HNO_3 liberated by the reaction of NO_3^- salts with particulate acids). Figure 12 plots the NO_3^- fraction reaching the afterfilter (nylon or NaCl/W41) against the ambient HNO_3 concentration. Despite the removal of >99 percent of the HNO_3 by the denuder, the NO_3^- fraction reaching the afterfilter correlates with the HNO_3 level.* The scatter in the results suggested that another variable might also be significant. Figure 13 plots the log of the product of HNO_3 and mole fraction of NO_3^- on the afterfilter against 1/T. The data partition into two sets. We infer from this that adsorbed or weakly bound HNO_3 may be significant. The division into two data sets may indicate differing aggregates of volatile and less volatile NO_3^-. Alternatively, the data may reflect increased volatilization of NH_4NO_3 in the presence of decreased NH_3 levels. The latter in turn was negatively correlated with HNO_3 levels. However, this alternative provides no obvious rationale for the partitioning of the Figure 13 data into two sets.

---

*Note added in proof. . . Additional trials of the efficiency of the acid gas denuder have been made. The overall mean result is 88 ± 5 percent (n = 10) for 85 to 135 ppb HNO_3 at 21 to 32°C, and 30 to 80 percent RH. Based on the higher mean results for atmospheric HNO_3 by the difference method compared to Fourier transform infrared results, the expected 12 percent HNO_3 penetration is more than offset by opposing sources of error (e.g., loss of large-particle nitrate in the denuder).

ACKNOWLEDGMENTS AND DISCLAIMER

These studies were supported by the California Air Resources Board, Research Section. The authors express their appreciation to Professor G. Kok, Harvey Mudd College, and to the staff and management of the South Coast and the Bay Area Air Quality Management Districts for providing facilities for conducting atmospheric sampling.

This report has been reviewed by the California Air Resources Board, and approved for publication. Approval does not signify that the contents necessarily reflect the views and policies of the California Air Resources Board, nor does mention of trade names or commercial products constitute endorsement or recommendation for use.

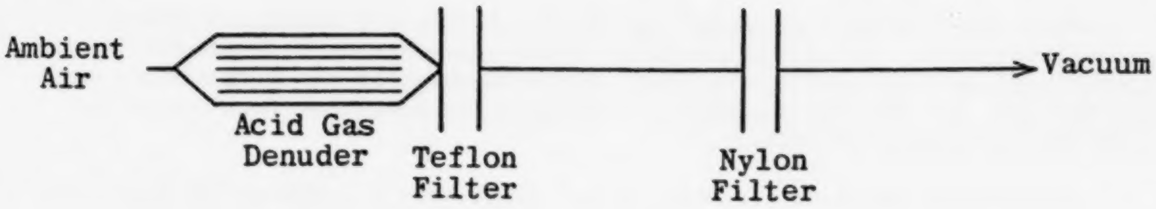
Ambient Air
Acid Gas Denuder
Teflon Filter
Nylon Filter
Vacuum

(TOTAL NITRATE)−(TOTAL PARTICULATE NITRATE) = AMBIENT HNO_3

Figure 1. Total particulate nitrate sampler.

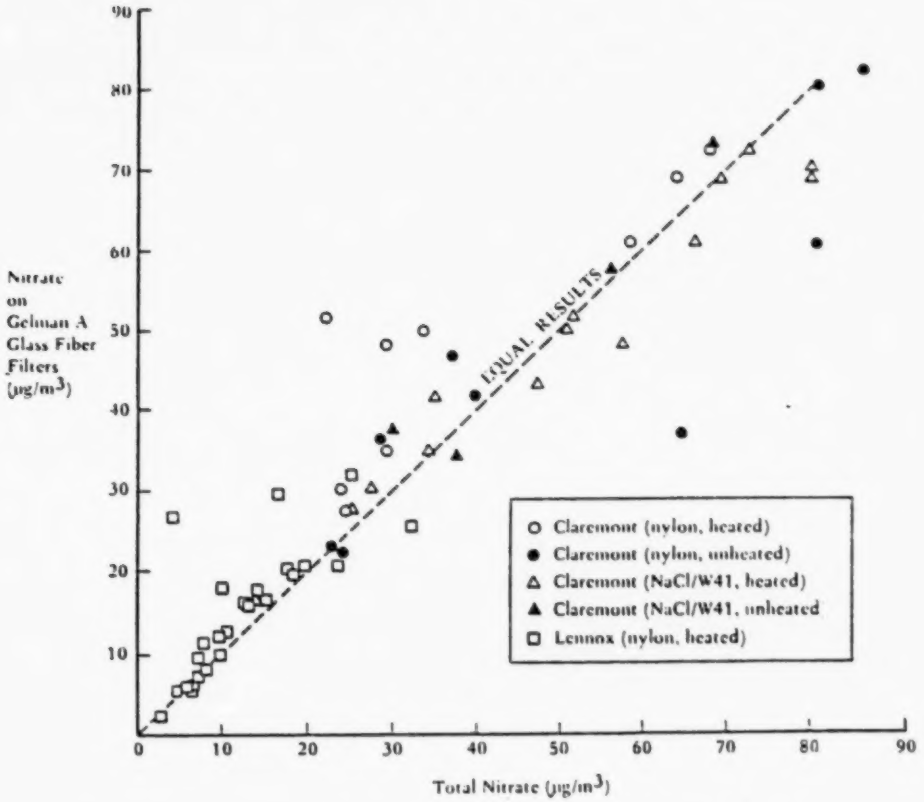

Figure 2. Glass fiber filters as total nitrate samplers.

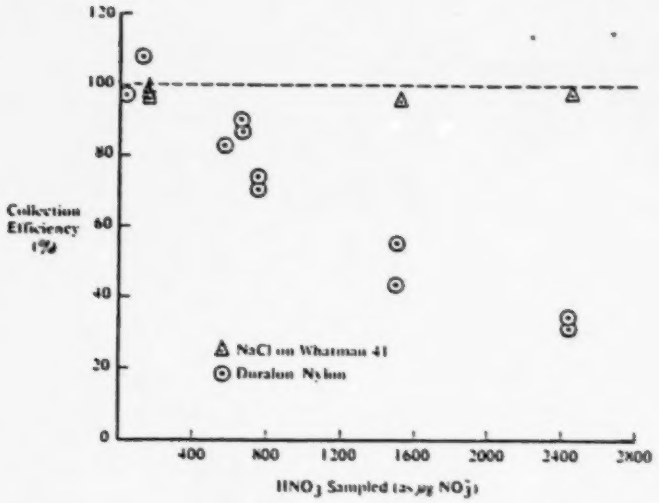

Figure 3. HNO_3 collection efficiency of nylon and NaCl-impregnated Whatman 41 filters (50 to 80 percent RH).

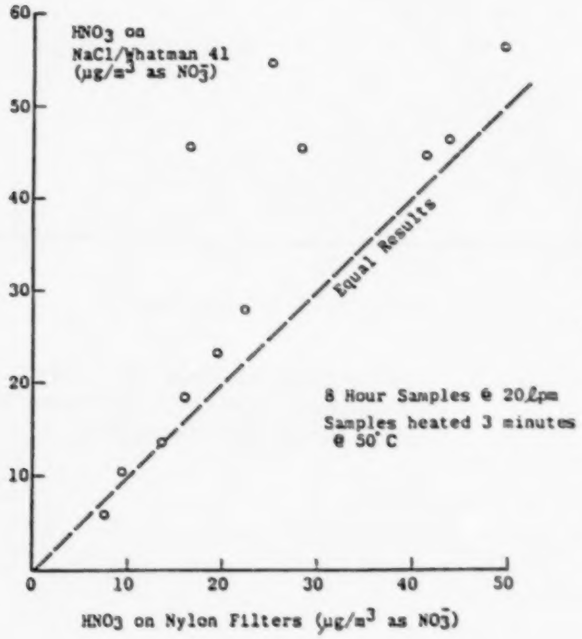

Figure 4. Atmospheric HNO_3 collection of nylon vs. NaCl/Whatman 41 filters.

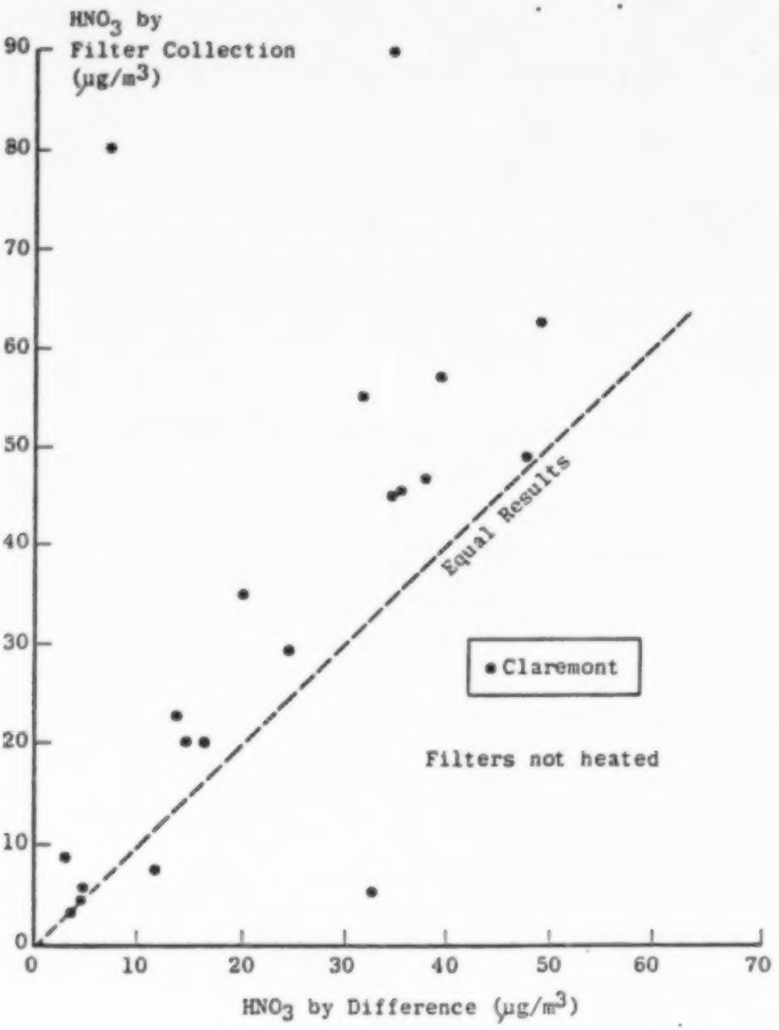

Figure 5. Comparison of HNO$_3$ by filter collection and "by difference" using unheated samplers.

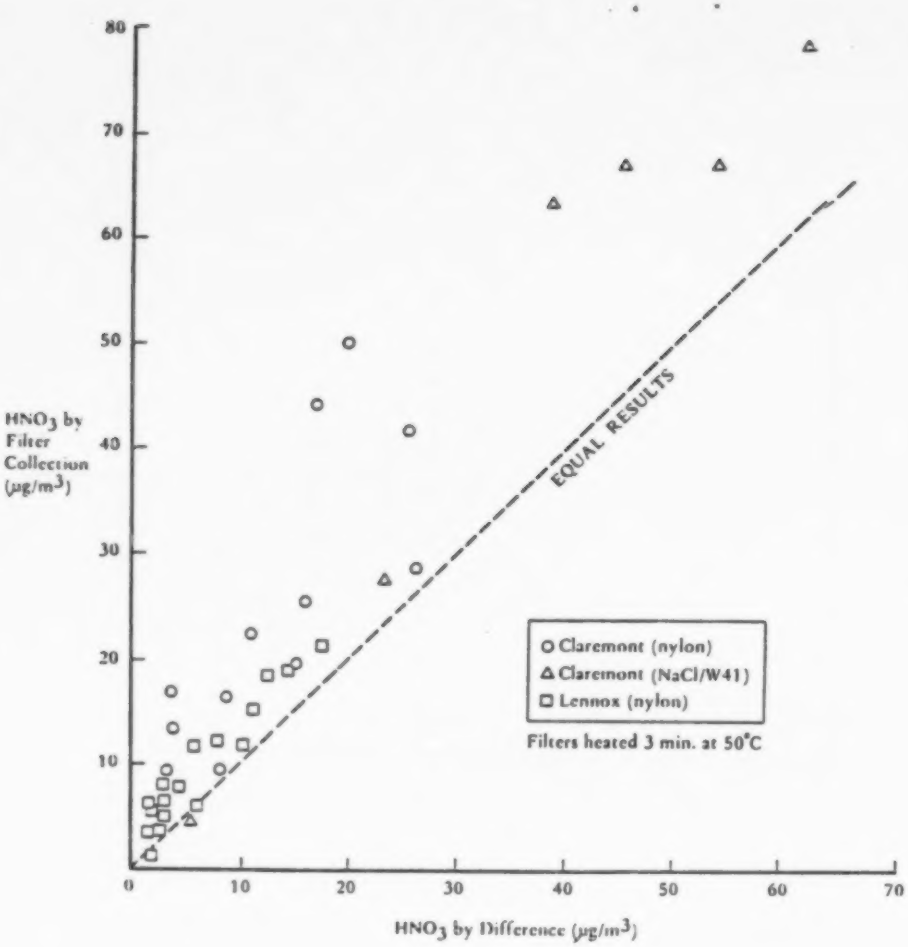

Figure 6. Comparison of HNO_3 by filter collection and "by difference" using heated samplers.

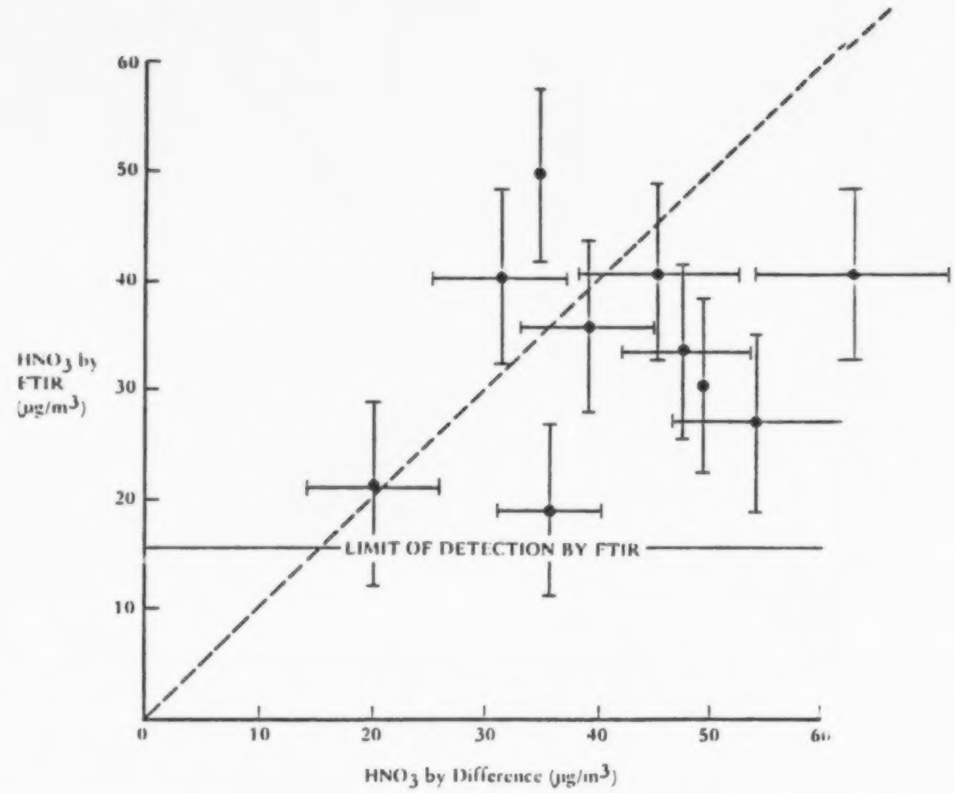

Figure 7. Comparison of HNO_3 by long path Fourier transform and "by difference."

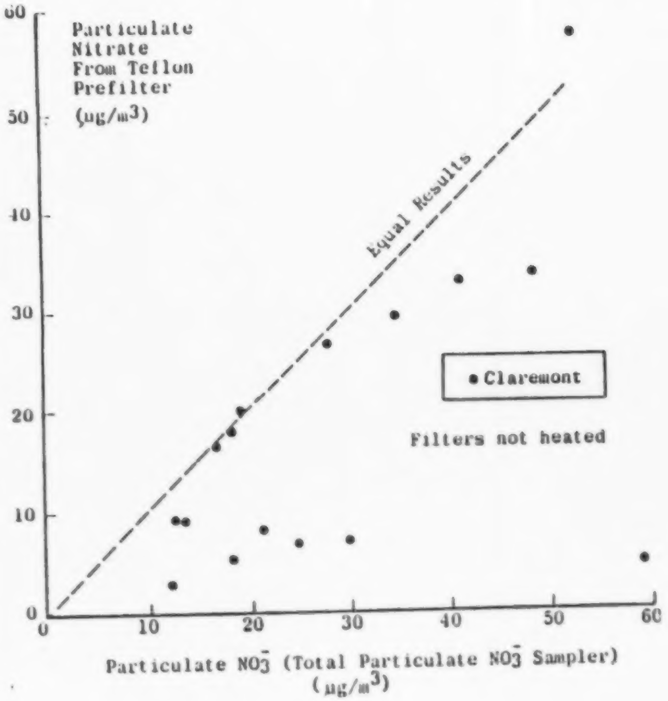

Figure 8. Comparison of particulate NO_3^- levels by Teflon prefilters and by the total particulate NO_3^- sampler with unheated samplers.

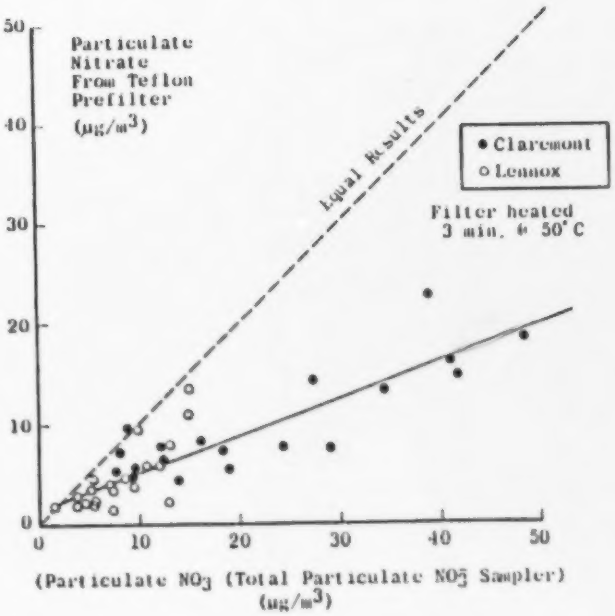

Figure 9. Comparison of particulate NO_3^- levels by Teflon prefilters and by the total particulate NO_3^- samplers with heated samplers.

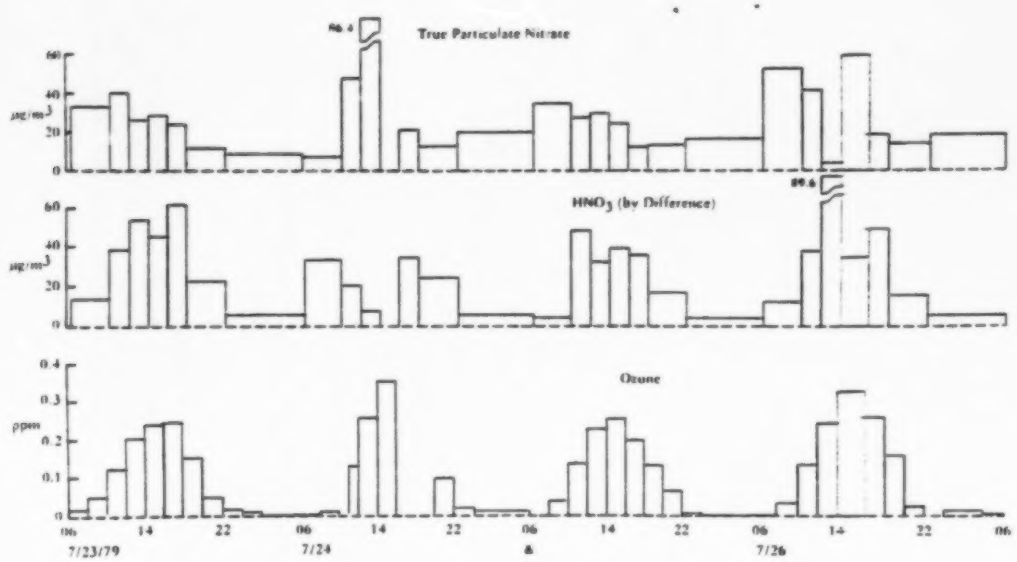

Figure 10. Diurnal variations for HNO_3, true particulate NO_3^-, and O_3 at Claremont, California.

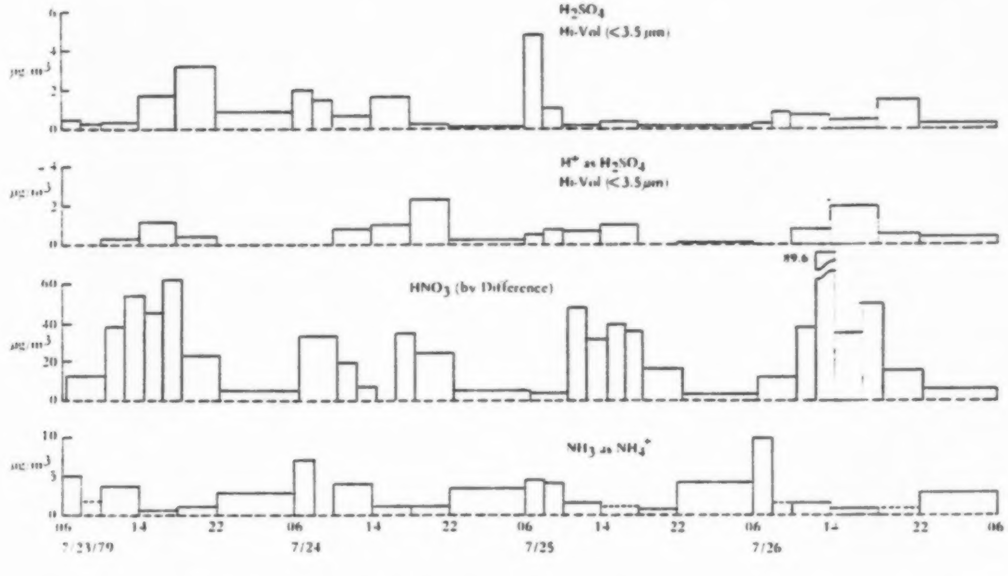

Figure 11. Diurnal variations for HNO_3, H_2SO_4, particulate acidity, and gaseous NH_3 at Claremont, California.

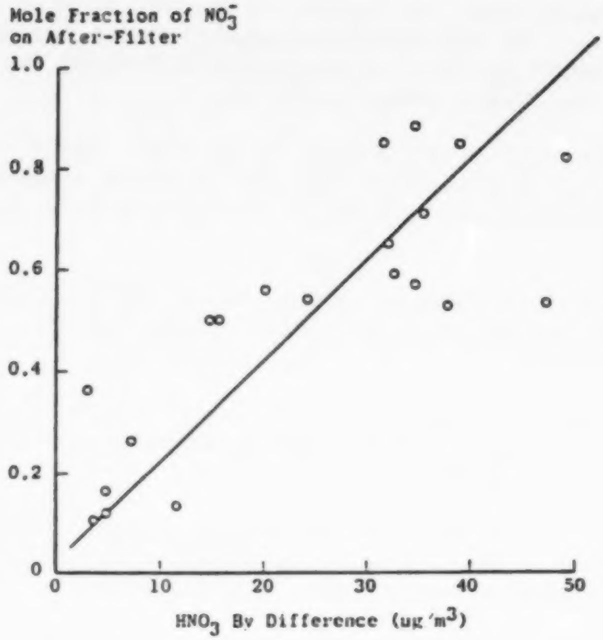

Figure 12. Fraction of NO_3^- on the after-filter of the total particulate NO_3^- sampler vs. "HNO_3 by difference."

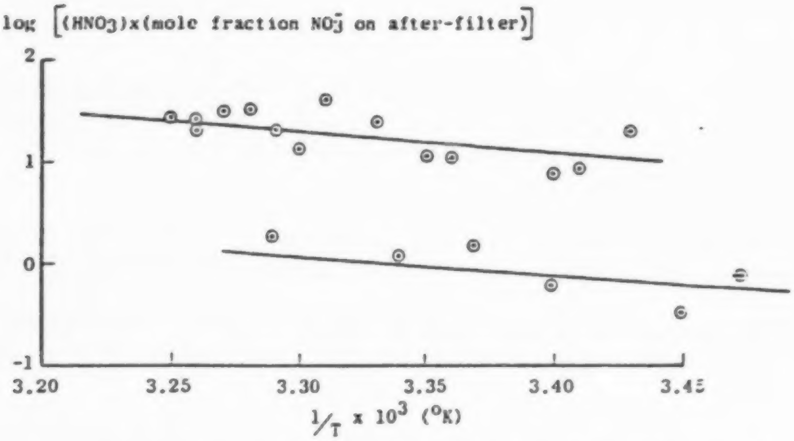

Figure 13. Fraction of NO_3^- on the afterfilter of the total particulate NO_3^- sampler as a function of "HNO_3 by difference" and temperature.

REFERENCES

Appel, B. R., J. J. Wesolowski, E. Hoffer, S. Twiss, S. Wall, S. G. Chang, and T. Novakov. 1976. An Intermethod Comparison of X-Ray Photoelectron Spectroscopic (ESCA) Analysis of Atmospheric Particulate Matter. Intern. J. Environ. Anal. Chem. 4:169-181.

Appel, B. R., E. L. Kothny, E. M. Hoffer, G. M. Hidy, and J. J. Wesolowski. 1978. Sulfate and Nitrate Data from the California Aerosol Characterization Experiment (ACHEX). Environ. Sci. Technol. 12:418-425.

Appel, B. R., S. M. Wall, Y. Tokiwa, and M. Haik. 1979a. Interference Effects in Sampling Particulate Nitrate in Ambient Air. Atmos. Environ. 13:319-325

Appel, B. R., S. M. Wall, Y. Tokiwa, and M. Haik. 1979b. Simultaneous Nitric Acid, Particulate Nitrate and Acidity Measurements in Ambient Air. Atmos. Environ. (in press)

Appel, B. R., S. M. Wall, M. Haik, E. L. Kothny, and Y. Tokiwa. 1979c. Evaluation of Techniques for Sulfuric Acid and Particulate Strong Acidity Measurements in Ambient Air. Atmos. Environ. (in press).

Harker, A. B., L. W. Richards, and W. E. Clark. 1977. The Effect of Atmospheric SO_2 Photochemistry upon Observed Nitrate Concentrations in Aerosols. Atmos. Environ. 11:87-91.

John, W., and G. Reischl. 1978. Measurement of the Filtration Efficiencies of Selected Filter Types. Atmos. Environ. 12:2015-2019.

Joseph, E. W., and C. W. Spicer. 1978. Chemiluminescence Method for Atmospheric Monitoring of Nitric Acid and Nitrogen Oxides. Anal. Chem. 50:1400-1403.

Lazrus, A., B. W. Ganrud, and J. P. Greenberg. Indophenol Ammonia Test in Measurement of HNO_3 and NO_3^-. In: Current Methods to Measure Atmospheric Nitric Acid and Nitrate Artifacts, R. K. Stevens, ed. EPA-600/2-79-051, pp. 45-50.

Leahy, D. F., R. Siegel, P. Klotz, and L. Newman. 1975. The Separation and Characterization of Sulfate Aerosol. Atmos. Environ. 9:219-229.

Okita, T., S. Morimoto, S. Izawa, and W. Konno. 1976. The Measurement of Gaseous and Particulate Nitrates in the Atmosphere. Atmos. Environ. 10:1085-1089.

Shaw, R. W., T. G. Dzubay, and R. K. Stevens. 1979. The Denuder Difference Experiment. In: Current Methods to Measure Atmospheric Nitric Acid and Nitrate Artifacts, R.K. Stevens, ed. EPA-600/2-79-051, pp. 79-84.

Spicer, C. W. 1977. Photochemical Atmospheric Pollutants Derived from Nitrogen Oxides. Atmos. Environ. 11:1089-1095.

Spicer, C. W. 1979. Measurement of Gaseous HNO_3 by Electrochemistry and Chemiluminescence. In: Current Methods to Measure Atmospheric Nitric Acid and Nitrate Arfifacts, R. K. Stevens, ed. EPA-600/2-79-051, pp. 27-35.

Spicer, C. W., and P. Schumacher. 1977. Interference in Sampling Atmospheric Particulate Nitrate. Atmos. Environ. 11:873-876.

Stevens, R. K., T. G. Dzubay, G. Russwurm, and D. Rickel. 1978. Sampling and Analysis of Atmospheric Sulfates and Related Species. Atmos. Environ. 12:55-68.

Technicon Industrial Systems. 1973. Nitrate and Nitrite in Water and Wastewater. Method No. 100-70W. Technicon Instruments Corp., Tarrytown, NY.

Tuazon, E. C., R. A. Graham, A. M. Winer, R. R. Easton, J. N. Pitts, Jr., and P. L. Hanst. 1978. A Kilometer Pathlength Fourier-Transform Infrared System for the Study of Trace Pollutants in Ambient and Synthetic Atmospheres. Atmos. Environ. 12:865-875.

Witz, S., and R. D. MacPhee. 1977. Effect of Different Types of Glass Filters on Total Suspended Particulates and their Chemical Composition. J. Air Pollut. Control Ass. 27:239-241.

NITRIC ACID MEASUREMENTS IN CLEAN AIR

Donald H. Stedman
Thomas J. Kelly

Chemistry Department
University of Michigan
Ann Arbor, Michigan 48109

INTRODUCTION

Atmospheric models of clean or polluted air predict concentrations of gaseous nitric acid (HNO_3-) which exceed those of nitrogen oxides (NO_x)--nitric oxide (NO) plus nitrogen dioxide (NO_2)--(Chameides 1978; Crutzen 1979). To test this prediction experimentally, all three species were measured simultaneously. Results of an initial study at a site east of Boulder, Colorado, have been published (Kelly and Stedman 1979).

EXPERIMENTAL

The chemiluminescence principle is used in a purpose-built, high sensitivity, NO detector. The adaptations to the inlet system are shown in Figure 1. The single sample inlet point to the vacuum system is a Teflon filter, connected to a glass and Teflon plumbing system, operating at a flow of 3 liters/min and a pressure of 6 torr. The detector has four sample flow channels, corresponding to the four Teflon solenoid valves (V1, V2, V3, and V4) in the inlet plumbing, which are controlled automatically by the detector electronics.

When V1 is opened, sample air passes directly into the reaction chamber where any NO in the sample is detected. Alternately, a background reading is taken by diverting the sample flow to a prereactor; here, the sample flow is mixed with an ozone flow, and the chemiluminescent reaction is completed before the fluid passes into the detection chamber (Ridley et al. 1973; Ritter et al. 1979). Opening V2 passes the sample air through a vessel containing 50 ml of granular iron sulfate ($FeSO_4$), which has been shown to convert 95 percent NO_2 to NO in streams from 1 to 500 ppb. The channel 2 signal thus indicates the sum of NO_2 + NO, and NO_2 is obtained by subtraction of the channel 1 NO signal.

Channel 3 passes the sample air through a trap of loose cotton or nylon fiber, which selectively removes HNO_3 from the sample (Joseph and Spicer 1978). In clean air, the levels of peroxyacetyl nitrate (PAN) and other interfering species are very low, so the trap in channel 3 is deleted. After traversing the trap, the stream passes through the HNO_3 converter. Channel 4 goes directly into the converter, a quartz tube heated to 350°C and packed with 4-mm diameter Pyrex beads.

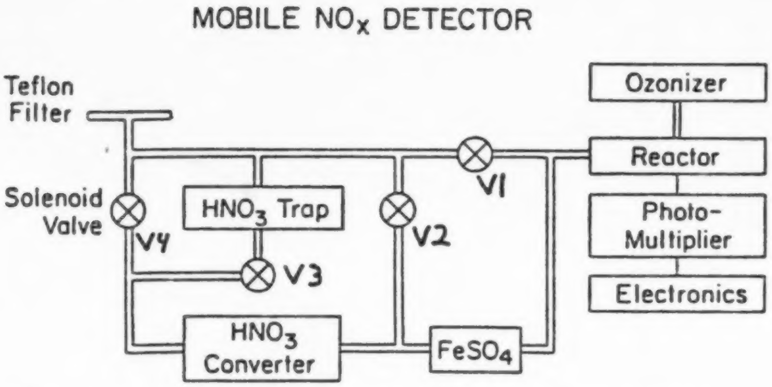

Figure 1. Inlet system block diagram for mobile NO_x detector.

In the converter, HNO_3 is quantitatively converted to NO_2; the $FeSO_4$ completes the conversion to NO. The quartz tube heat allows detection of organic nitrates or PAN, but it does not oxidize organic amines or ammonia. Any signal difference between channels 2 and 3 is a measure of undifferentiated, "total organic nitrate" present, provided it is not absorbed by the nylon. We have found PAN to be one component of this total organic nitrate, and studies are in progress to determine the detection efficiency for other organic nitrogen-containing compounds. The HNO_3 concentration is measured as the difference in signal between channels 3 and 4.

RESULTS

The trailer containing this measurement equipment was used at three sites during a 12-month period from 1978 to 1979. The first was Erie, Colorado, a rural site, but only 10 to 30 km from upwind urban sources. Figure 2 shows values from simultaneous measurements of NO_2 and HNO_3; for this figure, a large number of points with NO_2 between 0 and 7 ppb, and with HNO_3 less than the detection limit of 0.3 ppb, have been deleted. Figure 2 shows that at this site the NO_2/HNO_3 ratio was never less than 3 and frequently was greater than 10, contrary to expectation.

Reasoning that the departure from theory arose from proximity to local sources, we improved the detection limits to about 30 ppt and moved the trailer to a site nearly 10,000 ft in elevation on Niwot Ridge, 20 km west of Boulder. Here westerly winds brought very clean air, and occasionally

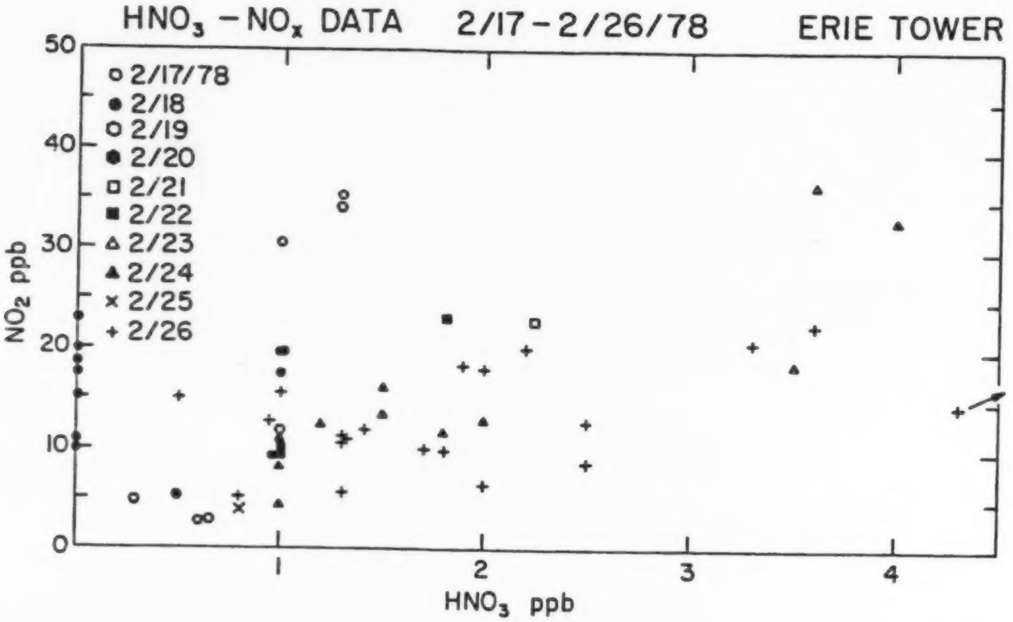

Figure 2. A plot of instantaneous values of the concentrations of NO_2 and HNO_3 in Erie, Colorado.

afternoon upslope winds brought well reacted front-range pollution. Figure 3 shows a set of data from Niwot Ridge. Note the change of scale to 1000 ppt, full scale, and the fact that the HNO_3 data (shown as a solid line) use the right hand scale of 400 ppt full scale. Figure 3 shows HNO_3 concentrations still considerably below NO_2, and clear evidence of the afternoon incursions of upslope winds bringing front range pollution.

Figure 4 shows a plot of the measured instantaneous NO_x/HNO_3 ratio versus $[NO_x]$. The lowest levels of NO_x were observed in the hours from midnight to sunrise; however, no diurnal variation in the NO_x/HNO_3 ratio was seen. Ratios of less than 2 were never observed, although the data may tend to extrapolate to a ratio nearer 1 as the air becomes cleaner. The apparent sharp slope on the left is an artifact of the detection limit for HNO_3 of 30 ppt. Points for HNO_3 <30 ppt were not plotted, but would fall in that gap. The open symbols in Figure 4 are data from B. Huebert (personal communication), who uses an impregnated filter technique to measure $[HNO_3]$ vapor.

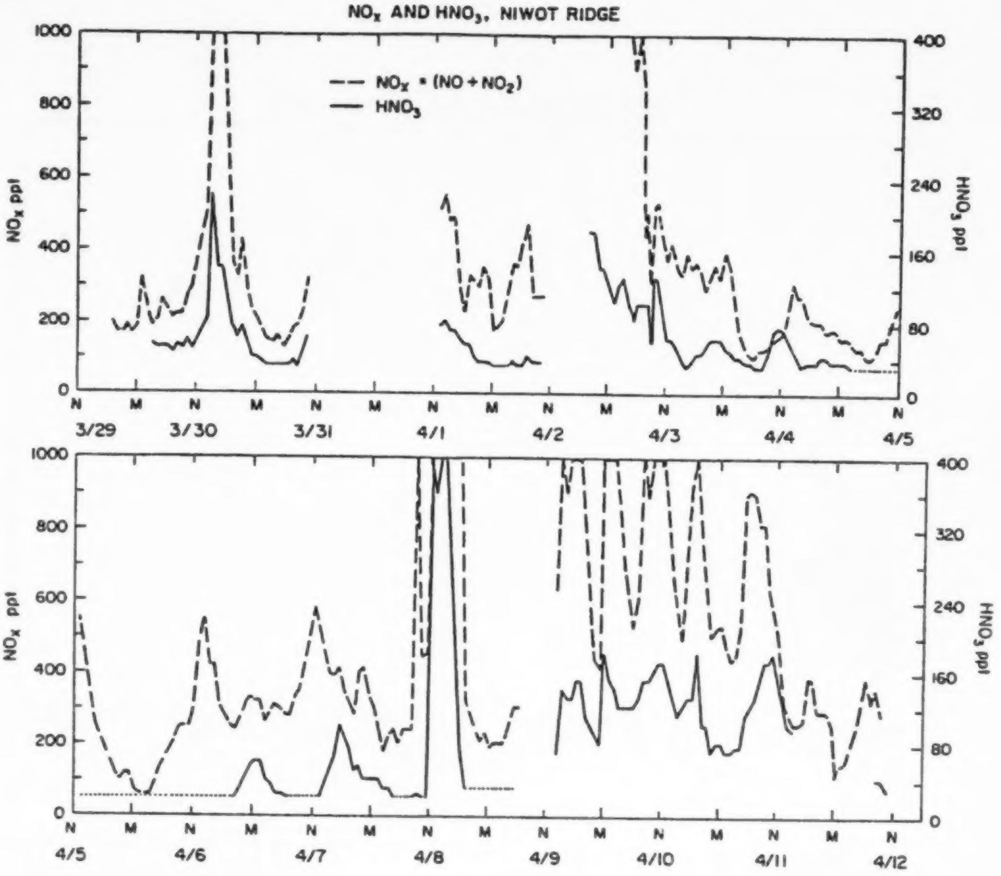

Figure 3. Typical NO$_x$ and HNO$_3$ data from the Niwot Ridge site.

The third site, Claremont, California, was visited in the last week of August 1979, and all techniques for measuring HNO$_3$ and NO$_3^-$ were utilized. Results for this experiment have not been completely reduced and analyzed, but preliminary analysis indicates that NO$_2$/HNO$_3$ ratios considerably larger than 1 were obtained, as might be expected in such an urban situation. The reasons for this departure from theory remain to be determined; either the source has been overestimated or the sink underestimated. Another departure from theory which we observe (Ritter et al. 1979) is that the photostationary state equation

$$j(NO_2)[NO_2] = k_3(NO)(O_3)$$

is not obeyed, implying larger free radical (HO$_2$) sources than hitherto expected.

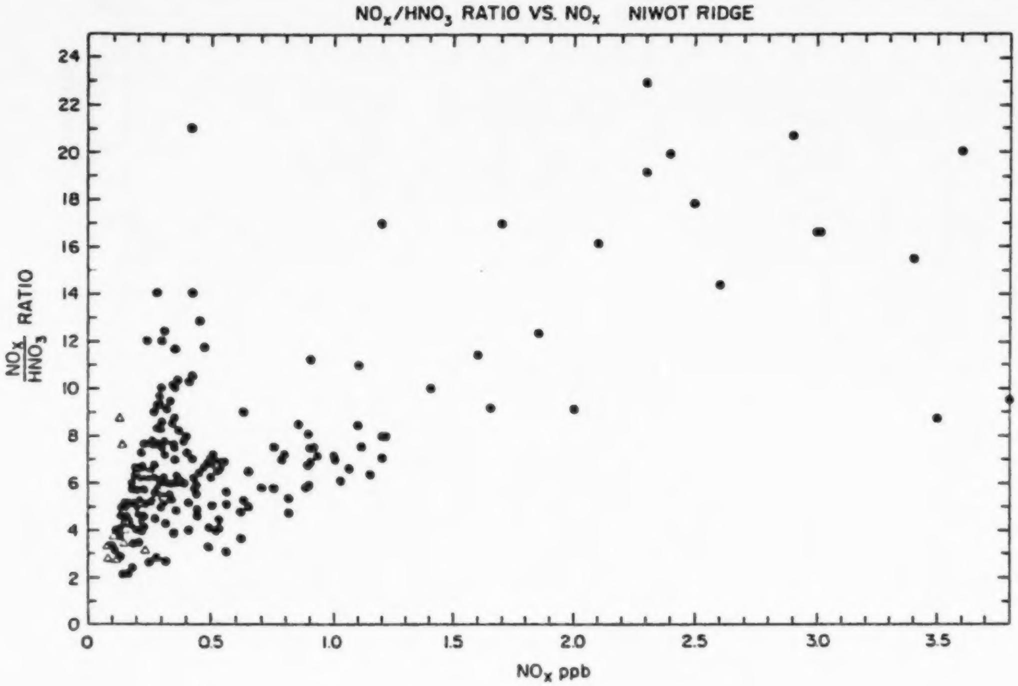

Figure 4. A plot of NO_x/HNO_3 ratio versus NO_x measured simultaneously from Niwot Ridge.

In a related effort, the important parameter, the dry deposition rate of NO_x (and SO_x), was measured experimentally using an eddy correlation technique in collaboration with B. Hicks and M. Weseley of Argonne National Laboratories. These measurements made in Lancaster, Pennsylvania, and Springfield, Ohio, in 1979 are also currently unreduced, but seem to indicate NO_x fluxes both into and out of the local agricultural land.

ACKNOWLEDGMENTS

These studies would not have been possible without support from the Atmospheric Science Division of the National Science Foundation, and the personal efforts of many of our colleagues at the University of Michigan, in Boulder, and in California.

REFERENCES

Chameides, W. L. 1978. The Photochemical Role of Tropospheric Nitrogen Oxides. Geophys. Res. Lett., 5:17-20.

Crutzen, P. J. 1979. The Role of NO and NO_2 in the Chemistry of the Troposphere and Stratosphere. Ann. Rev. Earth Planet. Sci., 7:443-472.

Joseph, D. W., and C. W. Spicer. 1978. Chemiluminescence Method for Atmospheric Monitoring of Nitric Acid and Nitrogen Oxides. Anal. chem. 50:1400-1403.

Kelly, T. J., and D. H. Stedman. 1979. Measurements of H_2O_2 and HNO_3 in Rural Air. Geophys. Res. Lett., 6:375-378.

Ridley, B. A., H. I. Schiff, A. W. Shaw, L. Bates, C. Howlett, H. LeVaux, L. R. Megill, and T. E. Ashenfelter. 1973. Measurements In Situ of Nitric Oxide in the Stratosphere Between 17.4 and 22.9 km. Nature, 245:310.

Ritter, J. A., D. H. Stedman, and T. J. Kelly. 1979. Ground-Level Measurements of Nitric Oxide, Nitrogen Dioxide and Ozone in Rural Air. In: Nitrogenous Air Pollutants: Chemical and Biological Implications, D. Grosjean, Ed. Ann Arbor Science, Ann Arbor, Michigan. Chapter 20.

HISTORY AND TRENDS OF ATMOSPHERIC NITRATE DEPOSITION IN THE EASTERN U.S.A.

M. L. Miller
A. G. Everett

Everett and Associates
416 Hungerford Drive
Rockville, Maryland 20850

INTRODUCTION

There has been a growing concern that nitrates of anthropogenic origin are resulting in increasingly acidic precipitation in the eastern United States.

The generally accepted, working definition of "acid precipitation" is any precipitation with a pH lower than about 5.7, the expected value for the equilibrium of atmospheric carbon dioxide (CO_2) and pure water (H_2O) (Barrett and Brodin 1955). This value is often assumed to be the pH of rainfall unpolluted by anthropogenic emissions, and for rainfall with a lower pH, anthropogenic pollution is assumed. Reasonably, however, it can be seen that the situation is not nearly this simple. Enormous natural sources of sulfur oxides (SO_x) and nitrogen oxides (NO_x) must be evaluated before the truly "natural" pH of precipitation can be estimated accurately.

Emissions of sulfur compounds from natural sources have variably been estimated by Granat et al. (1976) as contributing 60 percent of the tropospheric sulfur burden globally and 72 percent of the combined stratospheric and tropospheric global sulfur; for the Northern Hemisphere, natural sources are estimated to contribute 42.5 and 60 percent of tropospheric and total atmospheric sulfur, respectively. Friend (1973) had earlier estimated the overland flux of sulfur to represent 48 percent of the total atmospheric sulfur burden. Natural sources of sulfur include volcanic emanations, oceanic spray, hydrogen sulfide (H_2S) from decaying anaerobic vegetation, and gypsum from soil which is carried up in dust. The net impact of these natural sulfur sources on precipitation pH needs evaluation.

CONCLUSIONS

It seems clear that, if indeed a significant trend exists toward either increasing acidity or nitrate concentrations in rainfall, the ecosystem may be seriously threatened. However, it seems equally clear that we do not presently have the necessary knowledge to confirm either the trend or the magnitude of the threat.

NATURAL vs. ANTHROPOGENIC SOURCES

Nitrogen dioxide (NO_2) in the atmosphere has several sources. Certainly the burning of fossil fuels is one, but on a nationwide scale, natural sources of NO_2 from soil and lightning are quantitatively much more important than the anthropogenic sources.

Junge (1958) suggested that nitrate (NO_3^-) in the air is tied closely to natural processes in the soil. One source he suggested was the decay of organic matter to produce ammonia (NH_3), which in turn was oxidized to NO_3^-. Robinson and Robbins (1971) discounted this source of NO_2, but Chameides et al. (1977) later demonstrated that this pathway exists and estimated that about 25 to 50 percent of the annual NO_x produced comes from NH_3. The recent report (Chemical and Engineering News 1978) that desert sand is also a major NH_3 source is further evidence of a large contribution by this natural source.

A second possible source of natural NO_3^- in the atmosphere suggested by Junge (1958) is the production of nitric oxide (NO) by anaerobic bacteria in soils. The NO is oxidized to NO_2 and then to NO_3^-. No estimate of the significance of this source is made. Still another recently postulated NO source is the photocatalytically induced fixation of molecular nitrogen by near UV light. This has been demonstrated to occur on the surface of rutile, a common titanium-dioxide-containing mineral (Bickley and Vishwanathan 1979).

Nitrite (NO_2^-) from fertilizer has been shown by Bremer and Nelson (1968) to promote NO_2 emission from acidic soils. The failure of some previous investigators to detect NO_2 as an NO_2^- decomposition product is attributed to the use of closed experimental systems which promote absorption of the NO_2 and subsequent conversion to NO_3^- in the soil (Bremmer and Nelson 1968).

Lightning as an NO_2 source has been the subject of much debate in recent years. At one time, it was considered the major source. Later studies, which showed little correlation between lightning activity and NO_2 concentration (Junge and Werby 1958; Viemeister 1960; Visser 1961; Gambell and Fisher 1966) tended to downgrade the importance of lightning. Recent work by Noxon (1978a and 1978b) and Chameides (Chameides et al. 1977; Chameides 1979) has once again reinstated the importance of lightning. Noxon concluded the NO_2 contribution by lightning is roughly comparable to concentrations resulting from man's activities. Chameides estimated that as much as 50 percent of the total atmospheric NO_x comes from lightning, far more than the anthropogenic contribution. Previous failures to find a strong correlation of NO_3^- with lightning activity are attributed to the relatively long conversion time (12 to 20 h) required for NO--the NO_x form initially produced by lightning--to be converted to NO_2 and then to nitric acid (HNO_3) (Chameides et al. 1977).

Worldwide frequency of lightning flash maps were recently published (Turman 1979). The maps (Figure 1) show the highest density of lightning flashes is in the eastern U.S., this lightning storm track correlating well with the high NO_3^- levels in the eastern U.S. Although very few Australian data are included on these maps, the tremendously high NO_3^- levels observed by Johnson (1978) in the springtime in Australia (10 times the highest thunderstorm activity observed in the U.S.) may correlate with the increased thunderstorm activity occurring

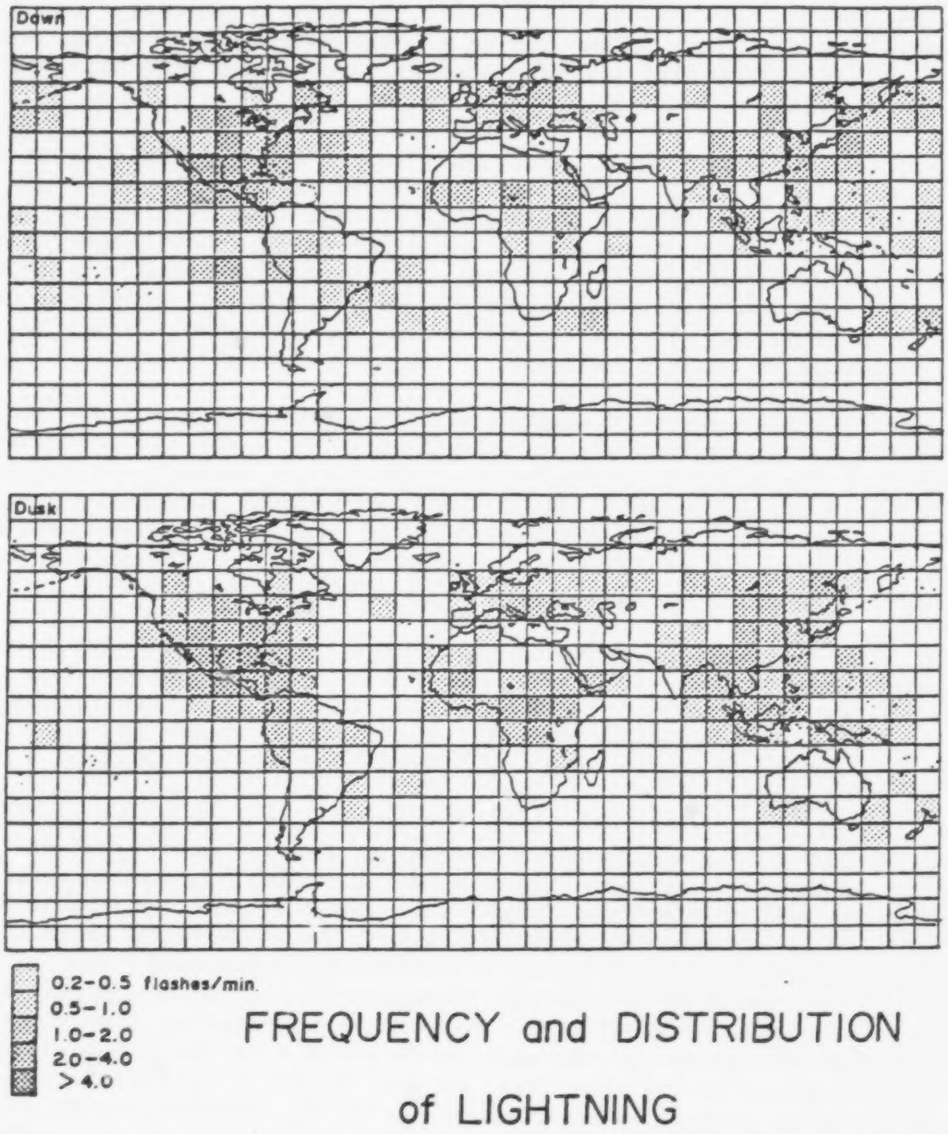
Dawn
Dusk
0.2–0.5 flashes/min.
0.5–1.0
1.0–2.0
2.0–4.0
>4.0
FREQUENCY and DISTRIBUTION
of LIGHTNING

(B.N. TURMAN, AMERICAN SCIENTIST, MAY-JUNE 1979, VOL. 67, USED WITH PERMISSION)

Figure 1. Frequency and distribution of lightning (B. N. Turman, American Scientist, May-June 1979, Vol. 67; used with permission).

during those months in Australia. An alternative possibility suggested by Johnson is that the high NO_3^- levels are caused by some kind of vegetative emission; however, they most surely do not emanate from anthropogenic sources.

Recent National Academy of Sciences (1978) estimates seem to concur that combustion of fuels is responsible for no more than 10 percent of the total NO_x. Local amounts may be higher, of course, although it seems readily apparent that the activities of man, while they may produce profound local effects, are not primarily responsible for the NO_3^- found in precipitation.

Long-term studies of the stratosphere do not suggest increasing concentrations of sulfate ($SO_4^=$) and NO_3^- over time, but they do suggest relatively steady-state concentrations that indicate a flux into the troposphere; this flux would make $SO_4^=$ and NO_3^- available for wet and dry deposition at the earth's surface. Lerman (1979) has shown that the pH of rainfall due to $SO_4^=$ and NO_3^- will range between 4.5 and 5.5. Thus, natural sulfates and nitrates lower the pH below the "normal" level of 5.7. The critical problem in future studies of acid precipitation is therefore to partition natural and man-made contributions so that realistic estimates of natural rainfall pH's can be made.

It is of interest to note that the pH of rainfall at Samoa, reputedly one of the cleanest places measured, is about 5.0 (Kerr 1979), suggesting that rainfall unbuffered by dust or neutral to basic gases, is acidic relative to the CO_2--H_2O equilibrium value of 5.7. The value of 5.0 at Samoa is quite low for an area surrounded by ocean, suggesting that the pH of a clean continental area may be in the range of 4.5.

Clearly, the pH of rainfall is quite variable, as a consequence of: 1) natural--as well as man-made--components such as dust, NH_3, and H_2S, which buffer pH or raise it to 7 or above, and 2) contributions by natural and anthropogenic NO_x and SO_x sources, which tend to result in a lowering of pH. Thus, rainfall composition and pH are functions of geographic (natural source distribution) as well as atmospheric processes under totally natural circumstances.

Anthropogenic emissions add local perturbations, which should be viewed as being superimposed on the natural gradient. The composition of surficial materials and the availability of surface dust to the atmosphere differ throughout the United States; west of the Mississippi, more dust of higher average calcium (Ca^{++}) content (both as calcium carbonate and calcium sulfate) is available. To the east of the Mississippi, we must factor in the recently recognized role of lightning in forming atmospheric NO_3^-. This becomes particularly significant when coupled with the information, based on satellite sensing systems, now emerging on the world geographic distribution of lightning.

Aside from the difficulty of separating natural from anthropogenic sources of nitrates and other acidifying components, many difficulties exist in interpreting the historical data used for establishing trends in either pH or NO_3^- levels in precipitation.

VARIABILITY IN SAMPLE COLLECTION

Because of the inherent difficulties in measuring the pH of rainwater--a very poorly buffered system--it is not surprising that very few good historical measurements exist.

Galloway (1978) has estimated that presently the analytical uncertainty in pH measurements using good techniques is 0.06. The design of the collector, the materials out of which it is made, and the collection technique are critically important factors which can introduce additional sources of error. An instrument which collects both wet and dry precipitation (i.e., a bulk collector) can never give satisfactory data concerning the composition of rain. For accurate assessment of precipitation components, dry deposition must be excluded; i.e., the collector must sample only during a precipitation event.

In a 1975 study, Galloway and Likens concluded that it "is apparent that regardless of the type of bulk collector used, the collection of dry deposition with wet precipitation can severely affect the apparent chemical composition of the rain and snow, sometimes by a factor of two to three." Dry deposition tends to neutralize some of the acidity of wet precipitation by interaction with the dry deposition components. Dry deposition also adds unknown quantities of various anions and cations (Galloway and Likens 1975). This ion contribution should be taken into consideration when evaluating data, particularly old data, since the use of bulk collectors, as was common until recent years, will result in falsely high pH readings. The simple act of filtering a precipitation sample was shown by Kramer (1974) to reduce NO_3^- levels by an order of magnitude.

The materials used in the construction of the collector are also important. Leaching from glass materials results in anomalously high sodium (Na^+), potassium (K^+), and NO_3^- levels, and anomalously high pH values following adsorption of the hydrogen ion (H^+) on the glass (Galloway and Likens 1975). An unknown factor was introduced into the 1932 data of Collison and Mensching by their use of a copper collection vessel and similarly into the 1952 data of Leland by his use of a "metal" collection vessel of unstated composition.

The technique employed in collecting a precipitation sample must also be considered. Even when dry deposition is excluded by opening the collector only during precipitation, a significant difference will frequently be found between samples collected by a vessel opening automatically versus an apparatus opened manually. The manually operated collector generally misses the initial fraction of rain. This is significant, since, as Lodge et al. (1968) have observed, "it is generally found that the highest concentrations of constituents are contained in the first fractions of precipitation to fall." The 1955-56 nationwide study on which the widely published 1955-56 isopleth map is based, employed manually operated collectors (Junge 1958; Junge and Werby 1958); the nationwide study of Lodge et al., on which the 1965-66 map is based, employed automatic collectors.

An additional source of error is introduced by sampling variability, the uncertainty between two samples collected at the same time in adjacent containers, and spatial variability, the uncertainty introduced when the collectors are placed apart (1 to 1000 km). These variabilities for pH were estimated at 0.11 and 0.09, respectively. Galloway (1978) concluded that "it seems doubtful that the reliability of [precipitation] composition data on a spatial scale (50 km in diameter) would be better than 20-60%."

In another study, Karol and Myatch (1958) found a measurement error of 35 to 45 percent when monitoring ionic concentrations in precipitation. Of this, 10 to 15 percent was attributed to instrumental error, the rest to sampling error.

ANALYTICAL UNCERTAINTIES

Several commonly cited studies are purported to substantiate the hypothesis of declining precipitation pH and concurrent increasing NO_3^- levels. Probably the most frequently cited evidence supporting the hypothesis of decreasing pH is the set of three isopleth maps constructed by Cogbill and Likens (1974).

The lack of historical pH data necessitated that the 1955-56 and the 1965-66 maps be based on "predicted" pH's, which were calculated from information about the concentrations of the various ionic species in rainwater. The difference between the sum of the milliequivalents of cations (magnesium, Mg^{++}; Ca^{++}; K^+; and ammonium, NH_4^+) and the sum of the milliequivalents of anions ($SO_4^=$; NO_3^-; and chloride, Cl^-) was assumed to be equal to the number of milliequivalents of H^+. This number was then converted to a pH. After satisfying themselves with the reliability of this method, Cogbill and Likens (1974) proceeded to construct isopleth maps of the eastern U.S., based primarily on historical ionic concentration.

The isopleth map of average pH for 1955-56 was constructed using data (Junge 1958; Junge and Werby 1958) on average ionic concentrations of $SO_4^=$, NO_3^-, Cl^-, Ca^{++}, K^+, and NH_4^+ for 22 collecting stations east of the Mississippi. Since the Junge studies lacked Mg^{++} concentration data, its value was estimated. The uncertainty in this estimated value, along with the 20 to 60 percent error expected for the values of the other ionic components (Galloway 1978), leads to a rather large uncertainty in the final, calculated pH. Additionally, Junge's precipitation collectors were manually operated, and hence, the ionic values undoubtedly contained a low bias.

The isopleth map for 1965-66 depends to a large extent on similarly calculated pH's based on the data of Lodge et al. (1968). Some of the points in the northeast and in North Carolina and Virginia are actually recorded pH's measured by Gambell and Fisher (1966) and Pearson and Fisher (1971).

According to Cogbill (1976), the isopleth map of 1972-73 is based on a Canadian study by Kramer (1974) and on a personal communication (J. Miller). Although the validity of these data could bear review, they seem to represent actually measured pH's. Another isopleth map for 1973 was based on results of a survey conducted by 16,000 high school students at 1100 stations (Current Science 1974); these results have since been widely reproduced (Nisbet 1975).

LONG-TERM STUDY RESULTS

Only a few examples of long-term pH and/or NO_3^- monitoring exist in the eastern U.S. One of these is the Hubbard Brook Experimental station, where monitoring has been continuous from 1964 (Likens et al. 1979). During this time, no significant trend in pH has been observed (Figure 2), even though NO_3^- did increase significantly.

USGS Network Results

Another precipitation network is the U.S. Geological Survey (USGS) water-quality of precipitation network in New York and adjacent Pennsylvania (USGS 1966-1978). The precipitation network was initiated in 1965 and has an extensive data record from 1966 through 1978 for eight stations and data for a ninth (Mineola) from 1966 to 1976 (Figures 3, 4, and 5).

Interpretation of these data must take into account the several changes made in precipitation collection techniques. The collection device used initially in 1965 consisted of a polyethylene funnel and bottle filled with a glass wool plug. Later (1966-76) a glass funnel with a fritted glass filter and a polyethylene bottle was used at the majority of sites. Most recently (1977), a polyethylene funnel with a looped plastic tube leading to a polyethylene bottle has been widely used. The incorporation of glass in some of these collecting devices and the use of the bulk collection method leads to uncertainties in pH and NO_3^- values.

Additionally, the analytical techniques employed have been substantially changed. From the initiation of the network in 1965 through Water Year 1968, NO_3^- was determined by use of the phenoldisulfonic acid method. Since 1969, an autoanalyzer colorimetric technique has been used (D. W. Fisher 1979, personal communication).

We have not found comparative data on the accuracy and precision of these different analytical techniques, despite inquiries of various analysts involved in the analyses during the past 12-year period. Comparative data would be most useful because of a pronounced increase in the magnitude of NO_3^- concentrations for all sites except Albany between Water Years 1968 and 1969.

Analysis of USGS Data--

Some summary statistical results for time trends of pH and NO_3^- and for pH regressed against NO_3^- are shown in Tables 1, 2, 3, and 4. Original data as they came from the USGS were analyzed. Additional analysis was made on data which were adjusted for obvious artifacts caused by contaminated samples or during transposition of data. These values are labeled "adjusted" in the figures.

Time-trend regression analysis of the pH data shows no significant trend for any of the nine sites. A regression analysis of the pooled data results in a line with a slope of -0.015 (original data) or -0.015 (adjusted data), hardly an alarming trend. Time-trend regression analysis of the NO_3^- data shows localized, individual station variability, with a large NO_3^- variability. Use

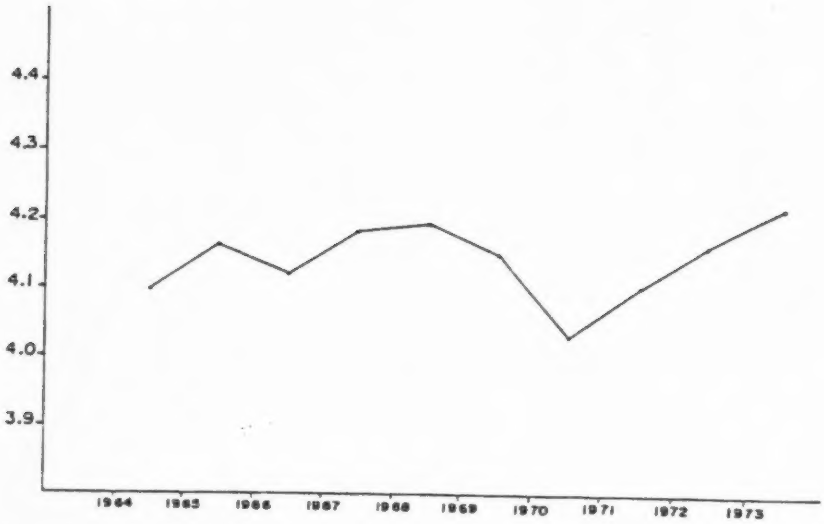

Figure 2. pH of precipitation at Hubbard Brook (Likens et al. 1979).

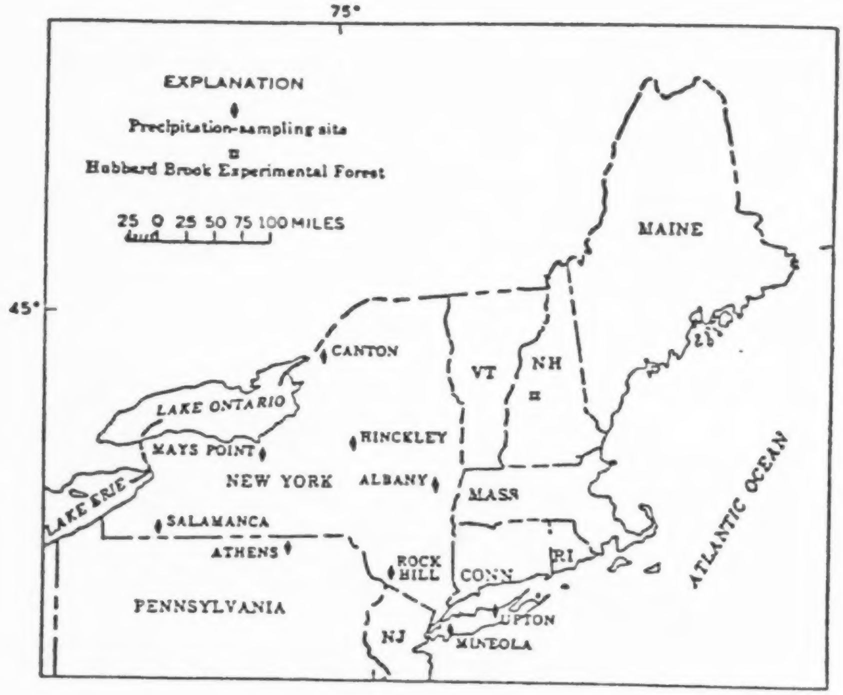
75°
EXPLANATION
Precipitation-sampling site
Hubbard Brook Experimental Forest
25 0 25 50 75 100 MILES
45°
MAINE
CANTON
VT
NH
LAKE ONTARIO
HINCKLEY
MAYS POINT
NEW YORK
ALBANY
MASS
LAKE ERIE
SALAMANCA
ATHENS
ROCK HILL
CONN
RI
ATLANTIC OCEAN
PENNSYLVANIA
UPTON
NJ
MINEOLA

Figure 3. Hubbard Brook precipitation sampling sites.

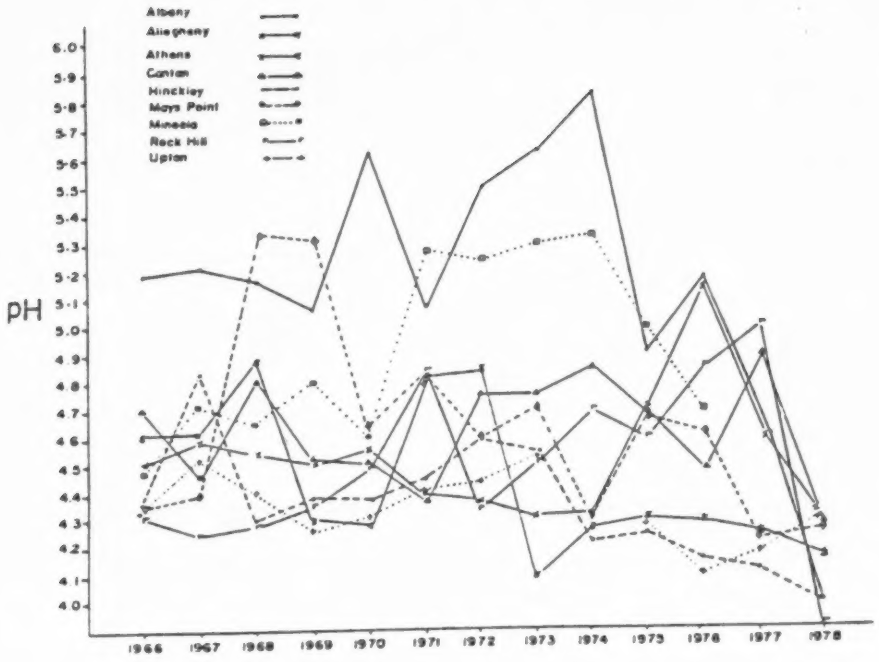

Figure 4. pH of precipitation vs. time at nine New York locations (USGS data base).

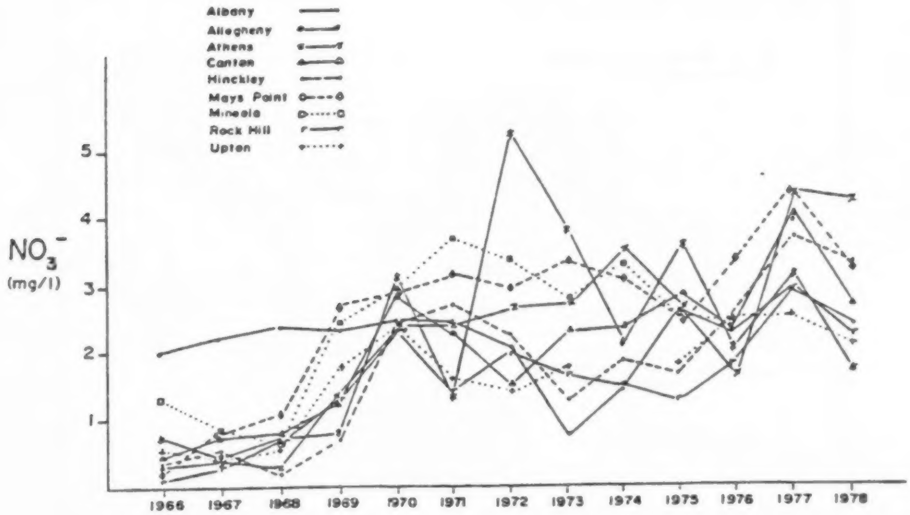

Figure 5. NO_3^- vs. time at nine New York locations (USGS data base).

TABLE 1. pH TRENDS FROM 1966 TO 1978 FOR NINE USGS DATA BASE SITES

Site	Data Set	Slope	r^2
Albany	Original	-0.047	0.174
	Adjusted	-0.041	0.122
Allegheny	Original	-0.045	0.439
	Adjusted	-0.045	0.376
Athens	Original	0.009	0.023
	Adjusted	0.009	0.025
Canton	Original	0.006	0.013
	Adjusted	-0.001	0.000
Hinckley	Original	-0.038	0.446
Mays Point	Original	-0.041	0.183
	Adjusted	-0.039	0.185
Mineola	Original	0.055	0.316
Rock Hill	Original	0.026	0.103
Upton	Original	-0.017	0.301
Average	Original	-0.015	0.023
	Adjusted	-0.015	0.020

TABLE 2. NO_3^- TRENDS FROM 1966 TO 1978 FOR NINE USGS DATA BASE SITES

Site	Data Set	Slope	r^2
Albany	Original	-0.011	0.004
	Adjusted	0.002	0.000
Allegheny	Original	0.160	0.093
	Adjusted	0.177	0.237
Athens	Original	0.544	0.486
	Adjusted	0.290	0.727
Canton	Original	0.213	0.712
Hinckley	Original	0.230	0.665
Mays Point	Original	0.252	0.720
Mineola	Original	0.573	0.462
	Adjusted	0.207	0.432
Rock Hill	Original	0.159	0.617
Upton	Original	0.4	0.616
Average	Original	0.230	0.241
	Adjusted	0.182	0.412

TABLE 3. NO_3^- TRENDS FROM 1969 TO 1978 FOR NINE USGS DATA BASE SITES

Site	Data Set	Slope	r^2
Albany	Original	-0.062	0.047
	Adjusted	-0.016	0.005
Allegheny	Original	-0.085	0.016
	Adjusted	0.029	0.005
Athens	Original	0.497	0.268
	Adjusted	0.213	0.456
Canton	Original	0.153	0.410
Hinckley	Original	0.166	0.367
Mays Point	Original	0.121	0.391
Mineola	Original	0.569	0.249
	Adjusted	-0.038	0.040
Rock Hill	Original	0.079	0.214
Upton	Original	0.049	0.194
Average	Original	0.126	0.045
	Adjusted	0.085	0.087

TABLE 4. NO_3^-/pH RELATIONSHIP FOR THE 13-YEAR, 9-SITE USGS DATA BASE

Location	Type of Data	No. Pairs	r	b
Albany	Original	13	0.27	-0.157
	Adjusted	13	0.40	-0.304
Allegheny	Original	13	0.05	0.006
	Adjusted	13	0.18	-0.036
Athens	Original	13	0.50	0.037
	Adjusted	13	0.28	-0.047
Canton	Original	13	0.18	0.036
	Adjusted	13	0.06	0.012
Hinckley	Original	13	0.53	-0.107
	Adjusted	-	-	-
Mays Point	Original	13	0.25	-0.082
	Adjusted	13	0.26	-0.079
Mineola	Original	11	0.02	0.003
	Adjusted	11	0.73*	0.226
Rock Hill	Original	13	0.36	0.141
	Adjusted	-	-	-
Upton	Original	12	0.65	-0.113
	Adjusted	-	-	-
Overall	Original	13	0.11	0.023
	Adjusted	12	0.04	0.014

*Statistically significant P between 0.05 and 0101.

of only the last 10 years of the data base, and only data generated by the autoanalyzer technique, demonstrates a marginally significant increase in NO_3^- levels. For the pooled data set, a slope of 0.126 is found if the original data are used, and 0.085 if spurious points are left out. The correlations are 0.045 and 0.087, respectively. For the 13-year set, the pooled data show a slope of 0.230 (original data) and 0.182 (adjusted data) with correlations of 0.241 and 0.412, respectively. The regression of pH versus NO_3^-, interestingly enough, shows a statistically significant correlation in only one instance (Mineola), and this is positive (i.e., indicating a rise in pH with increasing NO_3^- concentration). Correlation coefficients for precipitation versus 1) NO_3^-, 2) NH_3, and 3) pH do not indicate strong correlations among the parameters and have not been included here.

MAP3S Results

The Multistate Atmosphere Power Production Pollution Study (MAP3S), since its inception in 1976, has produced enough data for some initial interpretation. Work to date does not yet have sufficient time continuity to detect trends in the data. Galloway and Parker (1979) in the MAP3S progress report for 1977 and 1978, determined that sulfur deposition showed "no apparent geographical trends in the eastern United States," based on compilation of published and unpublished data. The progress report does not comment equally on NO_3^- deposition data.

Dana (1979) noted, on the basis of 2 years of data for 4 sites and 1 year for each of 3 additional sites, that both NO_3^- and NH_3 concentrations are quite uniform. in contrast to the summer peak and winter low pattern for $SO_4^=$. This observation is in apparent contrast with a tentative conclusion by Galloway and Parker (1979), postulating possibly similar scavenging mechanisms for $SO_4^=$ and NO_3^-. They point out that substantial variation of the $SO_4^=/NO_3^-$ ratio is a function of storm, possibly as a difference in origin of the air masses. The authors also concluded that the ratio was less a function of site and precipitation amount than of the individual storm. Scott (1979) observed that, in his studies of scavenging by winter storms, when NO_3^- concentrations are high, $SO_4^=$ concentrations can be either high or low; when NO_3^- concentrations are low, $SO_4^=$ concentrations are also low. Scott concluded that either the removal mechanisms for $SO_4^=$ and NO_3^- are different or that vertical distributions (i.e., source regions) for the pollutants are substantially different. Confirming an earlier study by Scott and Laulainen (1979), Scott found the greatest $SO_4^=$ washout when the precipitation particles grow by riming. The discussions of Scott (1979) and of Gatz and Hales (1979) in the MAP3S progress report indicate that a great deal of work is still needed to resolve the question of scavenging mechanisms for both NO_3^- and $SO_4^=$. The findings of Gatz and Hales tend to support those of Pack (1978) and Miller et al. (1979) that NO_3^- concentrations are related to local source areas rather than being regionally uniform.

ICE-CORE AND BUFFERING-EFFECT ANALYSES

Another approach used to detect pH and $SO_4^=$ trends has been the analysis of ice cores from glaciers. However, this type of analysis is fraught with difficulties. Reports of early snow and ice meltwater having low pH, commonly lower than the pH of bulk snow samples, indicate a partitioning of the strong mineral acids and of acid-dissolved heavy metals (Hagen and Langeland 1973; Hultberg 1977; Jeffries et al. 1979). The environmental consequences of this low pH, relatively heavy-metal-rich meltwater include an early spring shock to aquatic ecosystems, if the meltwater has not been buffered by inorganic and organic soil components prior to reaching water bodies.

In addition to the adverse biotic effect of this phenomenon, the partitioning effect on SO_x and heavy metals can be expected to decrease the total amount of atmospherically-deposited material in snow and ice as they age, thus reducing the certainty of quantitative estimates of anthropogenic--as opposed to natural--loadings of these chemical constituents. Presently, data are not available for tracing increases with time in NO_3^- in snow and ice, but it is reasonable to expect such an increase. The decrease in acidic and acid-soluble components due to partitioning into meltwater would exaggerate the present, apparent increase, which may be caused in part by increasing anthropogenic fossil fuel use. Data from Weiss et al. (1971) and Herron et al. (1977) indicate substantial fluctuations of trace metal and sulfur compound concentrations in ice cores. At present, no basis exists for reconstructing how much of the variation is a result of recrystallization and meltwater history, how much is due to natural variation, and how much is due to anthropogenic additions through time. Furthermore, the physical and chemical aging history of glacial ice will vary according to a number of factors that are a result of the location of the glacier of ice pack. It would not appear that NO_3^- data from ice and aged snow material would provide accurate quantitative data on atmospheric NO_3^- variations, but such data might give a qualitative indication of time trends.

It is important to recognize that various levels of pH buffering and nitrogen uptake will affect acid precipitation in its movement both as surface runoff and, through soil and rock, as ground water. Kramer has recently (1979) testified in Ontario that the buffering that results from carbonate-bearing glacial drift and till can be expected to reduce the originally projected estimates of damage to Canadian Shield lakes by about a factor of four. Data from the eastern United States do not indicate a trend of decreasing stream pH. Buffering in noncarbonate terrain is accomplished by aluminum-bearing silicate minerals, most notably feldspars and clays, and by organic materials.

Although the pattern of acid effects on Adirondack lakes is now emerging, literature on the eastern United States has few data on nutrient uptake from nitrate-rich precipitation or on the buffering effects of soil components. Changing patterns of forest fires, providing carbonate buffering in the upper soil zone, and other land uses are inadequately understood. Literature on vegetation growth effects does not indicate any demonstrated detrimental effects from the NO_3^- component of precipitation.

REFERENCES

Barrett, E., and G. Brodin. 1955. The Acidity of Scandinavian Precipitation. Tellus, 7:251-257.

Bickley, R. I., and V. Vishwanathan. 1979. Photocatalytically Induced Fixation of Molecular Nitrogen by near UV Radiation. Nature, 280:306-309.

Bremmer, J. M., and D. W. Nelson. 1968. Chemical Decomposition of Nitrite in Soils. 9th International Congress of Soil Sciences Trans., 2:495-503.

Chameides, W. L. 1979. Fate of NO_x in the Atmosphere and Implications for Tropospheric and Stratospheric Modifications. Proceedings of the Technical Symposium on Implications of a Low NO_x Vehicle Emission Standard, J. Romanovsky, Project Officer. Prepared by Ebon Research Systems, Reston, Virginia. U.S. Environmental Protection Agency, Ann Arbor, Michigan.

Chameides, W. L., D. H. Stedman, R. R. Dickerson, D. W. Rusch, and R. J. Cicerone. 1977. NO_x Production in Lightning. J. Atmos. Sci., 34:143-149.

Chemical and Engineering News. 1978. Desert Sands Catalyze Ammonia Formation. Chem. Eng. News, November 13, p.7.

Cogbill, C. V. 1976. The History and Character of Acid Precipitation in Eastern North America. Proceedings of the First International Symposium on Acid Precipitation and the Forest Ecosystem. Columbus, Ohio, May 12-15, 1975.

Cogbill, C. V., and G. E. Likens. 1974. Acid Precipitation in the Northeastern United States. Water Resources Res., 10:1133-1137.

Collison, R. C., and J. E. Mensching. 1932. Lysimeter Investigations--Composition of Rainwater at Geneva, New York, for a Ten-year Period. Tech. Bull., 193. New York State Agriculture Experiment Station, Geneva, New York.

Current Science. 1974. Acid Rain in the United States. Current Sci., 59:1.

Dana, M. T. 1979. The Multistate Atmospheric Power Production Pollution Study--MAP3S Progress Report for FY 1977 and FY 1978. M. C. MacCracken, Coord. U. S. Department of Energy, Washington, D.C. 404 p.

Friend, J. P. 1973. The Global Sulfur Cycle. In: Chemistry of the Lower Atmosphere, S. I. Rassol, ed. Plenum Press, New York, pp. 177-202.

Galloway, J. N. 1978. The Collection of Precipitation for Chemical Analysis. Tellus, 30:71.

Galloway, J. N., and G. E. Likens. 1975. Calibration of Collection Procedures for the Determination of Precipitation Chemistry. Proceedings of the First International Symposium on Acid Precipitation and the Forest Ecosystem. Columbus, Ohio, May 12-15, 1975.

Galloway, J. N., and G. G. Parker. 1979. The Multistate Atmospehric Power Production Pollution Study--MAP3S Progress Report for FY 1977 and FY 1978. M. C. MacCracken, coord. U.S. Department of Energy, Washington, D.C. 404 p.

Gambell, A. W., and D. W. Fisher. 1966. Chemical Composition of Rainfall--Eastern North Carolina and Southeastern Virginia. Water Supply Paper 1535-K, U.S. Geological Survey.

Gatz, D. E., and J. M. Hales. 1979. The Multistate Atmospheric Power Production Pollution Study--MAP3S Progress Report for FY 1977 and FY 1978. M. C. MacCracken, coord. U. S. Department of Energy, Washington, D.C. 404 p.

Granat, L., J. Rodhe, and R. O. Hallberg. 1976. The Global Sulphur Cycle. In: Nitrogen, Phosphorus and Sulphur--Global Cycles. B. H. Svensson and R. Soderlund, eds. SCOPE Report 7, Swedish Natural Science Research Council (NFR), Stockholm, Sweden, pp. 89-134.

Hagen, A., and A. Langeland. 1973. Polluted Snow in Southern Norway and the Effect of the Meltwater on Freshwater and Aquatic Organisms. Environ. Pollut., 5:45-57.

Herron, M. L., C. C. Longway, Jr., H. V. Weiss, and J. H. Crogin. 1977. Atmospheric Trace Metals and Sulfate in the Greenland Ice Sheet. Geochim. Cosmochim. Acta, 41:915-920.

Hultberg, H. 1977. Thermally Stratified Acid Water in Late Winter--A Key Factor Inducing Self-Accelerating Processes Which Increase Acidification. Water Air Soil Pollut., 7:279-294.

Jeffries, D. S., C. M. Cox, and P. J. Dillon. 1979. The Depression of pH in Lakes and Streams in Central Ontario During Snowmelt. Technical Report LTS79-1, Ontario Ministry of the Environment.

Johnson, M. 1978. Natural Water Quality. Botany Bay Project Working Paper 4, Australia.

Junge, C. E., 1958. The Distribution of Ammonia and Nitrate in Rainwater over the United States. Trans. Amer. Geophys. Union, 39:241-248.

Junge, C. E., and R. T. Werby. 1958. The Concentration of Chloride, Sodium, Potassium, Calcium, and Sulfate in Rain Water Over the United States. J. Meteorol., 15:417.

Karol, I. L., and L. T. Myatch. 1958. The Concentration of Chloride, Sodium, Potassium, Calcium, and Sulfate in Rain Water over the United States. J. Meteorol., 15:417.

Kerr, R. A. 1979. Global Pollution: Is the Arctic Haze Actually Industrial Smog? Science, 205:290-293.

Kramer, J. R. 1974. Atmospheric Loadings of the Upper Great Lakes. Acres Consulting Services. Prepared for the Canada Center for Inland Waters. p. 42

Kramer, J. R. 1979. Testimony Before the Standing Resources Development Committee of the Legislative Assembly of the Province of Ontario, February.

Leland, E. W. 1952. Nitrogen and Sulfur in Precipitation at Ithaca, NY. Agron. J., 44:172.

Lerman, A. 1979. Geochemical Processes: Water and Sediment Environments. Wiley-Interscience, New York. p. 481.

Likens, G. E., F. H. Bormann, and J. S. Eaton. 1979. Variations in Precipitation and Streamwater Chemistry at the Hubbard Brook Experimental Forest During 1964 to 1977. In: Proceedings from the NATO Advanced Research Institute on Effects of Acid Precipitation on Terrestrial Ecosystems. University of Toronto, Canada. In press.

Lodge, J. P., Jr., K. C. Hill, H. B. Pate, E. Lorange, W. Basbergill, A. L. Lazrus, and G. S. Swanson. 1968. Chemistry of United States Precipitation, Final Report, National Center for Atmospheric Research, Boulder, Colorado.

Miller, M. L., A. G. Everett, C. Sullivan, and W. F. Thall. 1979. A review of EPA's Comments on Acid Precipitation in Chapter 9, Nitrogen Oxides Criteria Document Draft, November 1978. Report to the American Petroleum Institute.

National Academy of Sciences (Panel on Nitrates of the Coordinating Committee for Scientific and Technical Assessments of Environmental Pollutants, Environmental Studies Board, National Research Council). 1978. Nitrates: An Environmental Assessment. National Academy of Sciences, Washington, D.C.

Nisbet, I. C. T. 1975. Sulfates and Acidity in Precipitation. Air Quality and Stationary Source Emission Control. A report prepared by the Commission on Natural resources, National Academy of Sciences, for the Committee on Public Works, U.S. Senate, 94th Congress, 1st Session. Committee Serial 94-4. U.S. Government Printing Office, Washington, D.C.

Noxon, J. F. 1978a. Nitrogen Dioxide in the Stratosphere and Troposphere Measured by Ground-Based Absorption Spectroscopy. Science, 189:547-549.

Noxon, J. F. 1978b. Stratospheric NO_2 in the Antarctic Winter. Geophys. Res. Lett., 5(12):1021-1022.

Pack, D. W. 1978. Sulfate Behavior in Eastern U.S. Precipitation. Geophys. Res. Lett., 5:673-674.

Pearson, F. J., and D. W. Fisher. 1971. Chemical Composition of Atmospheric Precipitation in the Northeastern United States. Water Supply Paper 1535-P, U. S. Geological Survey.

Robinson, E., and R. C. Robbins. 1971. Emissions, Concentrations and Fate of Atomospheric Precipitation in the Northwestern United States. In: Air Pollution Control, Part II, W. Strauss, ed. John Wiley and Sons, New York. pp. 1-93.

Scott, B. C. 1979. The Multistate Atmospheric Power Production Pollution Study--MAP3S Progress Report for FY 1977 and FY 1978. M. C. MacCracken, coord. U. S. Department of Energy, Washington, D.C. 404 p.

Scott, B. C., and N. S. Laulainen. 1979. On the Concentration of Sulfate in Precipitation. J. Appl. Meteorol., 18:138-147.

Turman, B. N. 1979. Lightning Detection from Space. Amer. Sci., 67:321-329.

USGS. 1966-1978. Water Resources Data for New York. Water-Data Reports for Water Years 1966-1978. U. S. Geological Survey, Albany, New York.

Viemeister, P. E. 1960. Lightning and the Origin of Nitrates Found in Precipitation. J. Meteorol., 17:681-683.

Visser, S. 1961. Chemical Composition of Rain Water in Kampala, Uganda, and Its Relation to Meteorological and Topographical Conditions. J. Geophys. Res., 66:3759-3765.

Weiss, H. V., M. Koide, and E. D. Goldberg. 1971. Selenium and Sulfur in a Greenland Ice Sheet: Relation to Fossil Fuel Combustion. Science, 172: 261-263.

AQUEOUS PHASE NO_x PROCESSES IN THE ATMOSPHERE

An Informal Presentation by

Stephen E. Schwartz
Environmental Chemistry Division
Brookhaven National Laboratory
Upton, New York 11973

Ongoing investigations for the Federal Aviation Administration (FAA) High Altitude Pollution Program (HAPP), dealing with aqueous phase processes, are described. Of specific concern are rainout and washout of nitrogen oxides and oxyacids, processes that impact upon removal of these species from the atmosphere, upon partition of these compounds into the aqueous phase, or upon any chemical transformations that may be taking place in the aqueous phase.

The species and processes and equilibria with which we are concerned are summarized in Figure 1. Below the dotted line on this figure is aqueous phase; above is the gas phase. The gas phase species of initial concern are NO and NO_2. In addition, the compound oxides are important to laboratory and, to a certain extent, atmospheric studies--for example, N_2O_5. Also, one has the oxyacids--nitrous acid and nitric acid. Each of these gaseous species is related by a Henry's Law coefficient to the corresponding aqueous phase species listed below the dotted line. Chemical equilibria relate these species in the gas phase and in the aqueous phase; additionally, the acid dissociation equilibria play a major role.

We have been addressing some of the chemical kinetics and chemical equilibria, chemical thermodynamics, relating these species in gas and aqueous phases. (In this phase of the work, we've been joined by Warren White). In our literature review, much information, some of it quite old, has been found applicable.

The well known equilibria are, first of all, the gas phase equilibria, and and, secondly, the overall mixed phase equilibria that include NO, NO_2, down to nitrous and nitric acid. What are not so well known are the Henry's Law coefficients relating these species, principally, NO_2. The NO Henry Law's coefficient is well known. Also not well established are the aqueous phase equilibria relating these.

Before solubility of a species--of one of the nitrogen oxides or oxyacids--is discussed, the term solubility should be defined. One can have a nonreactive solubility which is the Henry's Law coefficient. One can have acid dissociation, for example, with the nitrous and nitric acids. One can have reactive solubility, which is the overall solubility equilibrium illustrated in Figure 1.

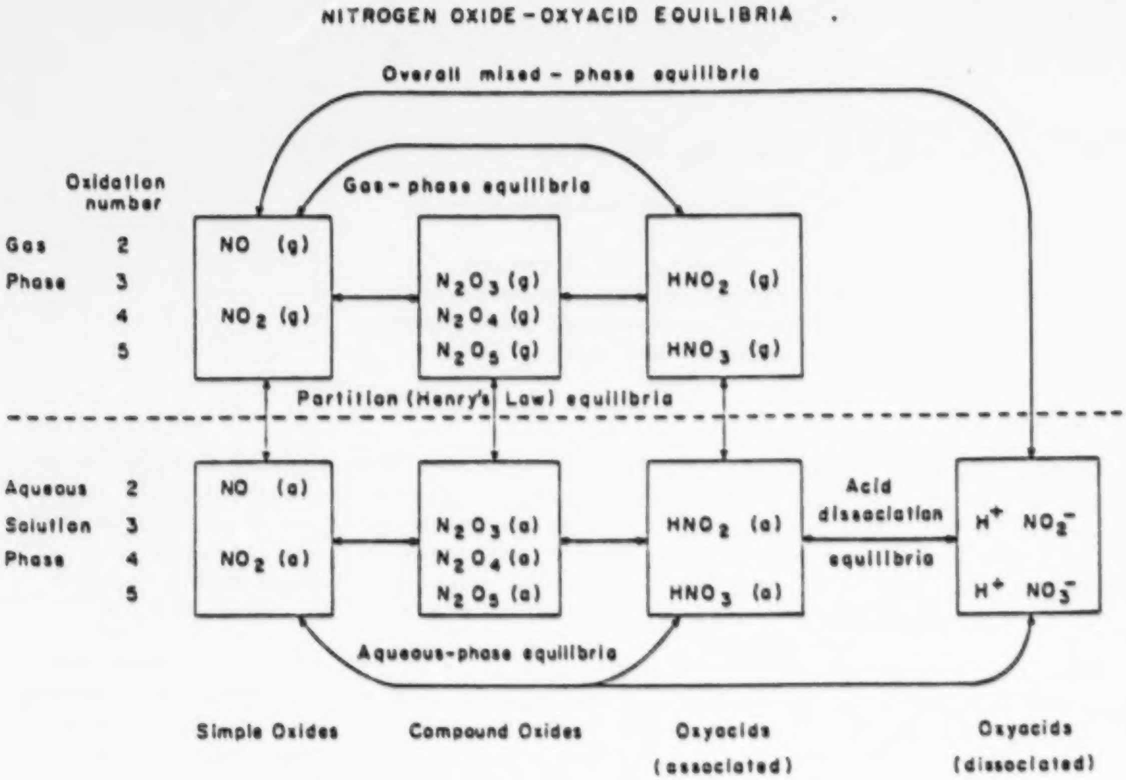
NITROGEN OXIDE-OXYACID EQUILIBRIA
Overall mixed-phase equilibria
Gas-phase equilibria
Oxidation number
Gas
Phase
2
3
4
5
NO (g)
NO_2 (g)
N_2O_3 (g)
N_2O_4 (g)
N_2O_5 (g)
HNO_2 (g)
HNO_3 (g)
Partition (Henry's Law) equilibria
Aqueous
Solution
Phase
2
3
4
5
NO (a)
NO_2 (a)
N_2O_3 (a)
N_2O_4 (a)
N_2O_5 (a)
HNO_2 (a)
HNO_3 (a)
Acid dissociation equilibria
H^+ NO_2^-
H^+ NO_3^-
Aqueous-phase equilibria
Simple Oxides
Compound Oxides
Oxyacids (associated)
Oxyacids (dissociated)

Figure 1. Summary of nitrogen oxide and oxyacid species, processes, and equilibria that occur in gas phase (above) and aqueous phase (below).

One speaker yesterday mentioned expected parallelism between, say, NO_2 and SO_2, and some of the aqueous phase chemistry. Actually a tremendously big difference exists between aqueous phase NO_2 and SO_2 behavior. SO_2 is the anhydride of sulfurous acid, which undergoes acid dissociation and is highly soluble; NO_2 by contrast, must undergo redox reaction to become one of the oxyacids.

The Henry's Law coefficients in Table 1 were chosen to express the concentration (C) of the aqueous phase, which is equal to a proportionality constant called H times partial pressure in the gas phase; this constant has units molar per atmosphere.

Listed in Table 1 are some of the numbers that are well known; SO_2 and O_3 are included for comparison. It's interesting to look at any of these Henry's Law coefficients as a function of physical properties, because the Henry's Law coefficient, in the absence of a chemical interaction, is a physical interaction between the solute and water.

TABLE 1. AQUEOUS PHASE CONCENTRATIONS USING HENRY'S LAW COEFFICIENTS*

Molecule	H	f_a† ($L = 10^{-6}$)‡
NO	1.9×10^{-3}	8×10^{-8}
HNO_2	54	
HNO_3	2.1×10^{5}	
NO_2	$\sim 4 \times 10^{-2}$??	1.6×10^{-6}
N_2O	2.5×10^{-2}	
CO_2	3.4×10^{-2}	

*$C = Hp$; $[H] = M\ atm^{-1}$.
†f_a = fraction of molecules in the aqueous phase.
‡L = liquid water volume fraction of a cloud.

In plotting this coefficient against, of all things, the boiling point of the gas (Figure 2), one finds a very good correlation for gases of similar kinds of properties. (Hydrocarbons, fluorocarbons, etc., must be excluded from this kind of plot.) Comparison of this unexpected quantity, the normal boiling

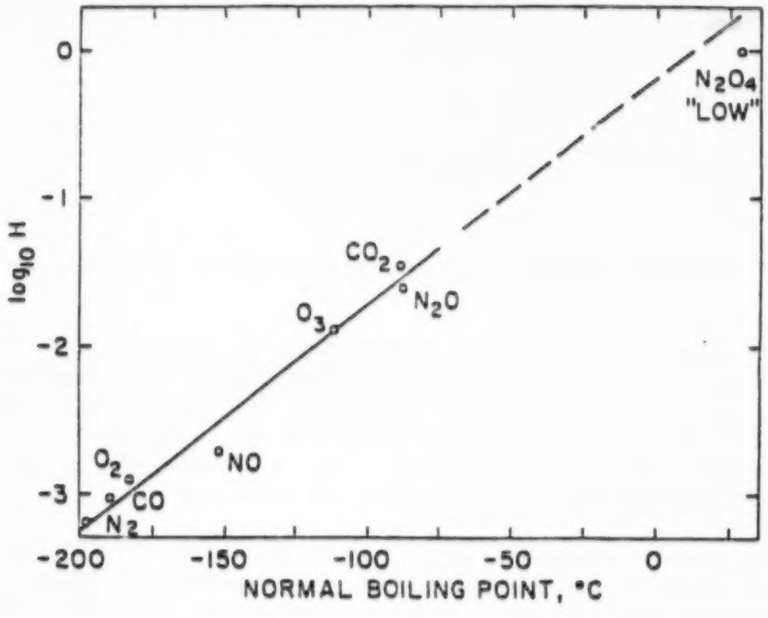

Figure 2. Henry's Law coefficient vs. normal boiling point for various gases.

point, shows O_3, CO_2, and N_2O clustered very closely; in this region, about 10^{-2} for a Henry's Law coefficient, we would expect to find NO_2 a priori, unless some specific chemical interaction interferes. That possibilty will be discussed later.

The solubility process for nitric acid is dominated by the acid dissociation constant. That solubility process is addressed in the plot of Figure 3.

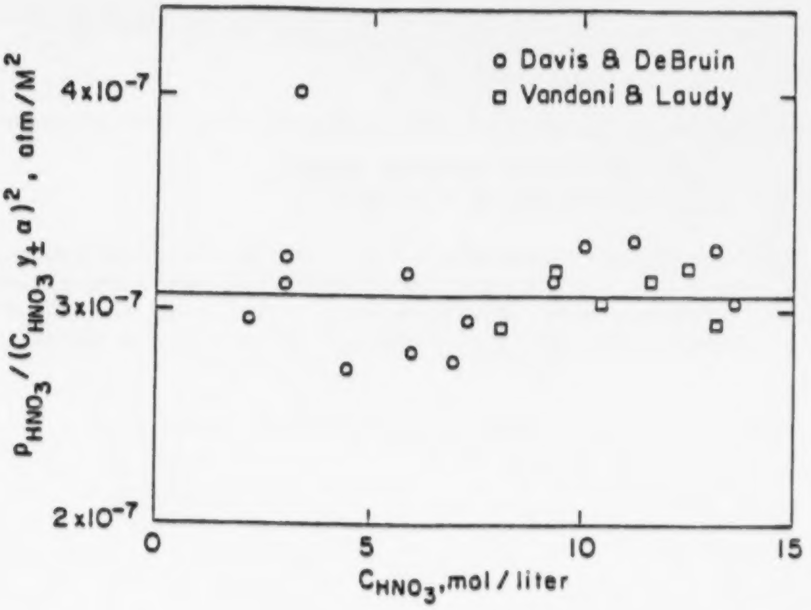

Figure 3. Partial pressure of nitric acid above a dilute solution.

The ratio of the partial pressure of nitric acid to the activity (the product of hydrogen ion times nitrate) spans about four orders of magnitude; this method of plotting yields a number of about 3×10^{-7} atm/M^2 as a partial pressure of nitric acid above a dilute solution, a number that's rather independent of nitric acid concentration. The squared power in this number results from multiplying the nitrate times the hydrogen ion.

That is the number extrapolated to dilute solution, and activity corrections were used in this plotting. For concentrations above 10^{-2} molar, activity corrections would be desirable, to the extent that data are available. They're available for pure nitric acid; for mixed solutions, new measurements would be required.

Figure 4 introduces one further concept that we have investigated--the partial pressure of nitric acid, say 1 ppb, what is the corresponding aqueous phase at a given concentration of nitric acid? Maintaining this concentration at 1 ppb, water is present in equilibrium; that concentration is about 10^{-1} molar nitric acid. Since nitric acid is very soluble, if water is present, the equilibrium is very much on the side of dissolved nitric acid.

ACID DISSOCIATION

$$HNO_{3\,(g)} = H^+ + NO_3^-$$

$$K = \frac{[H^+]\,[NO_3^-]}{P_{HNO_3}} = 3.26 \times 10^6\ M^2\ atm^{-1}$$

$$\text{for } P_{HNO_3} = 10^{-9}\ atm$$

$$C_{HNO_3} = 5.7 \times 10^{-2}\ M$$

$$\text{for } L = 10^{-6} \quad (1\ gm\ H_2O_{(l)}/m^3)$$

$$f_g = 4.3 \times 10^{-4}$$

Figure 4. Partial pressure of nitric acid at 1 ppb.

If we consider a cloud with a liquid water loading of 10^{-6}, or 1 g/m^3 of water content, and we turn on that phase equilibrium in such a cloud with 1 g/m^3 liquid water, the fraction of nitric acid remaining in the gas phase is of the order of 10^{-3}, a number that corresponds to these conditions. That number will change somewhat as the nitric acid gets more concentrated, and it is based upon holding the nitric acid at 10^{-9} atm and letting this climb to whatever equilibrium value it will reach.

FRIEDLANDER: What pH--well, I mean, there's no chloride in the equilibrium here; you don't take that into account?

SCHWARTZ: That will become relevant at lower concentrations. Figure 5 deals with your question. Pure nitric acid and nitric acid as a function of various pH values are shown. Calculations have been made for the partial pressure of nitric acid, above a specified concentration of nitric acid at various pH conditions. For instance, with a 10^{-3} nitrate concentration in a pH 5 solution, 10^{-14} atm nitric acid would be in equilibrium in that solution. In the context of this high solubility of nitric acid, some of the work that we've heard about at this workshop has new relevance.

Nitrous acid is a different kettle of fish (Figure 6). It's much less soluble. It's a weak acid. Henry's Law coefficient is quite different, indicating much less chemical interaction with water.

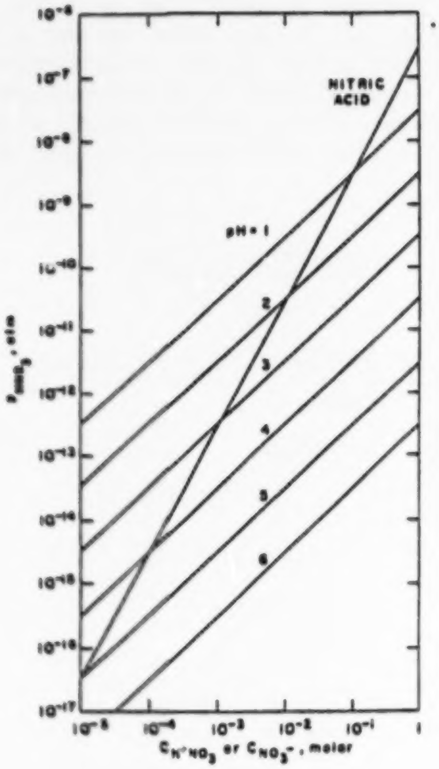

Figure 5. Partial pressure of nitric acid, above a specified concentration, as a function of various pH values.

HNO_2

WEAK ACID, pK = 3.3

SUBSTANTIAL VAPOR PRESSURE
AT LOW CONCENTRATION

for $P_{HNO_2} = 10^{-9}$ atm

$C_{HNO_2} + C_{NO_2^-} = 5 \times 10^{-6}$ M

for $L = 10^{-6}$ $\qquad f_g = 0.72$

Figure 6. Nitrous acid characteristics.

Figure 7, for nitrous acid, is similar to the figure (Figure 5) we've just seen for nitric acid. A given formal nitrite concentration is shown as a function again of pH, or as a function of nitrous acid for the pure solution, in order to address the partial pressure. Here, for example, 10^{-4} molar pure nitrous acid would result in a slightly greater than 100 ppb nitrous acid concentration equilibrium with water, so it's much less soluble. Alternatively stated, nitrous acid exerts a much greater vapor pressure than does nitric acid above the same concentration aqueous solution.

Briefly, these are the gas phase equilibria relating the nitrogen oxides and oxyacids:

$$NO + NO_2 + H_2O = 2HNO_2(g) \qquad (1a)$$

$$3\ NO_2 + H_2O = 2HNO_3(g) + NO \qquad (1b)$$

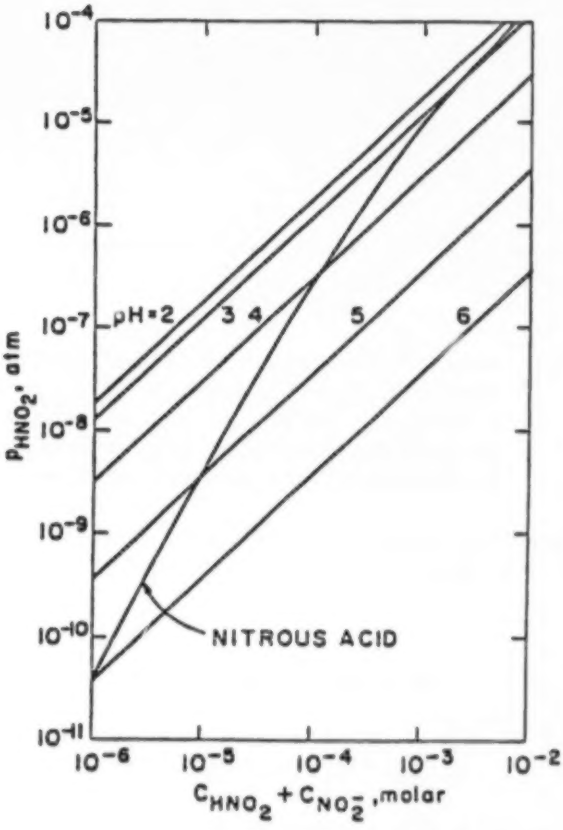

Figure 7. Partial pressure of nitrous acid as a function of pH (or of nitrous acid for the pure solution) for given nitrate concentrations.

These processes are rather well understood. They are our vehicle to address the overall mixed-phase equilibrium, which is of more interest and concern.

Figure 8 depicts one discrepancy in the literature that is concerned with free energy formation of nitrous acid in the gas phase. This discrepancy is between NBS 1968 (I think it's 270-3) data and the JANAF tables, the two primary literature sources, and we selected the NBS number.

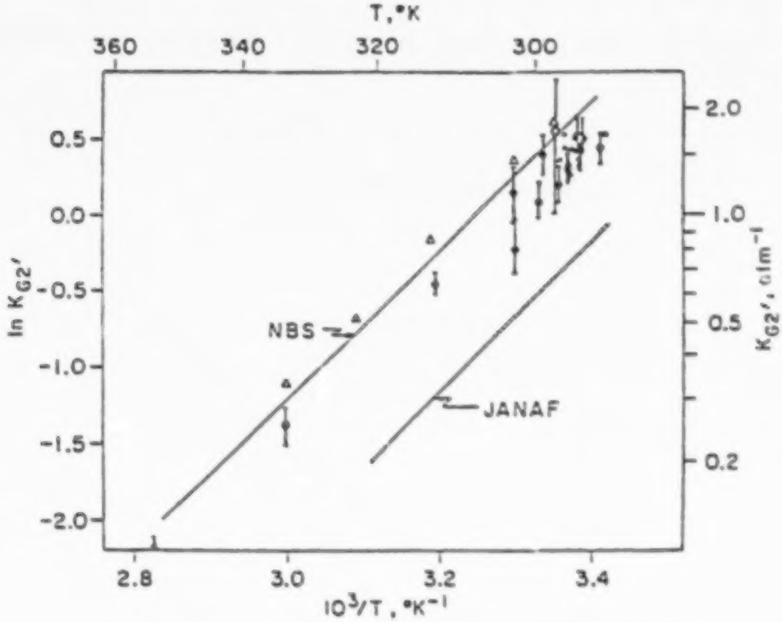

Figure 8. Plot of literature data for equilibrium constant $K_{G2'}$, of reaction $NO_{(g)} + NO_{2(g)} + H_2O_{(g)} = 2HONO_{(g)}$, and of values computed from tabulated free energies of formation of the several species.

Those data are combined with the solubility equilibria of nitrous acid and of nitric acid to get the mixed-phase reactive solubility equilibria for NO and NO_2:

$$NO + NO_2 \overset{W}{=} 2HNO_2(a) \qquad (2a)$$

$$3\ NO_2 \overset{W}{=} 2H^+ + 2NO_3^- + NO \qquad (2b)$$

One can think of these--NO + NO_2 giving twice nitrous, or thrice NO_2 giving twice nitric + NO--as the two equilibria that will lead to solubility of one or the other.

One can then use those numbers in two important contexts. One context is that of measurements that have been made on Whiteface, for example, by Mohnen and coworkers of the New York State Department of Environmental Conservation. These investigators report pH values in the 2's, and certainly less than 3, in fog water rising over their mountain-top device. Such low pH's are of great concern.

In a second context, Figure 9 addresses NO_2/NO ratios as the formal concentration of nitrous acid in equilibrium with a specified value of partial pressure of NO_2. These are equilibrium concentrations, however, and this equilibrium is not necessarily turned on; we must account for the chemical kinetics and requisite time for achieving this equilibrium.

The second equilibrium (Equation 2b) describes production of nitric acid and the much greater solubility of nitric acid versus nitrous acid. Comparison of Figure 10 with Figure 9 shows that production of nitric acid, rather than nitrous acid, yields a much more concentrated solution. For instance, at 10^{-9} atm, i.e., 1 ppb NO_2, and NO = NO_2, one has an equilibrium nitric acid concentration of approximately 3×10^{-2} molar, if equilibrium is in effect. However, as we shall see, the chemical kinetics will govern whether these equilibria are established.

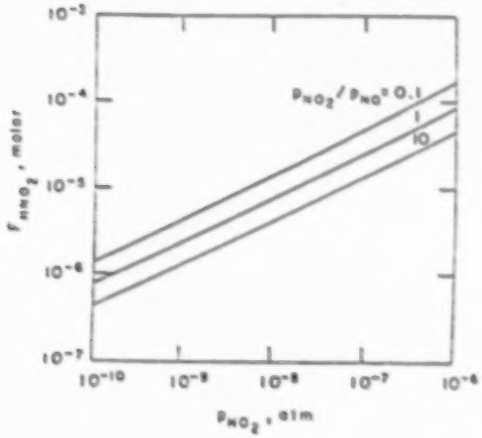

Figure 9. NO_2/NO ratio, or the formal concentration of nitrous acid in equilibrium with specified values of the partial pressure of NO_2, for indicated values of P_{NO_2}/P_{NO}.

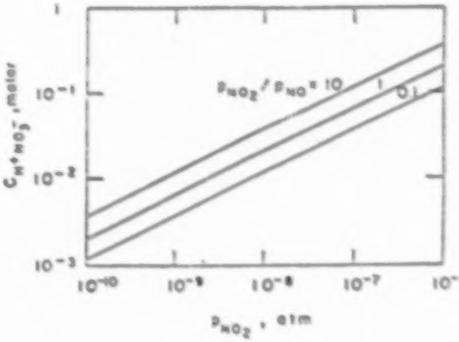

Figure 10. Concentration of nitric acid at various values of the partial pressure of NO_2, for indicated values of P_{NO_2}/P_{NO}.

Figure 11 depicts some relationships that are possibly relevant to some processes taking place in smog chambers and in the atmosphere. The partial pressure of nitric acid, or gas phase NO_2, is plotted against various equilibrium nitric acid concentrations. This pattern reflects a means of regenerating NO_2 from nitric acid. For example, a 10^{-3} molar nitric acid concentration producing that equilibrium, or an NO partial pressure of 10^{-8}, corresponds to about 1 ppb NO_2 that will be evolved with the more concentrated acids, such as in an aerosol--e.g., 10^{-2} molar, 10^{-1} molar. This NO_2 concentration in equilibrium with that nitric acid becomes increasingly high, much higher than the partial pressure of nitric acid. The HNO_3 partial pressure will exceed the NO_2 partial pressure only in rather concentrated acid solution.

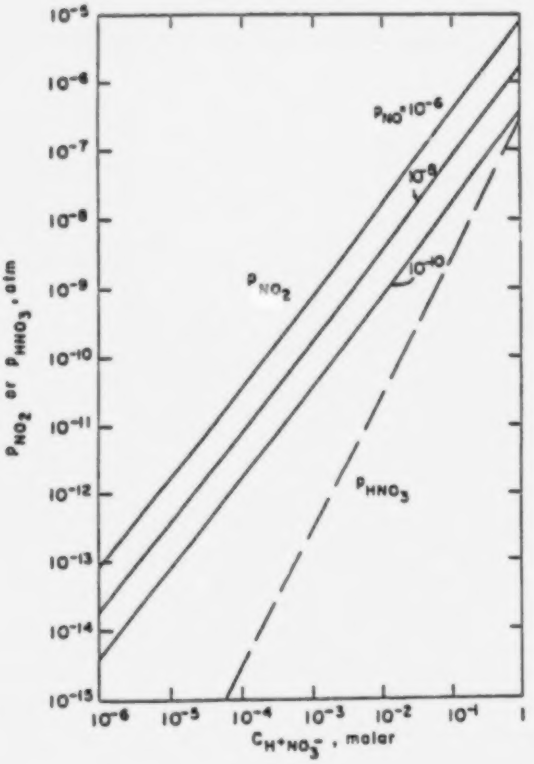

Figure 11. Partial pressure of gas phase NO_2, or HNO_3, at various equilibrium nitric acid concentrations.

We wanted to address as well the Henry's Law coefficient of NO_2 in particular, insofar as it plays a role in kinetic studies. Figure 12 displays a set of thermochemical cycles that we've been examining in order to address the Henry's Law coefficient of NO_2, of N_2O_3, of N_2O_4, of nitrous acid. Gas phase equilibria are above, aqueous phase equilibria below. The solid lines are numbers that we consider well known. The dashed lines represent numbers that were found somewhere in the literature but that are not well known; these numbers contain contradiction. Dotted lines represent processes for which no direct information or source is available.

Using the information of Figure 12, the Henry's Law coefficient was calculated for NO_2 by one or another route. One number gives us about 10^{-2} molar per atmosphere, as expected; the other number is about a factor of 70 higher. We anticipated that the discrepancy lay in this equilibrium, the dehydration of nitrous acid to form N_2O_3 in aqueous phase. Upon remeasuring this one in the laboratory, we get a number, which then leads to Henry's Law coefficient of NO_2 of about 10^{-2} molar per atmosphere, as we expect. So that aspect of it has been cleared up.

Concluding, now, on the chemical thermodynamics: Nitric acid is very soluble; nitrous acid is moderately soluble. NO_2 is sparingly soluble by the Henry's Law ($H \approx 1 \times 10^{-2}$ M atm $^{-1}$), which we expect to be rapid, very soluble by reaction. Solubility depends on the kinetics.

Many studies of the chemical kinetics of the reactive uptake of nitrogen oxides by aqueous solution have been conducted, motivated in part by nitric acid manufacture. These studies can be classfied by approach: i.e., direct absorption ($NO_2(g) + H_2O(l)$) studies; or indirect (nitrous acid decomposition) studies in 1928-30, by Abel and Schmid--excellent, first-rate kinetics; also, some pulse radiolysis measurements of aqueous phase reaction rates have been achieved; those measurements coupled with the Henry's Law coefficient will provide the desired number. So there are three approaches on that.

The mechanism of the chemical kinetics includes hydration of NO_2, a slow step involving twice NO_2, which gives nitrous and nitric acids. It's this slow step which is going to govern the overall kinetics. The mechanisms shown in Figure 13 describe a phase-mixed system, with all of the Henry's Law equilibria occurring. Conditions where chemical kinetics dominate cannot always be achieved in the laboratory studies.

The rate law that one expects based upon those kinetics is represented in Figure 14. Important to note is that it's second order rate law and partial pressure of NO_2; also, a large extrapolation is made, from tenths of atmospheres, based on results of laboratory kinetic studies. As this number is used in extrapolating down to low concentrations characteristic of the ambient atmosphere, a half-time is found for NO_2 removal. In a cloud with a liquid water content of 10^{-6}, or 1 g/m^3, that removal rate is about 3 months at 1 ppm.

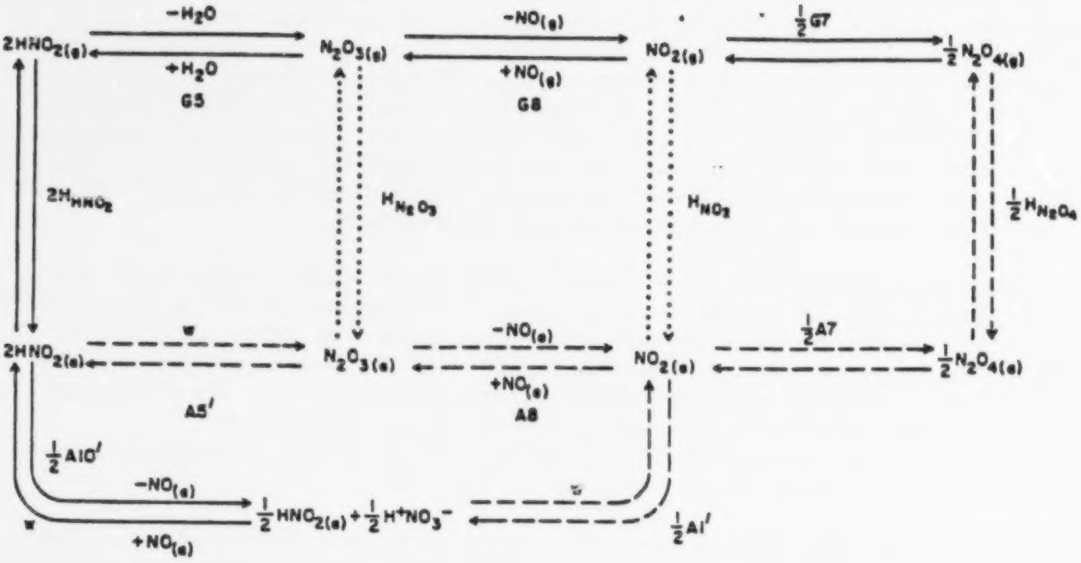

2HNO2(g)
−H2O
+H2O
G5
N2O3(g)
−NO(g)
+NO(g)
G8
NO2(g)
1/2 G7
1/2 N2O4(g)
2H_HNO2
H_N2O3
H_NO2
1/2 H_N2O4
2HNO2(a)
w
A5′
N2O3(a)
−NO(a)
+NO(a)
A8
NO2(a)
1/2 A7
1/2 N2O4(a)
1/2 A10′
−NO(a)
+NO(a)
w
1/2 HNO2(a) + 1/2 H+NO3−
1/2 A1′

Figure 12. Thermochemical cycles and Henry's Law coefficient of HNO_2, N_2O_3, NO_2, and N_2O_4.

MECHANISM

- Phase Mixed System
- $P_{NO_2} \gtrsim 0.01$ atm

$$
\begin{array}{lll}
(4) & NO_{2\,(g)} & \overset{1}{=} NO_{2\,(a)} \\
(2) & 2\,NO_{2\,(a)} & \xrightarrow{2} HNO_2 + H^+ + NO_3^- \text{ slow} \\
(1) & 2\,HNO_2 & \xrightarrow{3} NO_{2\,(a)} + NO_{(a)} \\
(1) & NO_{2\,(a)} & = NO_{2\,(g)} \\
(1) & NO_{(a)} & = NO_{(g)} \\
\hline
 & 3\,NO_{2\,(g)} & = 2H^+ + 2NO_3^- + NO_{(g)}
\end{array}
$$

Figure 13. Mechanism describing a phase mixed system, inferred from studies with $P_{NO_2} > 0.01$ atm.

$$\text{Rate} \equiv \tfrac{1}{2} \frac{d[NO_3^-]}{dt}, \quad M\ sec^{-1}$$

$$\text{Rate} = \tfrac{1}{2} k_2 [NO_2]^2 \ (a)$$

$$= \tfrac{1}{2} k_2 H^2{}_{NO_2}\ P^2{}_{NO_2}$$

$$\text{Rate}'\ (atm\ sec^{-1}) = (LRT)\ \text{Rate}$$

P_{NO_2}, atm	$\tau_{1/2}\ (NO_2)$, sec	$(L = 10^{-6})$
10^{-6}	6.8×10^{6}	= 3 months
10^{-7}	6.8×10^{7}	= 2 years
10^{-8}	6.8×10^{8}	
10^{-9}	6.8×10^{9}	
10^{-10}	6.8×10^{10}	

cf $\tau = 10^5$ sec for $OH + NO_2$ @ $[OH] = 10^6\ cm^{-3}$

Figure 14. Second-order rate law and partial pressure of NO_2.

This second-order rate law was investigated further in the laboratory to find if it holds at parts per million concentration. It does not. What we find is a first-order rate law:

$$2NO_2(g) \xrightarrow{w} H^+\ NO_3^- + H^+\ NO_2^-$$

If the rate = k P_{NO_2},

$$k = 2 \times 10^{-3}\ M\ atm^{-1}\ sec^{-1}$$

We put that into the number and find that still it's slow; with a liquid water content of 10^{-6}, $\tau = 10^7$ sec = 4 months. That is a 1/e time period for removal of NO_2 in cloud water, by a process involving only reaction of NO_2 in that water with NO_2 and with other reaction products, oxygen included, and other species excluded.

BUFALINI: My comment concerns reaction products, as measured by Greg Kok, as well as by our group. Assuming you're to extrapolate as to rain, or formation of rain droplets, or something like that, we find a tremendous amount of H_2O_2. So it would seem to me that--

SCHWARTZ: I agree. I think that's crucial. Those are obviously the kinetic studies to be done. We've addressed it as a function of the presence of oxygen; oxygen, itself, makes no difference. I just have to emphasize that--the importance of the chemical kinetics. One can make thermodynamic calculations for N_2 and O_2 in their atmospheric concentrations, and ask what's the nitric acid concentration equilibrium with that? It's 10^{-1} molar. So, the question is, how long does it take for this equilibrium to get turned on?

The presence of oxygen does not enhance the rate of NO_2 uptake. However, there remain other possible reaction paths that must be investigated.

- Transition metal catalysts
- Oxidants--H_2O_2 and ozone
- Reductants--SO_2 (somebody has mentioned a study indicating the participation of nitrous acid as an oxidizing agent, oxidizing SO_2)
- Rate of back reaction in concentrated solutions that may be back-liberating NO_2.

This concludes my presentation. Thank you.

WILSON: Questions or comments?

APPEL: Do I infer correctly that you're saying that the Orel and Seinfeld mechanism is largely insignificant on kinetic grounds?

SCHWARTZ: I'm not saying that quite yet. The Orel and Seinfeld study, as I recall, put forward some chemical thermodynamics; and did not explicitly address a mechanism whereby those chemical thermodynamics could be achieved. The indications that we have from the laboratory study, where we haven't doped it with anything other than water and oxygen, is that NO_2 dissolves slowly at ppm concentrations. It's very soluble, and it's a question of how long it takes to get there.

STEVENS: What about the role of ammonia?

SCHWARTZ: I don't think that's going to be very important. That's a big difference, now, between SO_2 and NO_2. If we write the solubility of SO_2 as sulfur IV, the concentration of sulfur IV is equal to a Henry's Law coefficient times the partial pressure of SO_2 times a quantity, η, where

$$\eta = 1 + k_1/[H^+] + k_1 k_2/[H^+]^2$$

a dimensionless quantity that tremendously increases the solubility of sulfur IV, with increasing pH. You don't have that with NO_2.

STEVENS: But in an extremely acid droplet, with NO_2 or nitric acid dissolved in it, wouldn't the solubility of ammonia be favored, where it might be less favorable for SO_2?

SCHWARTZ: Well, I'm not sure I'm getting the thrust of your question. The question I'm answering is the influence of ammonia upon the solubility of NO_2 in water. Because of the ammonia dissociation equilibria, if an acid is in the water, the ammonia becomes much more soluble as ammonium.

STEVENS: Yes, and the acid rain--or the rain that we see--is high in concentrations of ammonium ions, which affects the pH. This in turn would affect the solubility of components in the rain droplet itself.

DURHAM: Well, since the NO_2 mass, transferred to liquid in water, is pH independent, the only problem is in the distribution of the products--in regard to nitrite, which may be driven out as the pH goes down, as Steve presented. Now, the question is the rate of oxidation of the nitrate ion--

STEVENS: In the presence of ammonia.

DURHAM: Right. It turns out that the mass transfer of NO_2 in falling raindrops and fog drops is so slow that probably it is not an important consideration in pH.

SCHWARTZ: I'd just go a little further and try to distinguish between the mass transfer, which is a transport phenomenon, and the equilibrium solubility of nitrogen IV, which is so low being that it is soluble only according to Henry's Law. The big difference in the sulfur IV is that these acid dissociation and hydration equilibria are fast. One electron must be gained or lost before nitrogen IV can become appreciably soluble; a one-electron-transfer process is needed. And one electron is not required in sulfur.

DURHAM: In regard to the end result constant for nitrogen dioxide, have you rejected the value give by Andrew?

SCHWARTZ: Sure.

DURHAM: Okay. On what basis?

SCHWARTZ: I will make available to you a copy of an analysis that goes through every one of those dashed lines in Figure 12. I'm not sure I can recall offhand the number for Henry's Law of NO_2 that we got on the basis of Andrew and Hanson. Do you remember that, Warren? Andrew and Hanson measured, in a--no, Andrew and Hanson in fact just guessed a number.

WHITE: They pulled one out of the air.

DURHAM: They said in the paper that they measured by a falling film method, analogous to the carbon dioxide mass transfer.

SCHWARTZ: No, they were measuring the chemical kinetics in a film experiment. They interpreted that, using a Henry's Law coefficient which they obtained by "indirect methods." They gave no further indication of where that came from.

STEDMAN: I have a much less detailed question concerning nitric acid solubility. I think it is clear that when the air gets into a cloud, all of the gaseous nitrate--if it has any attraction to water--will be dissolved. The problem that I have is understanding what happens, because, when I talk to meteorologists, they tell me 90 percent of cloud droplets reevaporate. Now, what do you think hapens to just the gaseous nitrate--never mind all the other complications? What happens when that cloud droplet reevaporates?

SCHWARTZ: Just a real quick guess: Any nitric acid in an evaporating drop will go back into the gas phase as molecular nitric acid. I don't think any other chemical equilibrium can be sufficiently fast, based upon any calculated vapor pressure curve.

MUELLER: In a partial response to your question, we have some measurements with our filters from ground to 5,000 ft. And if you assume that the nitrate on our filters (always the same filter) is a function of the nitric acid concentration, then the findings could indicate a very rapid deposition of nitric acid. The gradient is extremely steep. For instance, while the concentration of nitrate at the ground station is less, maybe 0.1 $\mu g/m^3$, at higher altitudes the amount of nitrate recovered with our filters increases, up to several micrograms per cubic meter near the inversion base.

SCHWARTZ: Which, putting words in your mouth, there, infers that the nitrate comes from clouds that have evaporated and left it there?

MUELLER: Left nitrate there, or somehow produced there a sort of zone, and a very steep gradient. Much steeper than any other material that we've measured.

SCHWARTZ: One aspect of that goes along with what Joe Bufalini is suggesting. If one has clouds with hydrogen peroxide, which is quite soluble in cloud water, and NO_2, which is sparingly soluble, one has a chemical reactor up there which can process NO_2 into nitric acid. Most clouds don't rain; and then, gas phase nitric acid can be reemitted by that mechanism.

ALTSHULLER: Well, what fraction of time, in terms of formation reevaporation, is really involved for reactions within droplets per unit of time?

SCHWARTZ: Well, that depends on the chemical kinetics, Paul--

ALTSHULLER: Just a second. If the material is in the gas phase a certain fraction of time, and that fraction of time is large, doesn't this affect the heterogeneous kinetics here? Unless you assume about how long the droplet exists per unit of time, how can you make any further computations?

SCHWARTZ: I'm addressing the expectation that NO_2 in a finely dispersed system such as a cloud will exhibit phase equilibrium between the gas phase and the aqueous phase. I therefore will answer the question, not what fraction of the time a molecule spends in the aqueous phase, but rather what fraction of the molecules were present in the aqueous phase? Henry's Law coefficient tells me that. Given that number, and given also a rate coefficient for oxidation of aqueous phase NO_2 by some things, via H_2O_2, then I can tell you a rate--normalized to the total amount of gas present in that cloud--of oxidation in the aqueous phase.

DURHAM: One other point having to do with the evaporation of cloud droplets. When these droplets containing nitric acid and nitrous acid begin to evaporate, this is a concentration step: it will lower the pH. And I don't remember if you showed the redox reaction between nitric acid and nitrous acid. But as the pH is lowered, a molecular species of these acids is formed within the droplet at low pH. This redox reaction then generates a species, NO/NO_2, emitted in the gas phase. This may be what Harvey's seeing in his chamber.

SCHWARTZ: In fact, all three processes can take place. Nitrous and nitric acids will yield two NO_2's, and nitrous acid alone will yield an NO and NO_2.

DISCUSSION

Moderated by

William E. Wilson

Environmental Sciences Research Laboratory
Research Triangle Park, North Carolina 27711

NATURAL VS. ANTHROPOGENIC NO_x SOURCES

Pointing to the heavy (~90 percent) contribution by anthropogenic sources are the high NO_x levels in the eastern U.S., in comparison to those west of the Mississippi (Bufalini). Also, in springtime and summer measurements near the Canadian border (Stedman), winds from the south were observed to carry NO_2 concentrations greater than those in winds from the north; this observation would suggest anthropogenic NO_2 sources, since, in contrast with the U.S., Canada has more natural than anthropogenic sources.

Most evidence indicates relatively little contribution of NO_x ($\leq$10 percent) by natural sources such as lightning (Stedman) or conversion of ammonia to nitrate during fog and rain (Durham). An oxidation mechanism, possibly responsible for the conversion in the latter case, was demonstrated in laboratory experiments (Appel) to determine the stability of nitrate and ammonium in solution; at room temperature, nitrate concentrations increased with time, and ammonium concentrations decreased with time; frozen solutions showed negligible change.

WET DEPOSITION MEASUREMENTS

In order to demonstrate any trend in deposition of acidity, current measurement techniques must be refined, and operating influences to be considered in data interpretation must be determined, e.g. influences of cities on precipitation, and of possibly changing precipitation patterns (Wilson). (Gene Likens, and other experts on this subject did not attend the workshop, and thus no comment was offered in this regard).

The characteristics of the ideal measurement instrument should be agreed upon (Shaw). An instrument is being developed that will use electrochemistry, with specific ion electrodes, pH electrodes, to obtain information on rain dynamics through continuous rain measurements (Schwartz). A similar instrument was used in some Illinois Water Survey field studies (Stedman). The material used for fabricating these instruments must be accounted for (Bufalini), because leaching may cause problems unless precautions are taken. Several possible fabrication materials are available: glass, Teflon, stainless steel, Pyrex, or (Schwartz) a polymeric material.

Priorities must be ordered for existing and future sampling programs. To avoid unnecessary expense, established programs could be adapted to a "crash" program for measuring as many chemistries as possible (Mueller). Measurements of pH only would not produce valuable results, since (Schwartz) many substances could influence these measurements, and since (Mueller) the MAP3S data indicate a "fair amount" of correlation between "field pH" and "lab pH." Efforts should be directed toward achieving consistency within one measurement technology (Stedman), since certain variations among the various techniques appear unavoidable.

DRY DEPOSITION MEASUREMENTS

Dry deposition of sulfuric acid particles, nitric acid vapor, hydrochloric acid vapor, etc., has long remained an unrecognized, important influence in the acidification of the environment (Wilson). The proposal is made (Wilson) for nitrogen-compound measurements in terms of mass flow rates in a plume for information on transformation and removal rates.

Refining of measurements could begin with a study of previous experiments and the variety of techniques tested. Stedman used fast response instrumentation to measure deposition velocities by eddy correlation (Schwartz). Dry deposition work was performed by "the Harwell people in England" (Mueller). Dry deposition of lead as a function of particle size has been measured (Friedlander). Deposition of gases in a wind tunnel, using a water trough was studied by Chamberlain, but the simulation task was extremely burdensome, and interpretation of results is difficult (Durham).

New, direct methods are needed that measure nitrogen compounds in urban and rural settings (Durham). In most cases, use is prohibited of direct deposition measurement techniques that would include following the path of some tracer; although boron, used with a neutron generator and boosted to lithium, has been used as a tracer, the technique involves extensive scatter and requires several repetitions of measurements. On the other hand, inferred methods - eddy correlation, concentration gradient, etc. - allow for greater error. One direct method with good potential is the acid-drip method, analyzing forest drip water resulting from a rain that occurred several days earlier.

SMOG CHAMBER STUDIES

Interfering phenomena in these experiments are chemical transformations and wall deposition (Wilson). Nitric acid uptake and the degassing of nitric acid and other nitrogen dioxides have been observed in the aluminum Battelle chamber and in the Teflon UNC chamber.

Further experimental data involving wall deposition measurements are needed (Friedlander). In one ongoing chamber study (Fox), strips of film are positioned on the chamber walls and later examined by IC for sulfate deposition; an interference from high humidity is expected in this study. In another study (Spicer), the following observations were made concerning solution-phase chemistry: High NO_2 levels do not decrease after several hours - 1) in an aluminum chamber, 2) in a Teflon-lined chamber, or 3) at relatively high humidities. Also, in 5- or 10-h experiments (Spicer), particulate nitrate, certainly, is lost to chamber walls, and gaseous nitric acid, probably, forms a bond with the walls; ammonia level is controlled with acidic charcoal; and the ~30-percent observed nitrogen deficit appears attributable to N_2O_5/HNO_3 loss on the chamber walls.

LABORATORY STUDIES

Complementary laboratory studies that do not use smog chambers could provide needed data on chemical kinetics (Schwartz). Such investigations should first be supported by field evidence that aqueous-phase reactions are important (Wilson). One study (Appel) would indicate that gas-phase reaction studies alone provide an insufficient data base; observations of diurnal variation in nitric acid and in particulate nitrate reflected maximum nitric acid at midday or afternoon (paralleling the ozone maximum) and maximum particulate nitrate in the morning.

An understanding of aqueous-phase oxidation and an answer to the question, "How does the acid get into the rain?" are needed (Schwartz). Since the acid content of aerosols is not sufficient to account for the acidity measured in rain, NO_x and SO_x precursors to acid rain should be studied. As a starting point (Friedlander), the equilibrium hypothesis could be checked by comparing the ammonia/nitric acid equilibrium relationship in the Southwest to that in the North-Northeast, where humidities differ vastly; the FTIR technique appears to be the method of choice. Such a study could provide evidence for or against further aqueous-phase chemistry research.

Another valuable study (Wilson) might be laboratory measurements of the vapor pressure of ammonia and nitric acid above solutions of ammonium nitrate and ammonium nitrate plus chloride ions, sulfate ions, etc. Tang's article in Atmospheric Environment deals with this topic (Schwartz). A related study is ongoing at Brookhaven (Schwartz) to justify an assumed phase equilibrium, e.g., between ammonia plus ammonium, in order to determine where this material has partitioned.

Understanding the relationship between NO_x problems and O_3 problems (Schwartz) is part of continuing smog chamber work at Battelle (Spicer). Influential factors appear to be temperature, formation and decomposition of PAN, and several other subtle, secondary effects seen only after perhaps 2 days have elapsed.

Results of these laboratory studies should provide valuable applications to air quality simulation models (Altshuller), and results of smog chamber studies should be applicable to "real world" conditions (Bufalini).

GENERAL OBSERVATIONS

The effect on human health of atmospheric nitrogen pollutants appears to be important, although these nitrogen products - nitrate esters, olefins, toluene in combination with OH^- and NO_2, etc. - are not important in terms of mass (Wilson). This conclusion agrees with Pitts' report that passing NO_2 over a filter increases mutagenicity.

"One might expect the same type of nitration reactions to occur with polynuclear aromatics, and lead to increases in the mutagenicity of atmospheric organic material" (Wilson).

A reemphasis was placed on the need to refine measurement techniques (Wilson). The excess NO_2 observed in Stedman's work may result from measured conditions or from the particular measurement method. Perhaps techniques should be developed to measure particulate-phase nitrate in the presence of vapor phase; these techniques would abolish the requirement of removing the particle from the gas phase, where it is in equilibrium with vapor.

ATTENDEES

Bruce R. Appel
California Department of Health Services
Berkeley, California

A.P. Altshuller
U.S. Environmental Protection Agency
Research Triangle Park, North Carolina

H.M. Barnes
U.S. Environmental Protection Agency
Research Triangle Park, North Carolina

Basil Dimitriades
U.S. Environmental Protection Agency
Research Triangle Park, North Carolina

Thomas G. Dzubay
U.S. Environmental Protection Agency
Research Triangle Park, North Carolina

Jack Durham
U.S. Environmental Protection Agency
Research Triangle Park, North Carolina

A. Gordon Everett
Everett and Associates
Rockville, Maryland

Donald L. Fox
University of North Carolina
Chapel Hill, North Carolina

Sheldon K. Friedlander
University of California
Los Angeles, California

Bruce Gay
U.S. Environmental Protection Agency
Research Triangle Park, North Carolina

Dale G. Hendry
SRI International
Menlo Park, California

Barry J. Huebert
Colorado College
Colorado Springs, Colorado

Harvey E. Jeffries
University of North Carolina
Chapel Hill, North Carolina

Henry S. Judeikis
The Aerospace Corporation
El Segundo, California

Richard Kamens
Univeristy of North Carolina
Chapel Hill, North Carolina

Kenneth T. Knapp
U.S. Environmental Protection Agency
Research Triangle Park, North Carolina

Charles Lewis
U.S. Environmental Protection Agency
Research Triangle Park, North Carolina

William A. Lonneman
U.S. Environmental Protection Agency
Research Triangle Park, North Carolina

Peter Mueller
Environmental Research and Technology
Westlake Village, California

Leonard Newman
Brookhaven National Laboratory
Upton, Long Island, New York

Janet R. Parsons
Northrop Services, Inc.
Research Triangle Park, North Carolina

Richard Paur
U.S. Environmental Protection Agency
Research Triangle Park, North Carolina

T. Slater Raymond
Northrop Services, Inc.
Research Triangle Park, North Carolina

Stephen E. Schwartz
Brookhaven National Laboratory
Upton, Long Island, New York

Kenneth G. Sexton
University of North Carolina
Chapel Hill, North Carolina

Robert W. Shaw
U.S. Environmental Protection Agency
Research Triangle Park, North Carolina

John Sigsby
U.S. Environmental Protection Agency
Research Triangle Park, North Carolina

John W. Spence
U.S. Environmental Protection Agency
Research Triangle Park, North Carolina

Chester W. Spicer
Battelle Columbus Laboratory
Columbus, Ohio

Donald H. Stedman
University of Michigan
Ann Arbor, Michigan

Gary J. Stensland
Illinois State Water Survey
Urbana, Illinois

Robert K. Stevens
U.S. Environmental Protection Agency
Research Triangle Park, North Carolina

D. Bruce Turner
U.S. Environmental Protection Agency
Research Triangle Park, North Carolina

Jack Wagman
U.S. Environmental Protection Agency
Research Triangle Park, North Carolina

Warren H. White
Washington University
St. Louis, Missouri

William E. Wilson
U.S. Environmental Protection Agency
Research Triangle Park, North Carolina

Arthur M. Winer
University of California - SAPRC
Riverside, California